



Gas Phase Chemistry of Organic Anions involving Isomerisation

A Thesis submitted for the Degree

of

Doctor of Philosophy

in the

Department of Organic Chemistry

by

Kevin M. Downard B.Sc. (Hons.)



The University of Adelaide

July, 1991

"No amount of experimentation can ever prove me right; a single experiment can prove me wrong."

Albert Einstein (1879-1955)

Contents

Statement	Page	viii
Acknowledgements		ix
Figures		xi
Tables		xiii
Abstract		xvi
Chapter 1	An introduction to negative ion mass spectrometry	1
1.1	Introduction	1
1.2	Negative ion generation by direct electron capture	2
1.2.1	Associative resonance capture	2
1.2.2	Dissociative resonance capture	3
1.2.3	Ion-pair production	3
1.3	Negative ion chemical ionisation	4
1.3.1	Proton transfer	4
1.3.2	Nucleophilic displacement	5
1.3.3	Nucleophilic addition	5
1.3.4	Charge transfer	5
1.4	A double sector reverse-geometry mass spectrometer	6
1.4.1	Collisional activation mass analysed kinetic energy spectra	8

1.4.2	The fragmentations of even-electron organic anions on collisional activation	9
1.4.2.1	Simple homolytic cleavage	9
1.4.2.2	Fragmentations through an ion-molecule complex	9
1.4.2.3	Rearrangements	10
1.4.2.4	Charge remote fragmentations	10
1.4.3	Charge reversal mass spectra	11
1.5	A triple sector mass spectrometer	12
1.6	<i>Ab initio</i> molecular orbital calculations - a theoretical aid to studies of gas-phase ion chemistry	14
1.6.1	Introduction	14
1.6.2	Electronic and nuclear motion	15
1.6.3	Molecular orbital theory	16
1.6.4	Møller-Plesset perturbation theory	19
1.6.5	Nomenclature	20
1.7	Gas phase ion-molecule chemistry	21
1.7.1	Introduction	21
1.7.2	The flowing afterglow - S.I.F.T. instrument	23
1.7.2.1	Collision-induced dissociation in the S.I.F.T. instrument	24
1.7.2.2	Gas-phase acidity measurements	24
1.7.2.3	Reaction rates and branching ratios	26
1.7.2.4	Ion-molecule reaction efficiencies	29
Chapter 2	α and β substituted alkyl carbanions in the gas phase	30
2.1	Introduction	30

2.2	α -Substituted carbanions	32
2.2.1	Gas-phase experiments to generate carbanions $RXCH_2^-$	33
2.2.2	The hydroxymethylene anion	38
2.2.2.1	Theoretical considerations to the possible detection of the hydroxymethylene anion	38
2.2.2.2	The attempted formation of the hydroxymethylene anion	40
2.2.3	The methylene thiol anion	42
2.2.3.1	Theoretical considerations concerning the possible detection of the methylene thiol anion	42
2.2.3.2	Formation of the methylene thiol anion	43
2.2.3.3	The reactivity of the methylene thiol anion	49
2.2.3.3.1	Experimental determination of the proton affinity of $HSCH_2^-$	52
2.2.3.3.2	Reactions of $HSCH_2^-$ involving hydride ion transfer	53
2.2.3.4	Thermochemistry of the methylene thiol anion	59
2.2.4	The amino methylene anion	60
2.2.4.1	Theoretical considerations concerning the possible detection of the amino methylene anion	60
2.2.4.2	The attempted gas phase formation of the amino methylene anion	61
2.2.5	The methylthiomethylene anion	63
2.2.5.1	Theoretical considerations concerning the possible detection of the methylthiomethylene anion	63
2.2.5.2	The formation of the methylthiomethylene anion	63
2.2.6	The methoxymethylene anion	64
2.2.6.1	Theoretical considerations concerning the possible detection of the methoxymethylene anion	64

2.2.6.2	The attempted gas phase formation of the methoxy-methylene anion	65
2.2.7	The N-methyl amino methylene anion	66
2.2.7.1	Theoretical considerations concerning the possible detection of the N-methyl amino methylene anion	66
2.2.7.2	The attempted gas phase formation of the N-methyl amino methylene anion	67
2.2.8	The N,N-dimethyl amino methylene anion	67
2.2.8.1	Theoretical considerations concerning the possible detection of the N,N-dimethyl amino methylene anion	67
2.2.8.2	The attempted gas phase formation of the N,N-dimethyl amino methylene anion	68
2.3	β -Substituted carbanions	69
2.3.1	β -Keto ethyl anions	72
2.3.1.1	The β -formylethyl anion	72
2.3.1.2	The β -acetylethyl anion	76
2.3.1.3	The β -benzoylethyl anion	81
2.3.1.4	The β -hydroxycarbonylethyl anion	86
2.3.1.5	The β -methoxycarbonylethyl anion	86
2.3.2	The β -vinylethyl anion	88
2.4	Summary and conclusions	93
Chapter 3	The formation, structure and reactivity of HN_2O^- . A product ion study.	95
3.1	Introduction	95

3.2	The reactivity of $\text{HN}=\text{NO}^-$ in the flowing afterglow	100
3.2.1	Experimental determination of the basicity of $\text{HN}=\text{NO}^-$	100
3.2.2	Reactions of $\text{HN}=\text{NO}^-$ involving oxidation	102
3.3	Thermochemistry of the $\text{HN}=\text{NO}^-$ ion	109
Chapter 4	The elimination of ethene from deprotonated ethyl methyl sulphoxide. The formation, structure and reactivity of the methyl sulphinyl anion.	110
4.1	Introduction	110
4.2	Structure elucidation of the $(\text{CH}_3\text{SO})^-$ ion	112
4.3	Reactivity of the $(\text{CH}_3\text{SO})^-$ ion	115
4.3.1	Experimental determination of the basicity of $(\text{CH}_3\text{SO})^-$	116
4.3.2	The reactivity of the methyl sulphinyl anion	118
4.4	Thermochemistry of the methyl sulphinyl anion	126
4.5	Thermochemistry of the loss of ethene from deprotonated ethyl methyl sulphoxide	127
4.6	The methyl disulphide anion	129
4.6.1	Formation of the methyl disulphide anion	129
4.6.2	The reactivity of the methyl disulphide anion	131
4.6.2.1	Experimental determination of the basicity of CH_3SS^-	131
4.6.2.2	Reactivity of the methyl disulphide anion	131
4.6.3	Thermochemistry of the methyl disulphide anion	134
4.7	The formation and reactivity of the formyl sulphinyl anion	134

Chapter 5	Gas phase intramolecular anionic rearrangements involving the migration of silicon	137
5.1	Introduction	137
5.2	Trimethylsilylalkoxides	138
5.3	Trimethylsilylalkyl carboxylates	141
5.4	Deprotonated trimethylsilyl ketones	145
5.4.1	Deprotonated alkoyltrimethylsilanes	146
5.4.2	Deprotonated benzoyltrimethylsilane	152
5.5	Trimethylsilylaryl carboxylates	153
5.6	Trimethylsilylbenzyl carboxylates	158
5.7	Summary and conclusions	162
	Summary and conclusions	164
Chapter 6	Experimental	167
6.1	Instrumentation	167
6.2	Synthesis	170
6.2.1	Commercial samples used for experiments discussed in chapter 2	170
6.2.2	Synthesis of unlabelled compounds for chapter 2	170
6.2.3	Synthesis of labelled compounds for chapter 2	176
6.2.4	Synthesis of compounds for chapter 3	177
6.2.5	Synthesis of compounds for chapter 4	177

6.2.6	Synthesis of unlabelled compounds for chapter 5	178
6.2.7	Synthesis of labelled compounds for chapter 5	183
	References	185
	Publications	199

Statement

This thesis contains no material which has been accepted for the award of any other degree or diploma in any University.

To the best of my knowledge, this thesis contains no material previously published or written by any other person, except where due reference has been made in the text.

Kevin M. Downard

NAME: KEVIN M. DOWNARD COURSE: PH.D.

I give consent to this copy of my thesis, when deposited in the University Library, being available for loan and photocopying.

SIGNED: ..

DATE: 4/2/92

Acknowledgements

First and foremost, I would like to thank my supervisor Professor John Bowie for his guidance, tireless enthusiasm and timely assistance and advice throughout my postgraduate studies. More recently, I am indebted to him for suggesting many improvements to this thesis which have greatly improved its quality. I would also like to thank him for providing me with the opportunity to visit The University of Colorado at Boulder to utilise the F.A.-S.I.F.T instrument.

This opportunity would not have been possible without the support of Professor Charles DePuy and The University of Colorado. My sincere thanks to Professor DePuy and his entire research group for their kindness and helpful guidance during my stay. I am particularly grateful to Dr.'s Scott Gronert and Michelle Krempp for their initial help with the operation of the instrument and to Hilary Oppermann whose assistance throughout my visit was very much appreciated.

I gratefully acknowledge The University of Adelaide for providing financial assistance for my flight to Boulder in the form of a University of Adelaide Travel Grant and a Donald Stranks Travelling Fellowship. I acknowledge the financial support of a University of Adelaide Postgraduate Scholarship.

I would like to thank Dr. John Sheldon for performing the high-level *ab initio* calculations presented in this thesis which have provided a valuable insight into the chemistry studied. I also thank Dr. Roger Hayes, formerly of The University of Nebraska, Lincoln, for recording the triple M.S. spectra reproduced in this thesis.

My thanks to all the members of the Organic Chemistry department for their helpful advice, assistance and friendship. In particular, I would like to thank the members of the Bowie research group who provided many constructive suggestions regarding my research work during many lively and stimulating group seminars.

Finally, I am especially grateful to my family and friends for their support and encouragement throughout my years of study. A special thank you to my parents, Valerie and Michael, for their continual support and for putting up with this sometimes temperamental scientist. My thanks also to my mother for graciously proof-reading this thesis.

Figures

		Page
1.1	A schematic representation of a double-focussing mass spectrometer of reverse geometry	7
1.2	Representation of a Kratos MS-50 Triple Analyser mass spectrometer exhibiting EBE geometry	13
1.3	An electronic configuration diagram for ($\nu^{\alpha_1\alpha}$)($\nu^{\beta_1\beta}$)($\nu^{\alpha_2\alpha}$)($\nu^{\beta_2\beta}$)($\nu^{\alpha_3\alpha}$)	18
1.4	The tandem flowing afterglow-S.I.F.T.-drift instrument	23
2.1	Collisional activation mass spectra of isomeric CH_2SH^- and CH_3S^-	44
2.2	Charge reversal mass spectra of isomeric CH_2SH^- and CH_3S^-	45
2.3	Interaction between a doubly occupied p-orbital and an unoccupied σ^* -orbital of a (C-X) bond	70
2.4	Conformers of a β -substituted ethyl anion in which the hyperconjugation effect is maximised and minimised	70
2.5	The interaction of a p(C $^-$)-orbital and the π orbitals of an adjacent C=O group	76
2.6	C.A. MS/MS/MS spectrum of the ion (m/z 138) formed on loss of CO_2 from $\text{C}_6\text{D}_5\text{C}(\text{O})\text{CH}_2\text{CH}_2\text{CO}_2^-$	85
2.7	Reaction of the m/z 55 ion (formed on the loss of CO_2 from $\text{CH}_2=\text{CHCH}_2\text{CH}_2\text{CO}_2^-$) with nitrous oxide	92
2.8	Reaction of deprotonated 2-butene (m/z 55) with nitrous oxide	92

3.1	<i>Ab initio</i> calculations on the addition of hydride ion to nitrous oxide	97
3.2	Collision induced decomposition mass spectrum of HN_2O^-	99
3.3	Reaction of $\text{HN}=\text{NO}^-$ with carbon disulphide	104
4.1	Collisional activation mass spectrum of the m/z 63 ion (CH_3SO) ⁻ produced on loss of ethene from deprotonated ethyl methyl sulphoxide	113
4.2	Charge reversal mass spectrum of the m/z 63 ion (CH_3SO) ⁻ produced on loss of ethene from deprotonated ethyl methyl sulphoxide	113
4.3	Collision induced dissociation spectrum of deprotonated ethyl methyl sulphoxide produced in the flowing afterglow-S.I.F.T.	117
4.4	Two resonance forms of the methyl sulphanyl anion CH_3SO^-	118
4.5	The reaction of the methyl sulphanyl anion CH_3SO^- with carbon disulphide	120
4.6	The reaction of the methyl sulphanyl anion CH_3SO^- with oxygen	120
4.7	Thermochemistry of the loss of ethene from deprotonated ethyl methyl sulphoxide	128
4.8	Collision induced dissociation mass spectrum of CH_3SS^-	130
4.9	Collision induced dissociation mass spectrum of $\text{HC}(\text{O})\text{SO}^-$	130
5.1	Collisional activation mass spectrum of $\text{Me}_3\text{SiCH}_2\text{CO}_2^-$	143
5.2	Collisional activation mass spectrum of $^-\text{CH}_2\text{CO}_2\text{SiMe}_3$	143
5.3	Collisional activation mass spectrum of $^-\text{CH}_2\text{C}(\text{O})\text{SiMe}_3$	147
5.4	Collisional activation mass spectrum of $\text{c}(\text{CH}_2\text{OC}^-)\text{SiMe}_3$	147
5.5	Collisional activation mass spectrum of deprotonated α -trimethylsilylphenylacetic acid	159

Tables

2.1	<i>Ab initio</i> calculations on ions HXCH_2^- ($\text{X} = \text{S}, \text{O}, \text{NH}$)	Page 34
2.2	<i>Ab initio</i> calculations on radicals $\text{HXCH}_2\cdot$ ($\text{X} = \text{S}, \text{O}, \text{NH}$)	35
2.3	<i>Ab initio</i> calculations on neutrals HXCH_3 ($\text{X} = \text{S}, \text{O}, \text{NH}$)	36
2.4	Collisional activation mass spectra for the deprotonated bis-substituted ethane and carboxylate precursors to the α -hetero-substituted carbanions RXCH_2^- ($\text{X} = \text{O}, \text{S}, \text{NH}, \text{NCH}_3$; $\text{R} = \text{H}, \text{CH}_3$)	39
2.5	Collisional activation mass spectra of the α -hetero-substituted carbanions RSCH_2^- ($\text{R} = \text{H}, \text{CH}_3$). A comparison with the mass spectral data of their isomeric ions	46
2.6	Charge reversal mass spectra of the α -hetero-substituted carbanions RSCH_2^- ($\text{R} = \text{H}, \text{CH}_3$). A comparison with the mass spectral data of their isomeric ions	47
2.7	Reactions of HSCH_2^- with hydrogen containing compounds. Products and branching ratios	50
2.8	Reactions of HSCH_2^- with non-hydrogen containing compounds. Products and branching ratios	51
2.9	Collisional activation mass spectra for the alkoxide and carboxylate precursors of some β -substituted ethyl anions	73

- 2.10 Collisional activation and charge reversal mass spectra of the $C_3H_5O^-$ (m/z 57) product ion of the β -formylethyl anion precursor. A comparison with mass spectral data of $C_3H_5O^-$ ions of known structure. 74
- 2.11 Collisional activation and charge reversal mass spectra of the $C_4H_7O^-$ (m/z 71) ions from the β -acetylethyl anion precursors. A comparison with the mass spectral data of $C_4H_7O^-$ ions of known structure. 78
- 2.12 Collisional activation and charge reversal mass spectra of the $C_9H_9O^-$ (m/z 133) product ions of β -benzoylethyl anion precursors. A comparison of mass spectral data of $C_9H_9O^-$ ions of known structure 82
- 2.13 Collisional activation and charge reversal mass spectra of the $C_3H_5O_2^-$ ions (m/z 73) from the β -hydroxycarbonylethyl anion precursors. A comparison with the mass spectral data of $C_3H_5O_2^-$ ions of known structure 87
- 2.14 Collisional activation and charge reversal mass spectra of the $C_4H_7^-$ ions (m/z 55) of β -vinylethyl anion precursors. A comparison with the mass spectral data of $C_4H_7^-$ ions of known structure 89
- 3.1 Reactions of $HN=NO^-$ with hydrogen containing compounds. Products and branching ratios 101
- 3.2 Reactions of the $HN=NO^-$ with non-hydrogen containing compounds. Products, branching ratios, rate constants and reaction efficiencies 103
- 4.1 Collisional activation and charge reversal mass spectra of CH_3SO^- (m/z 63) prepared from deprotonated ethyl methyl sulphoxide 114

4.2	Reactions of CH_3SO^- with hydrogen containing compounds. Products and branching ratios	114
4.3	Reactions of CH_3SO^- with compounds containing no acidic hydrogens. Products, branching ratios, rate constants and reaction efficiencies	119
4.4	Reactions of CH_3SS^- with compounds containing acidic hydrogens. Products and branching ratios	132
4.5	Reactions of CH_3SS^- with compounds containing no acidic hydrogens. Products, branching ratios, rate constants and reaction efficiencies	133
4.6	Reactions of the formyl sulphinyl anion HC(O)SO^- with compounds containing acidic hydrogens. Products and branching ratios	132
5.1	Collisional activation mass spectra of trimethylsilylalkoxides	139
5.2	Collisional activation mass spectra of trimethylsilylalkyl carboxylates	142
5.3	Collisional activation mass spectra of deprotonated trimethylsilyl ketones	148
5.4	Collisional activation MS/MS/MS data for product ions from $\text{Me}_3\text{SiC(O)CH}_2^-$ and $^-\text{CH}_2\text{Si(Me)}_2\text{C(O)Ph}$, together with CA MS/MS data for MeC(O)CH_2^- and PhC(O)CH_2^-	150
5.5	Collisional activation mass spectra of trimethylsilyl substituted aryl carboxylates	154
5.6	Collisional activation mass spectra of α -trimethylsilylbenzyl carboxylates	160

Abstract

This thesis describes attempts to generate selected α - and β -substituted alkyl carbanions in the gas phase. Three concurrent experimental approaches are adopted, namely: (i) a nucleophilic displacement reaction on an suitably substituted trimethylsilyl-derivative, (ii) a collision induced dissociation of an appropriate carboxylate anion, and (iii) a collision induced dissociation of a deprotonated *bis*-substituted ethane derivative. Factors affecting the stability of the carbanions and their ultimate detection are discussed. Conclusions drawn from independent *ab initio* calculations are compared with the results in the gas phase. The stability of the carbanions to isomerisation in the gas phase is assessed based on collisional activation and charge reversal spectra, together with deuterium labelling studies.

The experimental approaches outlined above were successful in generating the α -heterosubstituted carbanions HSCH_2^- and $\text{CH}_3\text{SCH}_2^-$, though not their oxygen and nitrogen analogues. This is rationalised based on the instability of ions RXCH_2^- ($\text{R} = \text{H}, \text{CH}_3$; $\text{X} = \text{O}, \text{NH}, \text{NCH}_3$) to electron detachment. The formation of HSCH_2^- prompted its ion molecule chemistry to be investigated utilising a flowing afterglow - S.I.F.T. instrument. The ion HSCH_2^- was found to be an effective hydride donor, donating hydride ion to a wide variety of neutral reagents including nitrous oxide, carbon disulphide, oxygen and acrolein.

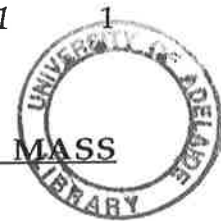
Attempts to detect several β -substituted ethyl anions have been unsuccessful. In most cases, the β -ethyl anions were unstable to isomerisation under the experimental conditions employed. Where no

isomer was detected, the β -ethyl anion is either not produced from the neutral precursors or is unstable to electron detachment.

The formation of the ion HN_2O^- , as the major product of the reaction between HSCH_2^- and nitrous oxide, prompted its ion molecule chemistry to be investigated. The structure of the HN_2O^- ion, in addition to its reactivity, is discussed in Chapter 3. The ion HN_2O^- was found to be an efficient oxidant transferring oxygen or hydroxide ion to a variety of neutrals. Oxidation products, or fragments therefrom, are produced on reaction of HN_2O^- with many electrophiles including carbon disulphide, carbonyl sulphide, sulphur dioxide and methyl *isocyanate*.

Chapter 4 describes an attempt to prepare the α -sulphinyl carbanion $^-\text{CH}_2\text{S}(\text{H})\text{O}$, a simple sulphur-oxidised analogue of the ion $^-\text{CH}_2\text{SH}$ (prepared in Chapter 2). The elimination of ethene from deprotonated ethyl methyl sulphoxide [the only suitable precursor of $^-\text{CH}_2\text{S}(\text{H})\text{O}$] affords an ion which is identified to be isomeric CH_3SO^- . The chemistry of this ion is interesting in its own right. The products of most reactions of CH_3SO^- are rationalised through initial nucleophilic attack by oxygen. However, the sulphur-oxygen bond of CH_3SO^- was found to exhibit some double character, as evidenced by its reaction with molecular oxygen. The major product of this reaction is the formyl sulphinyl anion.

This thesis also describes a preliminary investigation of intramolecular rearrangements involving the migration of silicon in the gas phase (see Chapter 5). Rearrangements involving the production of silicon-oxygen bonds are reported for most of the organosilicon systems studied. The extent of silicon migration as a function of intramolecular distance between the carbon and oxygen centres is discussed. Similarities between such rearrangements in the gas and solution phases are described.

Chapter 1AN INTRODUCTION TO NEGATIVE ION MASS SPECTROMETRY**1.1** Introduction

Gas-phase negative ions have been known to exist since the inception of mass spectrometry.¹ Despite this, there exists considerable disparity between the number of studies devoted to positive and negative ions. Positive ions have, until recently, received almost exclusive use in both analytical and research applications.

In spite of a possible lack of interest in the study of negative ions, early difficulties involving the production of anions in high concentration contributed to their neglect. With ionising electrons of 50-75 eV and low source pressures (typical of most common mass spectrometers) the production of negative ions on electron impact is, in general, at least one order of magnitude less efficient than for positive ions. Secondly, the generation of negative ions is strongly dependent on the electron energy used. Thus according to the nature of the molecule and the electron energy three non-concurrent ionisation processes are observed (see Section 1.2). In association with these problems of ion production, initial work in the area resulted in sensitivity and reproducibility difficulties.

Most of the early problems encountered in recording intense negative ion mass spectra were later attributed to the lack of a suitable mass spectrometer. The work of Large and Knof² in 1975 using a modified mass spectrometer contradicted that of Djerassi and co-workers³ just a decade before, who concluded that the negative ion mass spectra of various organic compounds at 70 eV contained little molecular weight or structural information.

The advent of negative ion chemical ionisation⁴⁻⁶ resulted in enhanced sensitivity in most spectra, whilst techniques such as fast atom bombardment⁷⁻¹⁰ and field desorption¹¹ have widened the applicability of

the negative ion mass spectrometric method. This, together with the availability of commercial mass spectrometers designed specifically for the study of negative ions, has led to a rapid expansion of the field.¹²⁻¹⁴

For the study of relatively stable anions, collisional activation (see Section 1.4.2) mass spectra are of analytical significance providing information often complementary to that obtained for positive ions. In addition to structure elucidation, the spectra can be used predict ion stability to fragmentation or rearrangement.

High pressure mass spectrometry¹⁵⁻¹⁷, ion cyclotron resonance¹⁸⁻¹⁹ and more recently the flowing afterglow technique²⁰ have enabled reactions and rates of a wide variety of gas phase anions to be recorded. This information, free of solvation and counter ion effects, enables the detail of reaction mechanisms to be probed.

1.2 Negative ion generation by direct electron capture

The generation of negative ions by the bombardment of sample molecules with electrons is particularly dependent on the electron energy used. Melton²¹ has classified the production of negative ions by electron impact according to the following three mechanisms.

1.2.1 Associative resonance capture

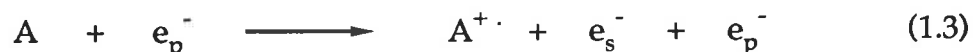


Associative resonance capture (equation 1.1) forms molecular ions AB^- at electron energies of 0-10 eV, provided molecules have a positive electron affinity.

1.2.2 Dissociative resonance capture

When AB captures a low energy electron (0-15 eV), an excited species, $(AB^-)^*$ is formed. Dissociation to A^- and B (equation 1.2) will occur if the captured electron has sufficient energy to produce an electronic transition of an energy higher than that for dissociation.

Many organic molecules produce molecular negative ions by these resonance capture processes at much higher electron beam energies (20-80 eV). This is due to the resonance capture of secondary thermal electrons (e_s^-) which are produced at metal surfaces or from competing gas phase positive ionisation²²⁻²³ (see equations 1.3 and 1.4).



Both associative and dissociative capture processes are enhanced under chemical ionisation conditions (see Section 1.3) where a reagent gas acts as both a means of producing thermal electrons and as a source of molecules for collisional stabilisation of the ions formed.

1.2.3 Ion-pair production

Ion-pair production is not restricted to a small range of ionisation energies. Any type of ionising radiation having an energy greater than, or equal to,

the appearance potential of A^- (typically ≥ 10 eV) can produce negative ions by this mechanism.

1.3 Negative ion chemical ionisation

Problems involved in the production of high concentrations of anions by electron impact may be overcome by employing negative ion chemical ionisation techniques.⁴⁻⁶ At the higher pressure of a chemical ionisation source, the abundance of low energy electrons present can lead to the formation of high concentrations of stable molecular anions.

The simplest N.I.C.I. process is that in which a reagent gas acts simply as a "buffer" to produce high concentrations of thermal electrons. The sample molecules can then undergo electron capture provided they possess positive electron affinities. For example, derivatised peptides give intense negative ion mass spectra with the addition of an appropriate inert gas,²⁴ but give no spectrum in the absence of the gas.

The second type of N.I.C.I. involves an ion-molecule reaction between a negatively charged reagent gas species (produced on electron impact) and a neutral sample molecule. Here, the reagent gas acts as a reactant upon its ionisation. Ion-production by ion-molecule reactions can be categorised as follows.

1.3.1 Proton transfer



Proton transfer reactions are generally very facile processes in the gas-phase. The extent to which a base will accept a proton from an acidic molecule AH depends on the proton affinity of B^- .

1.3.2 Nucleophilic displacement

De Puy^{25,26} and Bowie²⁷ have shown that specific anions can be generated in the gas phase upon nucleophilic displacement from an appropriately substituted trimethylsilyl-derivative using a suitable gas-phase nucleophile. For example, the $S_N2(Si)$ displacement reaction between trimethylsilylpropyne and fluoride ion (generated by electron impact of NF_3) produces the methylacetylide anion (equation 1.8).



The success of this method depends on the greater bond strength of Si-F relative to the C-Si bond

1.3.3 Nucleophilic addition

The nucleophilic attack of ions of low proton affinity generally form stable addition complexes (equation 1.9). For example, chloride ion (generated by electron impact from CCl_4) forms stable hydrogen-bonded complexes with a range of organic compounds including amides and phenols.²⁸

1.3.4 Charge transfer

The charge transfer reaction (equation 1.10) proceeds if the electron affinity of A is greater than that of B.

1.4 A double sector reverse-geometry mass spectrometer

The deflection of ions passing through a magnetic field results in the separation of ions of different mass to charge ratios m/z according to equation 1.11 where B is the magnetic field strength and r is the radius of the circular path of ions accelerated with a potential V .

$$\frac{m}{z} = \frac{B^2 r^2}{2V} \quad (1.11)$$

The resolving power of a single magnetic sector mass spectrometer is limited however. In practice, ions of the same mass to charge ratio experience slightly different potentials and so possess a spread of kinetic energies after acceleration.

A considerable increase in resolution is achieved by the incorporation of an electrostatic sector E . Ions which pass through an electrostatic field will follow paths of different radii according to their kinetic energy and hence velocity (v) (equation 1.12). Thus the ions are said to be "velocity-focussed". Instruments which employ both electrostatic and magnetic sectors achieve velocity and directional focussing and are described as "double focussing" mass spectrometers.

$$m v^2 = r z E \quad (1.12)$$

To record a conventional mass spectrum or make a precise mass determination, the order in which the ions experience the magnetic and

electric fields is immaterial. However, if the magnetic sector is situated before the electric sector, as is the case in the "reverse-geometry" instruments, then it is possible to characterise reactions or fragmentations occurring between the magnetic and electric sectors by scanning the latter at a constant magnetic field strength B and acceleration voltage V .

The arrangement employed in the ZAB instruments²⁹ is illustrated in Figure 1.1.

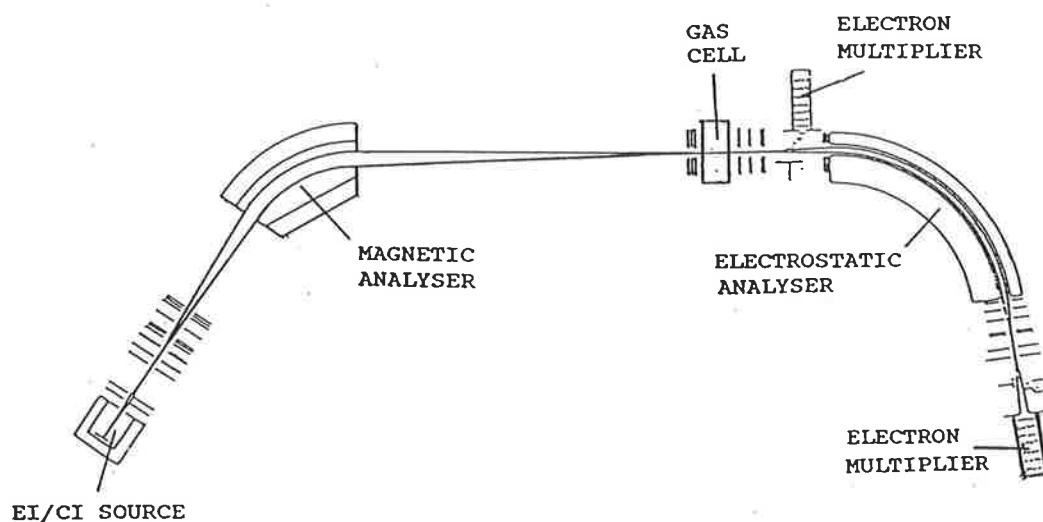


Figure 1.1 A schematic representation of a double-focussing mass spectrometer of reversed geometry. (VG-Analytical ZAB-2HF)

Here, ions are generated in the ion-source by electron impact or chemical ionisation with an ionisation energy of typically 70eV (for negative ions) and an operating pressure of approximately 10^{-1} Torr. This "soft-ionisation" technique gives information on molecular mass, yet the stability of the (generally) low energy ions produced hinders their fragmentation. The

presence of a "gas cell" between the sectors provides a confined region within which the beam of ions may undergo single or multiple collisions with a target gas (for example helium) depending on the pressure of the gas. The fragment ions produced are focussed by scanning the electric sector voltage. The result is a collision-induced (or collisional activated) decomposition spectrum.

1.4.1 Collisional activation mass analysed kinetic energy spectra

In the C.A. M.I.K.E. technique³⁰⁻³¹, of the ions produced in the chemical ionisation source, only those of a particular mass to charge ratio are allowed to transverse the magnetic sector.

The mass-selected primary beam enters the collision cell which contains inert helium at a typical pressure of 2×10^{-7} Torr (measured outside the collision cell). This produces essentially single ion-helium collisions, with the main beam signal intensity reduced by approximately 10%.

A MS/MS (or M.I.K.E.) spectrum is achieved by scanning the electric sector voltage. If the negative ion M_1^- selected upon emission from the source, fragments to ion M_2^- in the collision cell, then a reduction of the electric sector voltage (V) by the value M_2/M_1 , will transmit the M_2^- ion through that sector.

Most of the mass spectra reported in this thesis are CA MS/MS of even-electron organic anions produced in the source of a ZAB-2HF mass spectrometer (Figure 1.1) by proton abstraction (see Section 1.3.1) or nucleophilic displacement (Section 1.3.2). The spectra show fragment ions commensurate with the general fragmentations of even-electron negative ions recently classified by Bowie.³² The general fragmentation processes are now summarised.

1.4.2 The fragmentations of even-electron organic anions on collisional activation

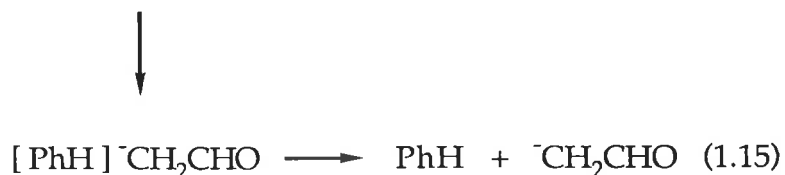
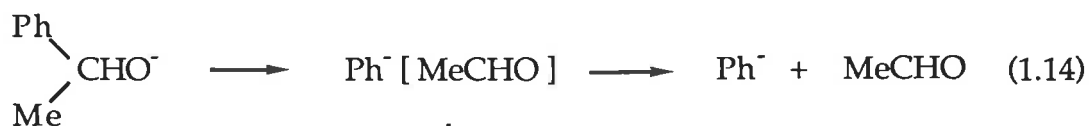
1.4.2.1 Simple homolytic cleavage

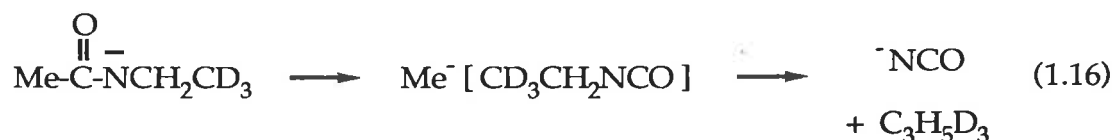
The loss of a radical by a simple homolytic cleavage process to yield a stable radical anion (for example, see equation 1.13³³) is common in the majority of (M-H⁺)⁻ spectra of organic ions. In particular, most (M-H⁺)⁻ ions exhibit some loss of H[·]. Indeed, for many ions this loss represents the base peak of the C.A. spectrum.



1.4.2.2 Fragmentations through an ion-molecule complex

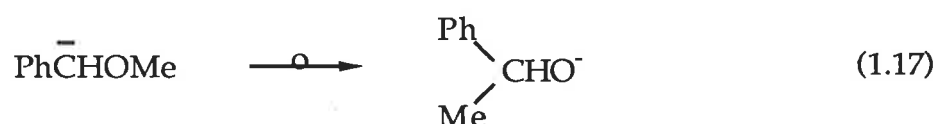
The formation of a solvated ion-molecule complex may occur directly from the initially formed (M-H⁺)⁻ ion or following a proton transfer reaction. The ion-molecule complex can collapse in several ways: (i) by direct dissociation of the "bound" anion from the complex (for example see equation 1.14³³), (ii) by dissociation of the complex following a proton transfer between the "bound" anion and the neutral (e.g. equation 1.15³³), or (iii) by a reaction (other than proton transfer) between the "bound" anion with the neutral molecule of the complex (e.g. equation 1.16³⁴).





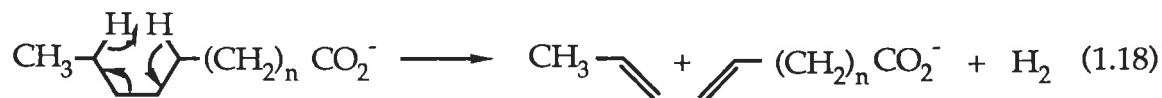
1.4.2.3 Rearrangements

Organic ions $(\text{M}-\text{H}^+)^-$ frequently undergo skeletal rearrangement prior to fragmentation. Several general rearrangement pathways have been reported including intramolecular nucleophilic displacement through a cyclic intermediate³⁵, 1,2-anionic (e.g. the Wittig rearrangement, equation 1.17³⁶) and six-centred³⁷⁻³⁸ rearrangements.



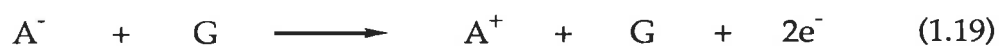
1.4.2.4 Charge remote fragmentations

This type of fragmentation results in the loss of a neutral molecule from a position remote to the charge site. Collisional activation mass spectra of large even-electron ions can exhibit fragments rationalised through charge remote fragmentations. For example, a charge remote 1,4-molecular hydrogen loss has been proposed to explain the loss of alkenes in the $(\text{M}-\text{H}^+)^-$ C.A. spectra of long chain saturated fatty acids.³⁹



1.4.3 Charge Reversal (C.R.) mass spectra

The charge reversal technique⁴⁰⁻⁴² was developed following the observation that, when high kinetic energy ions (A^-) collide with neutral gas target molecules (G), a non-decomposing negative ion can be converted into a positive ion ("charge reversal", "charge inversion" or "charge stripping") by a process shown in equation 1.19.



The energy required for the process (i.e. the electron affinity of A^- plus the ionisation energy of A^-) arises from a decrease in the translational energy of A^- during collision.

By decoupling the magnetic field from the electric sector voltage it became possible to detect products of the reaction shown in equation 1.19 with little interference from other ions or processes of the mass spectrometer. The development of reverse geometry instruments (see Figure 1.1) greatly facilitated the charge reversal experiment and extended its range of application.

In practice, ions A^+ are formed with excess internal energy and are often unstable to decomposition. Thus the charge reversal spectrum, produced by scanning the electric sector voltage at reversed potential (i.e. $-V$), records peaks corresponding to the daughter ions of A^+ . Parent ions A^+ are either recorded in low relative abundance or are not observed at all.

The charge reversal process can provide information on the structure of A^- , particularly useful when collision activation of A^- affords few daughter ions (see Section 2.2.3). However, the use of a charge reversal spectrum alone to determine the structure of a non-decomposing species requires caution⁴³ as reiterated recently by Grützmacher.⁴⁴ In particular instances, the positive ion produced by the charge reversal process may undergo a facile rearrangement

prior to detection. Consequently, the cation detected does not exhibit the same skeletal structure as the anion from which it was produced. For this reason, structural assignments in this thesis have been made on consideration of *both* the C.A. and C.R. spectra together, wherever possible, with a study of the ion's reactivity.

In addition, the charge reversal technique may be used to generate a cation A^+ which cannot be produced by conventional ionisation methods. For example the benzoate cation, $C_6H_5CO_2^+$, can be produced on charge reversal of its corresponding negative ion $C_6H_5CO_2^-$ but is not accessible by electron impact.⁴⁵

1.5 A Triple Sector Mass Spectrometer

A limitation of the double sector mass spectrometer is that whilst daughter ions produced in the collision cell are detected in the spectrum of the parent ion, their structure can at best only be implied.

To this end, spectrometers employing three independent stages of mass analysis are of particular use, since they allow one to select the ion beam from the source and utilise the latter two sectors to focus the products from each of the consecutive dissociations.

Of the possible combinations of triple analyser mass spectrometers incorporating only magnetic (B) and electric (E) sectors, three geometries have been applied, namely EBE, BEE and BEB. Several groups have added electric sectors to their double sector EB or reverse-geometry BE instrument to yield triple sector EBE and BEE designs respectively.

A triple analyser mass spectrometer of the EBE design, used to record the MS/MS/MS spectra in this thesis, is represented in Figure 1.2. Such an instrument has several modes of operation. In the first, the first two sectors are used for high resolution of the primary beam with the third sector

employed to detect the daughter ions.⁴⁶⁻⁴⁷ This mode is particularly useful in the analysis of mixtures containing compounds of the same nominal mass. A second mode involves the use of the first two sectors to transmit a fragment from a unimolecular or collision-induced dissociation of the parent, whilst the third sector detects the grand-daughter ions produced upon a consecutive dissociation. It is this second mode that has proved useful for the structure elucidation of the daughter ion which can only be generated on collision-induced dissociation of the parent.

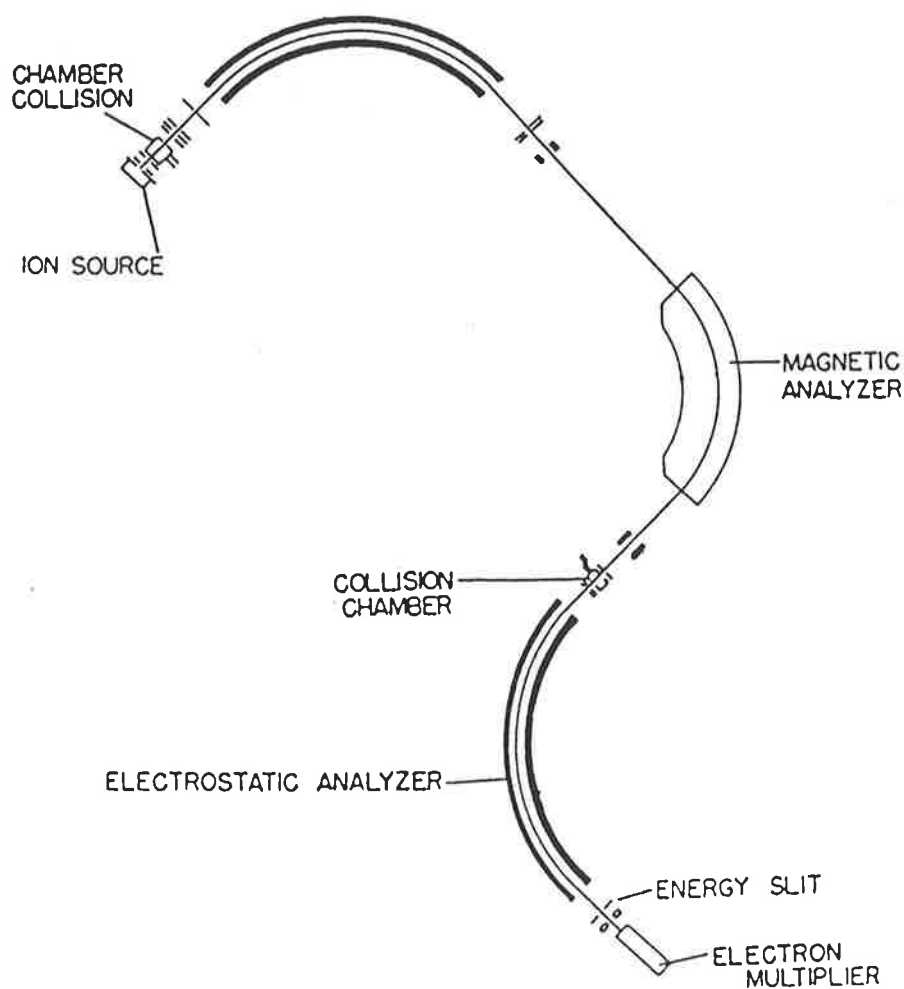


Figure 1.2 Representation of a Kratos MS-50 Triple Analyser mass spectrometer⁴⁸ exhibiting EBE geometry.

1.6 Ab initio molecular orbital calculations - a theoretical aid to studies of gas-phase ion chemistry.

1.6.1 Introduction

Early attempts to employ mathematical models to answer problems of a chemical nature were met with fierce opposition. Accusations that such work could only defile the science were issued by many. Comte described the mathematical methods "...profoundly irrational and contrary to the spirit of chemistry".⁴⁹ Whilst such opposition still exists to a lesser extent today, even the most ardent experimentalist will concede that an *ab initio* approach to chemistry (independent of experiment) is useful to aid the understanding of the properties of a discrete chemical species or the mechanism of a reaction process. Any chemical species or reaction process difficult or impossible to investigate experimentally can often be theoretically scrutinised. Theoretical calculations which lend support to experimental observations have obvious value, whilst those which yield results contrary to those obtained experimentally may highlight deficiencies or oversights in the experimental method.

The task of any model is to achieve an approximate solution to the Schrödinger partial differential equation⁵⁰ (equation 1.20) which defines the energy and properties of a stationary state of a molecule. The state of lowest energy is the ground state and most theoretical models are concerned with the calculation of the energy of this state.

$$H\psi = E\psi \quad (1.20)$$

In equation 1.20, H (the Hamiltonian operator) represents the total energy (kinetic and potential) of the system, E is the energy of an "allowed" quantised state relative to the constituent particles (nuclei and electrons)

infinitely separated, and ϑ is the wavefunction which defines the position (and spin) of all particles in cartesian co-ordinates.

The practice of attaining an approximate solution to the Schrödinger equation by employing mathematical models is now well established. The advent of efficient computer programs and developments in computing "power" has facilitated this.

The *ab initio* calculations in this thesis were performed on a Vax 11-750 computer by Dr. J.C. Sheldon of the Department of Physical & Inorganic Chemistry, The University of Adelaide. The conclusions drawn from these calculations by the author are presented in concert with the experimental approach. A full description of the theory cannot be discussed here. Instead, a brief introduction follows which emphasises the *ab initio* techniques and the level of theory presented in this thesis.

1.6.2 Electronic and nuclear motion

Since electrons adjust their positions in a molecule rapidly with nuclear motion, a reasonable approximation in solving the quantum mechanical problem is to assume that electron distribution depends only on the positions of the nuclei at any instant and not on nuclei-velocities. Thus in a field of fixed nuclei, electron motion may be defined by an effective electronic energy which is dependent on relative nuclear positions denoted $E(R)$. This separation of electronic and nuclear motion is called the Born-Oppenheimer approximation.⁵¹ It enables the Schrödinger equation to be expressed by equation 1.21 where ϑ^{elec} is the electronic wavefunction dependant on both electronic (r) and nuclear (R) co-ordinates.

$$H \vartheta^{\text{elec}}(r,R) = E(r) E(R) \vartheta^{\text{elec}}(r,R) \quad (1.21)$$

1.6.3 Molecular Orbital Theory

Molecular orbital theory is an attempt to define electron distribution and motion using one-electron wavefunctions. These wavefunctions, called spin orbitals, are the product of both spatial (x,y,z) and spin (α or β) functions and are denoted $\chi(x,y,z,\epsilon)$ where ϵ defines the spin co-ordinate.

To simplify the theory, an allocation of electrons to orbitals is often made, i.e. a single electron configuration is assigned. This simplification represents a constraint of the Hartree-Fock approximation.⁵²

For a n -electron system, these orbitals are combined to form a n -electron wavefunction ϑ which describes the simplest molecular orbital solution to the Schrödinger equation. Molecular orbital theory restricts the combination of the spin orbitals to a linear expression represented in equation 1.22 where ϕ_μ defines the assigned one-electron functions (or basis functions) $\phi_\mu(x,y,z,\epsilon)$ for each electron $\mu = 1, \dots, n$. Together these basis functions constitute the basis set.

$$\vartheta_i = \sum_{\mu=1}^n c_{\mu i} \phi_\mu \quad (1.22)$$

To define a basis set, well-described for any nuclear arrangement, it is convenient to define a particular set of basis functions associated with each nucleus. For simplicity, the atomic orbitals of the constituent atoms are represented by the basis functions. Thus, equation 1.22 represents a linear combination of atomic orbitals (L.C.A.O.). These functions contain the symmetry properties of the atomic orbitals, i.e. they exhibit the orbital geometries s,p,d ...etc. according to their angular properties.

One type of basis function used to represent the atomic orbitals are gaussian-type functions introduced to molecular orbital calculations by Boys.⁵³ Gaussian-type atomic functions $g(\alpha,r)$ are a function of a radial component, r , and a constant, α , which determines the size or radial extent of the orbital. A further representation involves the use of a linear combination of gaussian functions as basis functions. Basis functions of this type are known as "contracted-gaussians" whilst the individual gaussian functions of the linear combination are called "primitive gaussians".

Given the basis set, the unknown coefficients $c_{\mu i}$ can be determined so that the total electronic energy for the n -electron wavefunction is kept to a minimum. The wavefunction thus produced represents the Hartree-Fock (H.F.) approximation to the Schrödinger equation.

The theory described so far applies to molecules which have an even number of electrons in the ground (lowest energy) state. These molecules are said to be represented by closed-shell wavefunctions with orbitals either doubly occupied (with electrons of opposite spin) or empty.

For open-shell systems, i.e. those in which electrons are not completely assigned to orbitals in pairs, simple molecular orbital theory must be extended. Two approaches can be adopted. In the first, spin-restricted Hartree-Fock (R.H.F.) theory,⁵⁴⁻⁵⁵ singly occupied molecular orbitals have their electrons restrictively assigned to an α spin. The second approach in common use is spin-unrestricted Hartree-Fock (U.H.F.) theory.⁵⁶ Here, different spatial orbitals are assigned to α and β spins (see Figure 1.3). Hence, a previous doubly occupied orbital ϑ_i is now replaced by two distinct orbitals ϑ_i^α and ϑ_i^β (equations 1.23 and 1.24).

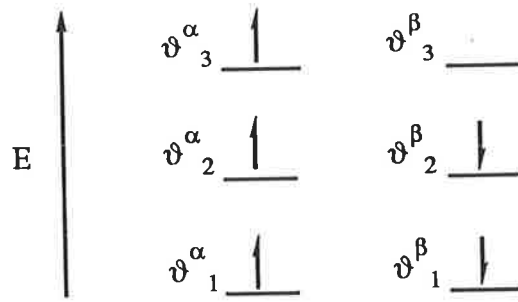


Figure 1.3 An electronic configuration diagram for
 $(\vartheta^{\alpha}_1\alpha)(\vartheta^{\beta}_1\beta)(\vartheta^{\alpha}_2\alpha)(\vartheta^{\beta}_2\beta)(\vartheta^{\alpha}_3\alpha)$

$$\vartheta^{\alpha}_i = \sum_{\mu=1}^n c_{\mu i}^{\alpha} \phi_{\mu} \quad (1.23)$$

$$\vartheta^{\beta}_i = \sum_{\mu=1}^n c_{\mu i}^{\beta} \phi_{\mu} \quad (1.24)$$

The main limitation of Hartree-Fock theory is its lack of correlation between the motion of electrons. Even with a large, flexible basis set, the exact solution to the Schrödinger equation cannot be expressed adequately by a unique assignment of electrons to orbitals, i.e. a single electron configuration. As a result, the exact energy required to solve the Schrödinger equation ($E(\text{exact})$) is higher than that predicted by Hartree-Fock theory ($E(\text{H.F.})$), the difference being the correlation energy, $E(\text{corr.})$, within the basis set used. (see equation 1.25)

$$E(\text{exact}) = E(\text{H.F.}) + E(\text{corr.}) \quad (1.25)$$

Whilst there are some important applications of *ab initio* wavefunctions for which Hartree-Fock energies are sufficient, energies accurate to a few millihartree require calculation of the correlation energy $E(\text{corr.})$.

1.6.4 Møller-Plesset Perturbation Theory

Calculation of the correlation energy, $E(\text{corr.})$, can be achieved using Møller-Plesset (M.P.) perturbation theory.⁵⁷ Møller-Plesset theory introduces a generalised electronic Hamiltonian H_λ to the Schrödinger equation which is the sum of the Hamiltonian according to Hartree-Fock theory H_0 and a perturbation $\lambda(H-H_0)$ (where H is the "correct" Hamiltonian and λ is a dimensionless integer) (equation 1.26).

$$H_\lambda = H_0 + \lambda(H - H_0) \quad (1.26)$$

The wavefunction ϑ_λ and energy E_λ , representing the exact solution to the Schrödinger equation for a given basis set, are now expanded to powers of λ according to Rayleigh-Schrödinger population theory⁵⁸ (equations 1.27 and 1.28) where ϑ_0 and E_0 represent the Hartree-Fock solutions to the Schrödinger equation.

$$\vartheta_\lambda = \vartheta_0 + \lambda\vartheta_1 + \lambda^2\vartheta_2 + \dots \quad (1.27)$$

$$E_\lambda = E_0 + \lambda E_1 + \lambda^2 E_2 + \dots \quad (1.28)$$

Setting $\lambda=1$, the first-order terms (ϑ_1 and E_1) can be determined by substituting the Hartree-Fock wavefunction ϑ_0 and energy E_0 . Subsequent increases in the parameter λ enables higher-order terms to be determined.

The level of calculation is defined by the highest-order energy term allowed, i.e. MP2 defines truncation to the second-order, MP3 to the third-order ...etc. The complexity of the computation increases rapidly with the order.

The calculations presented in this thesis have mostly been carried out to the fourth-order Møller-Plesset perturbation theory (MP4). At this level, single, double, triple and quadrupole substitutions contribute and hence this level of theory may be expressed MP4SDTQ.

1.6.5 Nomenclature

Complete specification of a theoretical model requires concise nomenclature to designate the Hartree-Fock or correlation procedure in addition to the basis set used. This notation is now discussed, with the theoretical level employed in this thesis used as a specific example.

For calculations at the 6-311++G** level,⁵⁹ G denotes the use of gaussian-type atomic functions to define the basis set. Each inner-shell atomic orbital is represented by a single function expressed in terms of six gaussian primitives. The outer-shell, or valence orbitals, are split into three functions represented by three, one and one gaussian primitives respectively.

The basis set is supplemented (**) by a single set of five d-type gaussian functions for "first-row" atoms and a single set of uncontracted p-type gaussians for hydrogen. The notation "++" denotes the incorporation of diffuse functions.⁶⁰ These overcome problems associated with anions where electron density may be far removed from a nuclear centre.⁶¹

Finally, the notation MP4SDTQ/6-311++G**//6-311++G** defines an energy calculation employing fourth-order Møller-Plesset theory and a 6-311++G**

basis set using a molecular geometry previously optimised at the Hartree-Fock level with an identical basis.

1.7 Gas Phase Ion-Molecule Chemistry

1.7.1 Introduction

Whilst many ion-molecule reactions can be carried out conveniently in solution, a recurrent concern regards the role of solvation in the chemical process. Indeed, it is well known that a change in solvent can, in some instances, completely alter the course of a reaction.⁶² As a result, our sometimes unconscious disregard of the role of solvation in a chemical reaction is a profound oversight.

Clearly, an investigation of the intrinsic reactivity of a discrete chemical species is best carried out free of the solvating medium. This primarily was the impetus for initiating reactivity studies in the gas phase. Here, reactions can be carried out which record the action of a totally unsolvated ion and a neutral molecule. Further, the role of solvation can be explored by allowing a partially solvated ion to react with a neutral species.

Such studies, however, presented initial experimental difficulties far in excess of those required to effect a reaction in solution. The generation of gaseous ions requires low pressures and short residence times which are the opposite conditions to those necessary to effect a gas phase reaction. In addition, studies involving the reaction of anions are complicated by the generally indirect processes required for their formation. These problems were addressed initially with the advent of high pressure¹⁵⁻¹⁷ and ion-cyclotron resonance¹⁸⁻¹⁹ mass spectrometers. The subsequent development of the flowing afterglow technique²⁰ has greatly facilitated the study of bimolecular ion-molecule reactions in the gas phase.

Constant instrumental advances have led to a continual expansion of this field, yet arguably the greater challenge is to persuade chemists of the fundamental importance of such studies. Many perceive that little relationship exists between the reactivity in gas and solution phases and thus any information obtained in the gas-phase will be of little practical use to those carrying out the same reaction in solution.

Such concern *does* have some foundation. In solution, ions are greatly stabilised by solvation and typically the encounter of an ion and neutral reactant requires an external energy (usually in the form of heat) to initiate a reaction. In contrast, ions in the gas-phase are attracted to neutrals by ion-dipole and ion-induced dipole forces. Hence, when an ion and neutral molecule reach a reaction distance, they may collectively contain up to 85 kJ mol⁻¹ ⁶³ in additional kinetic energy. This energy is sufficient to overcome many activation barriers. As a consequence, many gas-phase ion-molecule reactions are collision controlled, even at low temperatures.

However, once particular energetic differences between reactions in the two phases are accounted for, the similarities in the chemistry of the gas-phase and solution phase largely outweigh the differences. Since, the majority of synthetically useful organic reactions of negative ions are carried out in aprotic solvents where solvent effects on the reactant ion are minimised (with respect to the same reaction in a protic solvent), a remarkable parallel exists when an identical reaction is carried out in the condensed and gas phases.⁶⁴

The gas-phase ion-molecule chemistry presented in this thesis was carried out using the flowing afterglow technique. This technique is now discussed with the developments and capabilities of the method highlighted.

1.7.2 The Flowing Afterglow - S.I.F.T. instrument

The flowing afterglow technique was originally reported by Ferguson, Fehsenfeld and Schmeltekopf in 1969.²⁰ It enabled the authors to mimic, and subsequently study, the ion-molecule chemistry of the ionosphere initiated by solar-photoionisation of atmospheric gases. Bohme and Young⁶⁵ later applied the technique to study ion-neutral reactions of organic anions.

A further instrumental refinement involved the incorporation of a second flow tube. This allowed the preparation of anions via multi-step bimolecular reactions where direct electron impact of the appropriate neutral precursor proved unsuccessful. The introduction of quadrupole mass filter between the the two flow tubes produced a selected ion flow tube (S.I.F.T.)⁶⁶ enabling ions of a single mass to charge ratio to be injected solely into the second flow tube.

A representation of the tandem flowing afterglow-S.I.F.T.-drift⁶⁷⁻⁶⁸ currently in operation at Boulder is shown in Figure 1.4. It consists of four discrete sections: (i) a flow tube for ion preparation, (ii) a quadrupole mass filter for ion selection, (iii) a second flow tube for the reaction of the selected ions and (iv) an ion detection region.

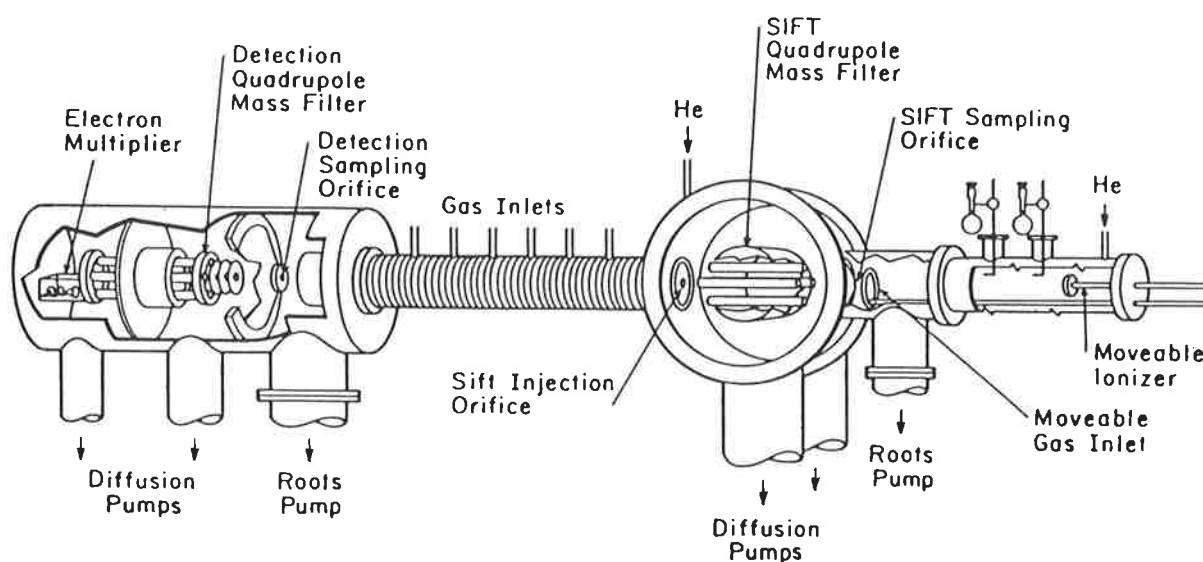


Figure 1.4 The Tandem Flowing Afterglow-S.I.F.T.-drift instrument.⁶⁷

In a typical experiment ions are generated in the first flow tube by direct electron impact, chemical ionisation or through multi-step bimolecular reactions. This is facilitated by a movable ioniser and inlets. The ions are thermalised by the helium buffer gas and sampled through the nose-cone orifice into the S.I.F.T. quadrupole mass filter. The mass-selected ions which exit are refocussed into the second flow tube. Introduction of a neutral reagent via one of the seven fixed inlets enables ion-molecule chemistry to proceed amidst the helium buffer gas. Whilst most of the reaction mixture is exhausted via a Roots blower pump, a small fraction is sampled in the low-pressure detection region. Here, the ions are refocussed via a series of lenses, analysed by a quadrupole mass filter and detected via an electron multiplier. Several experimental capabilities of the instrument are outlined in the subsequent sections.

1.7.2.1 Collision-induced dissociation in the S.I.F.T. instrument

To inject ions of the S.I.F.T. quadrupole into the higher pressure region of the second flow tube they must be extracted by an electrical potential. This potential imparts kinetic energy to the ions which is typically lost upon multiple collisions with the helium buffer gas. If the potential however is increased sufficiently, the ions can retain sufficient kinetic energy to undergo collision-induced dissociations.⁶⁷

The detection of the C.I.D. products produces a collision-induced dissociation spectrum providing information on the structure of the mass selected ion.

1.7.2.2 Gas-phase acidity measurements

The flowing afterglow method has found widespread utility in the measurement of experimental gas-phase acidities.⁶⁹ The reaction of a mass-

selected ion of the S.I.F.T.-quadrupole with a variety of acids of known acidity, permits the Gibbs free energy change of the proton transfer reaction ($\Delta G^{\circ}_{\text{acid}}$) to be obtained.

This bracketing method can be achieved since the ion-molecule collisions with the helium buffer gas ensure thermalisation of the excited ions produced on ionisation. Nevertheless, a limitation of this technique is that the error of the known acidity values is compounded in the experimental acidity measurement.

A second, more direct approach, involves the measurement of the proton transfer equilibrium constant K_{eq} for reactions of the type shown in equation 1.29.



The gas phase acidity of a compound AH can be determined by calculating the equilibrium constant K_{eq} from the ratio of the rates for forward and reverse reactions of equation 1.29.

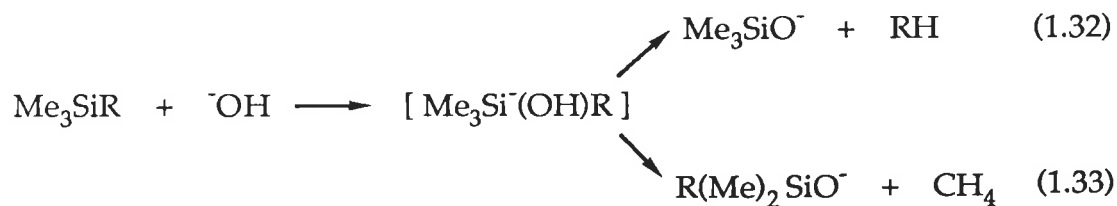
$$K_{\text{eq}} = \frac{k_1}{k_2} = \frac{[\text{A}^-][\text{BH}]}{[\text{AH}][\text{B}^-]} \quad (1.30)$$

Calculation of $\Delta G^{\circ}_{\text{acid}}$ (from equation 1.31 where R denotes the universal gas constant ($8.314 \text{ J mol}^{-1} \text{ deg}^{-1}$)) permits the establishment of quantitative gas phase acidity values.

$$\Delta G^{\circ}_{\text{acid}} = -R T \ln K_{\text{eq}} \quad (1.31)$$

A further kinetic method has been reported by De Puy.⁷⁰⁻⁷¹ This approach involves the reaction of an alkyltrimethylsilane with hydroxide ion. Two

siloxide ions are produced, resulting from competing losses of methane and alkane RH (see equations 1.32 and 1.33).



The relative concentrations of the siloxide ions $(\text{CH}_3)_3\text{SiO}^-$ and $\text{R}(\text{CH}_3)_2\text{SiO}^-$ reflects the ease of formation of carbanions CH_3^- and R^- after a statistical correction has been made for the differing degrees of substitution at silicon by the methyl (CH_3) and alkyl (R) groups. Assuming a linear relationship between the logarithm of the siloxide ratio and the acidity of RH, and making use of known acidities for methane and benzene, one can estimate the gas phase acidity of a compound RH.

The method has proved particularly useful in the determination of the acidities of alkanes whose conjugate bases have small or zero electron binding energies.

1.7.2.3 Reaction rates and branching ratios

In the S.I.F.T. instrument, the relationship between reaction time and the flow tube length allows the direct measurement of reaction kinetics. The reaction of a mass-selected ion with a neutral reagent added at each of the fixed inlets successively, permits the monitoring of reactant and product ion concentration as a function of inlet position and hence reaction time.

For a bimolecular ion-molecule reaction between anion A^- and neutral N, the decrease in concentration of anion A^- with time may be represented by equation 1.34 where k is the bimolecular rate constant.

$$\frac{d[A^-]}{dt} = -k [A^-] [N] \quad (1.34)$$

$$[A^-] d \ln [A^-] = -d[A^-] \quad (1.35)$$

Substitution of the identity shown in equation 1.35 into equation 1.34 yields equation 1.36.

$$d \ln [A^-] = -k [N] dt \quad (1.36)$$

Since \bar{v}_{ions} , the average velocity of the ions in the flow tube, is given by equation 1.37 (where x is the length of the reaction region), equation 1.36 can be simplified to the expression shown in equation 1.38, which affords equation 1.39 on rearrangement.

$$\bar{v}_{\text{ions}} = \frac{dx}{dt} \quad (1.37)$$

$$d \ln [A^-] = \frac{-k [N] dx}{\bar{v}_{\text{ions}}} \quad (1.38)$$

$$k = \frac{-d \ln [A^-]}{dx} \frac{\bar{v}_{\text{ions}}}{[N]} \quad (1.39)$$

The concentration of the neutral reagent N can be expressed by equation 1.40 where F_N is the neutral reagent flow rate, F_{He} is the buffer gas flow rate and P_{He} is the pressure of the buffer gas.

$$[N] = \frac{P_{\text{He}} F_N}{F_{\text{He}}} \quad (1.40)$$

The flow rate of the neutral can be determined by measuring the time the reagent takes to undergo a prescribed pressure increase within a calibrated volume.

Ferguson²⁰ has shown that the velocity of the ions is not simply that of the buffer gas since ions discharge at the flow tube walls. Hence ions have maximum density along the flow tube's central axis and zero density at the walls. The average velocities of the ions and helium buffer gas are related through equation 1.41 where α is a constant⁷² characteristic of the flow tube.

$$\bar{v}_{\text{ions}} = \alpha \bar{v}_{\text{He}} \quad (1.41)$$

$$\bar{v}_{\text{He}} = \frac{F_{\text{He}}}{P_{\text{He}} A} \quad (1.42)$$

Since the average buffer gas velocity can be represented by equation 1.42 where A is the cross-sectional area of the flow tube, equation 1.41 becomes equation 1.43.

$$\bar{v}_{\text{ions}} = \frac{\alpha F_{\text{He}}}{P_{\text{He}} A} \quad (1.43)$$

Substituting equations 1.40 and 1.43 into the rate equation (equation 1.39) affords equation 1.44.

$$k = \frac{-d \ln [A^-]}{dx} \frac{\alpha F_{\text{He}}^2}{A P_{\text{He}}^2 F_{\text{N}}} \quad (1.44)$$

Thus rate constants can be calculated from the experimental parameters expressed in equation 1.44 and are estimated to be accurate to within 25%.⁷³ A recent compilation of gas-phase reaction rate constants⁷⁴ highlights the importance of the flowing afterglow technique in such measurements.

Extrapolation of a plot of product ion concentration versus reaction time, t , towards $t = 0$, allows the branching ratios⁷⁵ for the product channels to be determined free from errors arising through secondary reactions.

In addition, the use of a variable temperature flow tube⁷⁶ enables studies to be carried out which monitor the temperature dependence of reaction rates.

1.7.2.4 Ion-molecule reaction efficiencies

The unique interactions between a particular ion and neutral molecule, results in an ineffectual comparison of rate constants between reactions. Thus, the magnitude of bimolecular reaction rate constants, k , are best correlated as reaction efficiencies.

The efficiency of a reaction is the ratio of the experimental rate constant to a theoretically calculated collision rate constant. The theoretical rate constant can be predicted using the "average dipole orientation theory" developed by Su and Bowers.⁷⁷

By extending the theory of Gioumouisis and Stevenson,⁷⁸ who defined a collision rate constant for reaction of a point charge at an induced dipole, Su and Bowers have derived a theoretical collision rate constant (equation 1.45).

$$k_{ADO} = 2 \Pi e \sqrt{\frac{\alpha}{\mu}} + c 2 e \mu_D \sqrt{\frac{2 \Pi}{\mu k T}} \quad (1.45)$$

Equation 1.45, together with an experimental rate constant, enables the calculation of a reaction efficiency using the following known or measured parameters: " μ_D " the dipole moment of the neutral, " μ " its reduced mass, " α " the polarisability of the neutral, " e " the charge of the ion, " T " the temperature, " k " the Boltzmann constant and " c " a constant which allows for the thermal rotation of the neutral.

Chapter 2 **α AND β SUBSTITUTED ALKYL CARBANIONS IN
THE GAS PHASE.**

2.1 **Introduction**

The importance of substituted carbanions in both synthetic and physical organic chemistry is well documented.⁷⁹⁻⁸³ Until recently however, the knowledge of substituent effects on the properties of alkyl carbanions was largely based on results obtained in solution.⁸⁴⁻⁸⁶ Over the past 15 years, the application of *ab initio* molecular orbital theory has enabled the properties of substituted alkyl carbanions to be predicted free from the effects of solvation.⁸⁷⁻⁹⁷ Despite suitable advances in instrumentation necessary for experimental observations in the gas phase, comparatively few studies have been reported.⁹⁸⁻¹⁰⁰ This is largely a consequence of the difficulties encountered in the generation of such carbanions in the gas phase.

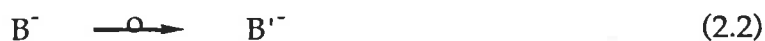
Three properties of fundamental importance in the detection of substituted alkyl carbanions in the gas phase are the basicity of the carbanion, its stability to isomerisation and the electron affinity of its corresponding radical. Substituted alkyl carbanions are amongst the strongest gas phase bases known and consequently their conjugate acids are weakly acidic. Therefore, the generation of a substituted alkyl carbanion from its conjugate acid by proton abstraction requires the generation of a reactant base not generally accessible in the gas phase. Further, if the conjugate acid of the carbanion of interest exhibits a substituent with an acidic site, proton abstraction may lead to the formation of an undesired isomer. To overcome these problems, this study attempts to produce substituted alkyl carbanions by the decomposition of an appropriate stable precursor (see Sections 2.2.1 and 2.3).

A second important property is the stability of substituted alkyl carbanions to isomerisation. Isomerisation of such a carbanion may occur through an

intramolecular or intermolecular process. If a substituted alkyl carbanion (B^-) is generated in the presence of a suitably acidic gas phase acid (AH), a facile intermolecular proton transfer may result. Further, if the conjugate acid of the carbanion (BH) which is produced exhibits an acidic site on its substituent, a second proton transfer reaction may occur to yield an isomer of the carbanion of interest (B'^-) (equation 2.1).



In the absence of a gas phase acid (AH), a substituted alkyl carbanion may undergo an intramolecular isomerisation reaction under the experimental conditions employed (equation 2.2).



The third property critical to the detection of substituted alkyl carbanions is the electron affinity of their corresponding radicals. It is well known that a radical can be stabilised through the interaction of its unpaired electron with a lone electron pair¹⁰¹⁻¹⁰² or π -bond¹⁰³⁻¹⁰⁴ of an adjacent substituent X. If the radical is stabilised sufficiently it may exhibit a negative electron affinity. Consequently the detection of a substituted alkyl carbanion may be hindered by its instability to electron detachment.

In this chapter, the attempted gas phase formation of selected α and β -substituted alkyl carbanions is described. Independent *ab initio* calculations which predict the basicity and stability of these ions to electron detachment are discussed together with the experimental approach. The stability of the carbanions to isomerisation is assessed based on collisional activation and charge reversal spectra, together with deuterium labelling studies.

2.2 α -Substituted carbanions

The stabilising effect of a substituent α to a carbanion centre can be measured by the energy difference of the substituted alkyl carbanion and the methyl anion. Largely positive values for the energy of the reaction represented in equation 2.3⁹² reflect the increased stabilisation of many α -substituted carbanions relative to the methyl anion.



This increase in stabilisation can be attributed to the interactions between the substituent X and the CH_2^- group. These interactions delocalise the charge on carbon resulting in positive stabilisation energies for XCH_2^- relative to the methyl anion.

To categorise the stabilisation processes, the substituents must first be classified in terms of their ability to donate or accept σ and π electrons. Electropositive groups, such as BH_2 , are σ -donors yet the presence of vacant π -orbitals allows them to act as π -acceptors. Thus electropositive groups stabilise α -substituted carbanions by the interaction between the π -orbital of the CH_2 group and a vacant p-orbital on X. In contrast, electronegative groups (e.g. OH) act as π -donors and σ -acceptors stabilising the carbanions through inductive σ -withdrawal.

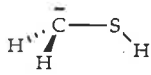
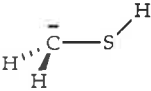
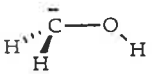
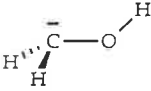
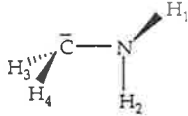
The choice of substituents X for this study was biased towards earlier interest in the hydroxymethylene anion ($\text{X} = \text{OH}$).¹⁰⁵ Attempts to directly detect the hydroxymethylene anion in addition to its sulphur and nitrogen analogues are described. In addition the effect of alkyl substitution at the heteroatom on carbanion stability is investigated. High level *ab initio* molecular orbital computations were performed by Dr. John C. Sheldon to calculate the energies and geometries for the α -substituted alkyl carbanions HXCH_2^- ($\text{X} =$

O, S, NH, NCH₃) and their corresponding radicals and neutrals. This data (presented in Tables 2.1 - 2.3) enables the basicity of the carbanions and the electron affinities of the corresponding radicals XCH₂· to be predicted. The use of a high level of theory which incorporates diffuse functions is essential to adequately calculate these parameters. As a result, similar *ab initio* calculations were not performed for the carbanions CH₃XCH₂⁻ (X = O, S, NH, NCH₃). The number of atoms in these systems required computations beyond those possible at the same level with the facilities available.

Reported stabilisation energies for the reaction shown in equation 2.3 are 46,⁹² 87⁹⁶ and 23⁹² kJ mol⁻¹ for X = OH, SH and NH₂ respectively. The increased stabilising effect of the SH group is noteworthy since it contradicts the value predicted based on the electronegativities of sulphur and oxygen. Further, the importance of the d-orbitals of sulphur in increasing carbanion stabilisation has been questioned.^{87,96} *Ab initio* molecular orbital calculations suggest the order of gas-phase carbanion stabilisation to be S>O>C for RXCH₂⁻ (R=H, CH₃) regardless of whether sulphur 3d orbitals are included in the basis set. Nevertheless, theoretical calculations have predicted that the interactions of the lone pair on carbon with the antibonding σ*-orbital of the SR group (R=H,CH₃) assist strongly to carbanion stabilisation. Indeed, it has been argued that the lower energy predicted for the σ*(S-R) orbital compared with that of σ*(O-R) will result in greater stability of α-thiocarbanions with respect to α-oxycarbanions.¹⁰⁶ This postulate is in strong agreement with the results presented in this thesis.

2.2.1 Gas-phase experiments to generate carbanions RXCH₂⁻

In view of the problems associated with the generation of substituted alkyl carbanions by proton abstraction (discussed in Section 2.1), three concurrent experimental methods to directly detect carbanions RXCH₂⁻ (X = O,S,NH; R =

Table 2.1 <i>Ab initio</i> calculations on ions HXCH_2^- ($\text{X} = \text{S}, \text{O}, \text{NH}$) ^a							
Structure of conformer (HF/6-311++G**//6-311++G**)							
Conformer number	1	2	3	4	5		
Symmetry	C _s (plane)	C _s	C _s	C _s	C ₁ (gauche)		
Total energies (au) hartrees HF/6-311++G**//6-311++G**	-437.08427	-437.08333	-114.38721	-114.39323	-94.55100		
MP4STDQ/6-311++G**//6-311++G**	-437.42700	-437.42543	-114.79451	-114.80102	-94.94758		
Zero point vibrational energies MP4SDTQ/6-311++G**//6-311++G**	0.0382	0.03310	0.03740	0.03800	0.05086		
Bond Lengths (Å)	C-S 1.8104 S-H 1.3586 C-H 1.0909	C-S 1.8455 S-H 1.3362 C-H 1.0917	C-O 1.4827 O-H 0.9402 C-H 1.1706	C-O 1.4884 O-H 0.9332 C-H 1.1022	C-N 1.4981 N-H ₁ 0.9981 N-H ₂ 1.1022	C-H ₃ 1.0981 C-H ₄ 1.1053	
Bond Angles (deg.)	CSH 109.18 HCS 109.40 HCSH 59.93	CSH 101.70 HCS 105.79 HCSH 122.80	COH 107.46 HCO 106.34 HCOH 55.97	COH 104.16 HCO 104.89 HCOH 124.97	CNH ₁ 109.69 CNH ₂ 114.12 H ₃ CN 107.67 H ₄ CN 110.37	H ₃ CNH ₄ 115.73 H ₁ NCH ₂ 119.39 H ₂ NCH ₄ 29.71	

^a Calculations performed by Dr. J.C. Sheldon, Department Physical & Inorganic Chemistry, The University of Adelaide on a VAX 11-750 computer using GAUSSIAN 86.¹⁰⁷

Table 2.2 <i>Ab initio</i> calculations on radicals HXCH_2 ($\text{X} = \text{S}, \text{O}, \text{NH}$) ^a			
Structure of radical (UHF/6-311++G**//6-311++G**)			
Structure number	1	2	3
Symmetry	C_1 CH_2 lies 24° below H_1CSH plane	C_1 CH_2 lies ca. 30° below H_1COH plane	C_s
Total energies (a.u.) hartress UHF/6-311++G**//6-311++G** MP4SDTQ/6-311++G**//6-311++G** Zero-point vibrational energies MP4SDTQ/6-311++G//6-311++G**	-437.11331 -437.41869 0.03347	-114.45353 -114.81642 0.03917	-94.62358 -94.97572 0.05313
Bond Lengths (Å)	C-S 1.7468 S-H 1.3299 C-H ₁ 1.0728 C-H ₂ 1.0728	C-O 1.3556 O-H 0.9402 C-H ₁ 1.0731 C-H ₂ 1.0776	C-N 1.3985 N-H ₄ 0.9968 C-H ₁ 1.0752
Bond Angles (deg.)	CSH 98.25 H ₁ CS 115.98 H ₂ CS 120.30 H ₁ CSH 177.85 H ₂ CSH -24.05	COH 110.75 H ₁ CO 113.34 H ₂ CO 117.94 H ₁ COH 182.05 H ₂ COH -31.11	CNH ₄ 114.42 H ₁ CN 116.19 H ₁ CNH ₂ 145.10 H ₄ NCH ₃ 129.00

^a Calculations performed by Dr. J.C. Sheldon, Department of Physical & Inorganic Chemistry, The University of Adelaide on a VAX 11-750 computer using GAUSSIAN 86.¹⁰⁷

Structure of neutral (RHF/6-311++G//6-311++G**)			
Structure number	1	2	3
Symmetry	C_s	C_s	C_s
Total energies (a.u.) hartress RHF/6-311++G**//6-311++G**	-437.74149	-115.08051	-95.24617
MP4SDTQ/6-311++G**//6-311++G**	-438.07924	-115.47645	-95.63103
Zero-point vibrational energies MP4SDTQ/6-311++G**//6-311++G**	0.04889	0.05477	0.06804
Bond Lengths (Å)	C-S 1.8183 S-H 1.3306 C-H ₁ 1.0819 C-H ₂ 1.0811	C-O 1.4003 O-H 0.9398 C-H ₁ 1.0817 C-H ₂ 1.0877	C-N 1.4541 N-H 0.9994 C-H ₁ 1.0907 C-H ₂ 1.0847
Bond Angles (deg.)	H ₁ CS 106.46 H ₂ CS 111.12 CSH 97.98 H ₂ COH ₁ ±118.45	H ₁ CO 107.24 H ₂ CO 111.78 COH 110.02 H ₂ COH ₁ 118.78	H ₁ CN 114.45 H ₂ CN 109.34 CNH 111.33 H ₂ CNH ₁ 121.38 HNCH ₁ 60.01

^a Calculations performed by Dr. J.C. Sheldon, Department of Physical & Inorganic Chemistry, The University of Adelaide on a VAX 11-750 computer using GAUSSIAN 86.¹⁰⁷

H, CH₃) were adopted. These approaches utilise a stable precursor ion or molecule which incorporates the desired carbanion as a moiety. Decomposition of the precursor may result in the formation of an α -substituted carbanion.

The first approach involves the collision-induced dissociation of a deprotonated bis-substituted ethane derivative with elimination of CH₂X as shown in equation 2.4.



The second approach involves the collision-induced dissociation of an appropriate carboxylate anion¹⁰⁸ (equation 2.5).



Thirdly, a nucleophilic displacement reaction on an appropriately substituted trimethylsilyl-derivative²⁵⁻²⁷ (equation 2.6) in the ion-source should generate RXCH₂⁻.



The three experimental approaches were employed separately for the attempted gas-phase formation of each of the α -substituted carbanions. Depending on the basicity of the α -substituted carbanion and the nature of the substituent X, an intermolecular proton transfer reaction (equation 2.1) may occur on the generation of the XCH₂⁻ by the approaches shown in equations 2.4 and 2.6. Any isomerisation of XCH₂⁻ from the method shown in equation 2.5, however, must proceed through an intramolecular process (equation 2.2).

2.2.2 The hydroxymethylene anion

2.2.2.1 Theoretical considerations concerning the possible detection of the hydroxymethylene anion

Previous interest in the hydroxymethylene anion¹⁰⁵ prompted a reinvestigation of its stability and ultimate detection. The generation of HOCH₂⁻ directly from methanol, however, cannot be achieved since proton abstraction occurs exclusively on oxygen. Further, methoxide ion was calculated to be stable to isomerisation to HOCH₂⁻ under collisional activation conditions; a process calculated to require an energy of 326 kJ mol⁻¹ 105.

While less thermodynamically stable than its isomer, the hydroxymethylene anion was nevertheless shown to be a theoretically stable species. In addition, since the reverse activation energy is some 194 kJ mol⁻¹, isomerisation of HOCH₂⁻ back to methoxide ion via an intramolecular hydride transfer (equation 2.7) should be unfavourable. Therefore, an experimental approach which could directly form the hydroxymethylene anion appeared intuitively useful.



The detection of HOCH₂⁻, however, is necessarily complicated by the ions predicted instability to electron loss. From the total energy of the more stable *anti* conformer of HOCH₂⁻ and that of its radical HOCH₂[·] (Tables 2.1 and 2.2), each corrected for zero point energies, the electron affinity of HOCH₂[·] is assigned a value -37 kJ mol⁻¹ using equation 2.8.

Ion (m/z)	C.A. MS/MS [m/z (loss) abundance in %]
HOCH ₂ CH ₂ O ⁻ (61) DOCH ₂ CH ₂ O ⁻ (62) HOCH ₂ CO ₂ ⁻ (75)	59(H ₂)100, 31(CH ₂ O)5, 29(H ₂ + CH ₂ O)1 61(H·)6, 59(HD)100, 31(CHDO)1 74(H·)100, 73(H ₂)18, 57(H ₂ O)6, 47(CO)61, 45(H ₂ + CO)15, 17(C ₂ H ₂ O ₂)4
HSCH ₂ CH ₂ S ⁻ (93) DSCH ₂ CH ₂ S ⁻ (94) HSCH ₂ CO ₂ ⁻ (91)	92(H·)12, 91(H ₂)3, 60(HS·)1, 59(H ₂ S)4, 58(H· + H ₂ S)3, 47(CH ₂ S)2, 46(H· + CH ₂ S)3, 33(C ₂ H ₄ S)100 93(H·)15, 92(H ₂ D·)8, 61(HS·)8, 60(H ₂ S, DS·)12, 59(HDS)9, 58(H ₂ DS)7, 48(CH ₂ S)6, 46(D· + CH ₂ S)7, 34(C ₂ H ₄ S)100, 33(C ₂ H ₃ DS)56 90(H·)100, 89(H ₂)15, 75(O·)78, 73(H ₂ O)54, 47(CO ₂)63, 46(HCO ₂ ·)12, 45(CH ₂ S)84
NH ₂ CH ₂ CH ₂ NH ⁻ (59) NH ₂ CH ₂ CO ₂ ⁻ (74)	58(H·)100, 57(H ₂)61, 42(NH ₃)46, 26(CH ₇ N)67 73(H·)100, 72(H ₂)12, 56(H ₂ O)4, 46(CO)8, 45(CH ₂ NH)9
CH ₃ SCH ₂ CH ₂ O ⁻ (91) CH ₃ SCH ₂ CO ₂ ⁻ (105)	90(H·)100, 89(H ₂)2, 73(H ₂ O)1, 61(CH ₂ O)2, 47(C ₂ H ₄ O)1 104(H·)50, 90(CH ₃ ·)63, 89(CH ₄)38, 61(CO ₂)100
CH ₃ OCH ₂ CH ₂ O ⁻ (75) CH ₃ OCH ₂ CO ₂ ⁻ (89) CD ₃ OCH ₂ CO ₂ ⁻ (92)	73(H ₂)86, 58(H ₂ + CH ₃ ·)13, 43(CH ₃ OH)3, 31(C ₂ H ₄ O)100 88(H·)100, 74(CH ₃ ·)85, 73(CH ₄)42, 58(CH ₃ O·)59, 45(C ₂ H ₄ O)5, 43(CH ₂ O ₂)4, 41(CH ₄ O ₂)2 31(CH ₂ CO ₂ ·), 29(C ₂ H ₄ O ₂ ·)1 91(H·)100, 90(D· + H ₂)84, 74(H ₂ O)83, 72-73 ^a (CD ₃ H)50, 58(CD ₃ O·)63, 45(C ₂ D ₃ HO)5, 34(CH ₂ CO ₂ ·)
CH ₃ NHCH ₂ CH ₂ O ⁻ (74) CH ₃ NHCH ₂ CO ₂ ⁻ (88)	72(H ₂)100 86(H ₂)23, 84(H ₂ + H ₂)18, 72(O·)14, 70(H ₂ O)9, 60(CO)100, 58(CH ₃ NH·)16, 45(C ₂ H ₅ N)54, 42(HCO ₂ H)8
(CH ₃) ₂ NCH ₂ CH ₂ O ⁻ (88) (CH ₃) ₂ NCH ₂ CO ₂ ⁻ (102) (CD ₃) ₂ NCH ₂ CO ₂ ⁻ (108)	86(H ₂)100 101(H·)100, 100(H ₂)30, 84(H ₂ O)65, 58((CH ₃) ₂ N·)51, 42(CH ₃ CO ₂ H)9 107(H·)100, 106(H ₂ + D·)45, 90(H ₂ O)61, 58((CD ₃) ₂ N·)52, 46(CH ₂ D _{CO} ₂ D)6

"a" denotes an unresolved peak

$$\begin{aligned} \text{E.A.}(\text{HXCH}_2^-) &= (\text{total energy of HXCH}_2^- + \text{zero point energy}) \\ &- (\text{total energy of HSCH}_2^- + \text{zero point energy}) \end{aligned} \quad (2.8)$$

The proton affinity of the hydroxymethylene anion can be calculated from equation 2.9 by substituting the computed energies for the most stable conformer of HOCH₂⁻ and neutral CH₃OH, each corrected for zero point energies.

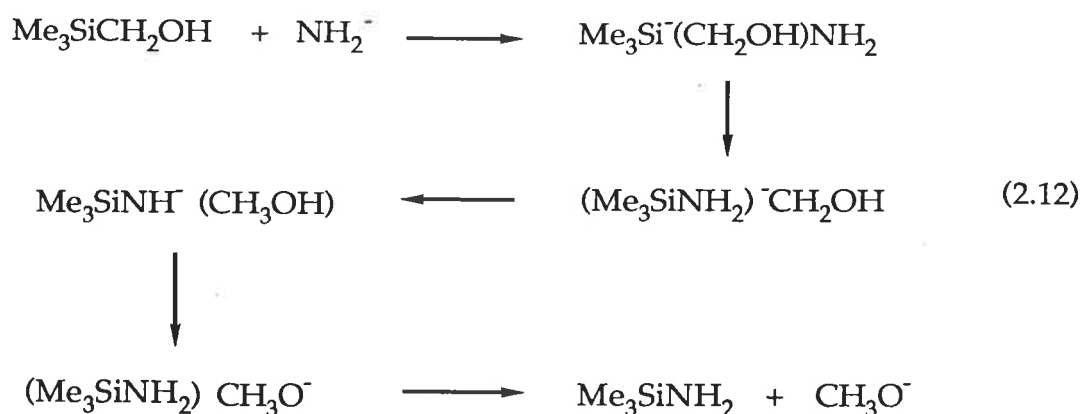
$$\begin{aligned} \Delta H_{\text{acid}}^{\circ}(\text{CH}_3\text{XH}) &= (\text{total energy of H}^+ + \text{total energy of HXCH}_2^- + \text{zero point energy}) \\ &- (\text{total energy of CH}_3\text{XH} + \text{zero point energy}) \end{aligned} \quad (2.9)$$

From equation 2.9, the proton affinity of HOCH₂⁻ was calculated to be 1730 kJ mol⁻¹. This value is considerably lower than that reported previously^{87,97}. This is believed to be a consequence of the higher level of theory used in calculations performed by Dr. John Sheldon.

2.2.2.2 The attempted formation of the hydroxymethylene anion

In accord with the predicted instability of HOCH₂⁻ to electron loss and its high basicity, attempts to directly detect the hydroxymethylene anion have failed. The C.A. mass spectrum of deprotonated glycolic acid (Table 2.4) shows no peak corresponding to carbon dioxide loss. It is instead dominated by losses corresponding to atomic hydrogen and carbon monoxide. The latter is thought to arise as shown in equation 2.10, i.e. the hydroxycarbonyl anion¹⁰⁹ acts as a hydroxyl anion donor within the ion complex.





Within the ion complex $[\text{Me}_3\text{SiNH}_2]^-\text{CH}_2\text{OH}$, the hydroxymethylene anion $[\Delta H^\circ_{\text{acid}}(\text{CH}_3\text{OH}) = 1730 \text{ kJ mol}^{-1}$; see above] deprotonates trimethylsilylamine $[\Delta H^\circ_{\text{acid}}(\text{Me}_3\text{SiNH}_2) = 1586 \text{ kJ mol}^{-1}$ ¹¹⁰] to yield Me_3SiNH^- solvated to methanol where subsequent deprotonation and dissociation yields methoxide ion and trimethylsilylamine.

In conclusion, the inability to detect the hydroxymethylene anion is in accord with: (i) the ion's predicted instability toward electron loss and (ii) its calculated basicity $[\Delta H^\circ_{\text{acid}}(\text{CH}_3\text{OH}) = 1730 \text{ kJ mol}^{-1}$; from above] which permits deprotonation of a suitably acidic solvated neutral within an ion complex as outlined above.

2.2.3 The methylene thiol anion

2.2.3.1 Theoretical considerations concerning the possible detection of the methylene thiol anion

The enhanced acidity of a C-H bond α to a sulphur atom compared to those of hydrocarbons has led to much debate. Several groups (in studies initiated independently^{87,88,97}) have questioned the importance of d-p π -bonding between the sulphur 3d-orbitals and the carbanion lone-pair. Indeed it has

been shown that the proton affinity of HSCH_2^- is unchanged whether or not d-type functions are included in the basis set.

The proton affinity of HSCH_2^- is calculated (using equation 2.9) to be 1669 kJ mol^{-1} . This value is in accord with a bracketing experiment carried out at Boulder (utilising the tandem flowing afterglow-S.I.F.T. instrument), which is discussed later (Section 2.2.3.3.1). The methylene thiol anion is calculated to be slightly less basic than amide ion [$\Delta H^\circ_{\text{acid}}(\text{NH}_3) = 1688 \text{ kJ mol}^{-1}$ ¹¹¹]. Nevertheless, proton abstraction of methane thiol with amide ion will occur preferentially on sulphur [$\Delta H^\circ_{\text{acid}}(\text{CH}_3\text{SH}) = 1493 \text{ kJ mol}^{-1}$ ¹¹²] and hence the experimental approaches outlined in Section 2.2.1 are required to enable the formation of the methylene thiol anion.

The methylene thiol anion is predicted to be stable to electron detachment. The electron affinity of radical $\text{HSCH}_2\cdot$ is obtained by substituting the total energies for the methylene thiol anion and radical (Tables 2.1 and 2.2) into equation 2.8. The *ab initio* calculations predict that the methylene thiol anion is more stable than its radical by 23 kJ mol^{-1} .

2.2.3.2 Formation of the methylene thiol anion

The experimental approach involved first recording the C.A. mass spectrum of deprotonated ethylene dithiol (Table 2.4). The spectrum shows a small peak at m/z 47 corresponding to the loss of thioformaldehyde whilst the C.A. spectrum of $\text{DSCH}_2\text{CH}_2\text{S}^-$ (Table 2.4) yields a peak at m/z 48 consistent with the formation of DSCH_2^- .

The C.A. mass spectrum of deprotonated thioglycolic acid (Table 2.4) shows a peak corresponding to carbon dioxide loss at m/z 47. The MS/MS/MS spectrum of this daughter ion produces a fragmentation pattern not dissimilar to that of isomeric MeS^- (Figure 2.1; Table 2.5), yet the charge reversal spectra are quite different (Figure 2.2; Table 2.6). The charge reversal

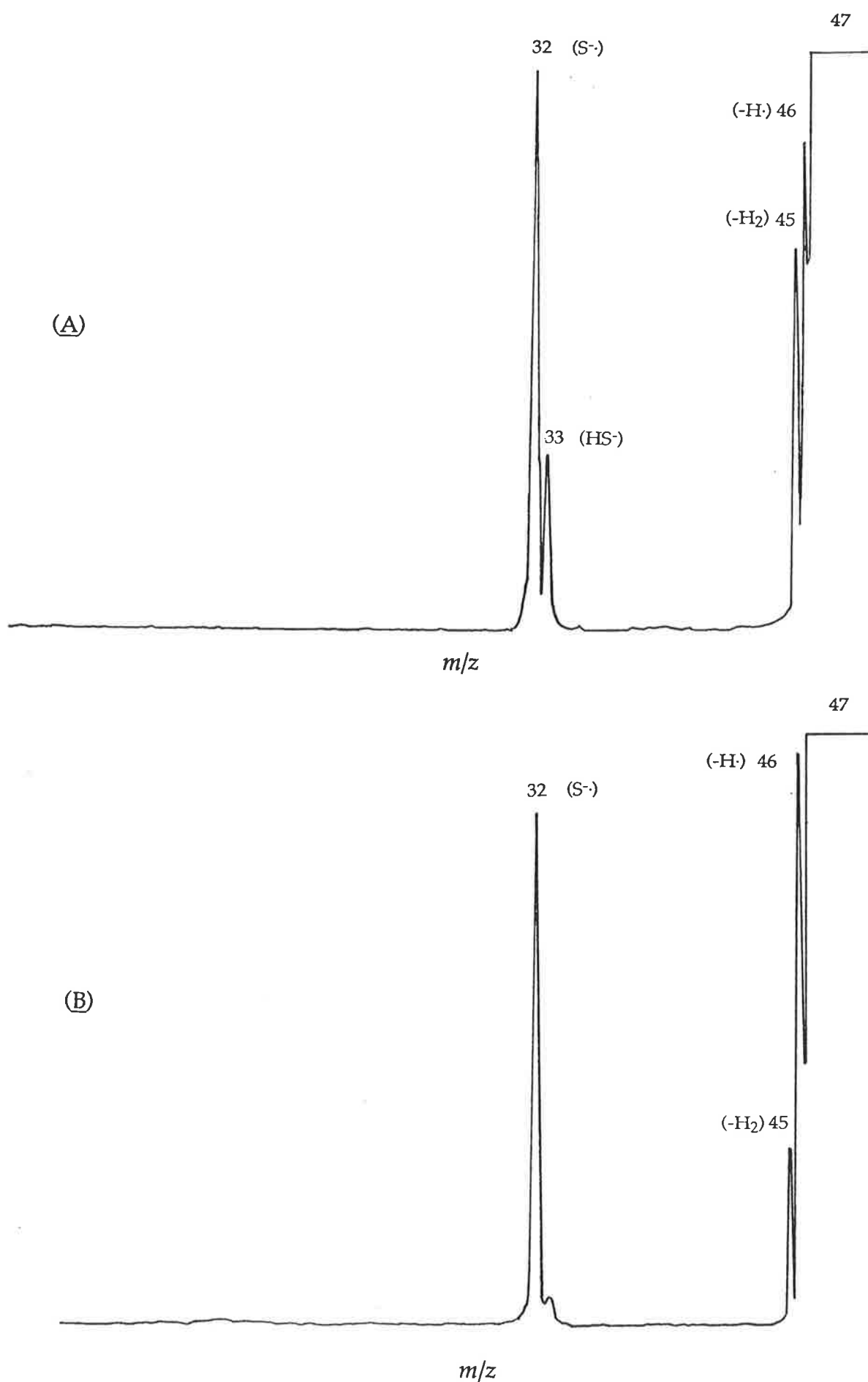


Figure 2.1 Collisional activation mass spectra of isomeric $^{-}\text{CH}_2\text{SH}$ (A) and CH_3S^{-} (B).

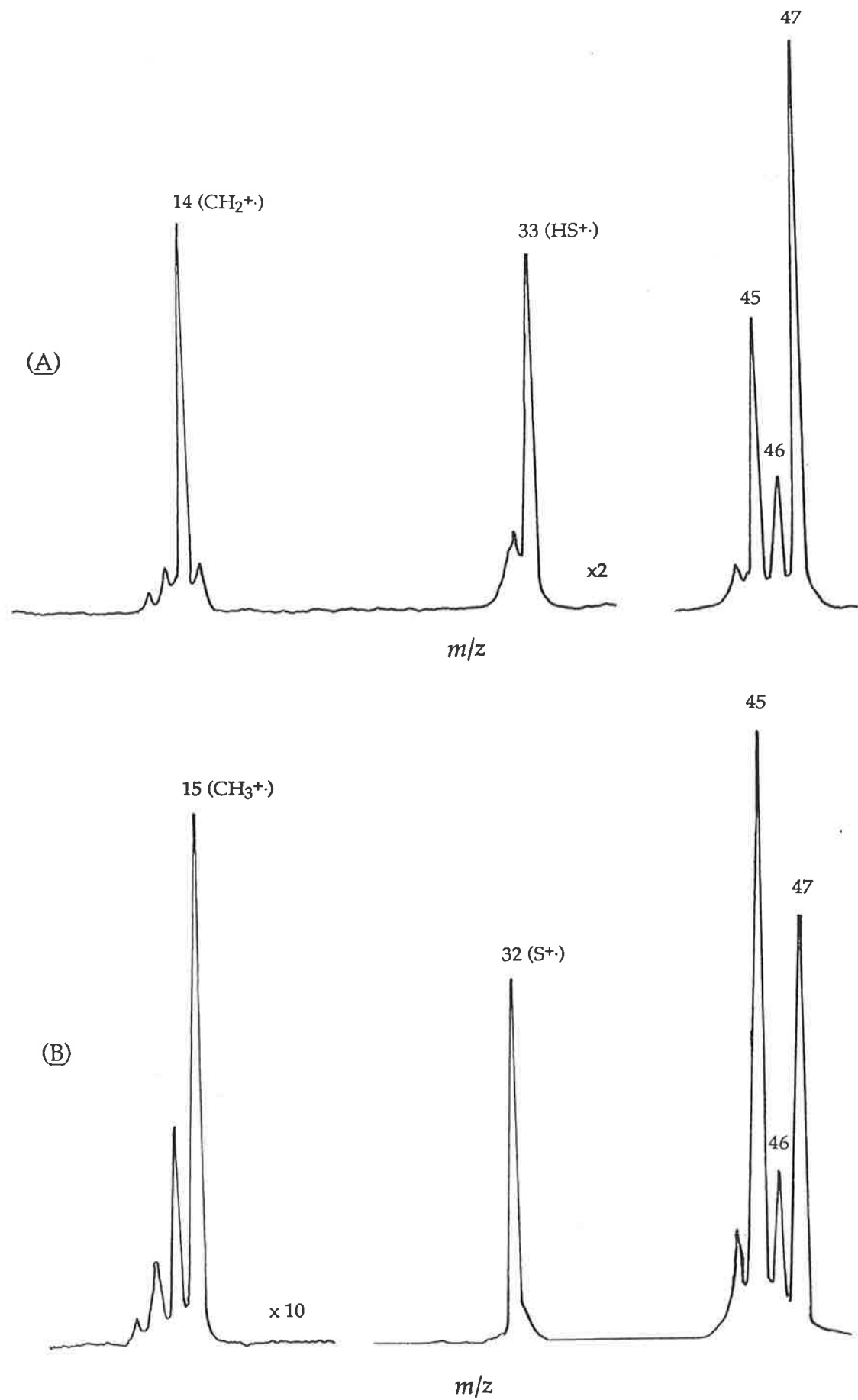


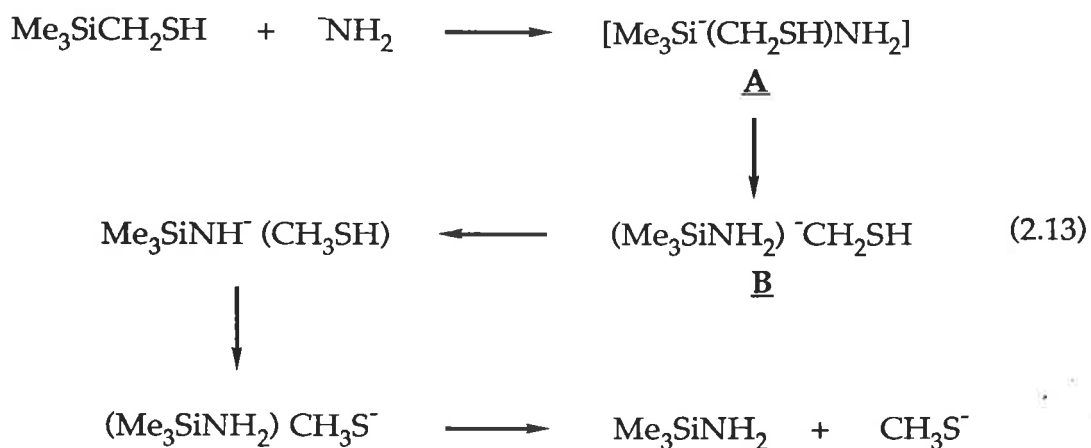
Figure 2.2 Charge reversal mass spectra of isomeric $^{-}\text{CH}_2\text{SH}$ (A) and CH_3S^{-} (B).

Table 2.5 Collisional activation mass spectra of the α -hetero-substituted carbanions RSCH_2^- ($\text{R} = \text{H}, \text{CH}_3$). A comparison with the mass spectral data of their isomeric ions.			
Ion (m/z)	Neutral Precursor	Spectrum type	Spectrum [m/z (loss) abundance in %]
HSCH_2^- (47)	$\text{HSCH}_2\text{CO}_2\text{H}$	CA MS/MS/MS ^a	46(H)81, 45(H ₂)63, 33(CH ₂)30, 32(CH ₃)100
CH_3S^- (47)	CH_3SSCH_3	CA MS/MS	46(H)100, 45(H ₂)29, 33(CH ₂)3, 32(CH ₃)92
$\text{CH}_3\text{SCH}_2^-$ (61)	$\text{Me}_3\text{SiCH}_2\text{SCH}_3$	CA MS/MS	59(H ₂)8, 46(CH ₃)100, 45(CH ₄)3, 33(C ₂ H ₄)2, 32(C ₂ H ₅)2
$\text{CH}_3\text{SCH}_2^-$ (61)	CH_3SCH_3	CA MS/MS	59(H ₂)5, 46(CH ₃)100, 45(CH ₄)6, 33(C ₂ H ₄)4, 32(C ₂ H ₅)4
$\text{CH}_3\text{CH}_2\text{S}^-$ (61)	$\text{CH}_3\text{CH}_2\text{SH}$	CA MS/MS	59(H ₂)56, 46(CH ₃)97, 45(CH ₄)11, 33(C ₂ H ₄)22, 32(C ₂ H ₅)100

^a MS/MS/MS spectra were recorded by Dr. R.N. Hayes using a Kratos MS-50 Triple Analyser mass spectrometer using operating conditions previously described.⁴⁸

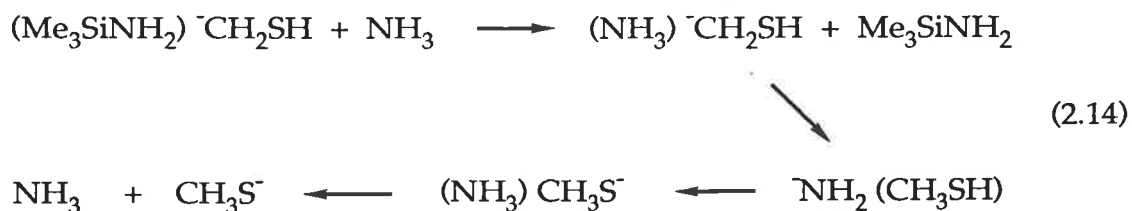
Table 2.6 Charge reversal mass spectra of the α -hetero-substituted carbanions RSCH_2^- ($\text{R} = \text{H}, \text{CH}_3$). A comparison with the mass spectral data of their isomeric ions.			
Ion (m/z)	Neutral Precursor	Spectrum type	Spectrum [m/z (abundance in %)]
HSCH_2^- (47)	$\text{HSCH}_2\text{CO}_2\text{H}$	CR MS/MS/MS	47(100), 46(22), 45(51), 33(31), 32(7), 15(4), 14(34), 13(4), 12(2)
CH_3S^- (47)	CH_3SSCH_3	CR MS/MS	47(68), 46(26), 45(100), 44(17), 33(6), 32(59), 15(9), 14(4), 13(1), 12(1)
$\text{CH}_3\text{SCH}_2^-$ (61)	$\text{Me}_3\text{SiCH}_2\text{SCH}_3$	CR MS/MS	61(12), 59(10), 58(10), 57(6), 47(13), 46(53), 45(100), 44(12), 35(26), 34(1), 33(1), 32(4), 27(21), 26(17), 15(3), 14(3)
$\text{CH}_3\text{SCH}_2^-$ (61)	CH_3SSCH_3	CR MS/MS	61(14), 60(1), 59(11), 58(11), 57(5), 56(1), 47(15), 46(50), 45(100), 44(12), 35(29), 34(2), 33(2), 32(3), 27(20), 26(14), 15(3), 14(3)
$\text{CH}_3\text{CH}_2\text{S}^-$ (61)	$\text{CH}_3\text{CH}_2\text{SH}$	CR MS/MS	61(52), 60(7), 59(29), 58(28), 57(14), 56(2), 46(25), 45(100), 44(21), 35(52), 34(3), 33(9), 32(38), 29(13), 28(7), 27(43), 26(11), 25(3), 15(1)

spectrum of MeS^- [generated by nucleophilic displacement from $(\text{MeS})_2$] shows fragment ions Me^+ (m/z 15) and S^+ (m/z 32). In contrast, the m/z 47 ion from $\text{HSCH}_2\text{CO}_2^-$ gives ions CH_2^+ (m/z 14) and HS^+ (m/z 33) substantiating the formation of the methylene thiol anion by equation 2.5. The $\text{S}_{\text{N}}2(\text{Si})$ reaction between trimethylsilyl-methylmercaptan and amide ion produces a pronounced peak at m/z 47 ion in the source of the mass spectrometer. However the C.A. and C.R. spectra of this ion identify it as MeS^- . In addition, the reaction of $\text{Me}_3\text{SiCH}_2\text{SD}$ and amide ion produces an ion at m/z 47, not 48. These results are best rationalised through the reaction sequence shown in equation 2.13.



Nucleophilic addition to silicon produces the penta-coordinate complex A which collapses to B. Within this solvated ion complex, HSCH_2^- [$\Delta H^\circ_{\text{acid}}(\text{CH}_3\text{SH}) = 1669 \text{ kJ mol}^{-1}$; see above] deprotonates Me_3SiNH_2 [$\Delta H^\circ_{\text{acid}}(\text{Me}_3\text{SiNH}_2) = 1586 \text{ kJ mol}^{-1}$ ¹¹⁰]. Subsequent deprotonation of MeSH [$\Delta H^\circ_{\text{acid}}(\text{MeSH}) = 1493 \text{ kJ mol}^{-1}$ ¹¹²] at sulphur followed by dissociation of the complex affords MeS^- .

An alternative mechanism involving the solvation of HSCH_2^- to a non-ionised ammonia molecule in the ion source is represented in equation 2.14.



This pathway appears less likely based on the relatively low probability of a three body reaction, despite the high concentration of ammonia in the ion source compared with that of the silyl parent. Secondly, deprotonation of ammonia by HSCH_2^- within the first solvated ion complex should be unfavourable based on known acidities. Nevertheless, the energy typically retained on ion-molecule complex formation of up to 85 kJ mol^{-1} ⁶³ does not enable this mechanism to be ruled out.

2.2.3.3 The reactivity of the methylene thiol anion

The successful generation of the methylene thiol anion through a process represented in equation 2.5 prompted a study of its reactivity (Tables 2.7 and 2.8) utilising the tandem flowing afterglow-S.I.F.T. at Boulder. During the course of this work, Kass reported some reactions of the methylene thiol anion¹¹³ using a variable temperature flowing afterglow. Whilst the results presented in this thesis largely mirror those of Kass, some differences exist.

The methylene thiol anion was produced in the flowing afterglow-S.I.F.T. by an identical procedure to that discussed above (Section 2.2.3.2). Deprotonation of thioglycolic acid with hydroxide ion (from the ionisation of N_2O and CH_4 ¹¹⁴) in the first flow tube afforded an $(\text{M} - \text{H}^+)^-$ (m/z 91) which was injected cleanly into the second flow tube by means of the S.I.F.T. quadrupole. Collision-induced dissociation of this ion results in decarboxylation of the parent to afford the methylene thiol anion HSCH_2^- .

Table 2.7 Reactions of HSCH_2^- with hydrogen containing compounds. Products and branching ratios.		
Neutral	Products ^a	Branching Ratios
C_6H_6	-	-
C_6D_6	-	-
D_2O	$\text{CH}_2\text{DS}^- + \text{HOD}$ $\text{DO}^- + \text{CH}_2\text{DSH}$	0.97 0.03
$\text{CH}_2=\text{CHCH}_3$	$\text{CH}_3\text{S}^- + \text{CH}_2=\text{CHCH}_3$	1.0
CH_3NO_2	$^-\text{CH}_2\text{NO}_2 + \text{CH}_3\text{SH}$	1.0
$\text{CH}_2=\text{CHCHO}$	$\text{HS}^- + (\text{C}_4\text{H}_6\text{O})^b$ $(\text{C}_3\text{H}_5\text{O})^- + \text{CH}_2\text{S}$ $^-\text{CH}_2\text{CHO} + \text{C}_2\text{H}_4\text{S}$	0.75 0.15 0.10
CH_3Cl	$\text{Cl}^- + \text{CH}_3\text{CH}_2\text{SH}$	1.0

"a" Neutral product structures rationalised through plausible mechanisms.

"b" Structure of neutral unknown.

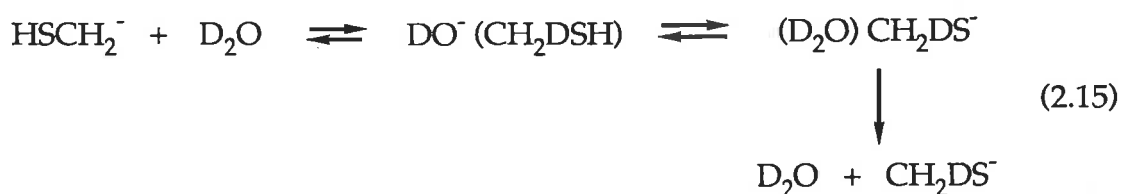
Table 2.8 Reactions of HSCH ₂ ⁻ with non-hydrogen containing compounds. Products and branching ratios.		
Neutral	Products ^a	Branching Ratios
N ₂ O ^b	HN ₂ O ⁻ + CH ₂ S	0.70
	HO ⁻ + CH ₂ S + N ₂	0.20
	HS ⁻ + (CH ₂ N ₂ O)	0.10
CS ₂	HCS ₂ ⁻ + CH ₂ S	0.95
	HS ⁻ + CH ₂ S + CS	0.05
COS	HSCH ₂ S ⁻ + CO	0.45
	HS ⁻ + CH ₂ S + CO	0.38
	⁻ SCH=C=O + H ₂ S	0.12
	HCOS ⁻ + CH ₂ S	0.05
SO ₂	SO ₂ ⁻ + HSCH ₂ ⁻	0.65
	HSO ₂ ⁻ + CH ₂ S	0.25
	HSCH ₂ SO ₂ ⁻	0.10
CO ₂	HSCH ₂ CO ₂ ⁻	0.93 ^c
	HCO ₂ ⁻ + CH ₂ S	0.07
O ₂	HCOS ⁻ + H ₂ O	0.45
	HO ₂ ⁻ + CH ₂ S	0.40
	O ₂ ⁻ + HSCH ₂ ⁻	0.15

"a" Neutral product structures rationalised through plausible mechanisms.
 "b" Reaction rate constant of $6.23 \times 10^{-11} \text{ cm}^3 \text{ molecule}^{-1} \text{ sec}^{-1}$. "c"
 Approximate branching ratio only. Parent and product ions have the same structure.

2.2.3.3.1 Experimental determination of the proton affinity of HSCH₂⁻

To find support for the theoretical proton affinity of HSCH₂⁻ [$\Delta H^{\circ}_{\text{acid}}(\text{CH}_3\text{SH}) = 1669 \text{ kJ mol}^{-1}$, Section 2.2.3], bracketing experiments were carried out.

The methylene thiol anion was observed to undergo no reaction with benzene [$\Delta H^{\circ}_{\text{acid}}(\text{C}_6\text{H}_6) = 1676 \text{ kJ mol}^{-1}$ ¹¹⁵] (Table 2.7) and hence the acidity of benzene represents an upper limit for the value of $\Delta H^{\circ}_{\text{acid}}(\text{CH}_3\text{SH})$. Determination of a lower limit for the proton affinity measurement, however, is complicated by the presence of an acidic proton on sulphur. Reaction with D₂O [$\Delta H^{\circ}_{\text{acid}}(\text{D}_2\text{O}) = 1644 \text{ kJ mol}^{-1}$ ¹¹⁶] produces an ion at m/z 48, together with only a trace of DO⁻ (m/z 18) (Table 2.7). This is consistent with the exchange process shown in equation 2.15



Indeed, any gas-phase acid with an acidity less than $\Delta H^{\circ}_{\text{acid}}(\text{CH}_3\text{SH})$, but greater than $\Delta H^{\circ}_{\text{acid}}(\text{CH}_3\text{SH}) = 1494 \text{ kJ mol}^{-1}$, should produce no conjugate base in the spectrum. For example, reaction with propene [$\Delta H^{\circ}_{\text{acid}}(\text{CH}_2=\text{CHCH}_3) = 1621 \text{ kJ mol}^{-1}$ ¹¹⁷] produces no ion corresponding to $\text{CH}_2=\text{CHCH}_2^-$ (m/z 41). However, reaction with nitromethane [$\Delta H^{\circ}_{\text{acid}}(\text{CH}_3\text{NO}_2) = 1491 \text{ kJ mol}^{-1}$ ¹¹²] affords $^-\text{CH}_2\text{NO}_2$ (m/z 60) (Table 2.7).

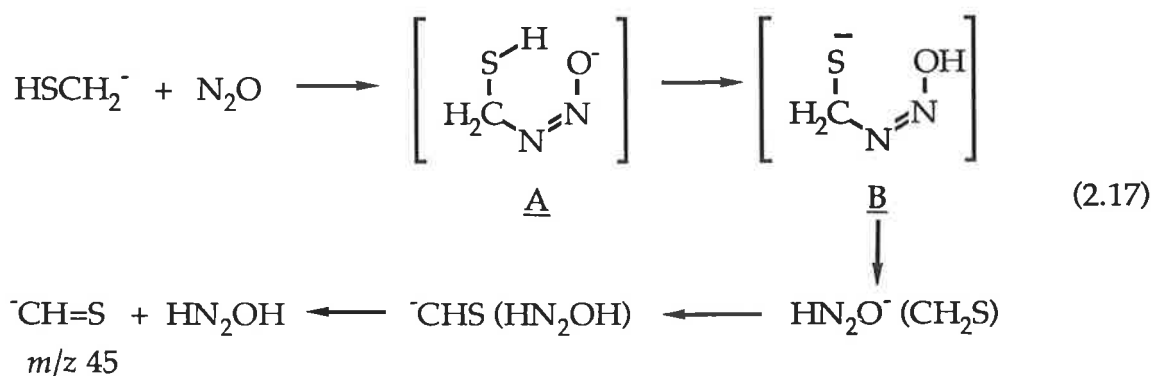
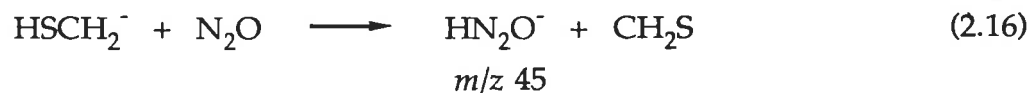
To ascertain that a similar mechanism did not operate for the reaction with benzene, HSCH₂⁻ was allowed to react with hexadeuterobenzene. No ion corresponding to CH₂DS⁻ (m/z 48) was detected. Thus, the $\Delta H^{\circ}_{\text{acid}}$ value of CH₃SH is between that of benzene and deuterium oxide, i.e. $1661 \pm 17 \text{ kJ}$

mol⁻¹, in good agreement with the theoretical value of 1669 kJ mol⁻¹ obtained above.

2.2.3.3.2 Reactions of HSCH₂⁻ involving hydride ion transfer

The reactivity of HSCH₂⁻ is dominated by its propensity to form hydride addition products. The ion HSCH₂⁻ donates hydride ion to nitrous oxide, carbon disulphide, carbonyl sulphide, carbon dioxide, sulphur dioxide, oxygen (Table 2.8) and acrolein (Table 2.7), although the relative extent of hydride transfer differs for each reaction. The reaction of the methylene anion with each of these reagents is now discussed.

The methylene thiol anion reacts with nitrous oxide ($k = 6.23 \times 10^{-11} \text{ cm}^3 \text{ molecule}^{-1} \text{ sec}^{-1}$) resulting in the formation of a major product ion at m/z 45. In principle, this product could arise by a hydride transfer to yield HN₂O⁻ (equation 2.16) or from the formation of ⁻CH=S (equation 2.17) since both product ions exhibit the same mass to charge ratio.

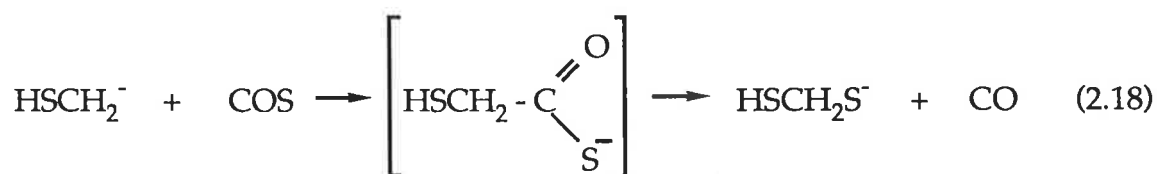


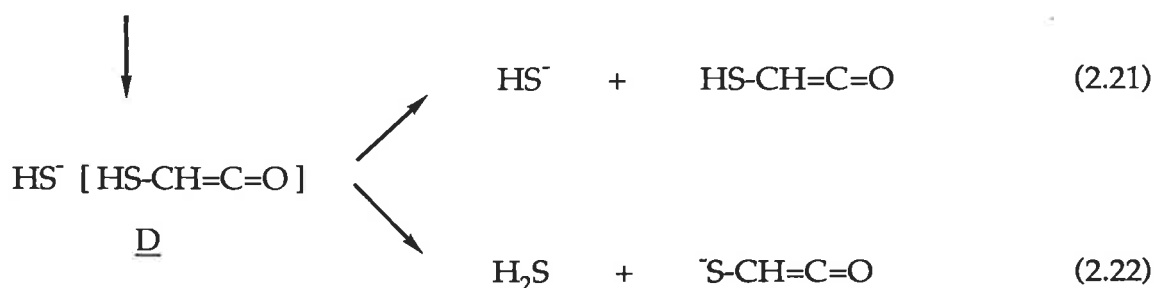
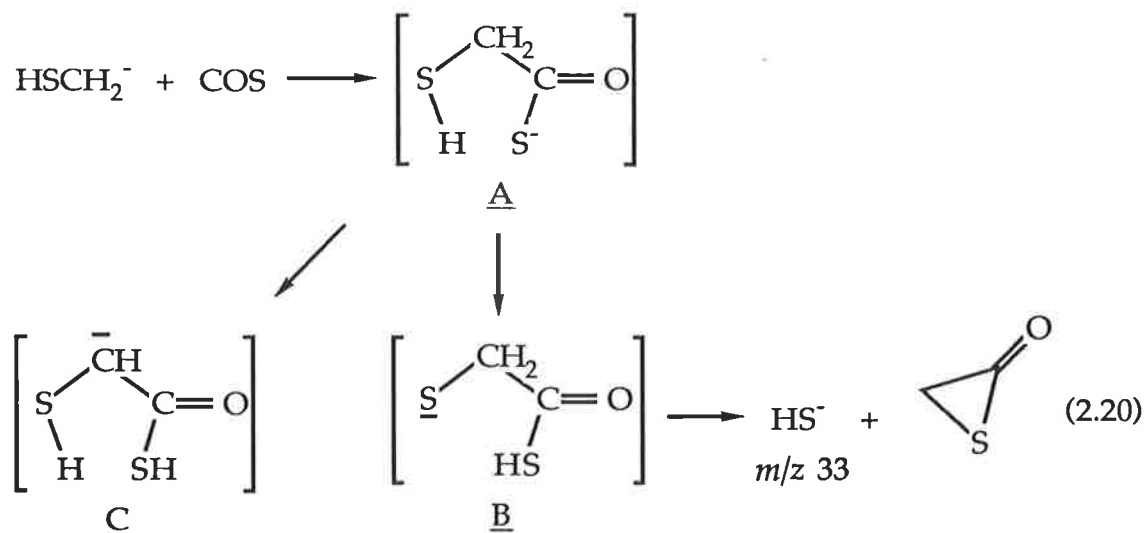
The reaction of DSCH₂⁻ with N₂O, however, has been shown¹¹³ to afford a major product ion at m/z 46. This observation is consistent with the formation of DN₂O⁻ through a deuteride ion transfer. The proton transfer

process in intermediate A (equation 2.17) will result (on dissociation of intermediate B) in unlabelled product ion $^{-}\text{CH}=\text{S}$ whose m/z value is unchanged.

Hydride ion donation to nitrous oxide has been observed previously,^{118,119} whilst another study has reported the formation of $(\text{HN}_2\text{O})^{-}$ via a different route.¹²⁰ Despite this, an investigation of the properties and reactivity of the $(\text{HN}_2\text{O})^{-}$ ion has not been undertaken. Subsequently, such a study was undertaken, the results of which are presented in Chapter 3.

Whilst the reaction of the methylene thiol anion with carbon disulphide is dominated by the formation of hydride addition product HCS_2^{-} (m/z 77), its reaction with carbonyl sulphide affords HCOS^{-} (m/z 61) as only a minor product. The major products in the reaction with COS correspond to HS^{-} (m/z 33) and $\text{HSCH}_2\text{S}^{-}$ (m/z 78). The latter product was not reported by Kass.¹¹³ Clearly, this product ion is the result of an efficient sulphur transfer reaction to HSCH_2^{-} (equation 2.18). Carbonyl sulphide has been previously reported to be an effective sulphur transfer reagent^{121,122} with the loss of stable carbon monoxide believed to be a driving force for this process.





The product ion HS^- (m/z 33) could be produced from the reaction of HSCH_2^- with COS by several pathways. Whilst HS^- could be produced by the elimination of thioformaldehyde from HSCH_2S^- (equation 2.19), it appears more likely (based on the branching ratio of HS^- for this reaction) that HS^- is produced from the collapse of either of two intermediates B and C (equations 2.20, 2.21 and 2.22). These intermediates result from internal proton transfer reactions within adduct A. The occurrence of minor amounts of product ion S-CH=C=O^- (m/z 73) (equation 2.22) in the reaction substantiates the intermediacy of complex D.

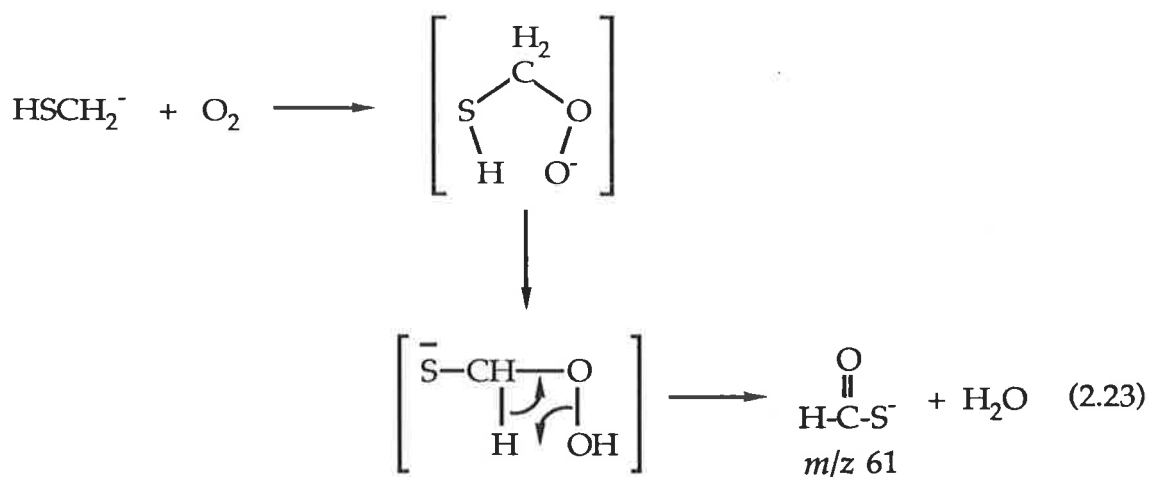
The reaction of HSCH_2^- with carbon dioxide produces small amounts of hydride addition product HCO_2^- (m/z 45). The major pathway for this reaction produces adduct $\text{HSCH}_2\text{CO}_2^-$ (m/z 91). This product is produced by the reverse reaction employed to generate the methylene anion, namely a carboxylation reaction. Whilst the reaction to form the adduct must require

only a small energy of activation, the reverse reaction obviously has a significant kinetic barrier as evident by the collisional activation conditions required to produce HSCH_2^- . However, even under collisional activation conditions, $\text{HSCH}_2\text{CO}_2^-$ undergoes only partial decomposition to generate the methylene thiol anion. As a result, the ratio of HSCH_2^- to $\text{HSCH}_2\text{CO}_2^-$ in the second flow tube before reaction with CO_2 was at best 3:2. An increase in this ratio in favour of $\text{HSCH}_2\text{CO}_2^-$ upon reaction with CO_2 is consistent with adduct formation though the relative extent of adduct formation vs. hydride transfer could only be estimated in this case.

With sulphur dioxide, the methylene thiol anion reacts primarily by an electron transfer process to afford product ion SO_2^- (m/z 64). Some hydride addition product HSO_2^- (m/z 65) is again detected together with minor amounts of adduct $\text{HSCH}_2\text{SO}_2^-$ (m/z 111). The detection of an electron transfer product suggests that the electron affinity of the methylene thiol radical is less than that of sulphur dioxide ($E.A.(\text{SO}_2) = 107 \text{ kJ mol}^{-1}$ ¹²³).

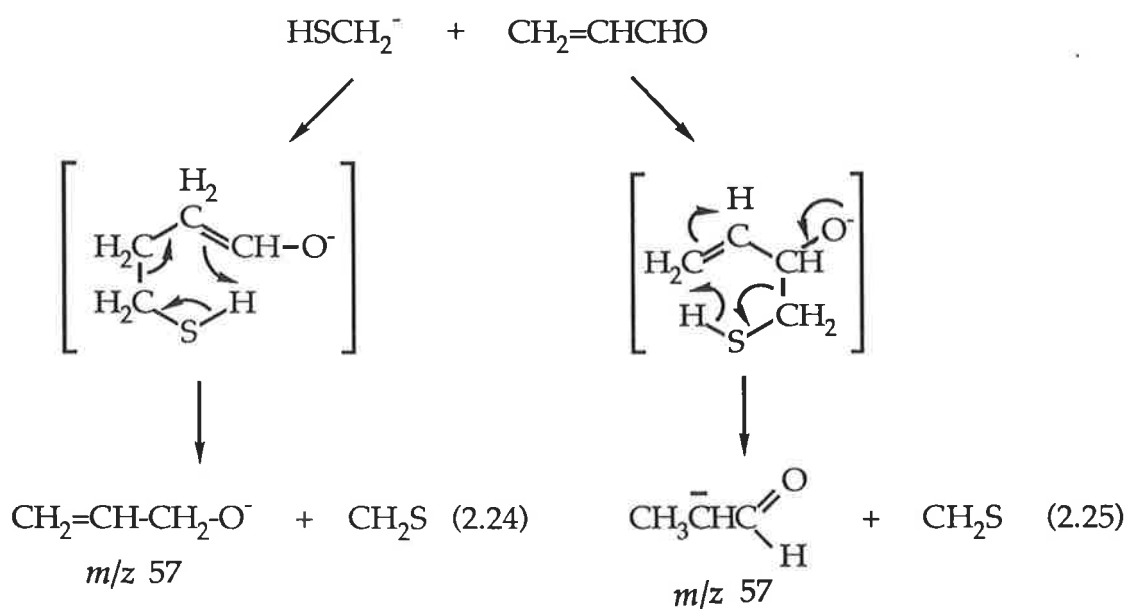
A further refinement on the upper limit for the electron affinity of HSCH_2^- was made following the reaction of HSCH_2^- with oxygen. This reaction produces electron transfer product O_2^- (m/z 32). Since no electron transfer process was observed between the reaction of HSCH_2^- and N_2O , the electron affinity of the HSCH_2^- radical is between that of oxygen (44 kJ mol^{-1} ¹²⁴) and nitrous oxide (21 kJ mol^{-1} ¹²⁵) in agreement with that calculated above (23 kJ mol^{-1} , Section 2.2.3.1).

The reaction of HSCH_2^- and oxygen is dominated by the formation of the hydroperoxy anion HO_2^- (m/z 33) (via a hydride transfer reaction) in addition to a product at m/z 61 rationalised plausibly by Kass to be HCOS^- ¹¹³(equation 2.23).



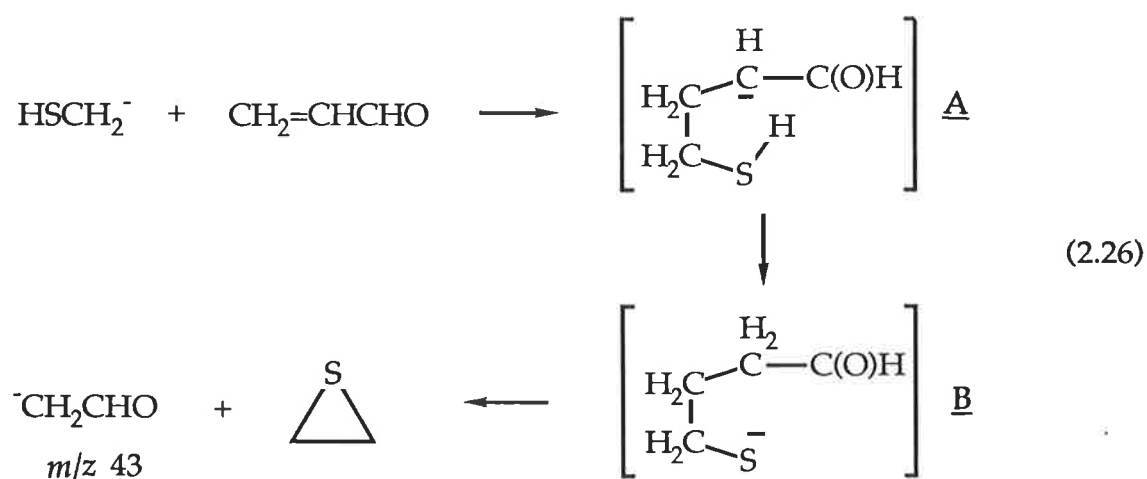
Recent interest in the reactions of carbanions with activated olefins,¹²⁶ prompted the reactivity of HSCH_2^- with acrolein to be investigated.

Consistent with its reported behaviour above, the methylene thiol anion was observed to undergo a hydride transfer to acrolein. In this instance, hydride ion transfer could be envisaged to proceed in a 1,2 or a 1,4-addition, a consequence of initial 1,4- or 1,2-nucleophilic attack by HSCH_2^- to acrolein respectively (equations 2.24 and 2.25).

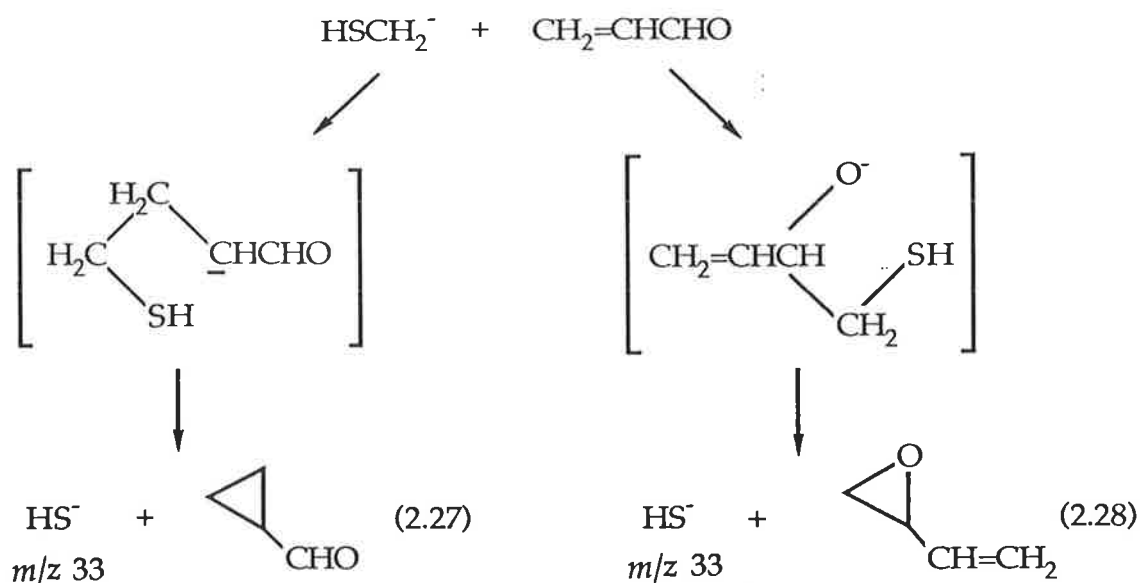


Two distinct product ions are produced, namely the allyloxy ion (by initial 1,4-attack of HSCH_2^-) (equation 2.24) and deprotonated propionaldehyde (by 1,2-addition) (equation 2.25).

The formation of a minor reaction product ion $^-\text{CH}_2\text{CHO}$ at m/z 43 is consistent with some 1,4-addition of HSCH_2^- to acrolein. Initial 1,4-nucleophilic attack is followed by a proton transfer from sulphur to carbon. Subsequent collapse of intermediate B will afford the acetaldehyde enolate ion (equation 2.26).



The major product of the reaction between HSCH_2^- and acrolein is HS^- (m/z 33). This product is plausibly formed following the insertion of a methylene group into either the carbon-carbon or carbon-oxygen double bond of acrolein (equations 2.27, 2.28).



A similar methylene insertion reaction has been suggested for the reaction of deprotonated nitromethane and acrolein.¹²⁶ Presumably such a reaction is facilitated since both HS^- and NO_2^- act as good leaving groups.

2.2.3.4 Thermochemistry of the methylene thiol anion

The propensity of HSCH_2^- to undergo hydride transfer reactions is reflected in the low hydride affinity of thioformaldehyde at sulphur. The hydride affinity of CH_2S at sulphur may be determined from equation 2.29 using known heats of formation of thioformaldehyde (105 kJ mol^{-1} ¹²⁷) and hydride ion (145 kJ mol^{-1} ¹²⁷) and a calculated value for the methylene thiol anion.

$$\text{H.A.}(\text{CH}_2=\text{S}) = \Delta H_f^\circ(\text{CH}_2=\text{S}) + \Delta H_f^\circ(\text{H}^-) - \Delta H_f^\circ(\text{CH}_2\text{SH}) \quad (2.29)$$

Substituting known heats of formation of CH_3SH (-23 kJ mol^{-1} ¹²⁷) and H^+ (1530 kJ mol^{-1} ¹²⁷), together with the theoretical proton affinity of HSCH_2^- (1669 kJ mol^{-1}) in equation 2.30, enables the heat of formation of HSCH_2^- to be assigned a value of 116 kJ mol^{-1} .

$$\Delta H_f^\circ(\text{CH}_2\text{SH}^-) = \Delta H_f^\circ(\text{CH}_3\text{SH}) - \Delta H_f^\circ(\text{H}^+) + \Delta H_{\text{acid}}^\circ(\text{CH}_3\text{SH}) \quad (2.30)$$

The hydride affinity of CH_2S at sulphur is hence determined to be 134 kJ mol^{-1} . This value is in accord with the observation that HSCH_2^- hydride transfers to N_2O ($\text{H.A.}(\text{N}_2\text{O}) \approx 154 \text{ kJ mol}^{-1}$ ¹¹³) but not benzene ($\text{H.A.}(\text{C}_6\text{H}_6) = 95 \text{ kJ mol}^{-1}$ ¹²⁸).

In a similar manner, the hydride affinity of thioformaldehyde at carbon is determined to be 309 kJ mol^{-1} (equation 2.31).



Thus, thioformaldehyde binds hydride ion at carbon more strongly than at sulphur accounting for the difference in reactivity of isomeric CH_2SH^- and CH_3S^- . Unlike its isomer, CH_3S^- undergoes no reaction with N_2O and O_2 , and produces only adducts upon reaction with CS_2 , COS , CO_2 and SO_2 .⁷⁴

2.2.4 The amino methylene anion

2.2.4.1 Theoretical considerations concerning the possible detection of the amino methylene anion

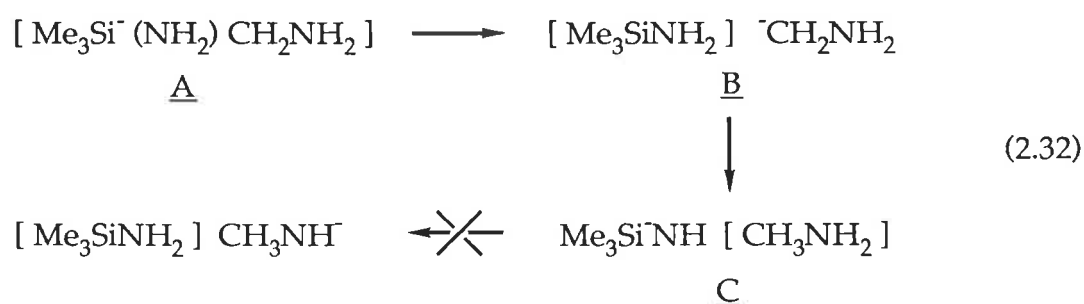
Unlike its analogues the hydroxymethylene and methylene thiol, the amino methylene anion has been calculated to adopt a single stable conformer of the gauche form (Table 2.1). From total energies of neutral CH_3NH_2 and the amino methylene anion, corrected for zero point energies, the proton affinity of the latter was determined to be 1749 kJ mol^{-1} (equation 2.9). This value predicts NH_2CH_2^- to be amongst the strongest gas phase bases known; it is only slightly less basic than the ethyl anion [$\Delta H_{\text{acid}}^\circ(\text{CH}_3\text{CH}_3) = 1761 \text{ kJ}$

mol^{-1} ⁷⁰]. Like the ethyl anion, however, the amino methylene anion is predicted to be unstable with respect to electron loss. Using the calculated value for the total energy of radical $\text{NH}_2\text{CH}_2\cdot$ (Table 2.2), its electron affinity was calculated from equation 2.8 to be -68 kJ mol^{-1} .

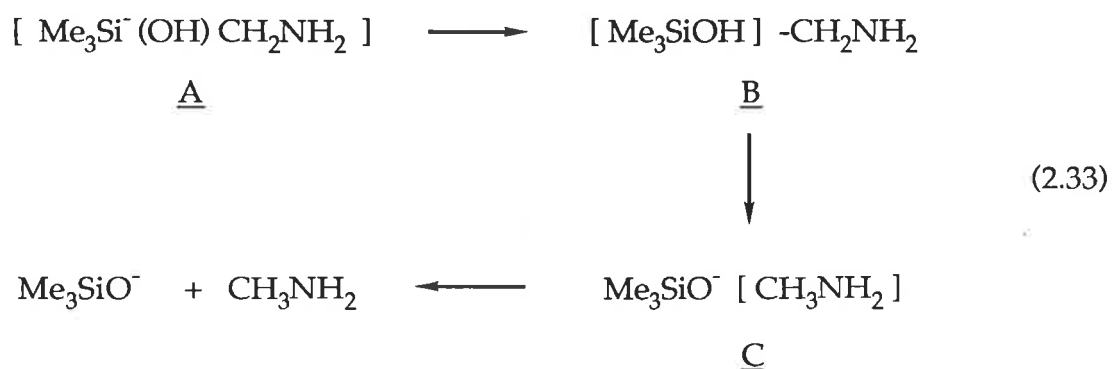
2.2.4.2 The attempted gas phase formation of the amino methylene anion

Each of the three experimental approaches for the direct generation of NH_2CH_2^- proved unsuccessful. The collisional activation mass spectrum of deprotonated 1,2-diaminoethane (Table 2.4) shows no ion at m/z 30. The spectrum is dominated by losses of atomic and molecular hydrogen and ammonia. Similarly, deprotonated glycine produces no ion corresponding to NH_2CH_2^- (m/z 30) in its C.A. spectrum (Table 2.4). The loss of carbon monoxide in this spectrum has been explained elsewhere.¹²⁹

The reaction of α -trimethylsilyl-methylamine with amide ion also affords no ion at m/z 30. Unlike the case for the hydroxymethylene anion, isomeric MeNH^- (m/z 30) is not observed here, a consequence of the unfavourable proton transfer step [$\Delta H^\circ_{\text{acid}}(\text{MeNH}_2) = 1686 \text{ kJ mol}^{-1}$ ¹¹¹, $\Delta H^\circ_{\text{acid}}(\text{Me}_3\text{SiNH}_2) = 1586 \text{ kcal mol}^{-1}$ ¹¹⁰] within complex C of the reaction sequence illustrated in equation 2.32.



The reaction between α -trimethylsilyl-methylamine and hydroxide ion, however, does produce Me_3SiO^- (m/z 89), a product best rationalised through the pathway shown in equation 2.33. This reaction supports the transient existence of NH_2CH_2^- within an ion-dipole (or ion-induced dipole) complex B.



The study of α -substituted carbanions is now extended to explore the effect of alkyl substitution on the heteroatom. Specifically, the formation of methyl heteroatom-substituted carbanions $\text{CH}_3\text{XCH}_2^-$ ($\text{X} = \text{O}, \text{S}, \text{NH}, \text{NCH}_3$) has been attempted through the approaches discussed in Section 2.2.1.

Lehn and Wipff⁸⁸ have reported that stabilisation of carbanions XCH_2^- increases along the series of substituents $\text{X} = \text{OH}, \text{OCH}_3, \text{SH}, \text{SCH}_3$. The enhanced stabilisation of an α -substituted carbanion upon alkyl substitution at the heteroatom was attributed to the increased polarisability of X-CH_3 over an X-H group. As a result, carbanions $\text{CH}_3\text{XCH}_2^-$ should be less basic than their non-heterosubstituted analogues HXCH_2^- . This, together with the ineffectual isomerisation of the ions $\text{CH}_3\text{OCH}_2^-$ and $\text{CH}_3\text{SCH}_2^-$ by a proton transfer mechanism, may facilitate their direct detection.

2.2.5 The methylthiomethylene anion

2.2.5.1 Theoretical considerations concerning the possible detection of the methylthiomethylene anion

Moran and Ellison¹³⁰ have recently reported the electron affinity of the radical $\text{CH}_3\text{SCH}_2\cdot$ to be 84 kJ mol^{-1} (0.87 eV). Using this value and the reported C-H bond strength (402 kJ mol^{-1} ¹³¹), the proton affinity of $\text{CH}_3\text{SCH}_2^-$ is calculated to be 1630 kJ mol^{-1} from equation 2.34. The slightly lower proton affinity of $\text{CH}_3\text{SCH}_2^-$ compared with HSCH_2^- [$\Delta H^\circ_{\text{acid}}(\text{CH}_3\text{SH}) = 1669 \text{ kJ mol}^{-1}$, Section 2.2.3.1] reflects the higher polarisability of substituent SCH_3 over SH . This value is in reasonable agreement with that reported by Nibbering and Ingemann¹³² ($\Delta H^\circ_{\text{acid}}(\text{CH}_3\text{SCH}_3) = 1645 \pm 8 \text{ kJ mol}^{-1}$) who produced the carbanion $\text{CH}_3\text{SCH}_2^-$ by the reaction of dimethylsulphide and amide ion in an F.T. I.C.R. spectrometer. The previous detection of $\text{CH}_3\text{SCH}_2^-$ enabled the applicability of the experimental approaches employed (Section 2.2.1) to be assessed.

$$\Delta H^\circ_{\text{acid}}(\text{CH}_3\text{SCH}_3) = \text{B.D.E.}(\text{H}-\text{CH}_2\text{SCH}_3) + \text{I.P.}(\text{H}^-) - \text{E.A.}(\cdot\text{CH}_2\text{SCH}_3) \quad (2.34)$$

2.2.5.2 The formation of the methylthiomethylene anion

The C.A. mass spectrum of deprotonated 2-methylthio-ethanol (Table 2.4) exhibits a peak at m/z 61 consistent with the formation of $\text{CH}_3\text{SCH}_2^-$ by a process shown in equation 2.4. Similarly, the C.A. spectrum of deprotonated methyl-thioglycolic acid is dominated by the loss of carbon dioxide (m/z 61) (Table 2.4). The reaction between α -methylthio-methyltrimethylsilane and amide ion produces an ion in the source of the mass spectrometer whose

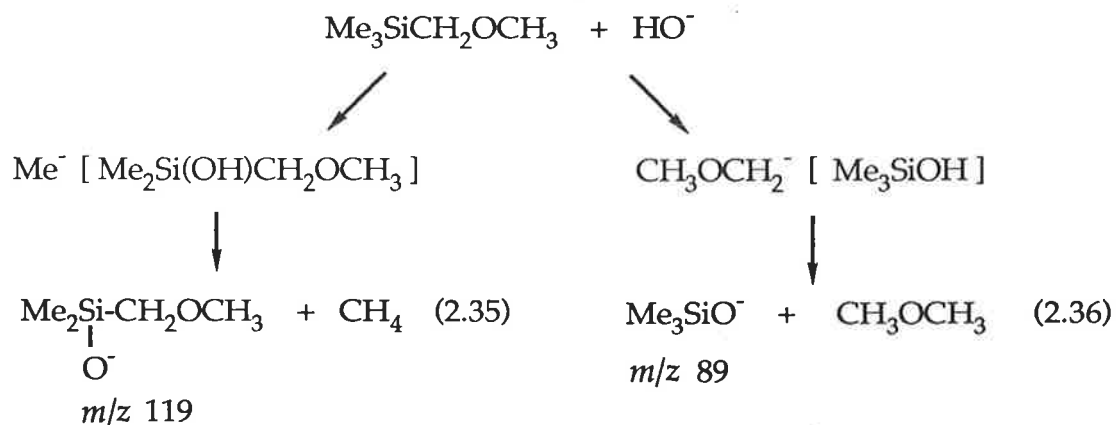
C.A. and C.R. spectra are identical (within experimental error) with those of authentic $\text{CH}_3\text{SCH}_2^-$ (formed from the reaction between amide ion and dimethylsulphide) (Tables 2.5 and 2.6).

Both the C.A. and C.R. spectra differ considerably from those of the ethyl sulphide ion prepared by the deprotonation of ethanethiol in the ion source. The C.A. spectrum of $\text{CH}_3\text{CH}_2\text{S}^-$ (Table 2.5) shows a base peak corresponding to the loss of ethyl radical (m/z 32) whilst the same peak represents only a minor fragmentation product in the C.A. spectrum of $\text{CH}_3\text{SCH}_2^-$ (Table 2.5). Similarly, whilst the C.R. mass spectra of $\text{CH}_3\text{SCH}_2^-$ and $\text{CH}_3\text{CH}_2\text{S}^-$ (Table 2.6) both exhibit base peaks due to the loss of methane (to form m/z 45), the loss of an ethyl radical from $\text{CH}_3\text{CH}_2\text{S}^-$ yields an ion which is approximately ten times more abundant as that produced by the same loss from $\text{CH}_3\text{SCH}_2^-$. Each of the three processes described in equations 2.4-2.6 affords $\text{CH}_3\text{SCH}_2^-$. This is consistent with: (i) the ions stability to electron loss, and (ii) it's ineffectual isomerisation by a proton transfer mechanism. The gas phase reactivity of $\text{CH}_3\text{SCH}_2^-$ has been reported in detail by Nibbering¹³² and is thus not studied further here.

2.2.6 The methoxymethylene anion

2.2.6.1 Theoretical considerations concerning the possible detection of the methoxymethylene anion

DePuy and co-workers⁷⁰ have reported an experimental value for the proton affinity of $\text{CH}_3\text{OCH}_2^-$ using the reaction of hydroxide ion with α -methoxymethyltrimethylsilane (equations 2.35 and 2.36).



Since the reaction of hydroxide at silicon is collision controlled, the statistically corrected ratio of Me_3SiO^- to $\text{Me}_2(\text{MeOCH}_2)\text{SiO}^-$ produced can be used to measure the proton affinity of $\text{CH}_3\text{OCH}_2^-$. From the known acidity of methane [$\Delta H^\circ_{\text{acid}}(\text{CH}_4) = 1743 \text{ kJ mol}^{-1}$ ¹³³], the acidity of dimethyl ether was determined to be 1703 kJmol^{-1} . This value is lower than $\Delta H^\circ_{\text{acid}}(\text{CH}_3\text{OH})$ (1730 kJ mol^{-1} , from Section 2.2.2.1) consistent with the substituent effect rationale outlined above.

The electron affinity of the radical $\text{CH}_3\text{OCH}_2\cdot$ is calculated (from an equation analogous to 2.34) to be -2 kJ mol^{-1} (using a reported C-H bond dissociation energy for dimethyl ether of 389 kJ mol^{-1} ¹³⁴). Hence, the methoxymethylene anion is predicted to be marginally unstable with respect to electron loss.

2.2.6.2 The attempted gas phase formation of the methoxymethylene anion

Consistent with the methoxymethylene anion's instability to electron loss, deprotonated 2-methoxy-ethanol (Table 2.4) produces no daughter ion on collisional activation formed by the loss of formaldehyde. In addition, the C.A. mass spectrum of deprotonated methoxy acetic acid (Table 2.4) shows no loss of CO_2 . The small peak at m/z 45 in this spectrum was identified to

be $(\text{HCO}_2)^-$, since an ion is produced with the same mass to charge ratio in the C.A. spectrum of deprotonated $\text{CD}_3\text{OCH}_2\text{CO}_2\text{H}$ (Table 2.4). Finally, the reaction between amide ion and methoxymethyl-trimethylsilane produces no ion at m/z 45 corresponding to $\text{CH}_3\text{OCH}_2^-$.

2.2.7 The N-methyl amino methylene anion

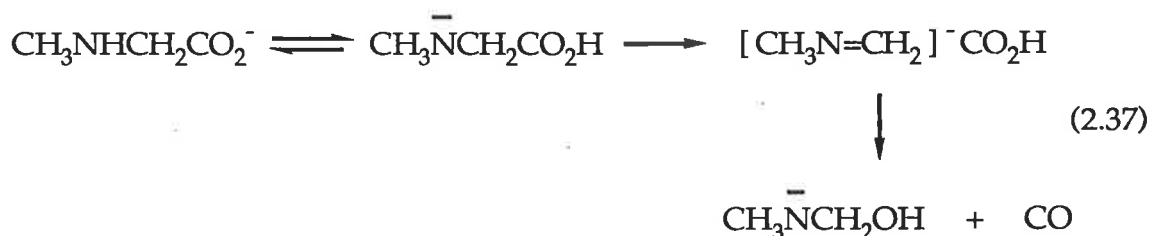
2.2.7.1 Theoretical considerations concerning the possible detection of the N-methyl amino methylene anion

If a linear relationship between the extent of nitrogen substitution and the proton affinity of the carbanions $\text{R}_1\text{R}_2\text{NCH}_2^-$ ($\text{R}_1, \text{R}_2 = \text{H}$ or CH_3) is assumed, the value for $\Delta\text{H}^\circ_{\text{acid}}(\text{CH}_3\text{NHCH}_3)$ may be estimated to be 1719 kJ mol^{-1} based on the proton affinities of NH_2CH_2^- [$\Delta\text{H}^\circ_{\text{acid}}(\text{CH}_3\text{NH}_2) = 1749 \text{ kJ mol}^{-1}$, Section 2.2.4.1] and $(\text{CH}_3)_2\text{NCH}_2^-$ [$\Delta\text{H}^\circ_{\text{acid}}((\text{CH}_3)_3\text{N}) = 1688 \text{ kJ mol}^{-1}$ 111]. This value appears reasonable, since it is greater than that of $(\text{CH}_3)_2\text{N}^-$ [$\Delta\text{H}^\circ_{\text{acid}}(\text{CH}_3\text{NHCH}_3) = 1658 \text{ kJ mol}^{-1}$ 111] and of the order of that reported for deprotonated dimethyl ether [$\Delta\text{H}^\circ_{\text{acid}}(\text{CH}_3\text{OCH}_3) = 1703 \text{ kJ mol}^{-1}$ 70].

The electron affinity of the N-methylamino methylene radical is estimated to be -43 kJ mol^{-1} from an equation analogous to 2.34 (using a reported homolytic carbon-hydrogen bond dissociation bond energy of CH_3NHCH_3 of 364 kJ mol^{-1} 135). Therefore, methyl substitution at nitrogen appears to stabilise the amino methylene anion to electron loss by some 25 kJ mol^{-1} . Nevertheless, the loss of an electron from $\text{CH}_3\text{NHCH}_2^-$ is still exothermic and consequently the direct detection of the ion is unlikely.

2.2.7.2 The attempted gas phase formation of the N-methyl amino methylene anion

The experimental approaches to detect the carbanion $\text{CH}_3\text{NHCH}_2^-$ have been unsuccessful. The C.A. spectrum of deprotonated N-methyl-2-aminoethanol (Table 2.4) exhibits no loss of formaldehyde whilst deprotonated sarcosine does not lose carbon dioxide on collisional activation. The C.A. spectrum of deprotonated $\text{CH}_3\text{NHCH}_2\text{CO}_2\text{H}$ (Table 2.4) is instead dominated by the loss of carbon monoxide; a fragment rationalised through a previously reported mechanism (equation 2.37).¹²⁹



The reaction between α -trimethylsilyl-trimethylamine and amide ion affords no ion at m/z 44 corresponding to $\text{CH}_3\text{NHCH}_2^-$.

2.2.8 The N,N-dimethyl amino methylene anion

2.2.8.1 Theoretical considerations concerning the possible detection of the N,N-dimethyl amino methylene anion

Bohme and co-workers have reported the proton affinity of $(\text{CH}_3)_2\text{NCH}_2^-$ to be in excess of 1688 kJ mol^{-1} . This value was obtained from the rates for the forward and reverse reactions in the equilibrium reaction shown in equation 2.38.¹¹¹



Substituting this figure (together with a reported homolytic bond strength for the carbon-hydrogen bond in trimethylamine of 352 kJ mol^{-1} ¹³⁵) into an equation analogous to 2.34, indicates that the electron affinity of $(\text{CH}_3)_2\text{NCH}_2\cdot$ should be greater than -24 kJ mol^{-1} .

Whilst this value is less negative than that of $\text{NH}_2\text{CH}_2\cdot$ (a consequence of the stabilising effect of the methyl substituents on nitrogen), it still suggests that the *N,N*-dimethylamino methylene anion will be unstable with respect to electron loss.

2.2.8.2 The attempted gas phase formation of the *N,N*-dimethyl amino methylene anion

The experimental evidence is in accord with the prediction that the *N,N*-dimethyl amino methylene anion will be unstable to electron loss. The C.A. spectrum of deprotonated *N,N*-dimethyl-2-aminoethanol (Table 2.4) exhibits no fragment ion corresponding to the loss of formaldehyde. Similarly, deprotonated *N,N*-dimethylglycine does not yield $(\text{CH}_3)_2\text{NCH}_2^-$ (m/z 58) on collisional activation (Table 2.4). It does, however, produce a daughter ion at m/z 58 but the structure of this ion is CH_2CO_2^- as evidenced by the C.A. spectrum of deprotonated $(\text{CD}_3)_2\text{NCH}_2\text{CO}_2\text{H}$. This spectrum also shows a fragment ion at m/z 58, inconsistent with the formation of $(\text{CD}_3)_2\text{NCH}_2^-$ (m/z 64) by a decarboxylation process.

Finally, the reaction of α -trimethylsilyl-trimethylamine with amide ion produces no ion at m/z 58. Thus it is concluded that if $(\text{CH}_3)_2\text{NCH}_2^-$ is produced from the nucleophilic displacement reaction, it undergoes spontaneous electron loss.

2.3 β -Substituted carbanions

Considerable theoretical interest^{94,95,136,137} has surrounded the stabilising effect of substituents beta to a carbanion centre. It has been shown⁹⁵ that both electronegative and electropositive groups are capable of stabilising β -substituted ethyl anions $XCH_2CH_2^-$ with respect to the ethyl anion, though the modes of stabilisation differ in each case.

The stabilising nature of a β -substituted substituent X can be assessed through calculations of the energy change for the reaction represented in equation 2.39.⁹⁵



Much debate has surrounded the stabilising effect of an electronegative substituent X beta to a carbanion centre.^{138,139} In particular, the controversy has involved the possibility of negative (or anionic) hyperconjugation in the stabilisation of such systems.

The concept of negative hyperconjugation was first reported by Roberts¹⁴⁰ though is best described later by Apeloig.¹⁴¹ Apeloig describes the hyperconjugative ability of a substituent X as the net result of a destabilising interaction of an occupied anion 2p orbital on carbon with a filled σ_{C-X} orbital and a stabilising interaction of the C-(2p) and σ^*_{C-X} orbitals. When X is an electronegative element or group the stabilising interaction of C-(2p) and σ^*_{C-X} orbitals is expected to be large and considerable stabilisation of the anion can be expected. However, when X = H, the C-(2p)- σ^*_{C-X} orbital interaction is weak, and the destabilising four electron C-(2p)- σ_{C-H} interactions are expected to predominate.

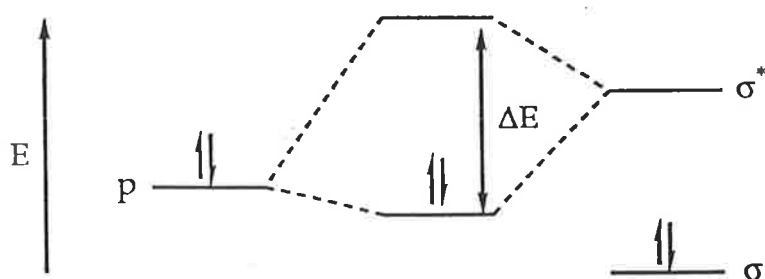


Figure 2.3 Interaction between a doubly occupied p-orbital and an unoccupied σ^* -orbital of a (C-X) bond.

The difficulty in assessing the importance of hyperconjugation arose from the problem of differentiating hyperconjugation from inductive effects. This was elegantly by Hoffman and co-workers⁹⁴ who compared the energies of β -substituted ethyl anions within conformations A and B (Figure 2.4).



Figure 2.4 Conformers of a β -substituted ethyl anion in which the hyperconjugation effect is maximised (A) and minimised (B).

Conformer A enables both hyperconjugative and inductive effects to operate. In conformer B, however, where the p-orbital on carbon and the C-X bond are perpendicular, only inductive effects should be stabilise the anion. As a result, the energy difference between the two conformers A and B provides a measure of the hyperconjugation effect, an effect evident in the significant barriers calculated for the internal rotation within $XCH_2CH_2^-$. Subsequent calculations¹³⁹ have estimated stabilisation effects through

negative hyperconjugation to be of the order of 40 kJ mol⁻¹; an effect comparable in magnitude to the inductive effect for several electronegative substituents X.

For electropositive substituents, β -substituted ethyl anions are stabilised by the direct overlap of the appropriately orientated 2p orbital on carbon with a vacant 2p orbital on X. The absence of a vacant 2p orbital on an electronegative substituent X precludes any stabilisation via this process.

In addition to the many theoretical studies devoted to these systems, several groups have attempted to produce stable β -substituted ethyl anions in the gas phase. Nibbering has studied the stabilising influence of β -substituents in carbanions $^-\text{CH}_2\text{C}(\text{CH}_3)_2\text{X}$ (X = NO, CHO)^{98,142} and more recently has inferred the intermediacy of the β -phenylethyl anion from a fluoro-desilylation reaction on β -trimethylsilylethyl benzene.¹⁴³ The latter ion, $\text{C}_6\text{H}_5\text{CH}_2\text{CH}_2^-$, has received previous interest from Bowie and co-workers¹⁴⁴ who reported it to be the first formed species on the loss of formaldehyde from deprotonated γ -phenylpropanol.

The following study describes attempts to directly detect several β -substituted ethyl anions in the gas-phase. A solely experimental approach was adopted. Pertinent theoretical data from the literature is cited when appropriate. The three experimental approaches described in Section 2.2.1 were extended for the attempted generation of selected β -ethyl anions. These approaches are illustrated in equations 2.40 to 2.42. Collisional activation of a deprotonated γ -substituted propanol and a β -substituted propionic acid could, in principle, produce β -ethyl anions by the loss of formaldehyde and carbon dioxide respectively (equations 2.40, 2.41). A nucleophilic displacement reaction on a β -substituted ethyl trimethylsilane may also result in the formation of $\text{XCH}_2\text{CH}_2^-$ (equation 2.42).



During the course of this investigation, Squires and Graul^{99,100} reported their attempts to detect several β -substituted ethyl anions from carboxylate precursors in a flowing afterglow apparatus. The results of this investigation are compared, where appropriate, with those obtained in this study.

2.3.1 β -Keto ethyl anions [RC(O)CH₂CH₂-]

2.3.1.1 The β -formyl ethyl anion

The simplest β -keto ethyl anion is the β -formyl ethyl anion. The collisional activation spectra of deprotonated γ -formyl propanol and β -formyl propionic acid (Table 2.9) both show a pronounced peak at m/z 57 corresponding to losses of formaldehyde and carbon dioxide respectively. The reaction of β -trimethylsilyl-propionaldehyde with amide ion or methoxide ion produces an intense ion at m/z 57 in the ion source. The C.A. and C.R. mass spectra of this ion, however, identify it to be largely deprotonated acetone (Table 2.10). The C.A. spectrum exhibits losses of atomic and molecular hydrogen, methane and water to form ions at m/z 56, 55, 41 and 39 in similar abundances to those from authentic CH₃C(O)CH₂- (Table 2.10). The losses of methane and water are rationalised from deprotonated acetone as shown in equations 2.43 and 2.44. The presence of a trace of product ion at m/z 27 corresponding to the loss of formaldehyde (equation 2.45) suggests

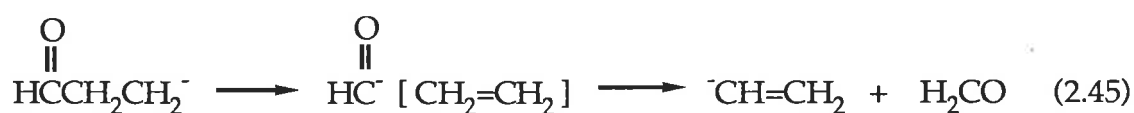
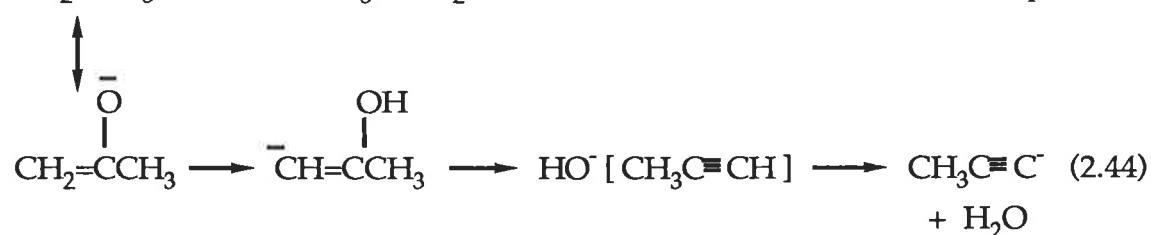
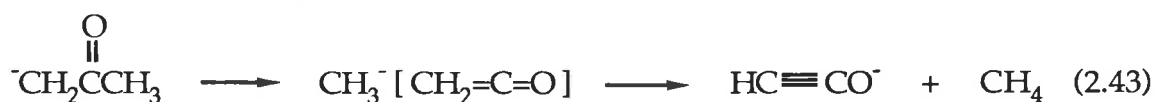
Table 2.9 Collisional activation mass spectra for the alkoxide and carboxylate precursors of some β -substituted ethyl anions.	
Ion ^a (<i>m/z</i>)	C.A. MS/MS [<i>m/z</i> (loss) abundance in %]
HC(O)(CH ₂) ₃ O ⁻ (101) HC(O)CH ₂ CH ₂ CO ₂ ⁻ (87)	71(CH ₂ O)100, 57(CO ₂)6 86(H·)13, 85(H ₂)36, 69(H ₂ O)20, 59(CO and C ₂ H ₄)100, 57(CH ₂ O)20
CH ₃ C(O)(CH ₂) ₃ O ⁻ (101) CH ₃ C(O)CH ₂ CH ₂ CO ₂ ⁻ (115) CD ₃ C(O)CD ₂ CH ₂ CO ₂ ⁻ (120)	100(H·)100, 99(H ₂)62, 85(CH ₄)78, 71(CH ₂ O)69, 55(H ₂ + CH ₃ CHO)25 114(H·)34, 113(H ₂)100, 97(H ₂ O)12, 71(CO ₂ and CH ₃ CHO)23 118(H ₂ and D·)34, 101(HOD)19, 100(D ₂ O)47, 76(CO ₂)100, 73(CD ₃ CHO)9
C ₆ H ₅ C(O)(CH ₂) ₃ O ⁻ (163) C ₆ H ₅ C(O)CH ₂ CH ₂ CO ₂ ⁻ (177)	162(H·)100, 145(H ₂ O)27, 133(CH ₂ O)87, 107(C ₃ H ₄ O)3, 85(C ₆ H ₆)5 77(C ₄ H ₆ O ₂)3, 57(C ₇ H ₆ O)2, 55(C ₇ H ₈ O)1 133(CO ₂)100, 103(C ₃ H ₆ O ₂)5, 77(C ₄ H ₄ O ₃)11, 71(C ₆ H ₅ CHO)1 55(C ₇ H ₆ O ₂)3
HOC(O)CH ₂ CH ₂ CO ₂ ⁻ (117)	116(H·)58, 92(H ₂ O)69, 91(C ₂ H ₂)2, 73(CO ₂)100, 58 ^b (C ₂ H ₃ O ₂)1,
CH ₃ OC(O)(CH ₂) ₃ O ⁻ (117) CH ₃ OC(O)CH ₂ CH ₂ CO ₂ ⁻ (131)	89(CO and C ₂ H ₄)2, 85(CH ₃ OH)100 130(H·)97, 99(CH ₃ OH)100, 31(C ₄ H ₄ O ₃)1
CH ₂ =CH(CH ₂) ₃ O ⁻ (85) CH ₂ =CHCH ₂ CH ₂ CO ₂ ⁻ (99)	84(H·)7, 83(H ₂)4, 67(H ₂ O)13, 55(CH ₂ O)100 97(H ₂)10, 55(CO ₂)100

"a" Parent ions are formed by deprotonation of the corresponding neutral with amide ion. "b" Peak is dish-shaped.

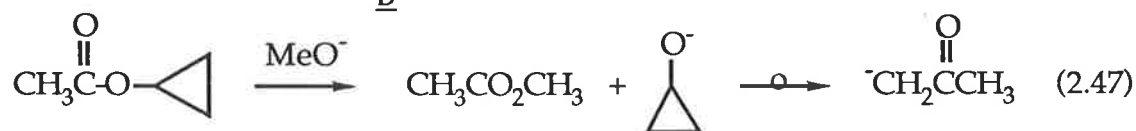
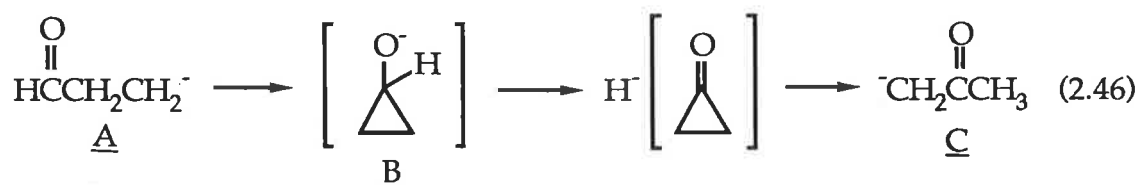
Table 2.10 Collisional Activation and Charge Reversal mass spectra of the C ₃ H ₅ O ⁻ (<i>m/z</i> 57) product ion of the β-formyl-ethyl anion precursor. A comparison with mass spectral data of C ₃ H ₅ O ⁻ ions of known structure.		<i>m/z</i> (abundances below in %)																		
ion (precursor)	spectrum type	56	55	54	53	43	42	41	40	39	38	37	29	28	27	26	25	15	14	13
"CH ₂ CH ₂ CHO" (3-TMS-propionaldehyde)	CA MS/MS	100	13					46		3				1		3				
	CR MS/MS	4	11	1	3	60	100	24	8	60	10	6	36	14	44	21	4	13	12	1
CH ₂ C(O)CH ₃ (acetone)	CA MS/MS	100						41		3										
	CR MS/MS	2	10	1	4	68	100	22	8	57	11	5	43	11	49	20	3	10	8	1
CH ₃ C(H)CHO (propionaldehyde)	CA MS/MS	98	100					7	11				1		4		2			
	CR MS/MS	17	43	3	4			3	9	4	46	6	3	100	32	63	31	3	3	4
c(C ₃ H ₅)O ⁻ (cyclopropylacetate)	CA MS/MS	100						35		2										
	CR MS/MS	2	12	1	3	60	100	22	8	61	12	4	51	15	50	22	3	9	9	1

"TMS" denotes a trimethylsilyl group. Enolate ions are represented in the carbanion form for convenience.

that a minor amount of unisomerised β -formylethyl anion remains after collisional activation.



The most probable mechanism for the conversion of the β -formylethyl anion to its isomer the acetone enolate is shown in equation 2.46. Initial cyclisation of the β -formylethyl anion (A) affords the cyclopropyloxy anion (B) which can subsequently undergo a concerted or stepwise hydride transfer reaction resulting in ring opening to generate deprotonated acetone (C).



In order to find support for this mechanism, a reaction was carried out between cyclopropylacetate and methoxide ion in the source of the mass spectrometer. The product ion $\text{C}_3\text{H}_5\text{O}^-$ (m/z 57) produced (equation 2.47), was identified to be deprotonated acetone based on its C.A. and C.R. mass spectra (Table 2.10). Thus the rearrangement of the β -formylethyl anion to

the acetone enolate through the cyclisation mechanism shown in equation 2.46 appears likely.

Similar interconversions have been predicted for the β -ethyl anion $^-\text{CH}_2\text{C}(\text{Me})_2\text{CHO}$. Noest and Nibbering^{98,142} have accounted for the low gas phase acidity of *tert*-butyl aldehyde based on hyperconjugative stabilisation resulting from the interaction of the $p(\text{C}^-)$ -orbital and the π bonding and anti-bonding orbitals of the $\text{C}=\text{O}$ group of the $(\text{M}-\text{H}^+)^-$ ion (Figure 2.5). Indeed, Noest and Nibbering report that a ring closure reaction to a cyclopropyloxy anion is energetically accessible in these systems.

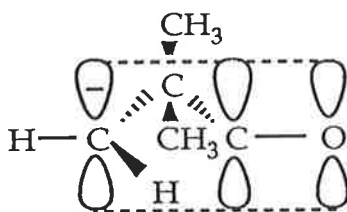


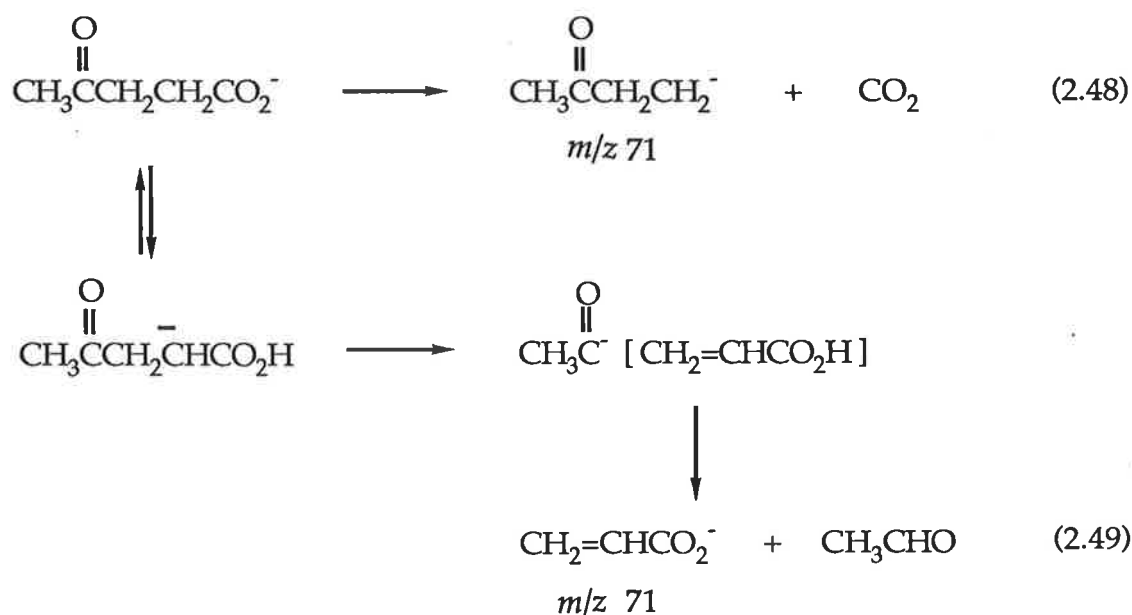
Figure 2.5 The interaction of a $p(\text{C}^-)$ -orbital and the π orbitals of an adjacent $\text{C}=\text{O}$ group.

In conclusion, the β -formylethyl anion is found to exhibit only a transient existence, rearranging to the more stable acetone enolate isomer by a process outlined in equation 2.46.

2.3.1.2 The β -acetylethyl anion $\text{CH}_3\text{C}(\text{O})\text{CH}_2\text{CH}_2^-$

Deprotonated γ -acetylpropanol (Table 2.9) exhibits a peak at m/z 71 in its C.A. mass spectrum. A product ion of the same mass is also detected in the C.A. spectrum of deprotonated β -acetylpropionic acid. In this instance, however, the ion could correspond to either the loss of carbon dioxide or acetaldehyde (equations 2.48 and 2.49). The C.A. spectrum of

$\text{CD}_3\text{C}(\text{O})\text{CD}_2\text{CH}_2\text{CO}_2^-$ (Table 2.9) shows product ions at m/z 76 and 73, which result from the respective losses of carbon dioxide and d_3 -acetaldehyde. However, the latter loss represents only a minor peak in the spectrum. Consequently, the C.A. and C.R. MS/MS/MS data of the daughter ion at m/z 71 from deprotonated β -acetylpropionic acid should largely correspond to either to the β -acetylethyl anion or a rearrangement product derived from it. The MS/MS/MS spectra of this ion are identical (within experimental error) to those produced from the reaction of methoxide ion and 4-trimethylsilylbutan-2-one. A comparison of both sets of spectra with those of ions of known structure (Table 2.11) identify the m/z 71 ion produced from the β -acetylethyl anion precursors to be deprotonated butan-2-one.



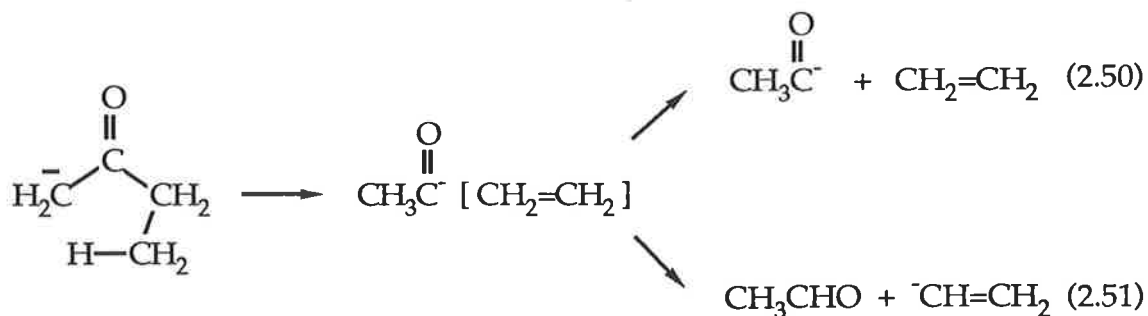
Of particular note in the C.A. spectra of the β -acetylethyl anion precursors is the presence of the acetyl anion CH_3CO^- (m/z 43). Squires¹⁰⁰ has reported that the formation of this ion is characteristic of the formation of the β -acetylethyl anion. However, since the ion is also detected in the C.A. spectrum of authentic deprotonated butan-2-one (Table 2.11), it appears

Table 2.11 Collisional Activation and Charge Reversal mass spectra of the C₄H₇O⁻ (*m/z* 71) ions from the β-acetylethyl anion precursors A comparison with mass spectral data of C₄H₇O⁻ ions of known structure.

ion (precursor)	spectrum type	<i>m/z</i> (abundances below in %)																			
		70	69	57	56	55	54	53	44	43	42	41	39	29	28	27	26	15	14	13	
"CH ₃ C(O)CH ₂ CH ₂ ⁻ " (β-TMS-butan-2-one)	CA MS/MS	100	27			5		6		7		11									
	CR MS/MS			5	16	20	8	10	26	72	100	42	28	41	26	61	37	3	2	2	
"CH ₃ C(O)CH ₂ CH ₂ ⁻ " (β-acetylpropionic acid)	CA MS/MS/MS	100	39			8		5		5		10			2						
	CR MS/MS/MS			4	10	13	13	13		62	100	35	28	40	30	72	37	17	9	2	
⁻ CH ₂ C(O)CH ₂ CH ₃ (butan-2-one)	CA MS/MS	100	71		15	41		9		15		65									
	CR MS/MS			5	7	10	4	7		68	100	31	23	24	21	40	21	1	1		
CH ₃ CH ₂ C-HCHO (butyraldehyde)	CA MS/MS	11	100			56				10											
	CR MS/MS	17	28			63	13	15				71	100	67		55	28	5	6	1	

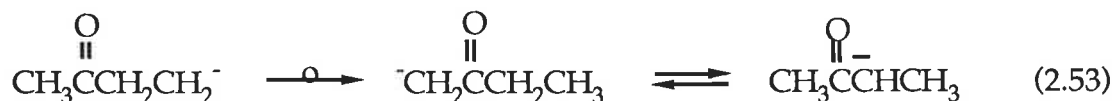
"TMS" denotes a trimethylsilyl group. Enolate ions are represented in the carbanion form for convenience.

more likely that it is produced from a butan-2-one enolate ion by the β -proton transfer elimination reaction shown in equation 2.50.



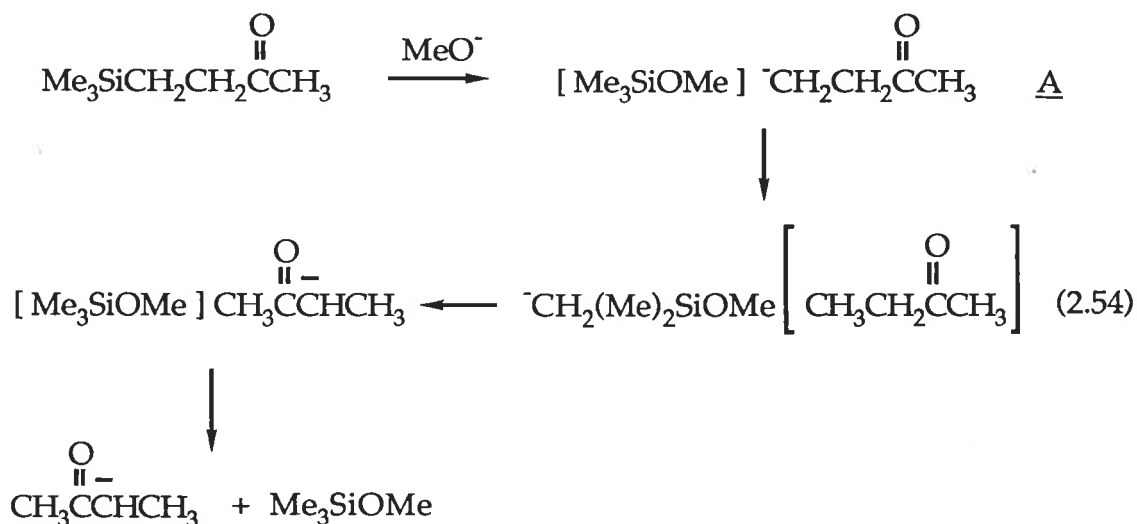
The C.A. MS/MS/MS spectrum of the m/z 71 ion from deprotonated β -acetylpropionic acid also exhibits a trace of vinyl anion at m/z 27. This product can be plausibly rationalised by a mechanism shown in equation 2.51, though conceivably it could arise from the decomposition of small amounts of deprotonated acrylic acid produced from the same precursor (see equation 2.49).

In summary, the β -acetylethyl anion readily isomerises to the enolate ions of butan-2-one under the experimental conditions used. In principle, this process can occur by either of the following two processes, namely (i) an intramolecular hydride transfer reaction (equation 2.52), or (ii) an intramolecular proton transfer process (equation 2.53).



Note that the isomerisation of the β -acetylethyl anion within an ion source by a nucleophilic $\text{S}_{\text{N}}2(\text{Si})$ displacement reaction can also be achieved

through a proton transfer reaction within a solvated ion-molecule complex (equation 2.54). The β -acetyethyl anion should be sufficiently basic to be able to deprotonate the solvated neutral silane [$\Delta H^\circ_{\text{acid}}((\text{CH}_3)_4\text{Si}) = 1636 \text{ kJ mol}^{-1}$ ¹⁴⁵] within complex A resulting in a α -silyl anion which can subsequently deprotonate solvated butan-2-one α to the carbonyl group. This approach therefore could not be employed for a mechanistic study.



The two intramolecular processes for the conversion of the β -acetyethyl anion to its isomeric enolate could be distinguished based on the position of the deuterium label in the collisional activation fragments of $\text{CD}_3\text{C}(\text{O})\text{CH}_2\text{CH}_2^-$ (m/z 74) produced from d_3 -acetyl propionic acid.

A 1,2-hydride transfer process within $\text{CD}_3\text{C}(\text{O})\text{CH}_2\text{CH}_2^-$ (equation 2.52) should yield $\text{CD}_3\text{C}(\text{O})\text{C}^-(\text{H})\text{CH}_3$ whose C.A. spectrum will exhibit losses of CD_3H and $\text{C}_2\text{H}_4\text{D}_2$ to form ions at m/z 55 and 42 respectively. In contrast, an intramolecular proton transfer reaction (equation 2.53) will result in the formation of $^-\text{CD}_2\text{C}(\text{O})\text{CH}_2\text{CH}_2\text{D}$ and/or $\text{CD}_2\text{HC}(\text{O})\text{C}^-(\text{H})\text{CH}_2\text{D}$. These enolate ions should show losses of CD_2H_2 and $\text{C}_2\text{H}_4\text{D}_2$ yielding ions at m/z 56 and 42 respectively.

Unfortunately, attempts to prepare β - d_3 -acetyl-propionic acid for use in such a study have proved unsuccessful. Consequently, no information can be

gained on the mechanism for isomerisation. An intramolecular proton transfer seems likely to contribute to the isomerisation process in accord with previous observations.¹⁴⁶ However, the possibility of the hydride transfer reaction cannot be excluded.

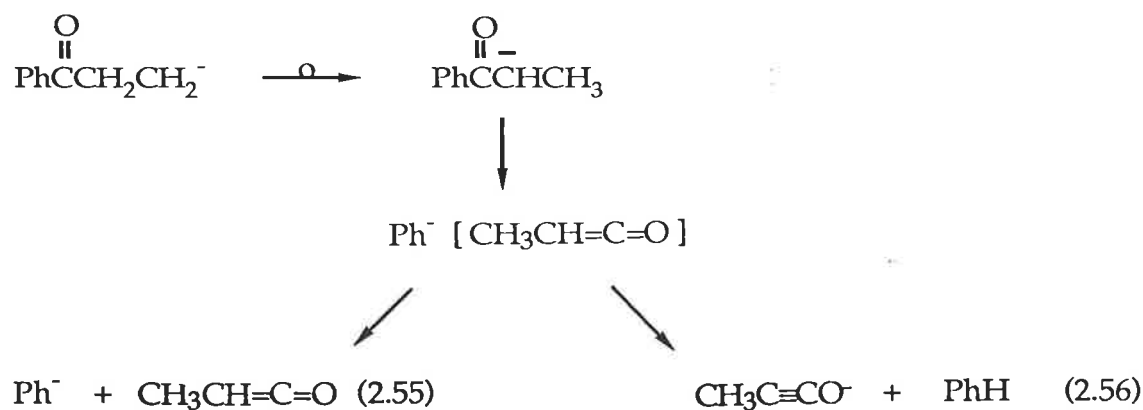
In conclusion, the β -acetylethyl anion isomerises under collisional activation conditions to form the butan-2-one enolate ions.

2.3.1.3 The β -benzoylethyl anion $\text{PhC(O)CH}_2\text{CH}_2^-$

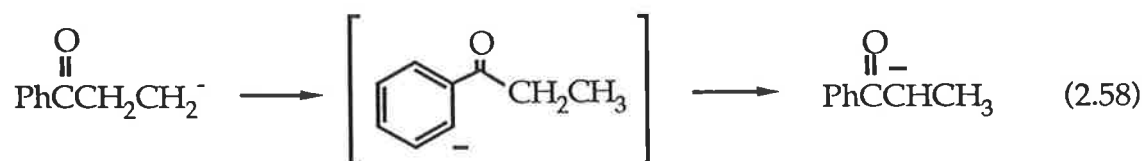
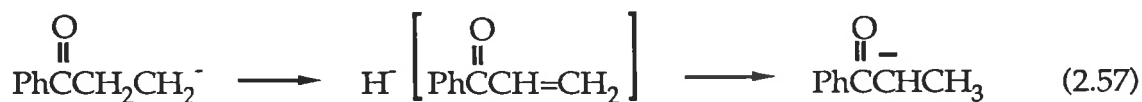
Deprotonated γ -benzoylpropanol exhibits a major fragment peak at m/z 133 corresponding to the loss of formaldehyde in its C.A. mass spectrum (Table 2.9). An ion of the same mass to charge ratio is detected in the C.A. spectrum of deprotonated β -benzoylpropionic acid (Table 2.9) corresponding to the loss of carbon dioxide. The C.A. and C.R. mass spectra of this daughter ion identify it as the enolate ion of phenyl ethyl ketone (Table 2.12). Similarly, the reaction of β -trimethylsilylethyl-phenyl ketone and methoxide ion in the source of the mass spectrometer also produces a product ion at m/z 133. The C.A. and C.R. spectra of this ion (Table 2.12) confirm it has the same structure as deprotonated phenyl ethyl ketone. Major fragment ions at m/z 131, 77 and 55 are consistent with the loss of molecular hydrogen, methyl ketene and benzene respectively. The latter two losses are rationalised through the phenylethyl ketone enolate ion by processes represented in equations 2.55 and 2.56. The β -benzoyl ethyl anion $\text{PhC(O)CH}_2\text{CH}_2^-$ should fragment to yield PhCO^- (at m/z 105) and C_2H_3^- (m/z 27) produced by the respective loss of ethene and benzaldehyde. No such fragmentations were observed.

ion (precursor)		<i>m/z</i> (abundances below in %)																		
spectrum type		132	131	118	117	115	105	103	102	91	90	89	88	77	63	55	50	43	41	39
"PhC(O)CH ₂ CH ₂ -" (3-TMS-1-phenylpropanone)	CA MS/MS	100	75							5				19		6				
	CR MS/MS		12		14	62		21				23		100	19		32			
"PhC(O)CH ₂ CH ₂ -" (3-benzoylpropionic acid)	CA MS/MS/MS	100	40		1		3							20		9				
	CR MS/MS/MS		4		34	29		17				14		100	12	5	30			6
PhC(O)C-HCH ₃ (1-phenylpropanone)	CA MS/MS	100	40					3		1				39		12				
	CR MS/MS		2		10	43		11				16		100	15	9	34			7
PhC-HC(O)CH ₃ (phenylacetone)	CA MS/MS	100	31		6	4		2		89				15		4				5
	CR MS/MS		20	22		26	24		18		86		100	68	44		46	38		16

"TMS" denotes a trimethylsilyl group. Enolate ions are represented in the carbanion form for convenience.

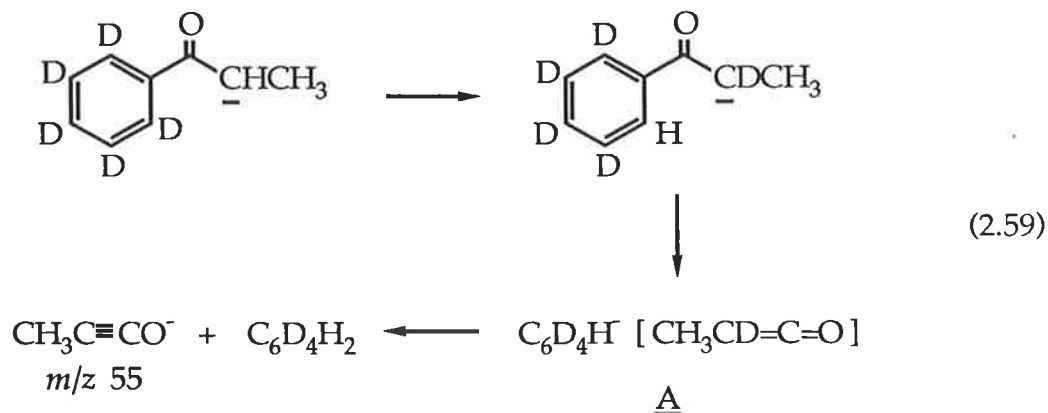


As in the case of the β -acetyethyl anion (Section 2.3.1.2), the β -benzoylethyl anion can isomerise to the more stable enolate ion of phenyl ethyl ketone under collisional activation conditions by two distinct mechanisms. The first involves a 1,2-hydride ion transfer (equation 2.57), whilst the second mechanism is an intramolecular proton transfer process shown in equation 2.58.



These mechanisms should be able to be distinguished based on the C.A. mass spectrum of $\text{C}_6\text{D}_5\text{C}(\text{O})\text{CH}_2\text{CH}_2^-$ (m/z 138) [formed by the loss of CO_2 from β -(d_5 -benzoyl)-propionic acid]. If a hydride transfer process operates the spectrum should show losses of $\text{C}_6\text{D}_5\text{H}$ and methyl ketene to form ions at m/z 55 and 82 respectively. However, if an intramolecular proton transfer mechanism occurs, the spectrum will exhibit losses of $\text{C}_6\text{D}_4\text{H}_2$ and CH_2DCHCO to yield ions at m/z 56 and 81. The C.A. mass spectrum of

$C_6D_5C(O)CH_2CH_2^-$ is shown in Figure 2.6. It exhibits major peaks corresponding to the loss of HD, methyl ketene, d₁-methyl ketene and d₅-benzene at m/z 135, 82, 81 and 55 respectively. At first sight these results appear contradictory. They can, however, be explained simply. The β -(d₅-benzoyl)-ethyl anion appears to isomerise exclusively through a 1,2-hydride transfer reaction to afford $C_6D_5C(O)C-HCH_3$ prior to hydrogen exchange with the aromatic ring. Collision-induced dissociation of this enolate ion affords $C_6D_5^-$ (m/z 82) or $CH_3C\equiv CO^-$ (m/z 55) by processes shown in equations 2.55 and 2.56 respectively. If, however, a proton exchange precedes dissociation, the enolate $C_6D_4HC(O)C-(H)CH_3$ will yield $C_6D_4H^-$ (m/z 81) (compare with equation 2.55) and $CH_3C\equiv CO^-$ (m/z 55). In the latter process, deuterium abstraction by $C_6D_4H^-$ occurs solely on the deuterium substituted carbon atom (complex A, equation 2.59); the product ion is consequently free of deuterium label and is again detected at m/z 55.



In support of a hydrogen exchange with the protons of the ring prior to isomerisation via a hydride transfer, the loss of ethyl radical (m/z 107) in the labelled spectrum (Figure 2.6) is di-deuterated. This is a result of deprotonated phenyl ethyl ketone undergoing two hydrogen exchanges with the ring prior to homolytic cleavage of the carbon-carbon bond in intermediate A (equation 2.60).

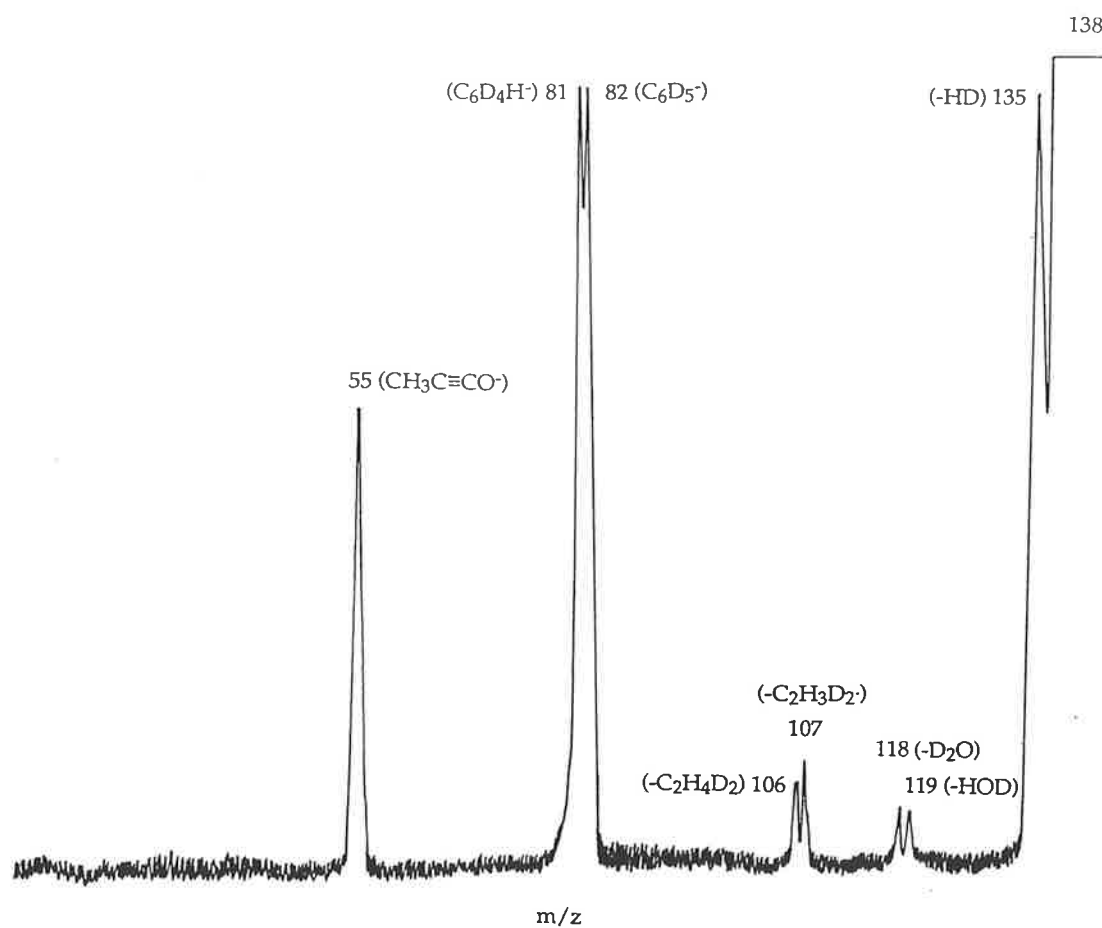
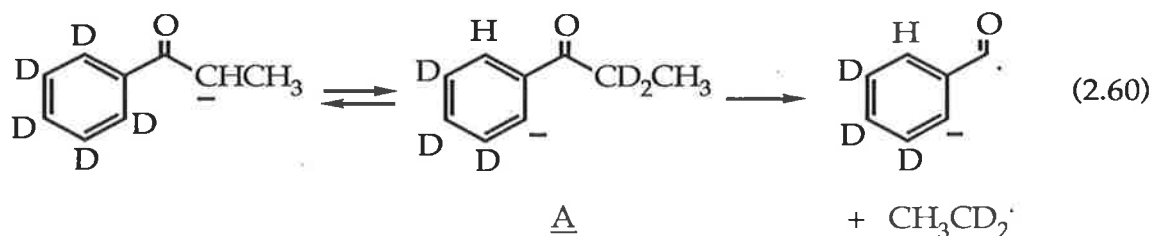


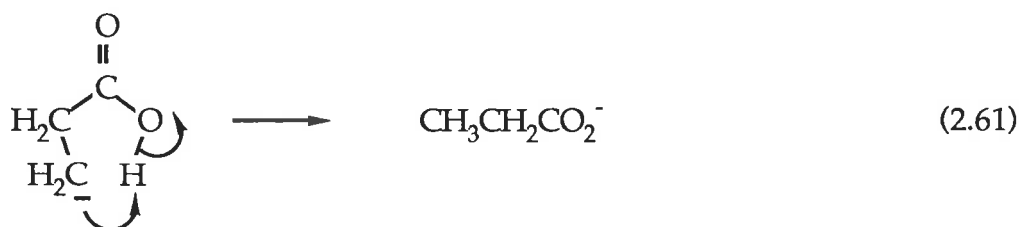
Figure 2.6 C.A. MS/MS/MS spectrum of the ion (m/z 138) formed on loss of CO_2 from $\text{C}_6\text{D}_5\text{C}(\text{O})\text{CH}_2\text{CH}_2\text{CO}_2^-$.



2.3.1.4 The β -hydroxycarbonylethyl anion

The C.A. spectrum of deprotonated succinic acid (Table 2.9) is dominated by the loss of carbon dioxide to afford an ion at m/z 73. The C.A. and C.R. mass spectra of this daughter ion (Table 2.13) identify it to be the propionate anion. Similarly, the reaction between methoxide ion and β -trimethylsilylpropionic acid in the source of the mass spectrometer produces an ion at m/z 73 which also corresponds to $\text{CH}_3\text{CH}_2\text{CO}_2^-$ (Table 2.13).

Clearly, under the experimental conditions employed the β -hydroxycarbonylethyl anion isomerises to the more stable propionate anion by a proton transfer mechanism shown in equation 2.61.



2.3.1.5 The β -methoxycarbonylethyl anion

Since the β -hydroxycarbonylethyl anion was observed to isomerise to a more stable carboxylate anion (Section 2.3.1.4), blocking of the carboxylate position would seem intuitively useful to prevent such an isomerisation and

Table 2.13 Collisional Activation and Charge Reversal mass spectra for the $C_3H_5O_2^-$ ions (m/z 73) from the β -hydroxycarbonylethyl anion precursors. A comparison with the mass spectral data of $C_3H_5O_2^-$ ions of known structure.

ion (precursor)	spectrum type	m/z (abundances below in %)																		
		72	71	59	58	56	55	52	45	44	42	41	31	29	28	27	26	15	14	13
"HO ₂ CCH ₂ CH ₂ " (β -TMS-propionic acid)	CA MS/MS	7	100				32			36										
	CR MS/MS					17	16	6	50	81	17		46	71	100	66	8	12	4	
"HO ₂ CCH ₂ CH ₂ " (succinic acid)	CA MS/MS	11	100		3		35			39										
	CR MS/MS					2	3	2	23	76	19		49	70	100	64	7	9	3	
CH ₃ CH ₂ CO ₂ ⁻ (propionic acid)	CA MS/MS	56	67		11		100			26										
	CR MS/MS					6	8	4	45	59	14		64	74	100	68	6	9	5	
-CH ₂ CO ₂ CH ₃ (methyl acetate)	CA MS/MS		5		1				1			100	1							
	CR MS/MS			3					9	10		100	22	14				10	5	

"TMS" denotes a trimethylsilyl group. Enolate ions are represented in the carbanion form for convenience.

perhaps facilitate the detection of a β -substituted ethyl anion. Consequently, the approaches shown in equations 2.40 to 2.42 have been employed to attempt to generate the β -methoxycarbonylethyl anion. All three approaches, however, have failed to yield such an ion.

The C.A. spectrum of deprotonated methyl 4-hydroxybutyrate (Table 2.9) shows no loss of formaldehyde. Instead, it is dominated by the loss of methanol. Similarly, deprotonated mono-methylsuccinate exhibits a base peak corresponding to the loss of methanol in its C.A. spectrum (Table 2.9) but shows no fragment ion at m/z 87 corresponding to the loss of carbon dioxide. Finally, the reaction between methoxide ion and methyl β -trimethylsilyl-propionate produces corresponding to $\text{MeOC(O)CH}_2\text{CH}_2^-$.

In conclusion, the methyl group attached to the carboxylate does not assist the detection of the β -methoxycarbonylethyl anion. The β -ethyl anion precursors for this ion are observed to undergo other reaction processes than those desired. If any β -methoxycarbonylethyl anion is formed through the processes summarised in equations 2.40 to 2.42, it is not detected. This is perhaps a consequence of the β -methoxycarbonylethyl anion's instability to electron detachment.

2.3.2 The β -vinylethyl anion

The C.A. and C.R. mass spectra of the m/z 57 ion produced on collisional activation of deprotonated 4-pentenol and 4-pentenoic acid are shown in Table 2.14. The spectra are very similar to those of the m/z 57 ion produced upon reaction of 4-trimethylsilyl-butene and methoxide ion in the source of the mass spectrometer (Table 2.14).

Table 2.14 Collisional Activation and Charge Reversal mass spectra of C₄H₇⁻ product ions (m/z 55) of β-vinylethyl anion precursors. A comparison with mass spectral data of C₄H₇⁻ ions of known structure.

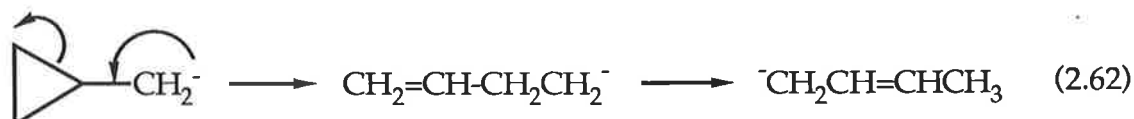
ion (precursor)	spectrum type	m/z (abundances below in %)																			
		54	53	52	51	50	49	41	40	39	38	37	29	28	27	26	25	15	14	13	
"CH ₂ =CHCH ₂ CH ₂ ⁻ " (4-TMS-butene) "CH ₂ =CHCH ₂ CH ₂ ⁻ " (4-pentenol) "CH ₂ =CHCH ₂ CH ₂ ⁻ " (4-pentenoic acid)	CA MS/MS	100	38																		
	CR MS/MS	41	49	15	29	24		5	13	100	34	28	36	24	67	39	12	4	3		
	CA MS/MS/MS	100	9																		
	CR MS/MS/MS	67	67	16	28	15		10	11	100	15	6	34	21	63	11					
	CA MS/MS/MS	100	7																		
	CR MS/MS/MS	49	59	15	25	16		7	10	100	14	7	29	19	55	13			2	1	
CH ₂ =C ⁻ (H)CHCH ₃ (1-butene)	CA MS/MS	100	41																		
	CR MS/MS	35	100	48	13				84	58	19			44	51	79	22	9			
⁻ CH ₂ CH=CHCH ₃ (2-butene)	CA MS/MS	100	35																		
	CR MS/MS	55	49	16	28	26		5	11	100	35	20	30	21	59	28		2	2	1	
c(C ₃ H ₅)CH ₂ ⁻ (cyclopropylacetic acid)	CA MS/MS/MS	100	10																		
	CR MS/MS/MS	18	41	22	32	30		31	15	100	41	17	43	24	73	31					

"TMS" denotes a trimethylsilyl group.

The C.A. spectra of m/z 57 produced from the β -vinylethyl anion precursors all exhibit a loss of atomic and molecular hydrogen (m/z 56 and 55 respectively) only, the former representing the base peak of the spectra. The spectra show no loss of ethene (to form an ion at m/z 27); a likely product of the direct fragmentation of the β -vinylethyl anion.

Whilst the C.A. mass spectra exhibit little fragmentation information, their corresponding C.R. spectra (Table 2.14) show a profusion of fragment ions. The fragment ions are present in similar abundances and at the same masses to those produced in the C.R. spectrum of deprotonated but-2-ene (Table 2.14). The C.R. spectrum of the 57 ion produced from collisional activation of deprotonated cyclopropyl acetic acid (Table 2.14) is noteworthy. It, too, exhibits fragment peaks and abundances which correspond closely to those of the C.R. spectrum of deprotonated but-2-ene.

These results suggest that the β -vinylethyl anion and the cyclopropyl methylene anion undergo rapid isomerisation to isomeric deprotonated but-2-ene (equation 2.62) under the experimental conditions employed.



One other possible explanation for the results obtained, however, must be considered. Namely, the β -vinylethyl anion, the cyclopropyl methylene anion and deprotonated but-2-ene, coincidentally show losses of atomic and molecular hydrogen with similar relative abundance. Their identical C.R. mass spectra are then merely the result of an isomerisation of the carbonium ions produced on charge reversal in the collision cell. (see Section 1.4.3).

In order to distinguish between these possibilities, the reactivity of the m/z 55 ion produced from collision induced dissociation of deprotonated

pentenoic acid was examined. DePuy and co-workers⁷¹ have recently predicted $\Delta H^{\circ}_{\text{acid}}(\text{CH}_2=\text{CHCH}_2\text{CH}_3)$ to be 1724 kJ mol^{-1} . However, the C_4H_7^- ion (m/z 55) produced on collision induced loss of CO_2 from deprotonated 4-pentenoic acid undergoes no reaction with $\text{d}_6\text{-benzene}^*$ [$\Delta H^{\circ}_{\text{acid}}(\text{C}_6\text{H}_6) = 1676 \text{ kJ mol}^{-1}$ ¹¹⁵], whilst with D_2O [$\Delta H^{\circ}_{\text{acid}}(\text{D}_2\text{O}) = 1644 \text{ kcal mol}^{-1}$ ¹¹⁶] a slow exchange reaction results. These results suggest the conjugate acid of the C_4H_7^- ion detected has an acidity of the order of 1644 kJ mol^{-1} consistent with that predicted for but-2-ene ($\Delta H^{\circ}_{\text{acid}}(\text{CH}_2=\text{CHCH}_3) = 1635 \text{ kJ mol}^{-1}$ ¹¹²). In addition, the C_4H_7^- ion (m/z 55) produced from the collision induced dissociation of deprotonated 4-pentenoic acid undergoes a reaction with N_2O characteristic of a primary carbanion.¹⁴⁷ The reaction affords a major product corresponding to the formation of a diazonium ion (m/z 81) (Figure 2.7). Whilst this product would be expected for a direct reaction of the β -vinylethyl anion, it appears more likely that, in conjunction with the above results, the product is produced from the reaction of the isomerisation product, deprotonated but-2-ene (see Figure 2.8) (equations 2.63 and 2.64). Initial attack of $^-\text{CH}_2\text{CH}=\text{CHCH}_3$ at a nitrogen of N_2O could form intermediate A which can undergo an intramolecular proton transfer to afford B. Subsequent elimination of hydroxide ion yields ion-molecule complex C, where the solvated neutral contains two acidic sites. Deprotonation of the neutral at either site by hydroxide ion affords diazonium ion D (m/z 81) (equation 2.63) or an ion of the same mass (E) (equation 2.64).

In conclusion, the β -vinylethyl anion appears to be unstable to isomerisation to $^-\text{CH}_2\text{CH}=\text{CHCH}_3$ under the experimental conditions employed. This is supported by recent work of Graul and Squires¹⁰⁰ who measured the appearance energy for the decarboxylation product of deprotonated 4-pentenoic acid and concluded the ion adopts the structure of

* Labeled $\text{d}_6\text{-benzene}$ was used in order to distinguish between the possibility of no reaction from that of an exchange process (see equation 2.15).

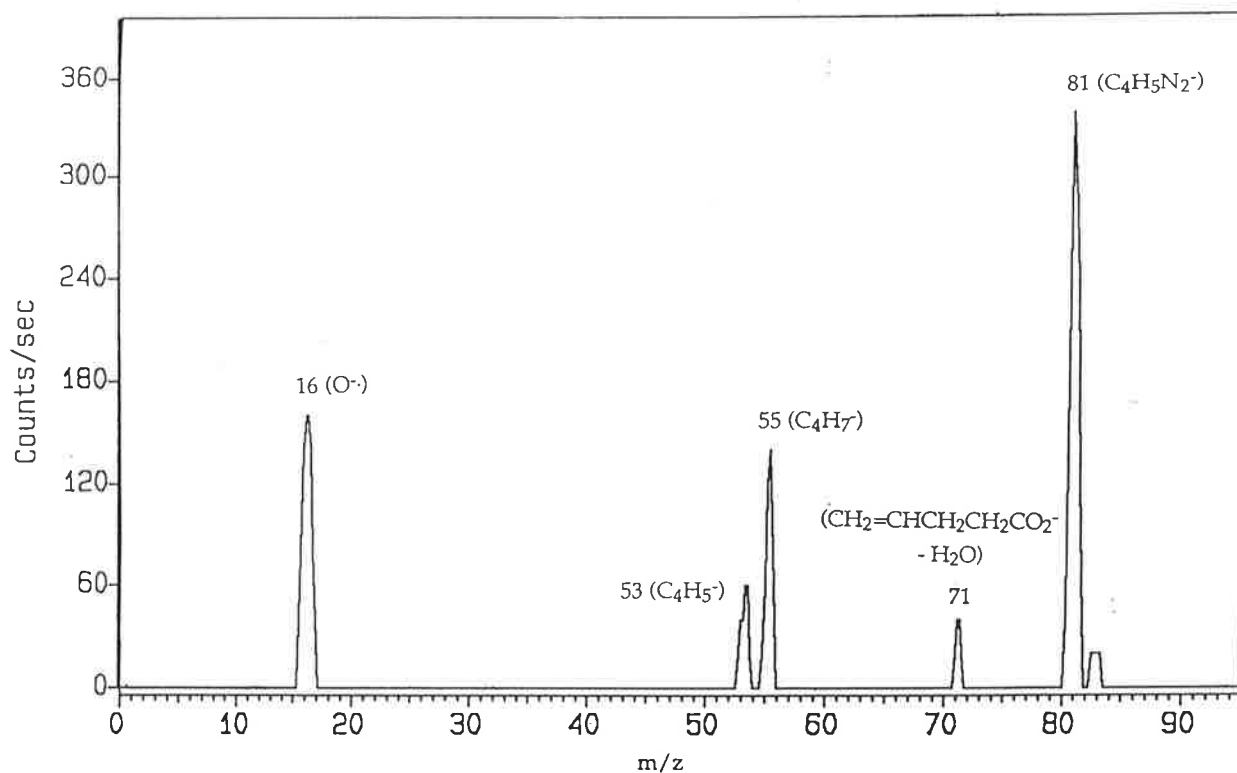


Figure 2.7 Reaction of the m/z 55 ion (formed on loss of CO_2 from $CH_2=CHCH_2CH_2CO_2^-$) with nitrous oxide. (The ion at m/z 71 is the product of a competing decomposition of the parent)

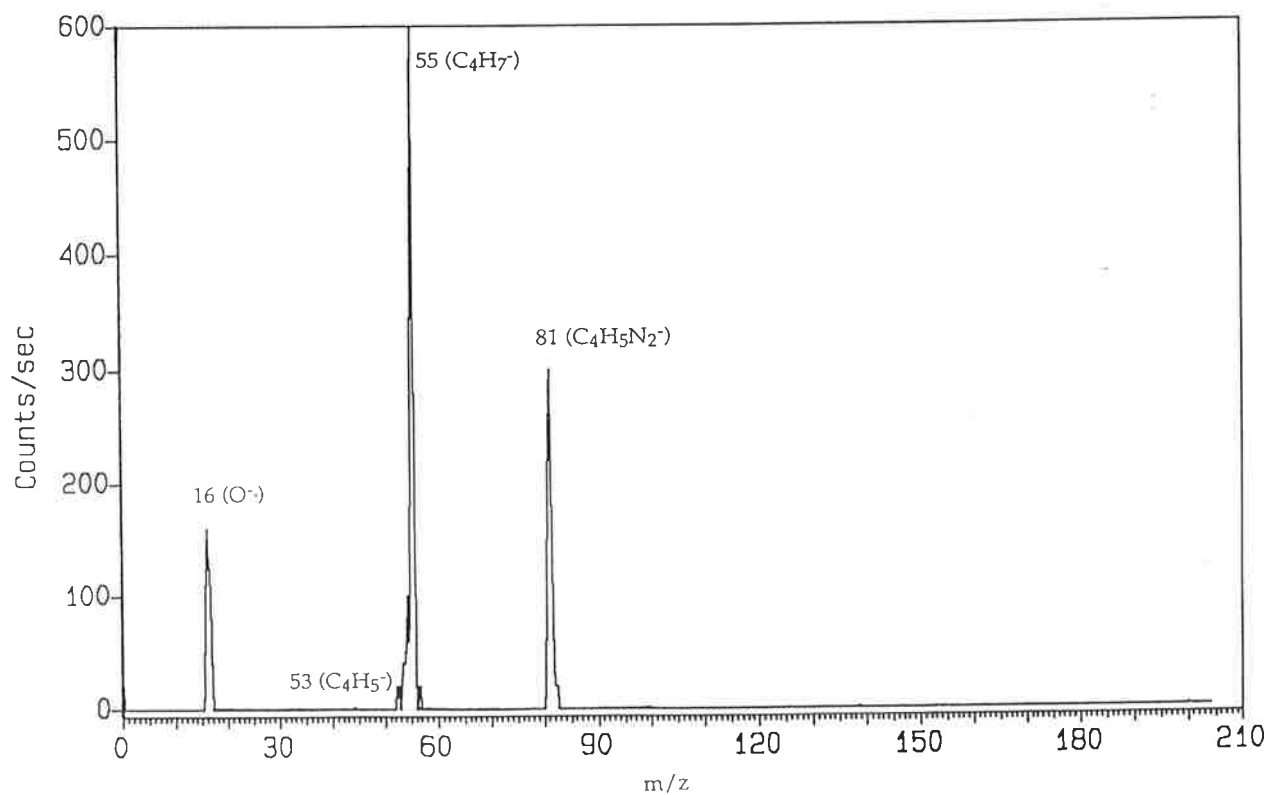
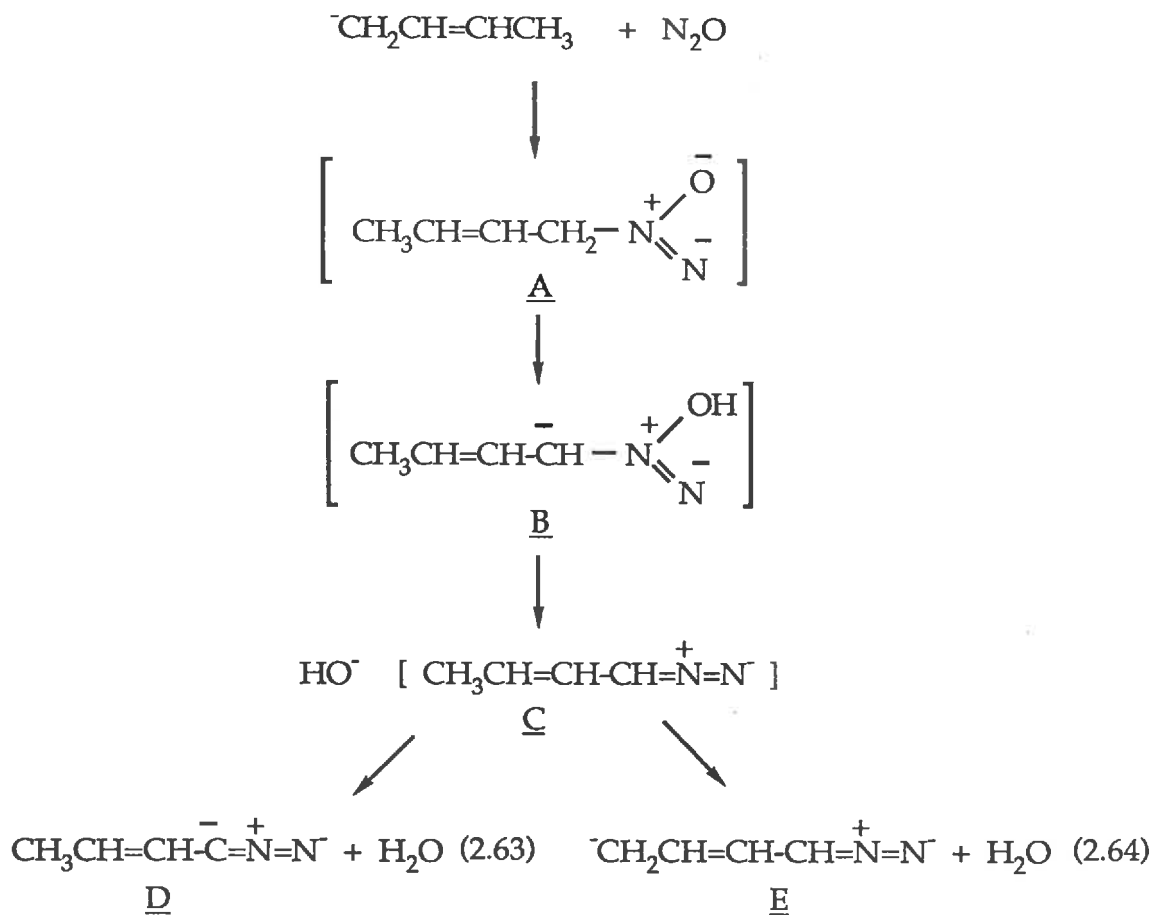


Figure 2.8 Reaction of deprotonated 2-butene (m/z 55) with nitrous oxide.



the allylic isomer $\text{CH}_2\text{CH}=\text{CHCH}_3$. A mechanistic study to determine the mode of isomerisation was not undertaken in this case due to the uncharacteristic fragmentation patterns exhibited in the C.A. spectra of the C_4H_7^- ions.

2.4 Summary and conclusions

This chapter describes attempts to generate selected α - and β -substituted alkyl carbanions in the gas phase. The experimental approach has been presented together, wherever possible, with conclusions drawn from independent theoretical calculations.

Of the α -hetero-substituted carbanions studied [RXCH_2^- ($\text{X} = \text{S}, \text{O}, \text{NH}, \text{NCH}_3$; $\text{R} = \text{H}, \text{CH}_3$)], only the methylene thiol anion and its methylated derivative, the methylthiomethylene anion, are predicted to be stable to electron detachment. In accord with this prediction, the experimental approaches were successful in generating the carbanions HSCH_2^- and $\text{CH}_3\text{SCH}_2^-$ but not their oxygen and nitrogen analogues. However, evidence is presented to support

the transient existence of the oxygen and nitrogen analogues within ion-molecule complexes. For example, the hydroxymethylene anion has been shown by labelling studies to have a transient existence within the ion-molecule complex $\text{HOCH}_2^- (\text{CH}_2\text{O})$ (Section 2.2.2.2). Within this complex, however, the highly basic carbanion ($\Delta H^\circ_{\text{acid}} (\text{CH}_3\text{OH}) = 1730 \text{ kJ mol}^{-1}$, Section 2.2.2.1) deprotonates formaldehyde. A second proton transfer followed by dissociation of the complex results in the formation, and subsequent detection, of isomeric methoxide ion. Such an intermolecular isomerisation is not possible if the hydroxymethylene anion is produced by the collision induced decomposition of deprotonated thioglycolic acid. However, in this case no ion at m/z 31 was detected and consequently either no loss of CO_2 from $\text{HSCH}_2\text{CO}_2^-$ occurs or the hydroxymethylene anion produced is unstable to electron loss [$E.A.(\text{HOCH}_2\cdot) = -37 \text{ kJ mol}^{-1}$, Section 2.2.2.1].

A similar scenario was found for the β -substituted ethyl anions studied. In these systems, however, isomerisation to a more stable isomer occurs intramolecularly [at least where the β -ethyl anions are formed from the decarboxylation approach (equation 2.41)]. In the case of the β -formylethyl anion, isomerisation to the acetone enolate ion occurs through a cyclopropyloxy anion intermediate. Both the β -acetyl ethyl and the β -benzoylethyl anion were found to isomerise to a more stable enolate ion, the latter through a 1,2-hydride ion transfer. No isomer was detected for the β -methoxycarbonylethyl anion. In this case, either the β -ethyl anion is not produced from the neutral precursors or its formation is accompanied by electron detachment.

Squires¹⁰⁰ has suggested that the isomerisation of β -substituted ethyl anions is dependent on the collision energy they experience. However, whilst low collision energies may prevent the isomerisation of a β -ethyl anion, they may also restrict the decomposition of a β -ethyl anion preventing its characterisation. Nevertheless, the different collision conditions employed by Squires may account for the reported formation of the β -acetylethyl anion with minimal isomerisation.¹⁰⁰

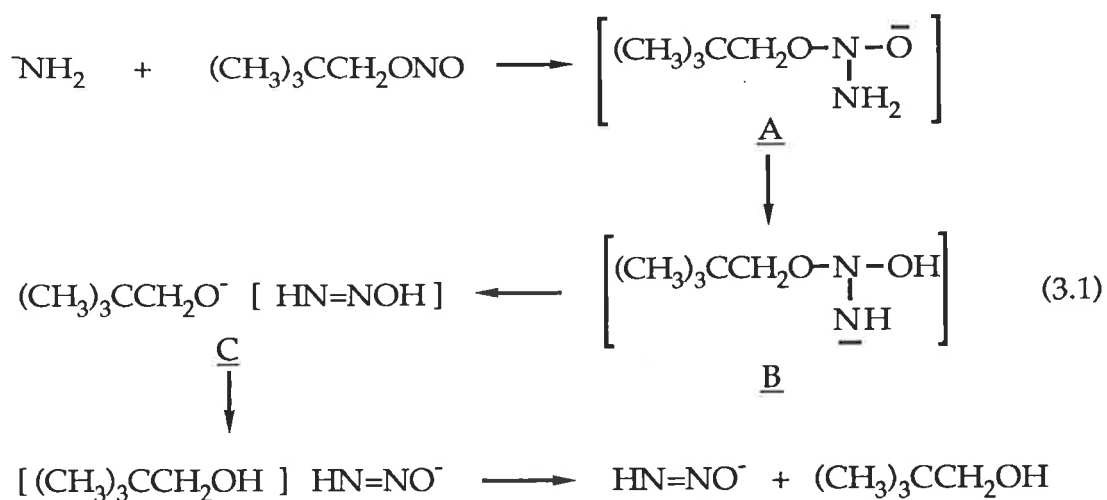
Chapter 3 **THE FORMATION, STRUCTURE AND REACTIVITY OF**
HN₂O⁻, A PRODUCT ION STUDY.

3.1 **Introduction**

The formation of product ion (HN₂O)⁻ from reaction of the methylene thiol anion with nitrous oxide in the flowing afterglow (Section 2.2.3.3.2) prompted a study to determine its structure and reactivity. Generation of the methylene thiol anion, however, was achieved in this instrument by collision-induced dissociation of deprotonated thioglycolic acid within the second flow tube of the flowing afterglow-S.I.F.T. (see Section 1.7.2.1). The subsequent formation of ion (HN₂O)⁻, in addition to its desired reaction, within this same flow tube would yield results difficult to interpret due to the presence of significant amounts of precursor ions HSCH₂CO₂⁻ and HSCH₂⁻.

Consequently, an alternative preparative method was sought which would enable (HN₂O)⁻ to be prepared within the first flow tube and be injected solely into the second by means of the quadrupole mass filter. Two previously reported procedures were adopted.

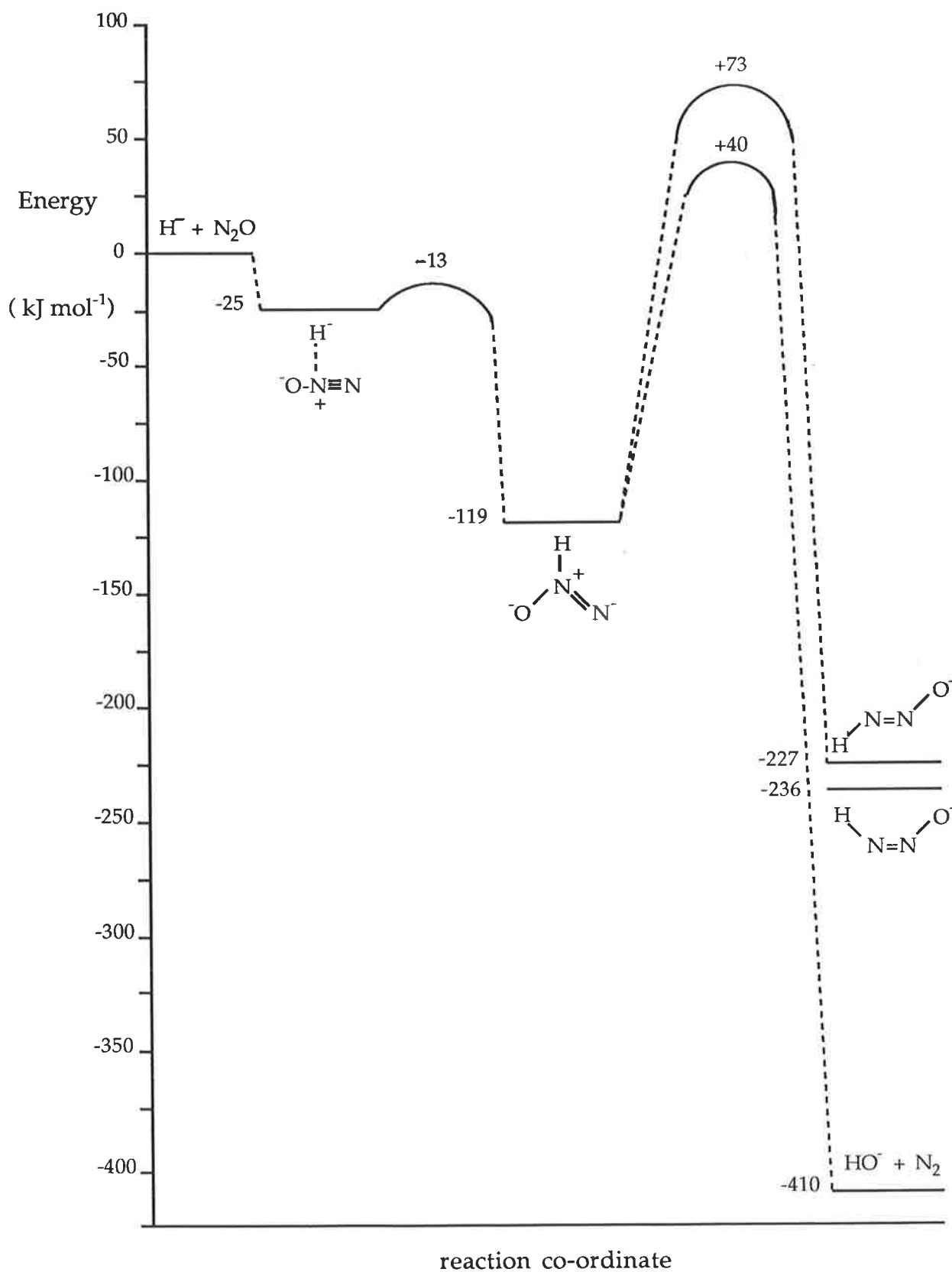
The first approach involves the reaction of amide ion with *neo*-pentyl nitrite¹²⁰ (equation 3.1).



1,2-hydrogen transfer reactions have not been generally observed in the gas phase.¹⁴⁸ Indeed, Radom and co-workers have reported that 1,2-hydrogen migrations are symmetry forbidden.¹⁴⁹ Consequently, a 1,2-hydrogen transfer between the nitrogen centres of intermediate A is unlikely to occur. Therefore the approach shown in equation 3.1 should generate only one isomeric form of ion HN_2O^- provided that proton abstraction in complex C occurs exclusively on oxygen. If proton abstraction occurs on nitrogen, the resulting ion should be unstable to dissociation (see below).

Consider now the isomer of HN_2O^- in which hydrogen resides on the terminal nitrogen. In this form, HN_2O^- can exist as two stable conformers, where the hydrogen and oxygen centres are *cis* and *trans* to the nitrogen-nitrogen double bond. The latter conformer has received previous theoretical interest.¹⁵⁰ Sheldon and co-workers showed that *trans* $\text{HN}=\text{NO}^-$ is a theoretically stable species and an energetically accessible product from a hydride transfer reaction from methoxide ion to nitrous oxide. Recent *ab initio* calculations by Dr. John C. Sheldon are summarised in Figure 3.1. The results predict that the *cis* conformer is some 9 kJ mol^{-1} more stable than the *trans* conformer. This is likely to be a consequence of the destabilising interaction in the *trans* conformer between the charge on oxygen and the lone electron pair on the nitrogen bearing hydrogen.

Figure 3.1 *Ab initio* calculations on the addition of hydride ion to nitrous oxide.



Ab initio calculations were performed by Dr. J.C. Sheldon (Department of Physical & Inorganic Chemistry, The University of Adelaide) at the MP2/6-311++G**//6-311++G** level using GAUSSIAN 86.¹⁰⁷

The second method employed to produce $(\text{HN}_2\text{O})^-$ involves a hydride transfer reaction from cyclohexadiene to nitrous oxide through hydride donor HNO^- ¹¹⁸ (equations 3.2 - 3.4).



In principle, this method could yield three isomeric forms of HN_2O^- in which the hydrogen atom resides on either the terminal or central nitrogen, or on oxygen. The latter isomer, $\text{HON}=\text{N}^-$, is expected to be unstable with respect to the loss of molecular nitrogen. Figure 3.1 shows the loss of N_2 from $\text{HON}=\text{N}^-$ is calculated to be exothermic by over 400 kJ mol^{-1} . This prediction is supported by the collision induced dissociation spectrum of $[\text{HN}_2\text{O}]^-$ formed by the hydride transfer reaction (Figure 3.2). The spectrum shows peaks corresponding to fragment ions H^- (m/z 1) and O^- (m/z 16). The former fragment ion H^- (m/z 1) is detected, either totally or in part, on its injection from the first flow tube. The low mass and hence short residence time of H^- within the quadrupole mass filter prevents its complete removal on injection of $(\text{HN}_2\text{O})^-$. The collision induced decomposition spectrum importantly shows no hydroxide ion (m/z 17), a likely C.I.D. product from the dissociation of $\text{HON}=\text{N}^-$. Thus if any $\text{HON}=\text{N}^-$ is produced from the hydride transfer process, it should dissociate rapidly within the first flow tube to HO^- and N_2 . As a result only the isomeric forms $\text{HN}=\text{NO}^-$ (*cis* and *trans*) and $^-\text{N}=\text{N}^+(\text{H})\text{O}^-$ should be present to react within the second flow tube. Preliminary *ab initio* calculations predict that an unbound hydride ion should add efficiently to both the central and terminal nitrogens

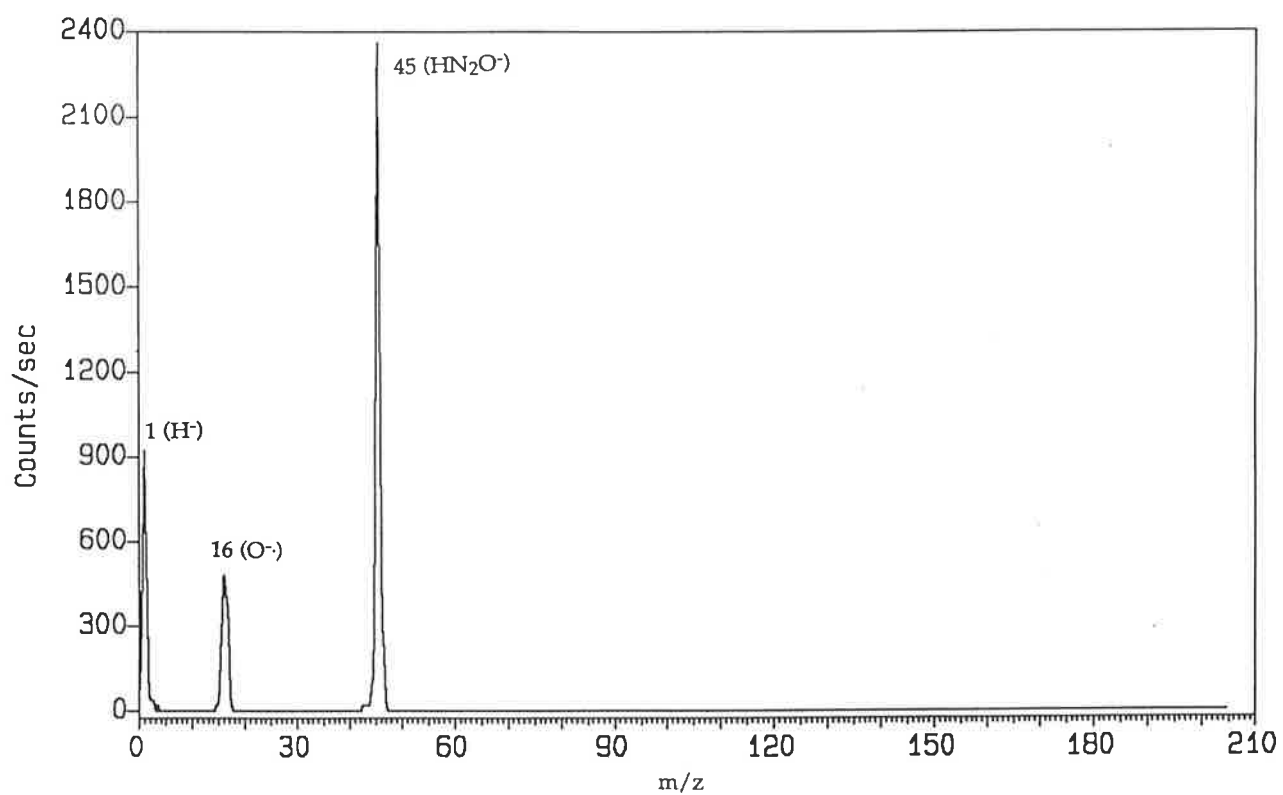


Figure 3.2 Collision induced decomposition mass spectrum of HN_2O^-

of N_2O .¹⁵¹ Isomerisation of these ions, however, is likely to be unfavourable. Figure 3.1 predicts the isomerisation (by a hydride transfer mechanism) of $\text{N}=\text{N}^+(\text{H})\text{O}^-$ to the more stable $\text{HN}=\text{NO}^-$ (equation 3.5) requires almost 200 kJ mol^{-1} whilst isomerisation in the reverse direction requires approximately 300 kJ mol^{-1} .



The generation of $[\text{HN}_2\text{O}]^-$ via the hydride transfer process resulted in a reactivity indistinguishable from that of $\text{HN}=\text{NO}^-$ from amide ion and neopentyl nitrite (Section 3.2). Thus if a mixture of isomers, or indeed one isomer of a different structure from $\text{HN}=\text{NO}^-$, is formed in this case no differentiation can be achieved based on reactivity.

The reactivity of $\text{HN}=\text{NO}^-$ generated by reaction of amide ion and neopentyl nitrite is now detailed. The inability to distinguish ions $\text{N}=\text{N}^+(\text{H})\text{O}^-$ and $\text{HN}=\text{NO}^-$ based on their reactivity is discussed.

3.2 The reactivity of $\text{HN}=\text{NO}^-$ in the flowing afterglow

3.2.1 Experimental determination of the basicity of $\text{HN}=\text{NO}^-$

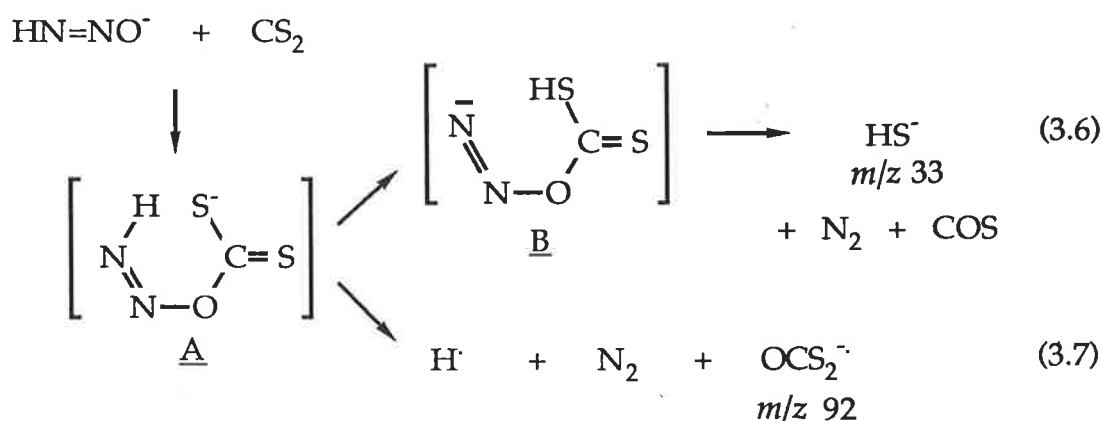
The basicity of the $\text{HN}=\text{NO}^-$ ion, prepared by the reaction of amide ion and neopentyl nitrite in the first flow tube, was determined by a bracketing experiment (see Section 1.7.2.2). The ion $\text{HN}=\text{NO}^-$ undergoes no reaction with acetophenone ($\Delta H^\circ_{\text{acid}}(\text{CH}_3\text{C}(\text{O})\text{Ph}) = 1512 \text{ kJ mol}^{-1}$ ¹¹²) but deprotonates nitromethane ($\Delta H^\circ_{\text{acid}}(\text{CH}_3\text{NO}_2) = 1491 \text{ kJ mol}^{-1}$ ¹¹²) (Table 3.1) and thus its proton affinity is estimated to be $1501 \pm 21 \text{ kJ mol}^{-1}$.

Table 3.1 Reactions of $\text{HN}=\text{NO}^-$ with hydrogen containing compounds. Products and branching ratios.		
Neutral	Products ^a	Branching Ratios
CH_3NO_2	$^-\text{CH}_2\text{NO}_2 + \text{HN}_2\text{OH}$ $^-\text{CH}_2\text{NO}_2(\text{CH}_3\text{NO}_2) + \text{HN}_2\text{OH}$	0.93 0.07
$\text{CH}_3\text{C}(\text{O})\text{Ph}$	-	-
CH_3Cl	$\text{Cl}^- + \text{HN}_2\text{OCH}_3$	1.0
CH_3NCO	$\text{CH}_3\text{NHCO}_2^- + \text{N}_2$ $(\text{C}_2\text{H}_3\text{N}_3\text{O}_2)^-\cdot \text{b} + \text{H}\cdot$ $\text{NCO}^- + \text{HN}_2\text{OCH}_3$	0.83 0.11 0.06
CH_3NCS	$\text{HS}^- + \text{CH}_3\text{NCO} + \text{N}_2$ $(\text{C}_2\text{H}_3\text{N}_3\text{OS})-\cdot \text{b} + \text{H}\cdot$ $\text{NCS}^- + \text{HN}_2\text{OCH}_3$	0.51 0.36 0.13

"a" Neutral product structures rationalised through plausible mechanisms. "b" Product ion structure unknown.

3.2.2 Reactions of $\text{HN}=\text{NO}^-$ involving oxidation

The reactions of $\text{HN}=\text{NO}^-$ with non-hydrogen containing compounds (Table 3.2) proceed typically by initial oxygen attack to produce an adduct which collapses either prior to or following an internal proton transfer. For example, consider the reaction of $\text{HN}=\text{NO}^-$ and carbon disulphide (Figure 3.3). The reaction proceeds, in the main, with the formation of HS^- (m/z 33) rationalised through a process shown in equation 3.6. Initial formation of adduct A is followed by an internal proton transfer (from the terminal nitrogen to sulphur) through a six-centred transition state. Subsequent decomposition of the intermediate B yields N_2 , COS and HS^- .



Alternatively, the adduct A can decompose prior to proton transfer by homolytic cleavage of the nitrogen-oxygen bond (equation 3.7). This results in the formation of OCS_2^- (m/z 92) as a minor product.

In this context, the isomeric ion $^-\text{N}=\text{N}^+(\text{H})\text{O}^-$ [possibly produced in the formation of $(\text{HN}_2\text{O})^-$ by hydride addition] is expected to react similarly to that $\text{HN}=\text{NO}^-$. The reaction of $^-\text{N}=\text{N}^+(\text{H})\text{O}^-$ with CS_2 may produce HS^- and OCS_2^- by the mechanisms shown in equations 3.8 and 3.9.

Table 3.2 Reactions of $\text{HN}=\text{NO}^-$ with non-hydrogen containing compounds. Products, branching ratios, rate constants and reaction efficiencies. ^a				
Neutral	Products ^b	Branching Ratios	k_{expt} ($\text{cm}^3 \text{ molecule}^{-1} \text{ sec}^{-1}$)	$k_{\text{expt}}/k_{\text{ADO}}^{\text{c}}$
CS_2	$\text{HS}^- + \text{COS} + \text{N}_2$	0.96	1.5×10^{-11}	0.01
	$\text{OCS}_2^- + \text{H} \cdot + \text{N}_2$	0.04		
COS	$\text{HO}^- + \text{COS} + \text{N}_2$	0.70	6.3×10^{-11}	0.05
	$\text{HS}^- + \text{CO}_2 + \text{N}_2$	0.28		
	$\text{HN}_2\text{S}^- + \text{CO}_2$	0.02		
SO_2	$\text{HO}^- + \text{SO}_2 + \text{N}_2$	0.66	1.6×10^{-10}	0.11
	$\text{SO}_3^- + \text{H} \cdot + \text{N}_2$	0.30		
	$\text{SO}_2^- + \text{HN}_2\text{O} \cdot$	0.02		
	$\text{HN}_2\text{OSO}_2^-$	0.02		
CO_2	$\text{HO}^- + \text{CO}_2 + \text{N}_2$	0.73	$< 5 \times 10^{-12}$	< 0.01
	$\text{HCO}_3^- + \text{N}_2$	0.27		
$^{13}\text{CO}_2$	$\text{HO}^- + ^{13}\text{CO}_2 + \text{N}_2$	0.73	-	-
	$\text{H}^{13}\text{CO}_3^- + \text{N}_2$	0.27		
O_2	-	-	-	-

"a" Products and branching ratios are identical to those observed for the reactions of $(\text{HN}_2\text{O})^-$ produced from the hydride addition process. "b" Neutral product structures rationalised through plausible mechanisms. "c" k_{ADO} calculated by the method of Su and Bowers.⁷⁷

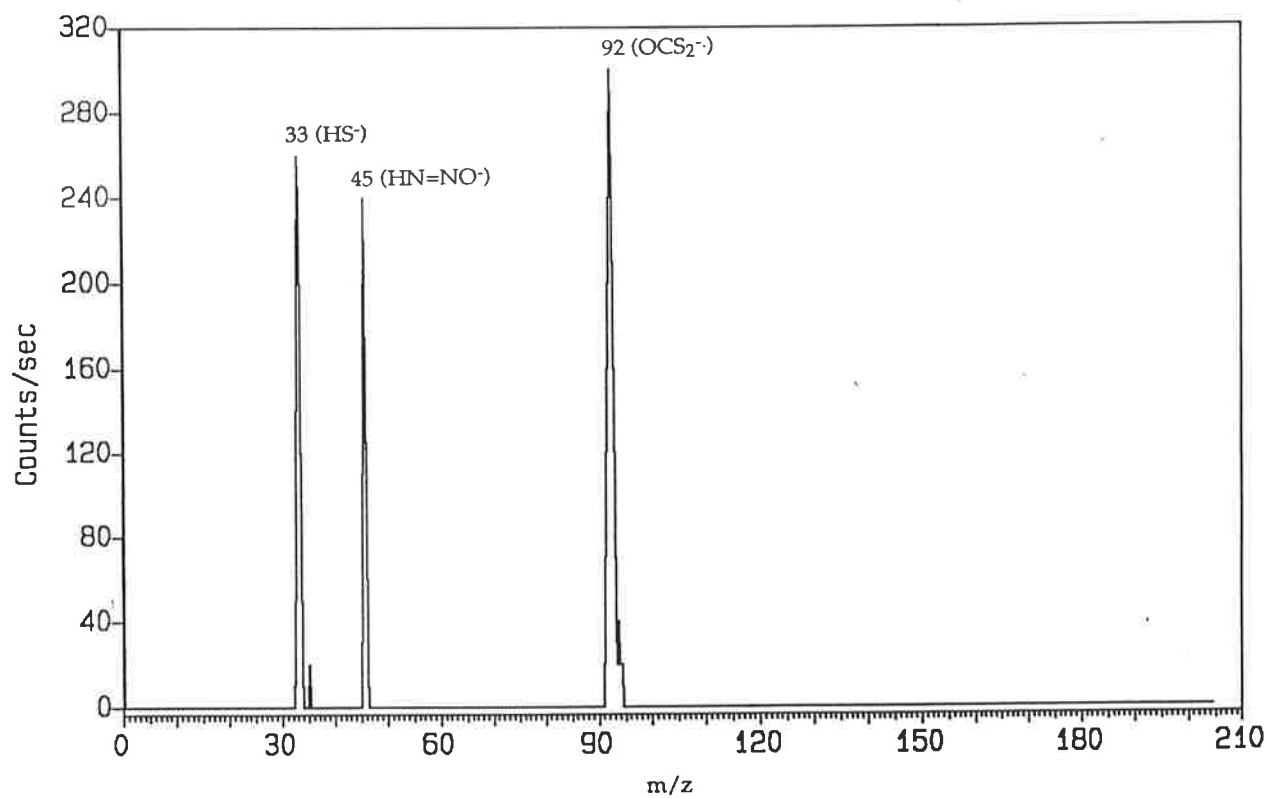
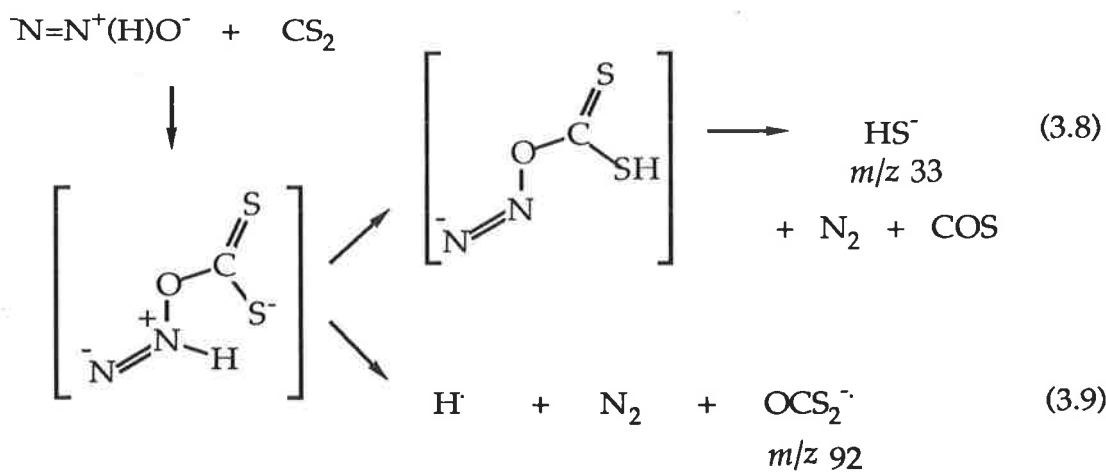
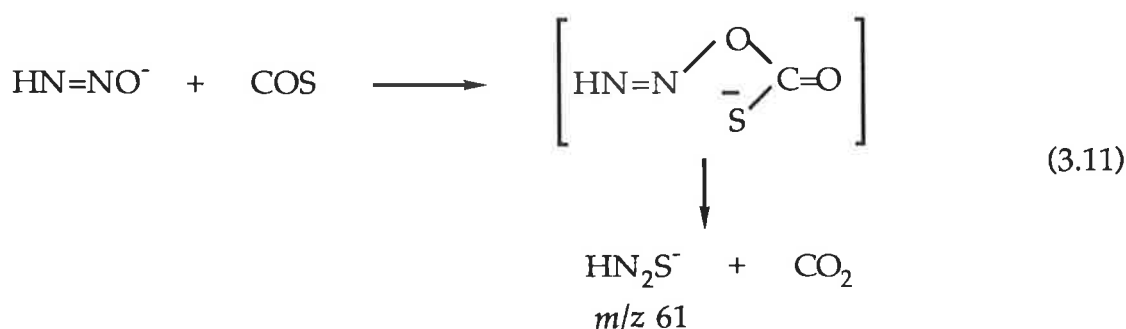
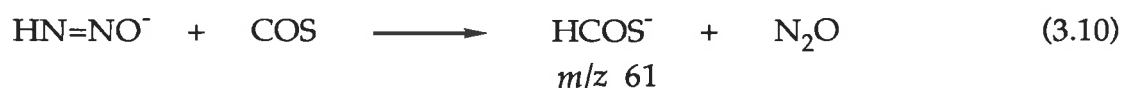


Figure 3.3 Reaction of $\text{HN}=\text{NO}^-$ with carbon disulphide.



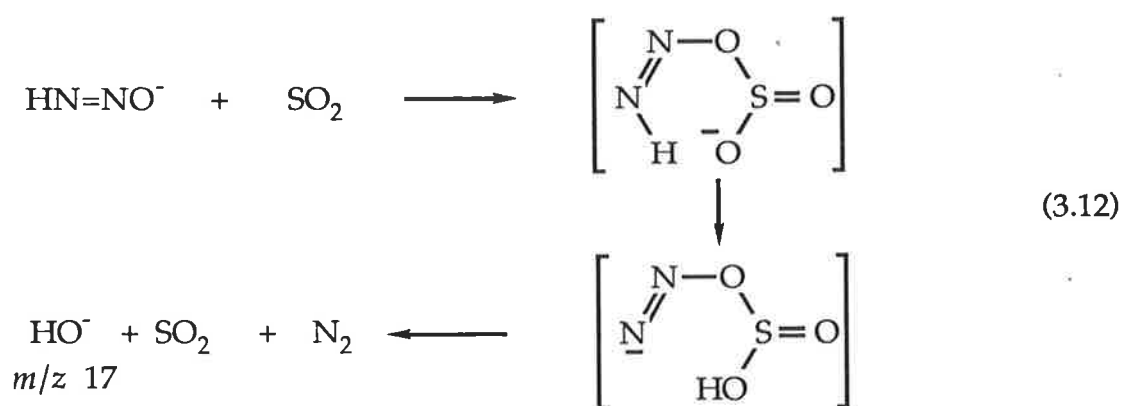
The reaction of $\text{HN}=\text{NO}^-$ with carbonyl sulphide (Table 3.1) affords major products best rationalised through a process analogous to that shown in equation 3.6. In this case, however, proton transfer in the first formed adduct can take place from nitrogen to either oxygen or sulphur. As a result, both HO^- (*m/z* 17) and HS^- (*m/z* 33) are observed products. The favoured formation of HO^- over HS^- reflects the increased basicity of the oxygen centre over sulphur.

A minor product of the reaction with carbonyl sulphide could correspond to HCOS^- (*m/z* 61), produced from a hydride ion transfer reaction (equation 3.10), or HN_2S^- (*m/z* 61) from a sulphur-oxygen exchange reaction represented in equation 3.11.



Of these two processes, the latter is more likely since despite the similar hydride affinities of carbon disulphide and carbonyl sulphide (281¹⁵² and 278¹⁵² kJ mol⁻¹ respectively) no hydride addition product was detected upon the reaction of HN=NO⁻ and CS₂. In addition, carbonyl sulphide is known to undergo sulphur transfer reactions,^{121,122} whilst product HN₂S⁻ has been reported elsewhere to be a stable species.^{153,154}

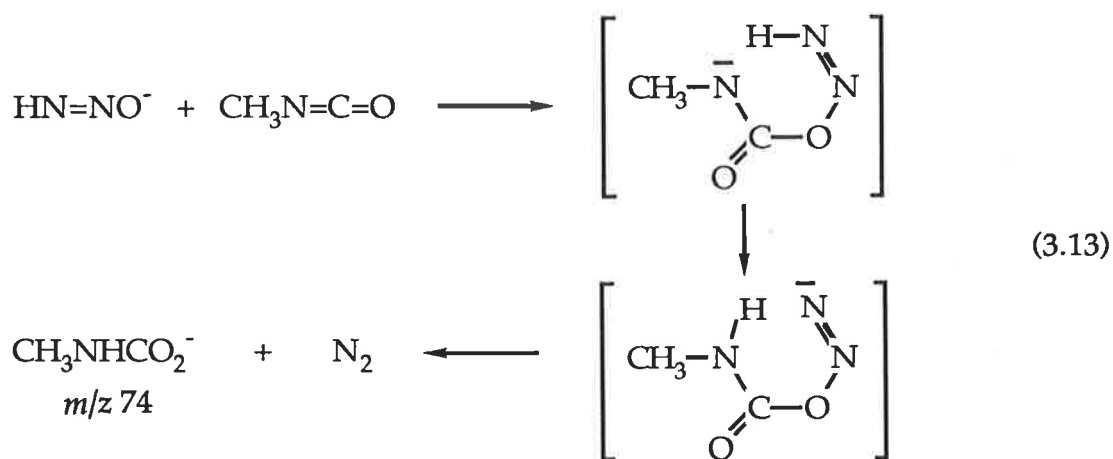
The ion HN=NO⁻ undergoes a reaction with sulphur dioxide with a reaction efficiency of 0.1. The major product of this reaction is HO⁻ (*m/z* 17) (equation 3.12). Oxygen transfer product SO₃⁻ (*m/z* 80) is produced by a process analogous to that shown in equation 3.7. Traces of adduct (*m/z* 109) and electron transfer product SO₂⁻ (*m/z* 64) were also detected.



With carbon dioxide, HN=NO⁻ reacts to afford HO⁻ (*m/z* 17) and HCO₃⁻ (*m/z* 61). The possibility of a hydride transfer reaction must also be considered here. Such a reaction will result in the formation of product ion HCO₂⁻ which has the same nominal mass (*m/z* 45) as the reactant ion HN=NO⁻. Therefore reaction with ¹³C-labelled carbon dioxide was performed. No product at *m/z* 46 (H¹³CO₂⁻) was detected; thus a hydride transfer does not occur in this reaction.

The ion $\text{HN}=\text{NO}^-$ undergoes no reaction with oxygen, yet reacts nucleophilically with methyl chloride to generate chloride ion (m/z 35,37) (Table 3.1).

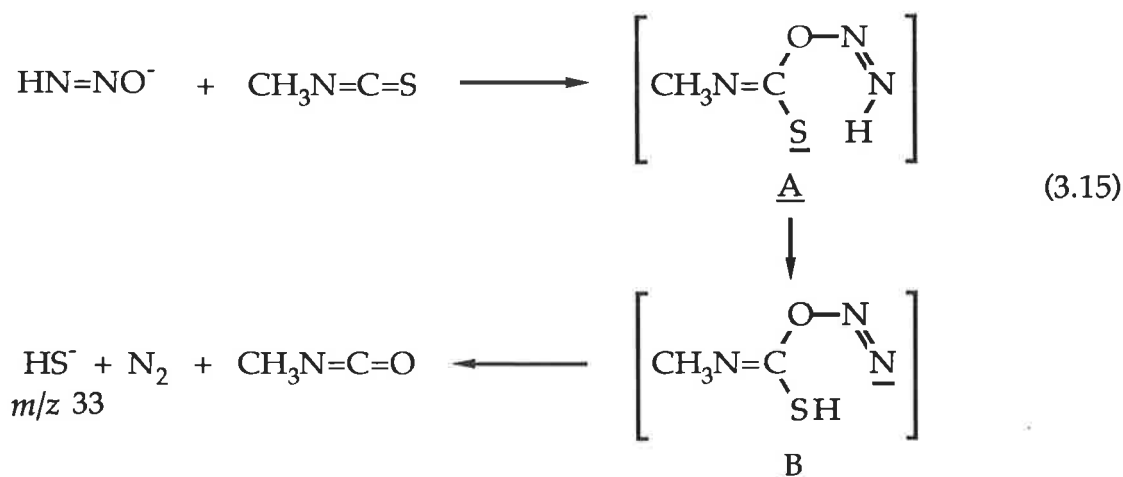
To determine the propensity of $\text{HN}=\text{NO}^-$ to undergo both oxidation and nucleophilic substitution reactions, it was allowed to react with both methyl isocyanate and methyl isothiocyanate (Table 3.1). These reactions enable the extent of oxidation versus nucleophilic substitution to be gauged within the same molecule.¹⁵⁵ With methyl isocyanate, $\text{HN}=\text{NO}^-$ reacts to produce oxidation product $\text{CH}_3\text{NHCO}_2^-$ (m/z 74) (equation 3.13).



This oxidation reaction results effectively in the transfer of hydroxide ion from $\text{HN}=\text{NO}^-$ to methyl isocyanate. This mirrors the chemistry observed on reaction of $\text{HN}=\text{NO}^-$ with SO_2 and CO_2 described above. By comparison, the nucleophilic substitution reaction between $\text{HN}=\text{NO}^-$ and methyl isocyanate to afford NCO (m/z 42) (equation 3.14) is observed to a much lesser extent.

The major reaction pathway of $\text{HN}=\text{NO}^-$ with methyl isothiocyanate is also an initial oxidation reaction. However, in this case no hydroxide addition product $\text{CH}_3\text{NHCOS}^-$ (m/z 90) is observed. Instead, the spectrum is

dominated by the formation of HS^- (m/z 33) rationalised by the mechanism shown equation 3.15.



In this instance, it is proposed that proton transfer within adduct A occurs from nitrogen to sulphur. The result is an unstable intermediate B which may decompose to HS^- (m/z 33), molecular nitrogen and methyl isocyanate. The dissociation of intermediate B directly to HS^- [with no hydroxide addition product $\text{CH}_3\text{NHCOS}^-$ (m/z 90) being observed] is consistent with the fact that HS^- is a better leaving group than HO^- based on its lower basicity. The reaction of $\text{HN}=\text{NO}^-$ with methyl isothiocyanate affords NCS^- (m/z 58) by nucleophilic substitution as only a minor product. Thus the reaction of $\text{HN}=\text{NO}^-$ with both methyl isocyanate and methyl isothiocyanate result primarily in the formation of products from oxidation processes.

In summary, $\text{HN}=\text{NO}^-$ prepared exclusively by the reaction of amide ion and neopentyl nitrite has a reactivity indistinguishable from that of $(\text{HN}_2\text{O})^-$ formed via the hydride transfer process. Oxygen and hydroxide addition products are produced by fragmentation of either (i) the initially formed adduct, or (ii) an adduct formed following a proton transfer reaction. Since hydride ion addition is predicted to occur to both the central and terminal nitrogen of N_2O (based on *ab initio* calculations), both $\text{N}=\text{N}^+(\text{H})\text{O}^-$ and

HN=NO⁻ are expected to be present to some extent by this process. The indistinguishable reactivity of HN=NO⁻ (produced from amide ion and neopentyl nitrite) from that of HN₂O⁻ from the hydride addition process can be accounted for through similar reactive pathways to products (see equations 3.6 - 3.9).

3.3 Thermochemistry of the HN=NO⁻ ion

The determination of the basicity of HN=NO⁻ by a bracketing experiment [$\Delta H^{\circ}_{\text{acid}}(\text{HN}=\text{NOH}) = 1501 \text{ kJ mol}^{-1}$, Section 3.2.1] permits the heat of formation of this ion to be calculated. $\Delta H^{\circ}_f(\text{HN}=\text{NO}^-)$ is estimated to be 117 kJ mol⁻¹ (from equation 3.16) using a reported value for $\Delta H^{\circ}_f(\text{HN}=\text{NOH})$ of 146 kJ mol⁻¹.¹⁵⁶

$$\Delta H^{\circ}_f(\text{HN}_2\text{O}^-) = \Delta H^{\circ}_f(\text{HN}_2\text{OH}) - \Delta H^{\circ}_f(\text{H}^+) + \Delta H^{\circ}_{\text{acid}}(\text{HN}_2\text{OH}) \quad (3.16)$$

This value is in agreement with an upper limit for $\Delta H^{\circ}_f(\text{HN}=\text{NO}^-)$ of 130 kJ mol⁻¹ calculated by Kass and DePuy.¹¹⁹ It is not consistent, however, with a recent estimate by Kass¹¹³ who reported $\Delta H^{\circ}_f(\text{HN}_2\text{O}^-) \leq 73 \text{ kJ mol}^{-1}$.

Calculation of $\Delta H^{\circ}_f(\text{HN}_2\text{O}^-)$ enables the hydride affinity of N₂O to be determined. Using a reported value of $\Delta H^{\circ}_f(\text{N}_2\text{O})$ of 82 kJ mol⁻¹¹⁵⁷, the hydride affinity of N₂O is calculated to be 110 kJ mol⁻¹ from equation 3.17.

$$\text{H.A.}(\text{N}_2\text{O}) = \Delta H^{\circ}_f(\text{N}_2\text{O}) + \Delta H^{\circ}_f(\text{H}^-) - \Delta H^{\circ}_f(\text{HN}_2\text{O}^-) \quad (3.17)$$

**Chapter 4 THE ELIMINATION OF ETHENE FROM DEPROTONATED
ETHYL METHYL SULPHOXIDE. THE FORMATION,
STRUCTURE AND REACTIVITY OF THE METHYL
SULPHINYL ANION.**

4.1 Introduction

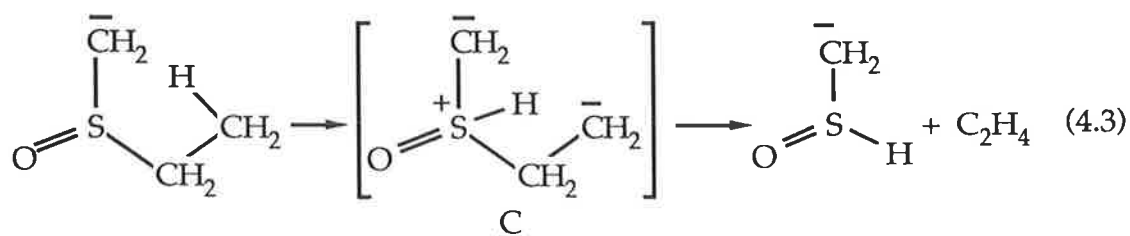
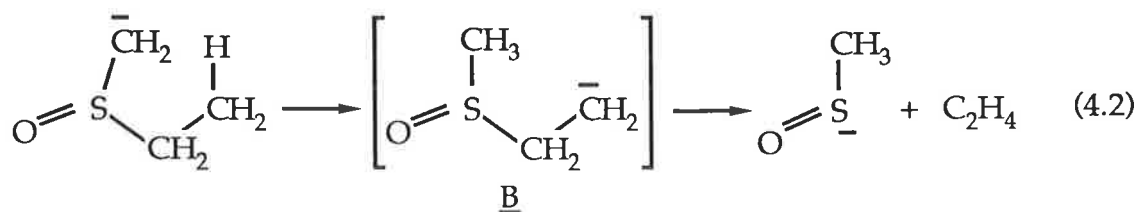
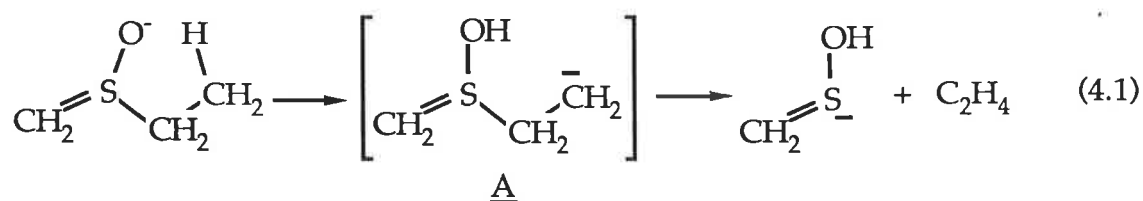
The successful generation of the methylene thiol anion (Section 2.2.3.2) prompted interest in its sulphur-oxidised analogue, the α -sulphinyl carbanion $^{-}\text{CH}_2\text{S}(\text{O})\text{H}$. This ion, and its isomer the methyl sulphinyl anion CH_3SO^{-} , are simple sulphur analogues of the acetaldehyde enolate and the acetyl anion which have been shown to exist in the gas phase as discrete species, stable to isomerisation under collision activation conditions.¹⁴⁸

Whilst the α -sulphinyl carbanion has received considerable theoretical interest by Wolfe and colleagues¹⁵⁸⁻¹⁶⁰ it has eluded direct detection in the gas phase. The most probable reason for this is the lack of a stable neutral precursor. Simple alkane sulphenic acids are known to be extremely unstable species which can only be isolated for short life times at low temperatures.¹⁶¹⁻¹⁶³ They exhibit high reactivity as either electrophiles or nucleophiles and undergo facile dimerisation to thiosulphinate esters.^{164,165} Similarly, α -trimethylsilyl-methane sulphenic acid, a useful precursor for the attempted formation of $^{-}\text{CH}_2\text{S}(\text{O})\text{H}$ (see Section 2.2.1), is unstable to dimerisation at ambient temperatures, albeit in solution.¹⁶⁶ Its transient existence is at best inferred based on the products isolated. Attempts to prepare α -trimethylsilyl-methane sulphenic acid [which could provide a direct route to the generation of $^{-}\text{CH}_2\text{S}(\text{H})\text{O}$ for this study] have proved unsuccessful.

The preferred precursors for the generation of simple sulphenic acids by flash vacuum pyrolysis are appropriately substituted sulphoxides.¹⁶¹⁻¹⁶³ By

analogy, a deprotonated sulphoxide may undergo an elimination reaction to afford a deprotonated sulphenic acid. A base-catalysed elimination reaction¹⁶⁷⁻¹⁷⁶ of ethyl methyl sulphoxide does occur in the ion source of the ZAB-2HF mass spectrometer to produce an ion at m/z 63. Three possible isomeric forms need to be considered for the structure of the m/z 63 ion.

The loss of ethene from deprotonated ethyl methyl sulphoxide can be accompanied by β -proton transfer to either oxygen, carbon or sulphur. If proton transfer occurs to oxygen (equation 4.1) the product of the ethene elimination is $\text{CH}_2=\text{S}^--\text{OH}$; a resonance form of the α -substituted carbanion $^-\text{CH}_2\text{SOH}$. Alternatively, β -proton transfer to the α -carbon (equation 4.2) produces the methyl sulphanyl anion $\text{CH}_3\text{S}^--\text{O}$. This ion exhibits two resonance forms in which the charge resides on either sulphur or oxygen. A third possibility must also be considered. Namely, a proton transfer from the β -carbon to sulphur through a four-centred transition state (equation 4.3) can result in a loss of ethene. The product of this process is the elusive α -sulphanyl carbanion $^-\text{CH}_2\text{S(O)H}$.



Each of these three processes (equations 4.1 - 4.3) could be envisaged to generate an ion (m/z 63) corresponding to the loss of C_2H_4 . Depending on the energetics of each pathway and the stability of the product ions, a single isomer may possibly be produced in favour of the others. Alternatively, two or all three of the isomers may be generated.

4.2 Structure elucidation of the $(CH_3SO)^-$ ion

In order to distinguish the existence of a single isomer from that of several isomers, the collisional activation and charge reversal mass spectra of the m/z 63 ion (produced from the reaction of hydroxide ion and ethyl methyl sulphoxide in the ion source of the ZAB-2HF mass spectrometer) were recorded.

The C.A. mass spectrum (Figure 4.1, Table 4.1) is dominated by the loss of atomic hydrogen (m/z 62) yet it also exhibits fragments at m/z 48 and 45 resulting from the losses of methyl radical and water respectively. The loss of $CH_3\cdot$ can only arise from the methyl sulphanyl anion by a simple homolytic cleavage of the carbon-sulphur bond, whilst the loss of H_2O can be explained by the fragmentation of isomeric ions $^-CH_2SOH$ (equation 4.4) or $^-CH_2S(O)H$ (equation 4.5). In the absence of collision gas, the abundance of the fragment ions from the loss of $CH_3\cdot$ and H_2O are considerably reduced (Table 4.1). These fragmentations are therefore almost entirely collision induced; unimolecular decomposition of the m/z 63 ion contributes to the formation of the daughter ions at m/z 48 and 45 by approximately 5%.

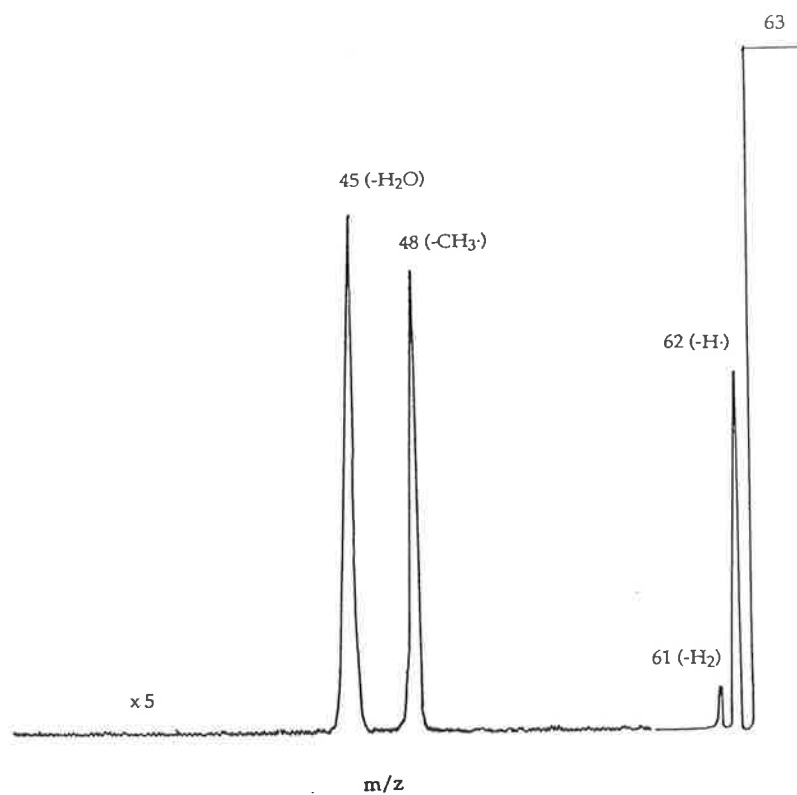


Figure 4.1 Collisional activation mass spectrum of the m/z 63 ion (CH_3SO^-) produced on loss of ethene from deprotonated ethyl methyl sulphoxide.

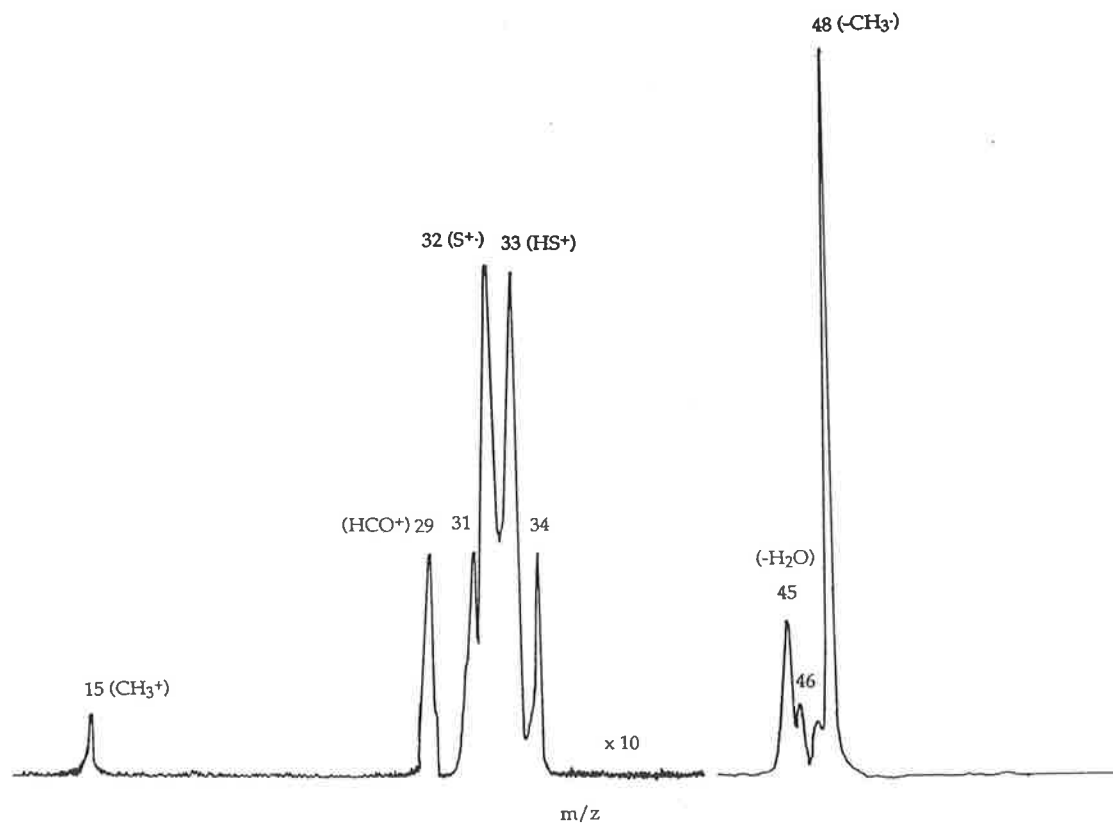


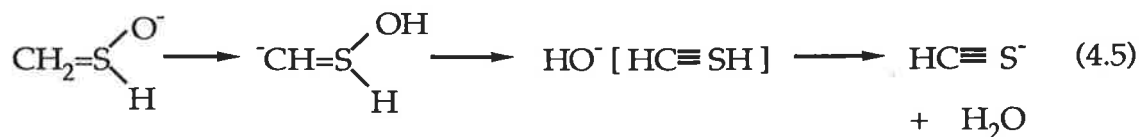
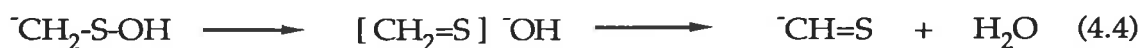
Figure 4.2 Charge reversal mass spectrum of the m/z 63 ion (CH_3SO^-) produced on the loss of ethene from deprotonated ethyl methyl sulphoxide.

ion	spectrum type	m/z (abundance)											
		62	61	48	47	46	45	34	33	32	31	29	15
CH_3SO^-	CA MS/MS ^a	100	8	25			28						
	CR MS/MS			100	11	13	24	3	8	9	3	5	1

"a" When a potential of +1000 V is applied to the collision cell, 95% of decompositions at m/z 45 and 48 are shifted to lower voltages. Consequently, 5% of the decompositions at m/z 45 and 48 occur outside the collision cell i.e. are unimolecular. (Note that due to the possibility of some leakage of collision gas from the cell, this unimolecular component may be, in part, collision induced.)

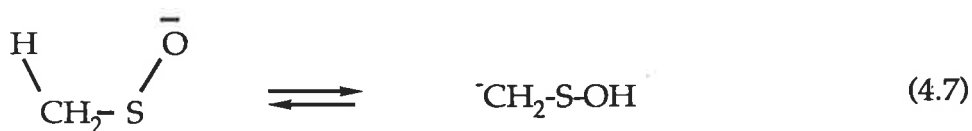
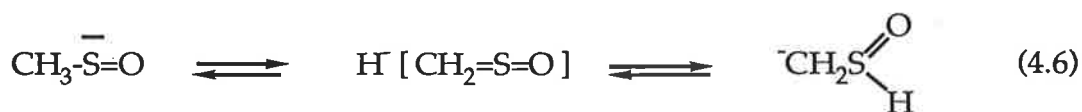
Neutral	Products ^a	Branching Ratios
CH_3NO_2	$^-\text{CH}_2\text{NO}_2 + \text{CH}_3\text{SOH}$	1.0
$\text{CF}_3\text{CH}_2\text{OH}$	-	-
CH_3NCO	$\text{CH}_3\text{SO}^- (\text{CH}_3\text{NCO})$	0.72
	$\text{CH}_3\text{NHCO}_2^- + \text{CH}_2\text{S}$	0.26
	$^-\text{CN} + \text{CO}_2 + \text{CH}_3\text{SH}$	0.02
CH_3NCS	$\text{CH}_3\text{SO}^- (\text{CH}_3\text{NCS})$	0.76
	$\text{NCS}^- + \text{CH}_3\text{SOCH}_3$	0.24
$\text{HCO}_2\text{CH}_2\text{CH}_3$	$\text{CH}_3\text{SO}^- (\text{HCO}_2\text{CH}_2\text{CH}_3)$	0.68
	$\text{CH}_3\text{SO}^- (\text{CH}_3\text{CH}_2\text{OH}) + \text{CO}$	0.32
D_2O	$\text{CH}_3\text{SO}^- (\text{D}_2\text{O})$	0.90
	$\text{CH}_3\text{SO}^- (\text{D}_2\text{O})_2$	0.10

"a" Neutral product structures rationalised through plausible mechanisms.



Similarly, the C.R. mass spectrum of $(\text{CH}_3\text{SO})^-$ (Figure 4.2, Table 4.1) shows major fragment peaks corresponding to the losses of methyl radical and water.

Whilst these spectra infer the existence of isomers CH_3SO^- , $\text{CH}_2\text{S-OH}^-$ and/or $\text{CH}_2\text{S(O)H}^-$ on collisional activation, they do not distinguish whether a particular isomer is produced initially in the ion source or by isomerisation proceeding or accompanying collisional activation (equations 4.6 - 4.8).

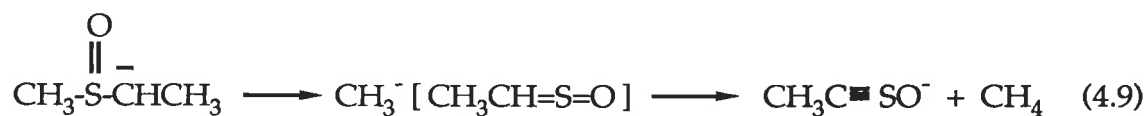


In order to differentiate between these possibilities, the reactivity of the m/z 63 ion was probed within the flowing afterglow-S.I.F.T. (Section 1.7.2).

4.3 Reactivity of the $(\text{CH}_3\text{SO})^-$ ion

Deprotonation of ethyl methyl sulphoxide with hydroxide ion in the first flow tube of the F.A.-S.I.F.T. results in the formation of parent ion (m/z 91)

in addition to decomposition products arising from the loss of ethene (m/z 63) (equations 4.1 - 4.3) and methane (m/z 75) (equation 4.9) (see Figure 4.3). The m/z 63 ion was injected solely into the second flow tube (utilising the quadrupole mass filter) and its reactivity was subsequently investigated.



4.3.1 Experimental determination of the basicity of (CH₃SO)⁻

A guide to the structure of an ion is its basicity. The m/z 63 ion deprotonates nitromethane [$\Delta H^\circ_{\text{acid}}(\text{CH}_3\text{NO}_2) = 1491 \text{ kJ mol}^{-1}$ ¹¹²] but not 2,2,2-trifluoroethanol [$\Delta H^\circ_{\text{acid}}(\text{CF}_3\text{CH}_2\text{OH}) = 1514 \text{ kJ mol}^{-1}$ ¹¹²] (Table 4.2) and thus its basicity is estimated as $1501 \pm 22 \text{ kJ mol}^{-1}$. This basicity is considerably less than that predicted for the α -substituted carbanion $\text{-CH}_2\text{SOH}$ whose proton affinity would be anticipated to be in the order of 1670 kJ mol^{-1} [based on that of $\text{-CH}_2\text{SH}$ ($\Delta H^\circ_{\text{acid}}(\text{CH}_3\text{SH}) = 1669 \text{ kJ mol}^{-1}$, Section 2.2.3.1)]. It is also less basic than that predicted for $\text{-CH}_2\text{S(O)H}$ since the proton affinity of this ion should be of the same order as that of deprotonated dimethylsulphoxide [$\Delta H^\circ_{\text{acid}}(\text{CH}_3\text{S(O)CH}_3) = 1563 \pm 10 \text{ kJ mol}^{-1}$ ¹¹²].

DePuy and co-workers have recently studied the reaction of a variety of gas phase nucleophiles with alkyl halides.¹⁷⁷ They showed that some correlation exists between the basicity of a nucleophile and its reaction efficiency with an alkyl halide. The effect was rationalised by suggesting that an increase in the basicity of a nucleophile lowers the energy of the products for reaction. Consequently the reaction becomes more exothermic.

As a result of this investigation, the measurement of the reaction rate (and hence reaction efficiency) of an ion with several alkyl halides enables the

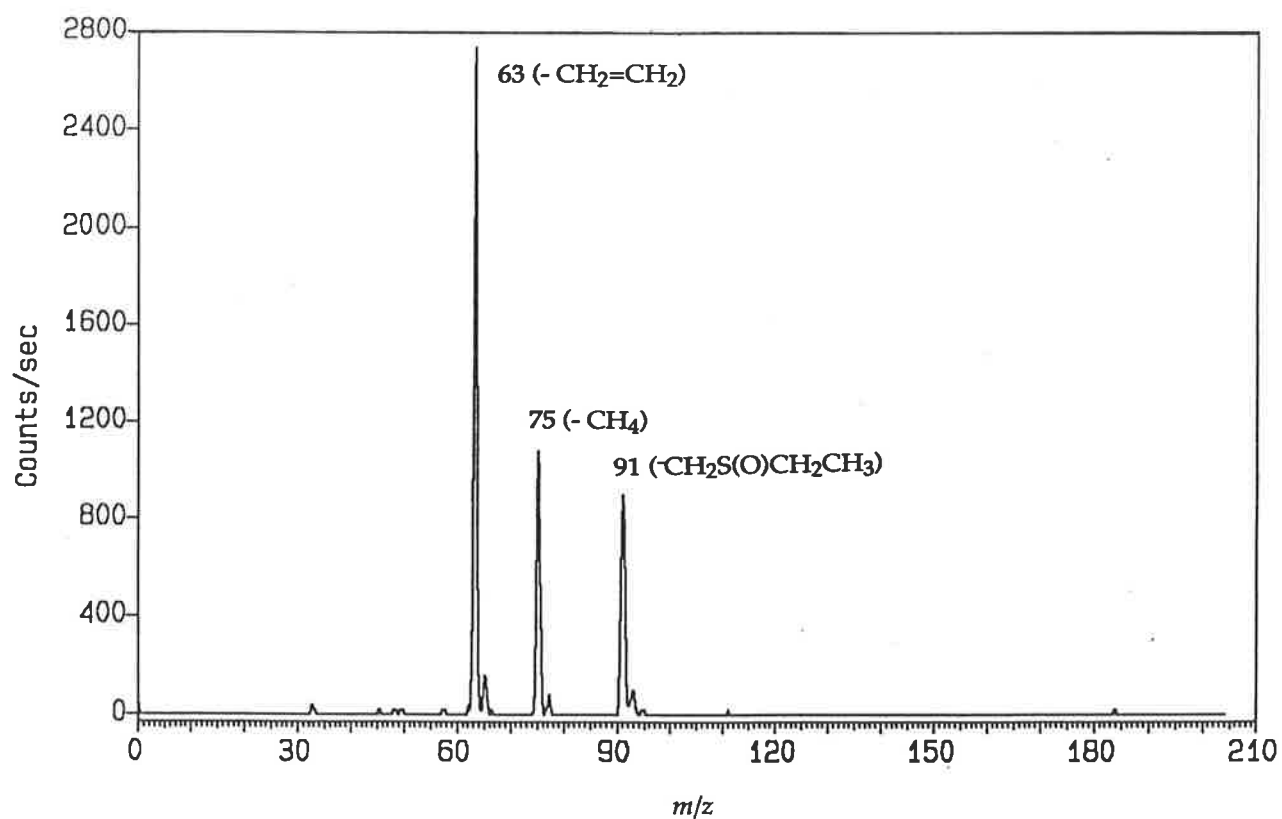


Figure 4.3 Collision induced dissociation spectrum of deprotonated ethyl methyl sulphoxide produced in the flowing afterglow - S.I.F.T.

basicity of the ion to be estimated. The reaction of the m/z 63 ion with methyl chloride ($k_{\text{expt}} = 1.5 \times 10^{-10} \text{ cm}^3 \text{ molecule}^{-1} \text{ sec}^{-1}$) and *iso* propyl chloride ($k_{\text{expt}} = 4.5 \times 10^{-11} \text{ cm}^3 \text{ molecule}^{-1} \text{ sec}^{-1}$) produces exclusively chloride ion (m/z 35,37) (Table 4.3), rationalised through S_N2 and E2 reaction processes respectively. The reaction efficiencies for these reactions, 0.09 and 0.02 respectively, are in accord with the reactivity of an anion whose conjugate acid has an acidity in the order of 1510 kJ mol^{-1} .

It appears, then, that the m/z 63 ion produced by the base-catalysed elimination of ethyl methyl sulphoxide exhibits a structure corresponding to the methyl sulphanyl anion CH_3SO^- . If this is so, then the possible isomerisation processes shown in equations 4.6 - 4.8 must occur primarily following or accompanying collisional activation.

4.3.2 The reactivity of the methyl sulphanyl anion

The methyl sulphanyl anion has two resonance forms which correspond to a sulphenate-like (A) or sulphoxide-like (B) form (Figure 4.4).



Figure 4.4 Two resonance forms of the methyl sulphanyl anion CH_3SO^- .

In support of an ion whose charge resides on oxygen, CH_3SO^- exhibits the reactivity of an effective oxidising agent. Oxidation products, or fragments produced therefrom, are detected in a variety of reactions of CH_3SO^- (Table 4.3). For example, CH_3SO^- reacts rapidly with carbon disulphide (Figure 4.5) to afford oxygen transfer product OCS_2^- (m/z 92) (equation 4.10).

Neutral	Products ^a	Branching Ratios	$k_{\text{expt}}^{\text{b}}$	$k_{\text{expt}}/k_{\text{ADO}}^{\text{c}}$
CS_2	$\text{HS}^- + \text{CH}_2\text{S} + \text{COS}$	0.73 ^d	3.69	0.31
	$\text{CH}_3\text{SS}^- + \text{COS}$	0.20		
	$\text{OCS}_2^- + \text{CH}_3\text{S}^-$	0.06		
	$\text{CH}_3\text{SOCS}_2^-$	0.01		
COS	$\text{HS}^- + \text{CH}_2\text{S} + \text{CO}_2$	0.95 ^d	0.32	0.03
	$\text{HSCO}_2^- + \text{CH}_2\text{S}$	0.03		
	$\text{CH}_3\text{SOCOS}^-$	0.02		
SO_2	$\text{SO}_2^- + \text{CH}_3\text{SO}^-$	0.95	16.1	1.2
	$\text{SO}_3^- + \text{CH}_3^-$	0.02		
	$\text{HSO}_3^- + \text{CH}_2\text{S}$	0.03		
CO_2	$\text{CH}_3\text{SOCO}_2^-$	0.86	< 0.05	< 0.01
	$(\text{C}_2\text{HSO}_2^-)^{\text{e}} + \text{H}_2\text{O}$	0.14		
O_2	$\text{HC(O)SO}^- + \text{H}_2\text{O}$	0.40	1.96	0.31
	$\text{SO}_3^- + \text{CH}_3^-$	0.23		
	$\text{HCSO}^- + \text{H}_2\text{O}_2$	0.20		
	$\text{O}^- + \text{CH}_3\text{SO}_2^-$	0.17		
N_2O	-	-	-	-
CH_3Cl	$\text{Cl}^- + \text{CH}_3\text{S(O)CH}_3$	1.0	1.45	0.09
$(\text{CH}_3)_2\text{CHCl}$	$\text{Cl}^- + \text{CH}_2=\text{CHCH}_3 + \text{CH}_3\text{S(O)H}$	1.0	0.45	0.02

"a" Neutral product structures rationalised through plausible mechanisms, "b" $\times 10^{-10} \text{ cm}^3 \text{ molecule}^{-1} \text{ sec}^{-1}$, "c" k_{ADO} calculated by the method of Su and Bowers⁷⁷, "d" The formation of the HS^- product from this reaction is complicated by the presence of small amounts of impurity H_2S in the neutral sample used. Branching ratios therefore may be subject to larger errors. "e" Structure of ion unknown.

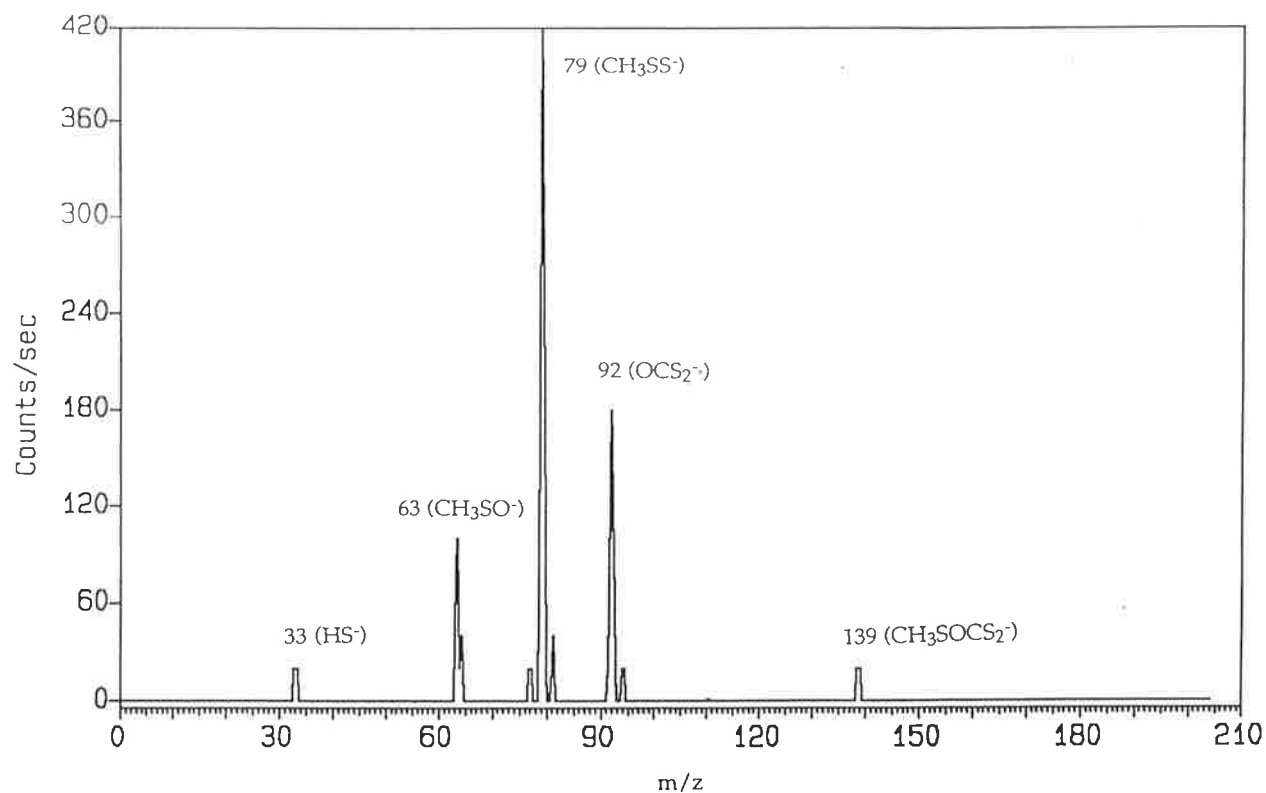


Figure 4.5 The reaction of the methyl sulphinyl anion CH_3SO^- with carbon disulphide.

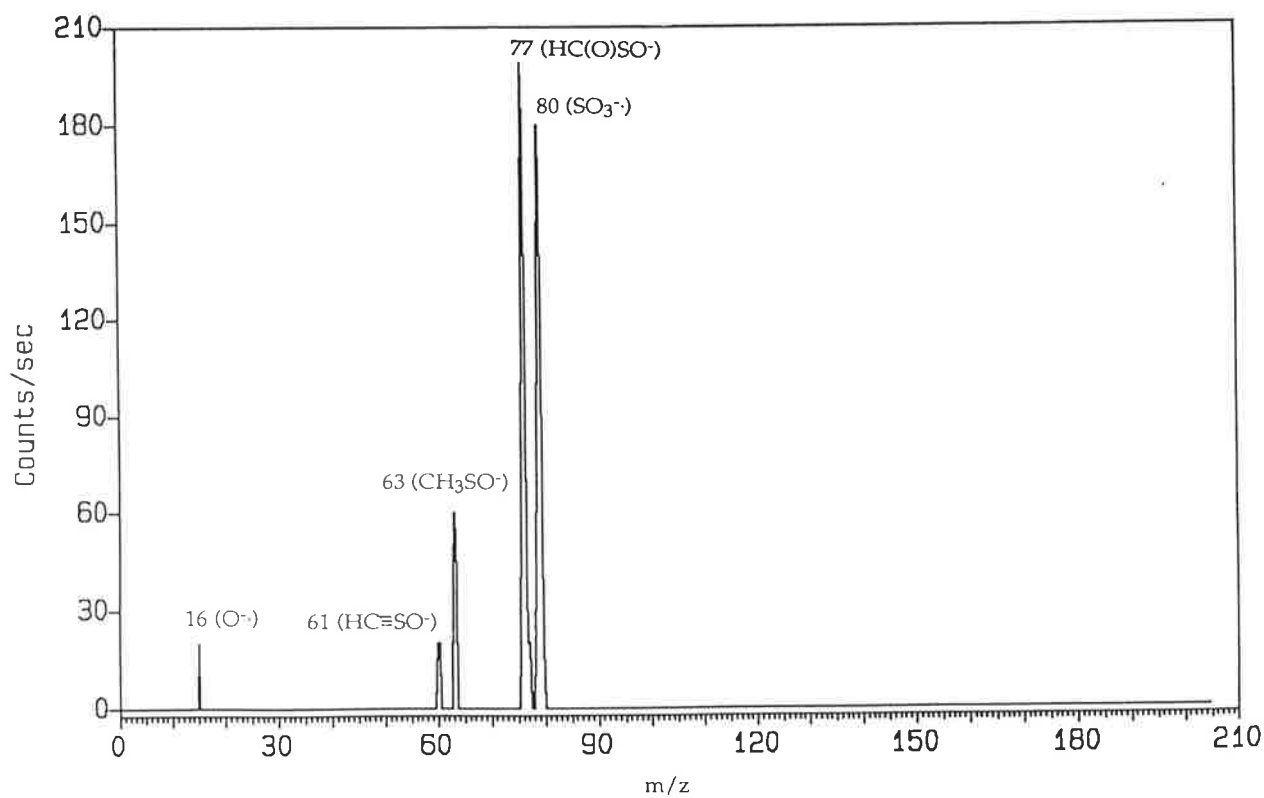
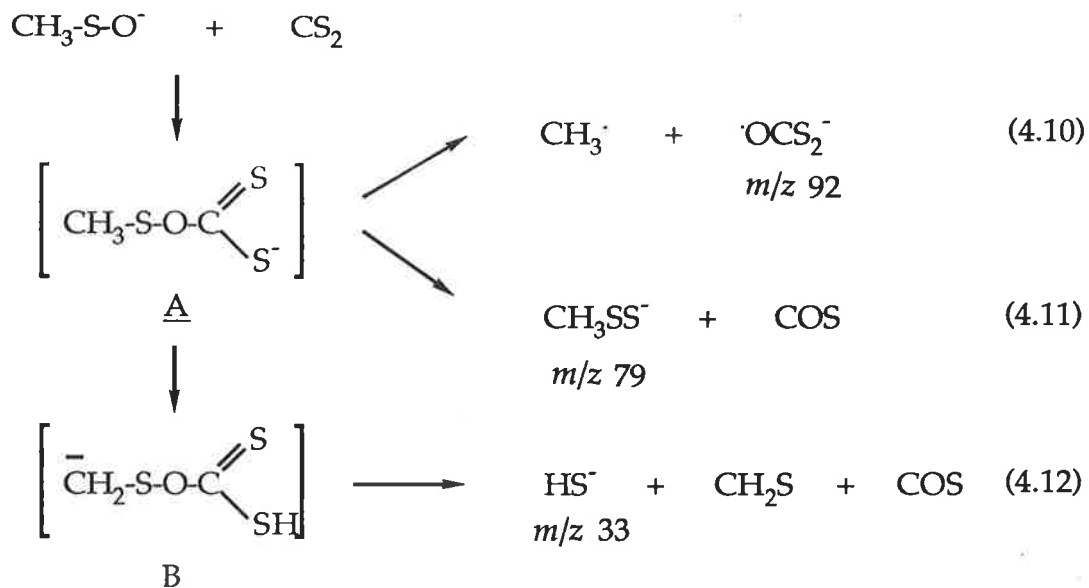
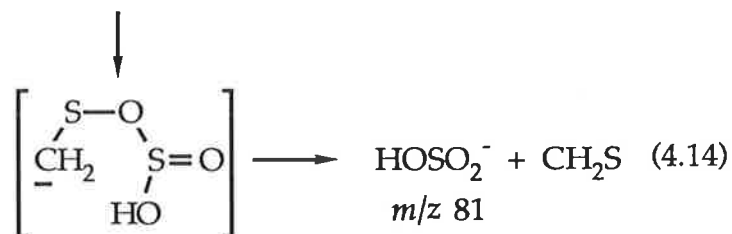
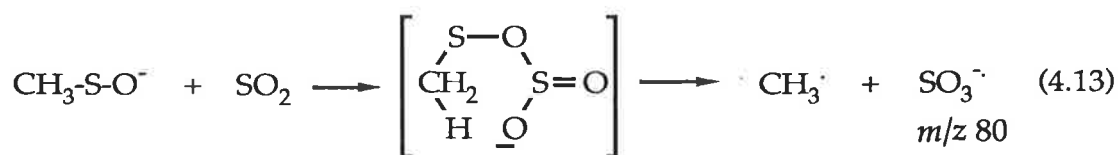


Figure 4.6 The reaction of the methyl sulphinyl anion CH_3SO^- with oxygen.

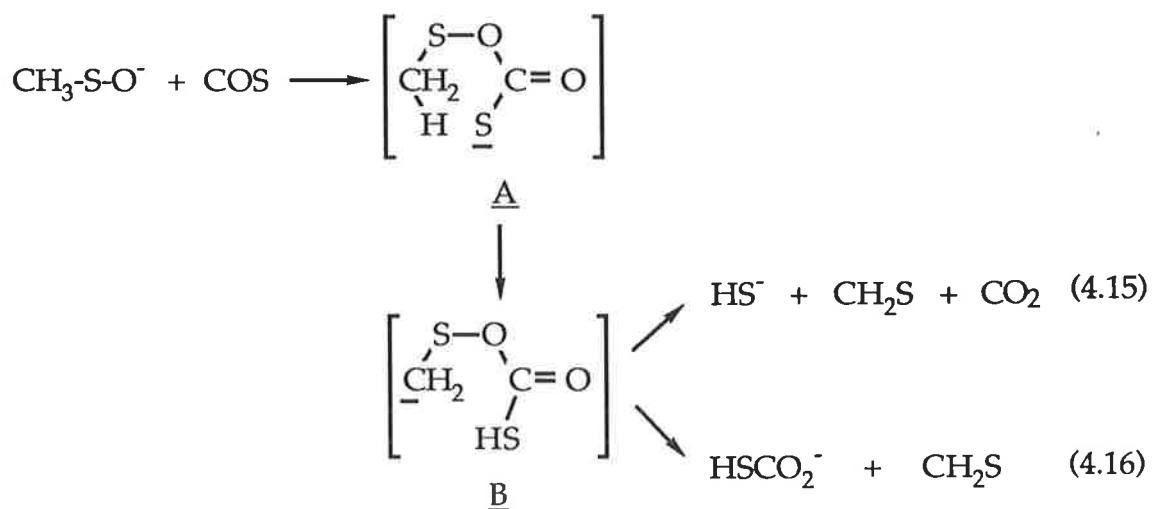


Initial attack through oxygen to CS₂ affords adduct A which may undergo homolytic cleavage of the S-O bond to produce oxidation product OCS₂⁻ (*m/z* 92). The same intermediate (A) can account for the formation of CH₃SS⁻ (*m/z* 79) through a sulphur-oxygen exchange reaction (equation 4.11). The chemistry of CH₃SS⁻ is discussed briefly in Section 4.6. The major product of the reaction between CH₃SO⁻ and CS₂, however, is HS⁻ (*m/z* 33). This product ion can again occur from intermediate A by a process shown in equation 4.12. Proton transfer from carbon to sulphur in intermediate A produces intermediate B. Subsequent elimination of thioformaldehyde and carbonyl sulphide from B yields HS⁻ (*m/z* 33).

The methyl sulphonyl ion CH₃SO⁻ also oxidises sulphur dioxide resulting in the formation SO₃⁻ (*m/z* 80) (equation 4.13) and the hydroxide addition product HOSO₂⁻ (*m/z* 81) (equation 4.14). However, the major product of this collision controlled reaction is SO₂⁻ (*m/z* 64), a species formed by electron transfer.



The reaction of CH_3SO^- with carbonyl sulphide produces products corresponding to HS^- (*m/z* 33) and HSCO_2^- (*m/z* 77) best rationalised by initial attack of CH_3SO^- through oxygen (equations 4.15, 4.16). Sufficient energy in the complex permits an internal proton transfer within adduct (A) to afford intermediate (B). Subsequent elimination of thioformaldehyde and carbon dioxide affords HS^- (*m/z* 33) (equation 4.15), whilst sole loss of CH_2S yields hydroxide addition product HSCO_2^- (*m/z* 77) (equation 4.16).

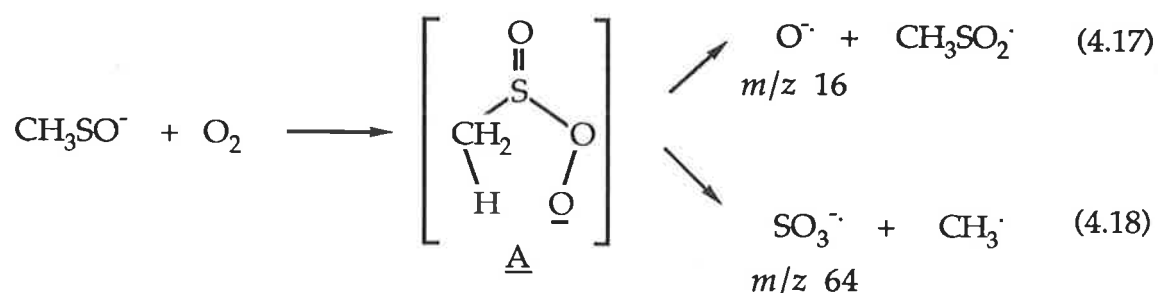


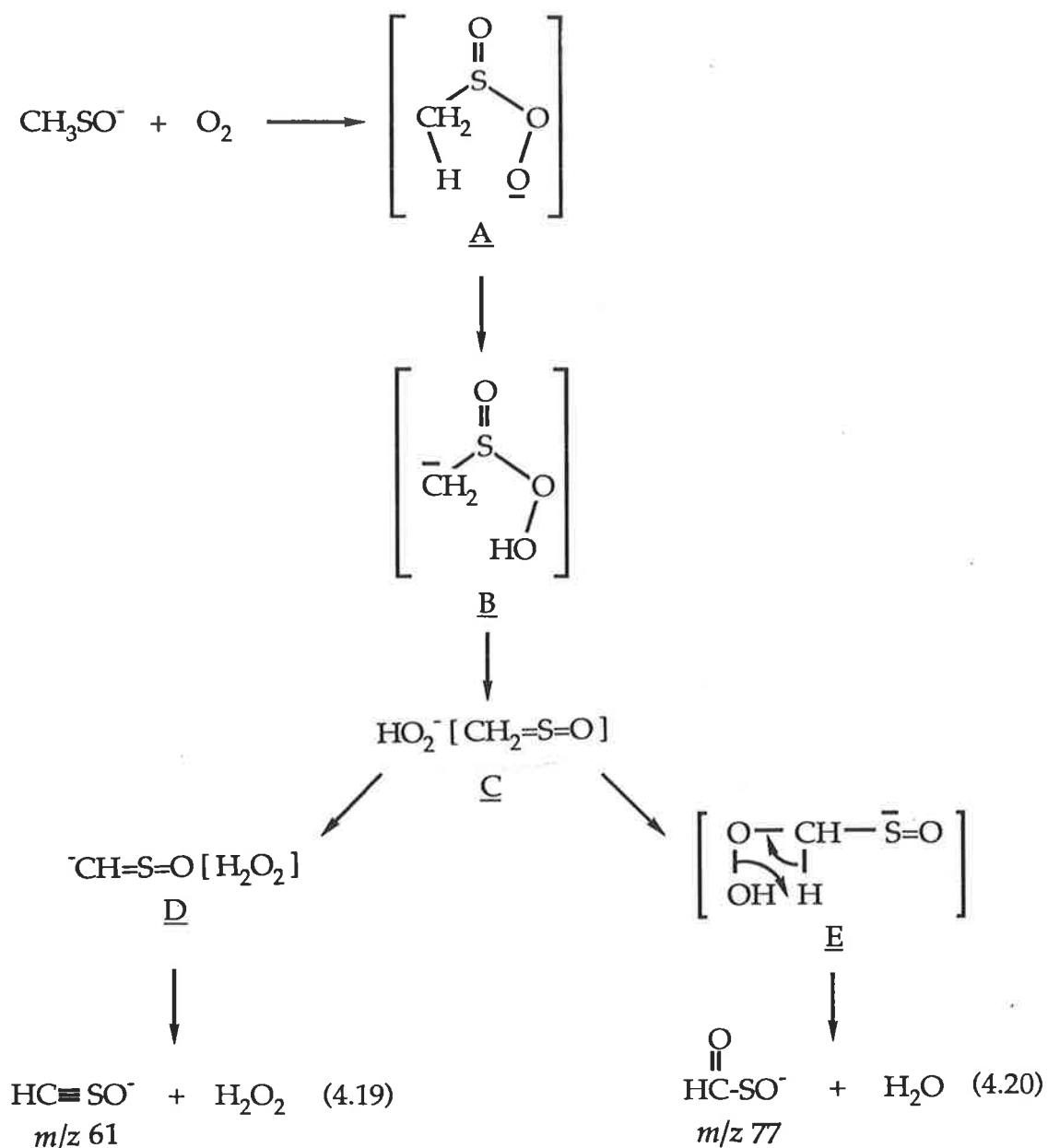
It is interesting to note that whilst the reactions of CH_3SO^- with both carbon disulphide and carbonyl sulphide afford HS^- as a major product (through mechanisms shown in equations 4.12 and 4.15), the reaction with CS_2 produces an oxygen transfer product (OCS_2^-) as opposed to the hydroxide addition product found with COS . Furthermore, CH_3SO^- reacts with CS_2 (but

not COS) to yield sulphur-oxygen exchange product CH_3SS^- despite the observation that carbonyl sulphide is an efficient sulphur transfer reagent.^{121,122}

The reactivity of CH_3SO^- summarised so far supports the localisation of the charge on to the oxygen atom. Thus resonance form A in Figure 4.4 appears to be the major contributing structure. The reaction of CH_3SO^- with oxygen (described below), however, affords products which can only be rationalised by initial attack of CH_3SO^- through sulphur. The sulphur-oxygen bond in CH_3SO^- is therefore expected to exhibit partial double bond character similar to the Si-O bond of HSiO^- .¹⁷⁸ Thus the S-O bond length in CH_3SO^- is predicted to lie between that for methane sulphenic acid, $\text{CH}_3\text{S(O)H}$, (1.490 Å¹⁷⁹) and hydrogen thioperoxide, HSOH , (1.662 Å¹⁸⁰).

The products of the reaction between CH_3SO^- and oxygen are shown in Figure 4.6 and Table 4.2. All products can be rationalised by the initial formation of adduct A (equations 4.17-4.20). The major product of the reaction corresponds to HC(O)SO^- (m/z 77) rationalised through a mechanism shown in equation 4.20. Evidence for the assignment of the structure of this ion is presented in Section 4.7.





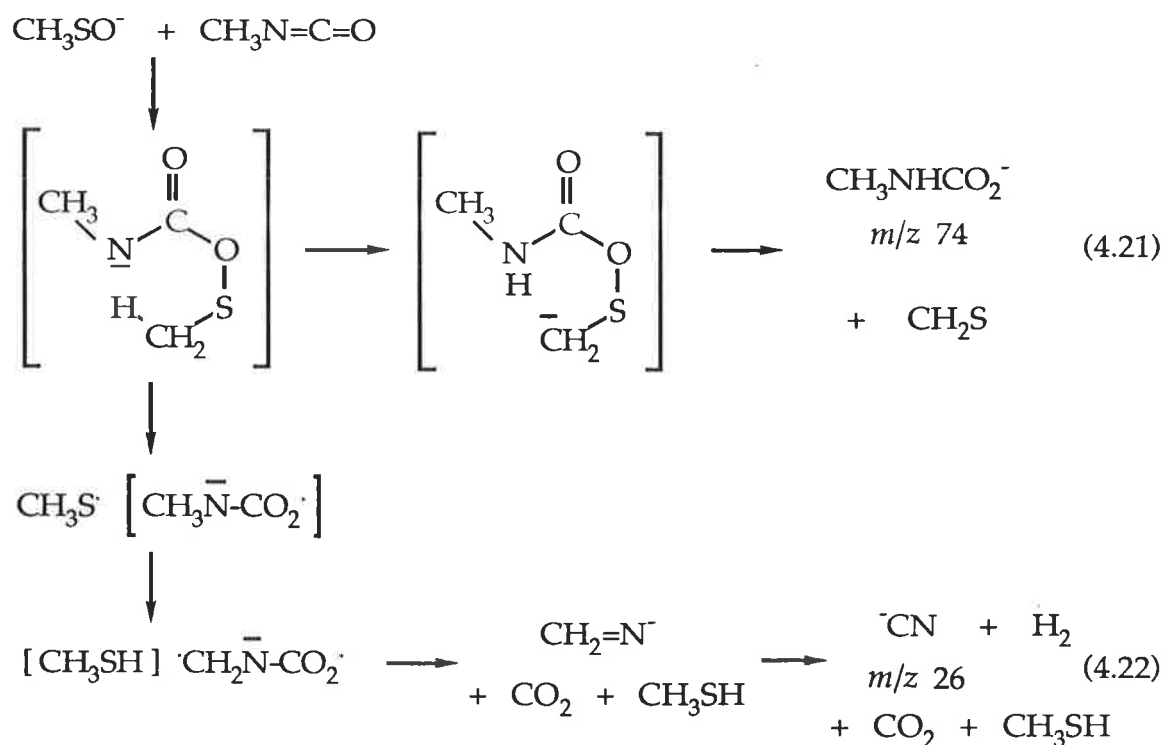
Initial attack of CH_3SO^- at oxygen through sulphur results in the formation of an adduct A. The collapse of this adduct by homolytic cleavage of the oxygen-oxygen and carbon-sulphur bonds results in the formation of ions at m/z 16 (O^-) and 80 (SO_3^-) (equations 4.17 and 4.18 respectively). If, however, a proton transfer from carbon to oxygen precedes the decomposition of A, intermediate B is produced. Elimination of thioketene from B yields the hydroperoxide anion HO_2^- within solvated ion-molecule complex C. The hydroperoxide anion, reported elsewhere,^{155,118} was found to be a powerful base and oxidising agent. Therefore, within ion complex C, HO_2^-

can undergo a competitive deprotonation and nucleophilic addition to thioketene.

If HO_2^- acts as a base, it will deprotonate thioketene resulting in the formation of ion-molecule complex D. Dissociation of this ion-molecule complex affords deprotonated thioketene (m/z 61) (equation 4.19).

Alternatively, the hydroperoxide anion may act as an oxidant. Addition of HO_2^- to thioketene produces intermediate E which can subsequently eliminate water to afford major product ion HC(O)SO^- (m/z 77) (equation 4.20). A similar process to that shown in equation 4.20 was previously reported for the oxidation reaction between the hydrogen peroxide anion and *tert*-butylaldehyde.¹⁵⁵

Other reactions of CH_3SO^- are shown in Table 4.2. The reactions of CH_3SO^- with both methyl isocyanate and methyl isothiocyanate are of interest. These reactions enable a comparison of oxidation and substitution processes within the same molecule.¹⁵⁵ The reaction with methyl isothiocyanate produces adduct (m/z 120), oxidation product $\text{CH}_3\text{NHCO}_2^-$ (m/z 74) (equation 4.21) and the cyanide ion (m/z 26). The latter product can be produced through a previously reported mechanism shown in equation 4.22.¹⁵⁵ No substitution product NCO^- (m/z 42) was detected.



With methyl isothiocyanate, CH_3SO^- reacts to afford adduct (m/z 136) and the nucleophilic substitution product NCS^- (m/z 58). In this case, no oxidation processes are observed.

The difference in reactivity of CH_3SO^- with methyl isocyanate and methyl isothiocyanate reflects the lower basicity of NCS^- [$\Delta H^\circ_{\text{acid}}(\text{HSCN}) = 1375 \text{ kJ mol}^{-1}$ ¹²¹] compared with NCO^- [$\Delta H^\circ_{\text{acid}}(\text{HOCN}) = 1443 \text{ kJ mol}^{-1}$ ¹⁸¹]. Thus NCS^- is expected to be a better leaving group than NCO^- .

4.4 Thermochemistry of the methyl sulphanyl anion

The experimental determination of the basicity of the methyl sulphanyl anion (Section 4.3.1) enables the heat of formation of CH_3SO^- to be determined. Using an equation analogous to 2.30, and a reported value for $\Delta H^\circ_f(\text{CH}_3\text{SOH})$ of -190 kJ mol^{-1} ¹⁶², the heat of formation of CH_3SO^- can be assigned a value of -219 kJ mol^{-1} .

4.5 Thermochemistry of the loss of ethene from deprotonated ethyl methyl sulphoxide

The evidence presented above suggests that the loss of ethene from deprotonated ethyl methyl sulphoxide forms exclusively (or almost so) the methyl sulphanyl anion CH_3SO^- .

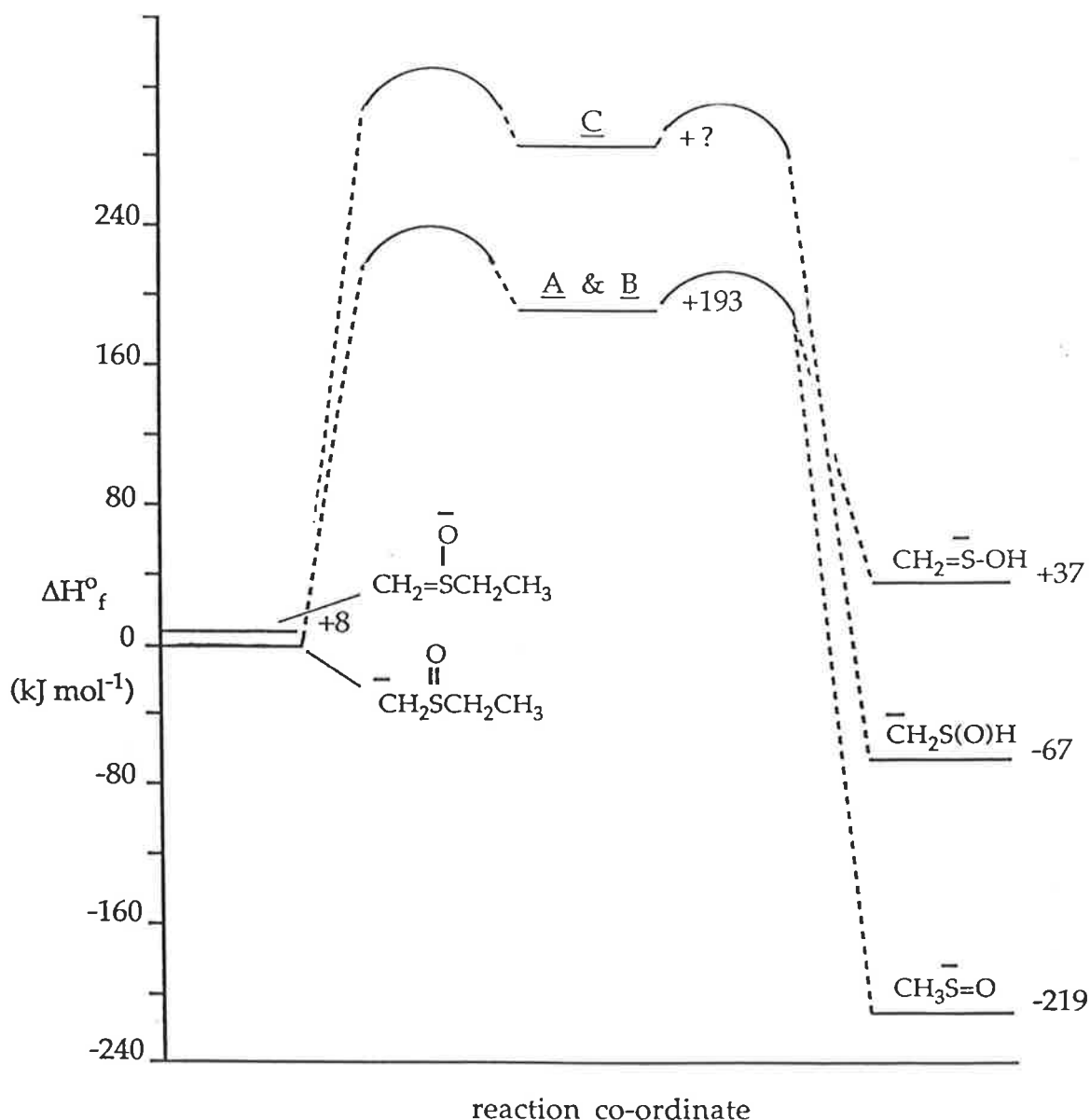
Previous studies involving base-catalysed gas phase elimination reactions¹⁷³⁻¹⁷⁶ have suggested that they likely follow an E1cB mechanism (namely, a stepwise reaction in which proton transfer to form a high energy intermediate, precedes elimination) in favour of a concerted E2 process.

Assuming that an E1cB mechanism operates in this instance (equations 4.1 - 4.3), the heats of formation of the parent ions, the intermediates (A - C; produced on proton transfer) and the products of ethene elimination were estimated using Benson's additivity rules.¹⁸² The results of these calculations are summarised in Figure 4.7.

The heat of formation of the intermediate C (the result of a β -proton transfer to sulphur) could not be calculated from available data. Nevertheless, it is likely that this intermediate (produced through a four-centred transition state) is of higher energy than that of intermediates A and B. The intermediates A and B are predicted to have similar energies, yet the products produced from them on ethene elimination are calculated to have vastly different energies. The methyl sulphanyl anion (the product of ethene elimination from intermediate B) is approximately 250 kJ mol^{-1} more stable than its isomer $\text{CH}_2=\text{S}^-\text{OH}$ (from A).

In addition, the change in enthalpy for the reactions shown in equations 4.1 and 4.2 differ markedly. The overall thermicity of the reaction shown in equation 4.2 (producing the methyl sulphanyl anion) is largely exothermic, whilst the reaction shown in equation 4.1 is endothermic.

Figure 4.7 Thermochemistry of the loss of ethene from deprotonated ethyl methyl sulphoxide



Heats of formation calculated using Benson's additivity rules.¹⁸² Activation energy barriers shown are assumed. ΔH°_f (intermediate C) unknown. Assumed: $\Delta H^\circ_f(\text{SO-C,H}) = \Delta H^\circ_f(\text{SO-C,C})$, $\Delta H^\circ_{\text{acid}}(\text{CH}_3\text{S}(\text{O})\text{CH}_3) = \Delta H^\circ_{\text{acid}}(\text{CH}_3\text{S}(\text{O})\text{CH}_2\text{CH}_3) = \Delta H^\circ_{\text{acid}}(\text{CH}_3\text{S}(\text{O})\text{H})$, $\Delta H^\circ_{\text{acid}}(\text{CH}_3\text{SH}) = \Delta H^\circ_{\text{acid}}(\text{CH}_3\text{S-OH})$, $\Delta H^\circ_{\text{acid}}(\text{CH}_2=\text{S}(\text{OH})\text{CH}_2\text{CH}_3) = \Delta H^\circ_{\text{acid}}(\text{HOOH})$, $\Delta H^\circ_{\text{acid}}(\text{CH}_3\text{S}(\text{O})\text{CH}_2\text{CH}_3) = \Delta H^\circ_{\text{acid}}(\text{CH}_3\text{CH}_3)$. A represents intermediate $\text{CH}_2=\text{S}(\text{OH})\text{CH}_2\text{CH}_2^-$, B represents $\text{CH}_3\text{S}(\text{O})\text{CH}_2\text{CH}_2^-$, C represents $^-\text{CH}_2\text{S}^+(\text{O})\text{HCH}_2\text{CH}_2^-$.

The product ion $^{-}\text{CH}_2\text{S}(\text{O})\text{H}$ (equation 4.3) is intermediate in energy to its isomers produced in equations 4.1 and 4.2. However, the higher energy predicted for intermediate C (and subsequently the larger activation barrier for the formation of C) is expected to hinder the E1cB elimination process shown in equation 4.3.

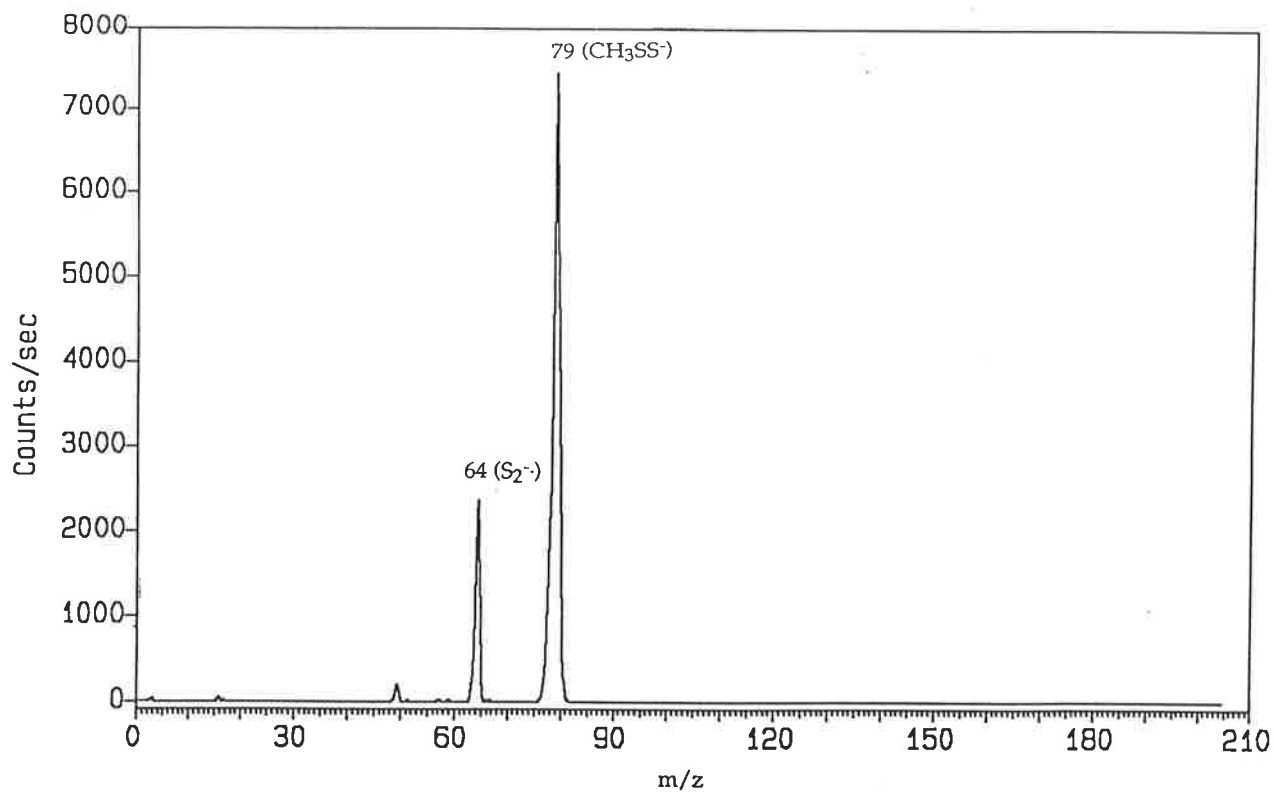
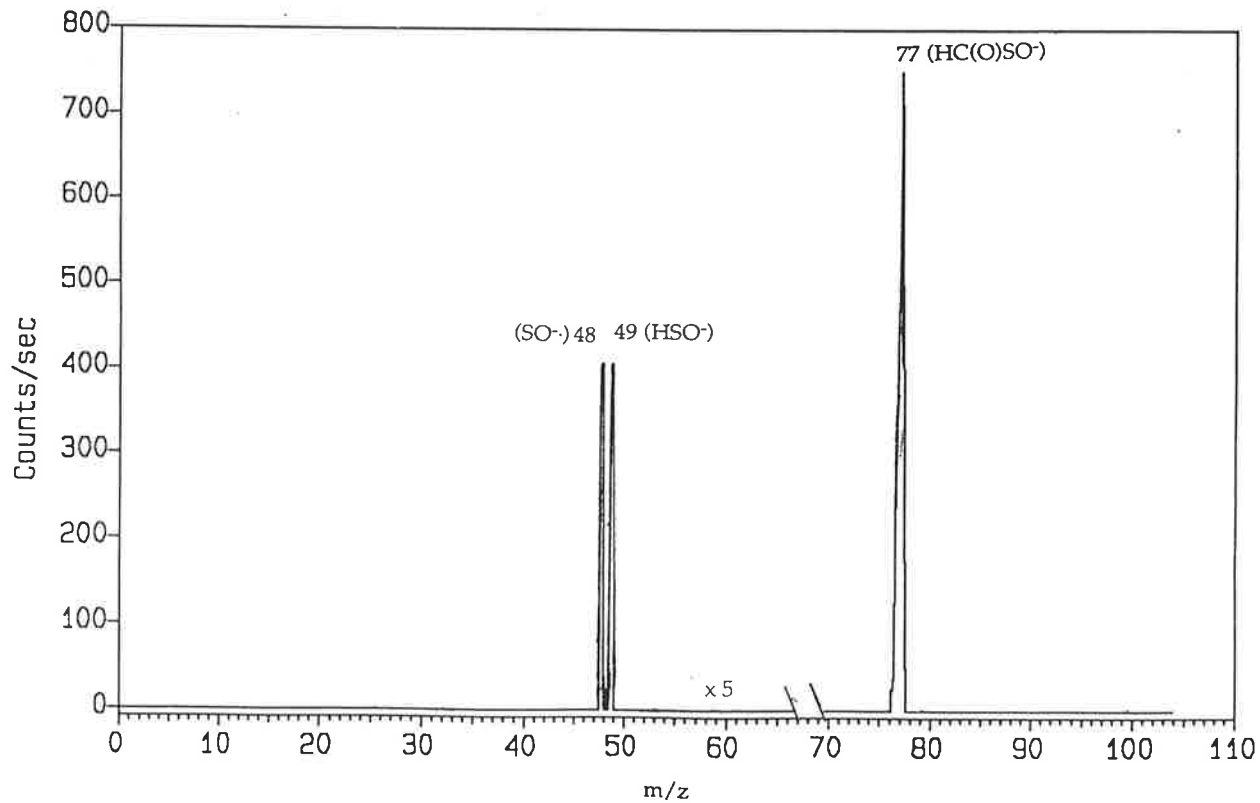
Whilst the energy profiles in Figure 4.7 provide only a rough estimation of the energetics of the three processes shown in equations 4.1 - 4.3, they nevertheless provide some insight into the favoured formation of the methyl sulphonyl anion (over its isomers) on elimination of ethene from deprotonated ethyl methyl sulphoxide. Note that the description above assumes that the loss of ethene from deprotonated ethyl methyl sulphoxide is thermodynamically controlled. No data are available to indicate whether $\text{CH}_3\text{S}^-\text{=O}$ is also the kinetic product.

4.6 The methyl disulphide anion

The generation of the methyl disulphide anion through a sulphur-oxygen exchange reaction (equation 4.11) has prompted a brief study of its reactivity.

4.6.1 Formation of the methyl disulphide anion

The methyl disulphide anion CH_3SS^- (m/z 79) was prepared from the reaction of CH_3SO^- (produced from hydroxide ion and ethyl methyl sulphoxide) and carbon disulphide within the first flow tube and injected solely into the second flow tube. It is a relatively stable species, undergoing little decomposition under collision activation conditions. The fragment in its C.I.D. spectrum (Figure 4.8) corresponds to the loss of a methyl radical to form the S_2^- ion (m/z 64).

Figure 4.8 Collision induced dissociation mass spectrum of CH_3SS^- Figure 4.9 Collision induced dissociation mass spectrum of HC(O)SO^-

4.6.2 The reactivity of the methyl disulphide anion

4.6.2.1 Experimental determination of the basicity of CH₃SS⁻

The methyl disulphide anion deprotonates 2,4-pentan-dione [$\Delta H^{\circ}_{\text{acid}}(\text{CH}_3\text{C}(\text{O})\text{CH}_2\text{C}(\text{O})\text{CH}_3) = 1466 \text{ kJ mol}^{-1}$ ¹⁸³], does so sparingly for 1,1,1-trifluoroacetone [$\Delta H^{\circ}_{\text{acid}}(\text{CF}_3\text{COCH}_3) = 1466 \text{ kJ mol}^{-1}$ ¹⁸³] but does not deprotonate *tert*-butyl thiol [$\Delta H^{\circ}_{\text{acid}}(t\text{-(CH}_3)_3\text{SH}) = 1475 \text{ kJ mol}^{-1}$ ¹¹²] (Table 4.4). Thus the basicity of CH₃SS⁻ is given by $\Delta H^{\circ}_{\text{acid}}(\text{CH}_3\text{SSH}) = 1472 \pm 16 \text{ kJ mol}^{-1}$. This value is considerably higher than that previously reported by Grabowski¹⁸⁴ who calculated $\Delta H^{\circ}_{\text{acid}}(\text{CH}_3\text{SSH})$ to be 1436 kJ mol^{-1} using a thermochemical cycle.

The lower basicity of CH₃SS⁻ compared with that of CH₃SO⁻ is mirrored in its diminished reactivity (summarised in Tables 4.4 and 4.5). The ion CH₃SS⁻ undergoes a very slow reaction with methyl chloride ($k < 5 \times 10^{-12} \text{ cm}^3 \text{ molecule}^{-1} \text{ sec}^{-1}$) and shows no reaction with isopropyl chloride consistent with the acidity of its conjugate acid (compare with Section 4.3.1).¹⁷⁷

4.6.2.2 Reactivity of the methyl disulphide anion

The methyl disulphide ion does not react with carbon disulphide. The possibility of a sulphur exchange reaction with CS₂ was eliminated by repeating the reaction using isotopically enriched CH₃S³⁴S⁻ (m/z 81). No product ion CH₃S³²S⁻ was formed at m/z 79. Similarly, no reaction was observed with carbonyl sulphide, carbon dioxide or oxygen (Table 4.5).

A slow reaction was observed with sulphur dioxide ($k_{\text{expt}} = 3.45 \times 10^{-11} \text{ cm}^3 \text{ molecule}^{-1} \text{ sec}^{-1}$). This reaction occurs in approximately three in every hundred collisions between CH₃SS⁻ and SO₂ to afford adduct CH₃SS⁻(SO₂)

Table 4.4 Reactions of CH_3SS^- (m/z 79) with compounds containing acidic hydrogens. Products and branching ratios.		
Neutral	Products	Branching Ratios
$[\text{CH}_3\text{C}(\text{O})]_2\text{CH}_2$	$\text{CH}_3\text{C}(\text{O})\text{C}-\text{HC}(\text{O})\text{CH}_3 + \text{CH}_3\text{SSH}$ $\text{CH}_3\text{SS}^-[\text{CH}_3\text{C}(\text{O})\text{CH}_2\text{C}(\text{O})\text{CH}_3]$	0.80 0.20
$\text{CF}_3\text{C}(\text{O})\text{CH}_3$	$\text{CH}_3\text{SS}^-(\text{CF}_3\text{C}(\text{O})\text{CH}_3)$ $\text{CF}_3\text{C}(\text{O})\text{CH}_2^- + \text{CH}_3\text{SSH}$	0.98 0.02
<i>t</i> - $(\text{CH}_3)_3\text{CSH}$	-	-
CH_3NCO	-	-
CH_3NCS	$\text{CH}_3\text{SS}^-(\text{CH}_3\text{NCS})$	1.0

Table 4.6 Reactions of the formyl sulphinyl anion $\text{HC}(\text{O})\text{SO}^-$ (m/z 77) with compounds containing acidic hydrogens. Products and branching ratios.		
Neutral	Products ^a	Branching Ratios
$[\text{CH}_3\text{C}(\text{O})]_2\text{CH}_2$	$\text{CH}_3\text{C}(\text{O})\text{C}-\text{HC}(\text{O})\text{CH}_3$ $+ \text{HC}(\text{O})\text{SOH}$	1.0
$\text{PhC}(\text{O})\text{CH}_3$	-	-
CH_3NO_2	$(\text{CH}_2\text{SO}_3)^-\cdot + \text{CH}_2\text{NO}\cdot$ $-\text{CH}_2\text{NO}_2 + \text{HC}(\text{O})\text{SOH}$	0.89 0.11
CD_3NO_2	$(\text{CHDSO}_3)^-\cdot + \text{CD}_2\text{NO}\cdot$ $-\text{CD}_2\text{NO}_2 + \text{HC}(\text{O})\text{SOD}$	0.90 0.10

^a Neutral product structures rationalised through plausible mechanisms.

Table 4.5 Reactions of CH_3SS^- with compounds containing no acidic hydrogen ^a . Products, branching ratios, rate constants and reaction efficiencies.				
Neutral	Products ^b	Branching Ratios	$k_{\text{expt}}^{\text{c}}$	$k_{\text{expt}}/k_{\text{ADO}}^{\text{d}}$
SO_2	$\text{CH}_3\text{SS}^- (\text{SO}_2)$ $\text{CH}_3\text{SO}^- + (\text{S}_2\text{O})^{\text{e}}$	0.65 0.35	0.35	0.03
CH_3Cl	$\text{Cl}^- + \text{CH}_3\text{SSCH}_3$	1.0	< 0.05	< 0.01

"a" No reactions detected between CH_3SS^- and CS_2 , COS , CO_2 , O_2 and $(\text{CH}_3)_2\text{CHCl}$, "b" Neutral product structures rationalised through plausible mechanisms, "c" $\times 10^{-10} \text{ cm}^3 \text{ molecule}^{-1} \text{ sec}^{-1}$, "d" k_{ADO} calculated by the method of Su and Bowers⁷⁷, "e" Structure of the neutral is unknown.

(m/z 143) and sulphur-oxygen exchange product CH_3SO^- (m/z 63).

Unlike its analogue CH_3SO^- , the methyl disulphide cannot act as an oxidant. Consequently it undergoes no reaction with methyl isocyanate. With methyl isothiocyanate, no substitution reaction was detected to form NCS^- (m/z 58). The diminished basicity (and therefore nucleophilicity; see Section 4.3.1) of this anion results in the formation of only an adduct from this reaction.

4.6.3 Thermochemistry of the methyl disulphide anion

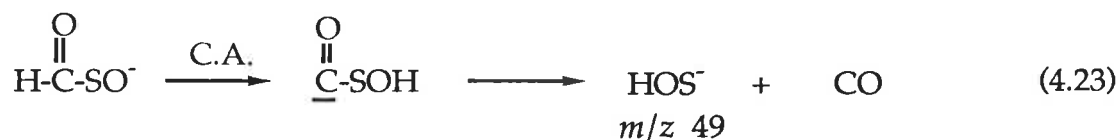
The heat of formation of the methyl disulphide anion can be estimated in a similar way to that of its oxygen analogue [CH_3SO^- (Section 4.4)]. Substituting a reported value for $\Delta H_f^\circ(\text{CH}_3\text{SSH})$ of -3.8 kJ mol^{-1} ¹⁸⁴, together with the basicity of CH_3SS^- determined above (Section 4.6.2.1), the heat of formation of the methyl disulphide anion is assigned a value of -59 kJ mol^{-1} .

4.7 The formation and reactivity of the formyl sulphinyl anion

The formyl sulphinyl HC(O)SO^- , produced by the reaction of CH_3SO^- with oxygen (equation 4.20), is an interesting ion previously unreported. It is a simple sulphur analogue of the peroxyformate anion HCO_3^- reported by Bowie and co-workers.¹⁵⁵

The formyl sulphinyl anion is produced in sufficient abundance from the reaction of CH_3SO^- with O_2 to enable it to be prepared in the first flow tube of the flowing afterglow-S.I.F.T. Selection of this ion using the quadrupole mass filter permits its chemistry to be investigated (Table 4.6). Under collision activation conditions (Section 1.7.2.1), the formyl sulphinyl ion (m/z 77) fragments by competitive loss of carbon monoxide and the formyl radical $\text{HCO}\cdot$ to form m/z 49 and 48 respectively (Figure 4.9). The loss of $\text{HCO}\cdot$ can occur by simple radical cleavage of the carbon-sulphur bond,

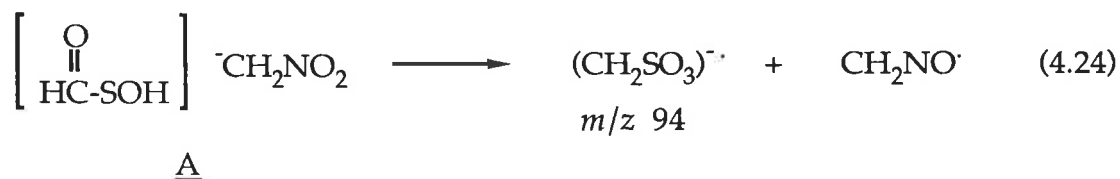
whilst carbon monoxide loss must be preceded by proton transfer from carbon to oxygen (equation 4.23).



The fragment ion HOS^- (m/z 49) has been reported previously. DePuy and co-workers have reported its formation upon reaction of hydroxide ion and carbonyl sulphide.¹²¹ More recently, Bowie¹⁸⁵ has detected HOS^- as a fragmentation product from the collisional activation of deprotonated dimethyl sulphoxide.

As anticipated, the formyl sulphinyl anion has a similar basicity to that of the methyl sulphinyl anion. It deprotonates 2,4-pentadione [$\Delta H^\circ_{\text{acid}}(\text{CH}_3\text{C}(\text{O})\text{CH}_2\text{C}(\text{O})\text{CH}_3) = 1466 \text{ kJ mol}^{-1}$ ¹⁸³] and nitromethane ($\Delta H^\circ_{\text{acid}}(\text{CH}_3\text{NO}_2) = 1491 \text{ kJ mol}^{-1}$ ¹¹²) but not acetophenone [$\Delta H^\circ_{\text{acid}}(\text{PhC}(\text{O})\text{CH}_3) = 1512 \text{ kJ mol}^{-1}$ ¹¹²]. Thus, the gas phase acidity of the conjugate acid of the formyl sulphinyl anion is $\Delta H^\circ_{\text{acid}}(\text{HC}(\text{O})\text{SOH}) = 1501 \pm 22 \text{ kJ mol}^{-1}$.

The reaction of $\text{HC}(\text{O})\text{SO}^-$ with nitromethane, however, does not produce solely proton abstraction product $^-\text{CH}_2\text{NO}_2$ (m/z 60). A subsequent oxygen transfer product (m/z 94) is also observed which, based on the reported oxidative ability of $^-\text{CH}_2\text{NO}_2$,^{186,187} can be explained by a mechanism shown in equation 4.24.



Within ion-molecule complex A (the result of an initial proton transfer from nitromethane to the formyl sulphinyl anion, deprotonated

nitromethane can transfer O^- to neutral HC(O)SOH to afford product $(\text{CH}_2\text{SO}_3)^-$ (m/z 94). This mechanism is supported by the analogous reaction of HC(O)SO^- and CD_3NO_2 which yields product $(\text{CHDSO}_3)^-$ (m/z 95) in addition to $^- \text{CD}_2\text{NO}_2$ (m/z 63).

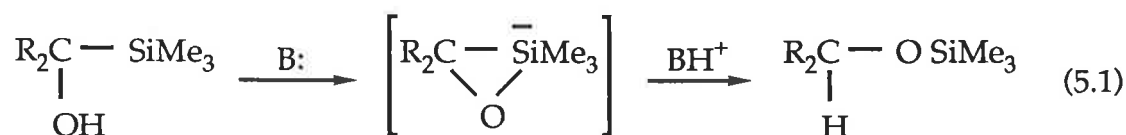
Chapter 5 GAS PHASE INTRAMOLECULAR ANIONIC REARRANGEMENTS INVOLVING THE MIGRATION OF SILICON.

5.1 Introduction

Extensive studies of molecular rearrangements in solution involve the migration of a silyl group to a neighbouring atom.^{188,189} This reflects the high migratory aptitude of a silyl group compared with both aryl and alkyl groups and hydrogen.

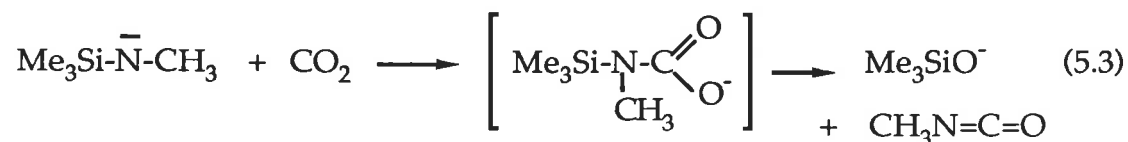
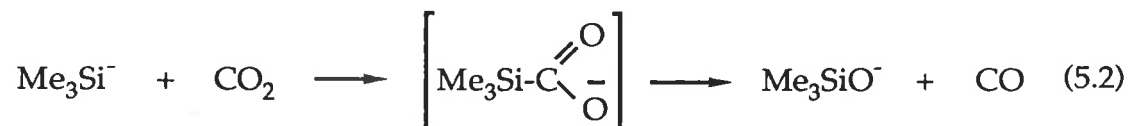
With a few exceptions, rearrangements involving organosilicon compounds proceed via nucleophilic attack on silicon by the lone electron pair of a sterically accessible adjacent atom.¹⁹⁰⁻¹⁹² These rearrangements are thought to proceed through a five co-ordinate silicon intermediate which provides a lower energy pathway than that if the empty d-orbitals on silicon were not available. The retention of configuration at silicon for most rearrangements involving a chiral silicon centre lends support for such an intermediate.

The migration of a silyl group to an adjacent atom is common where an electronegative atom, such as oxygen, carries a formal negative charge.¹⁹³ The formation of a strong Si-O bond provides a driving force for such a rearrangement. For example, when silyl-methanols are treated with a catalytic amount of base, their corresponding silyl ethers are produced¹⁹⁴ (equation 5.1).



In contrast to the wealth of anionic rearrangements involving the migration of silicon in solution, few gas phase analogies have been reported.

Noteworthy is the work of Bowie and colleagues^{195,196} who have reported the intermolecular migration of silicon to a charged oxygen centre upon reaction of Me_3Si^- and $\text{Me}_3\text{SiN}^-\text{CH}_3$ with carbon dioxide (equations 5.2, 5.3).



The preparation of a variety of organosilicon compounds as precursors for the specific generation of gas phase anions by nucleophilic displacement reactions (see Section 1.3.2) prompted a preliminary study of intramolecular rearrangements involving the migration of silicon.

This chapter describes the collision induced dissociations of a variety of deprotonated organosilicon compounds in the gas phase. Rearrangements involving the production of silicon-oxygen bonds are observed to predominate. The extent of silicon migration from carbon to oxygen as a function of the intramolecular distance between these centres has been investigated.

5.2 Trimethylsilylalkoxides

The collisional activation mass spectra of the trimethylsilylalkoxides $\text{Me}_3\text{Si}(\text{CH}_2)_n\text{O}^-$ $n=1-5$ prepared by specific deprotonation at oxygen in the source of the mass spectrometer are recorded in Table 5.1.

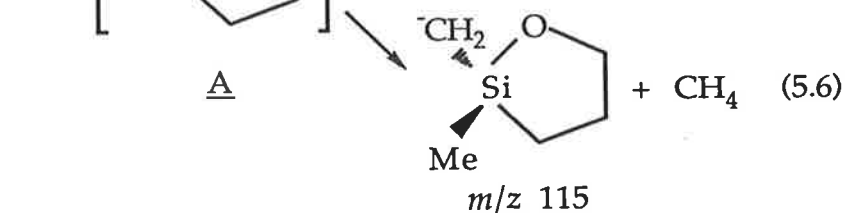
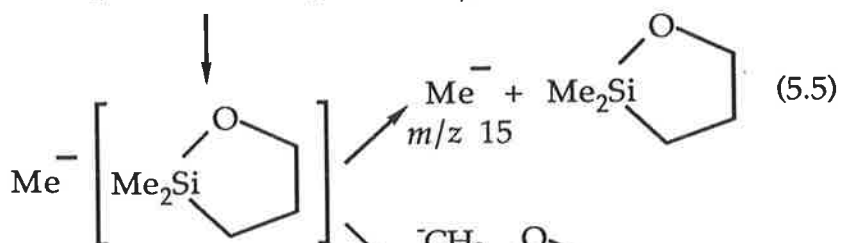
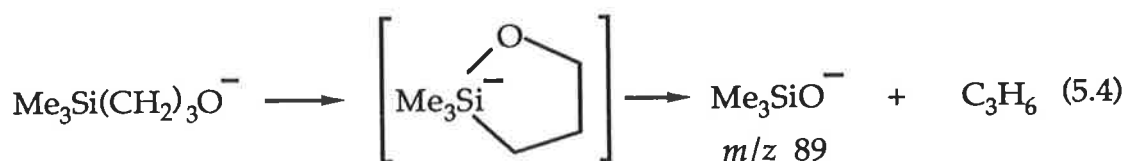
In the case of $\text{Me}_3\text{Si}(\text{CH}_2)_n\text{O}^-$ ($n=2-5$), all major fragment ions can be rationalised through silicon-oxygen bond formation which either precedes or accompanies fragmentation. The formation of the trimethylsilyl-oxy

Table 5.1 Collisional activation mass spectra of trimethylsilylalkoxides	
Ion (<i>m/z</i>) ^a	C.A. MS/MS [<i>m/z</i> (loss) abundance in %]
Me ₃ SiCH ₂ O ⁻ (103)	102(H·)100, 73(CH ₂ O)1
Me ₃ Si(CH ₂) ₂ O ⁻ (117)	89 ^b (C ₂ H ₄)100
Me ₃ Si(CH ₂) ₃ O ⁻ (131)	115(CH ₄)100, 89(C ₃ H ₆)12, 15(C ₅ H ₁₂ SiO)1
Me ₃ Si(CH ₂) ₄ O ⁻ (145)	129(CH ₄)100, 89(C ₄ H ₈)0.5, 15(C ₆ H ₁₄ SiO)0.7, 113(CH ₂ O)0.3, 73(C ₄ H ₈ O)0.1
Me ₃ Si(CH ₂) ₅ O ⁻ (159)	143(CH ₄)100

"a" Deprotonation was effected solely at oxygen by the reaction of DO⁻ (from D₂O) with the d₁-trimethylsilylalkoxides Me₃Si(CH₂)_nOD. Fragmentations arising from an α-silyl anion must follow a proton transfer reaction from a carbon adjacent to silicon to oxygen. "b" Dish-shaped peak, width at half-height 128.5 ± 2 V

anion Me_3SiO^- (m/z 89) and the methyl anion (m/z 15), in addition to ions corresponding to the loss of methane,* are consistent with a rearrangement involving initial silicon-oxygen bond formation.

Suggested mechanisms for the formation of daughter ions in the C.A. spectrum of $\text{Me}_3\text{Si}(\text{CH}_2)_3\text{O}^-$ (Table 5.1) are shown in equations 5.4 - 5.6.



Each product fragment results from the initial nucleophilic attack of oxygen at the silicon centre. The penta-coordinate silicon intermediate may then decompose by ejection of a methyl anion (equations 5.5 - 5.6) or through a decyclisation process to yield Me_3SiO^- (equation 5.4). In principle, the solvated methyl anion [$\Delta H_{\text{acid}}^{\circ}(\text{CH}_4) = 1741 \text{ kJ mol}^{-1}$ ¹³³] in the ion-molecule complex A (equations 5.5 and 5.6) can deprotonate at a carbon adjacent to silicon [$\Delta H_{\text{acid}}^{\circ}((\text{CH}_3)_4\text{Si}) = 1636 \text{ kJ mol}^{-1}$ ¹⁴⁵] or oxygen ($\Delta H_{\text{acid}}^{\circ}(\text{CH}_3\text{OCH}_3) = 1702 \text{ kJ mol}^{-1}$ ⁷⁰). The former process (equation 5.6) is favoured based on the quoted acidities.

* Note that deprotonation is effected solely on oxygen using DO^- (from D_2O) and the d_1 -labelled trimethylsilylalkoxides $\text{Me}_3\text{Si}(\text{CH}_2)_n\text{OD}$. Consequently, fragmentations arising from an α -silyl anion can only occur following an initial proton transfer reaction from the carbon adjacent to silicon to oxygen.

A comparison of the C.A. spectra of $\text{Me}_3\text{Si}(\text{CH}_2)_n\text{O}^-$, $n=2-5$, demonstrates that the loss of methane occurs preferentially over the formation of Me_3SiO^- (m/z 89) (based on the relative fragment ion abundances for these processes) as n is increased. Conversely, the formation of product ion Me_3SiO^- is favoured over other fragments as n decreases. Clearly, as the value of n increases, the ring size of the penta-coordinate intermediate increases, resulting in an alleviation of ring strain. No loss of methane is detected in the C.A. spectrum of $\text{Me}_3\text{Si}(\text{CH}_2)_2\text{O}^-$. This is consistent with a spontaneous collapse of the penta-coordinate silicon intermediate to Me_3SiO^- .

The simplest trimethylsilylalkoxide studied, $\text{Me}_3\text{SiCH}_2\text{O}^-$, undergoes no intramolecular rearrangements on collisional activation. Its C.A. spectrum is dominated by simple cleavage fragments corresponding to losses of H· and CH_2O to form m/z 102 and 73 respectively.

5.3 Trimethylsilylalkyl carboxylates

The C.A. mass spectra of the trimethylsilylalkyl carboxylates studied, $\text{Me}_3\text{Si}(\text{CH}_2)_n\text{CO}_2^-$ $n=1-3$ (Table 5.2), all exhibit pronounced peaks corresponding to the formation of rearrangement ion Me_3SiO^- (m/z 89). In the case of $\text{Me}_3\text{Si}(\text{CH}_2)\text{CO}_2^-$, this ion produces the base peak in the spectrum. The almost identical C.A. spectra of the isomeric ions $\text{Me}_3\text{SiCH}_2\text{CO}_2^-$ and $^-\text{CH}_2\text{CO}_2\text{SiMe}_3$ (Figures 5.1 and 5.2, Table 5.2) provide additional evidence for an intramolecular migration of silicon from carbon to oxygen. Interestingly, Brook has reported a base catalysed conversion of $\text{Me}_3\text{SiCH}_2\text{CO}_2\text{H}$ to $\text{Me}_3\text{SiCO}_2\text{CH}_3$ in the condensed phase.¹⁹⁷ The daughter ions detected in both spectra are believed to occur through the fragmentation of the latter ion $^-\text{CH}_2\text{CO}_2\text{SiMe}_3$; the product of a silicon migration from carbon to oxygen through a penta-coordinate silicon intermediate (equations 5.7 - 5.8).

Table 5.2 Collisional activation mass spectra of trimethylsilylalkyl carboxylates	
Ion (<i>m/z</i>)	C.A. MS/MS [<i>m/z</i> (loss) abundance in %]
Me ₃ SiCH ₂ CO ₂ ⁻ (131)	115(CH ₄)0.1, 89(CH ₂ CO)100, 73(CH ₂ CO ₂)3, 41(Me ₃ SiOH)6
Me ₃ SiOCOCH ₂ ⁻ (131)	115(CH ₄)0.5, 89(CH ₂ CO)100, 73(CH ₂ CO ₂)2, 41(Me ₃ SiOH)6
Me ₃ Si(CH ₂) ₂ CO ₂ ⁻ (145)	144(H·)14, 143(H ₂)3, 129(CH ₄)100, 101(CH ₄ + CO)7, 89(C ₃ H ₄ O)33, 75(C ₃ H ₂ O ₂)5, 73(CH ₂ =CHCO ₂ H)2, 71(Me ₃ SiH)1, 55(Me ₃ SiOH)4, 27(HCO ₂ SiMe ₃)0.2
Me ₃ Si(CH ₂) ₃ CO ₂ ⁻ (159)	158(H·)10, 143(CH ₄)100, 129(C ₂ H ₆)9, 115(CO ₂)3, 101(CH ₂ CO ₂)20, 89(C ₄ H ₆ O)48, 71(Me ₄ Si)38, 58(C ₅ H ₁₃ Si)1, 41(C ₂ H ₄ + Me ₃ SiOH)1

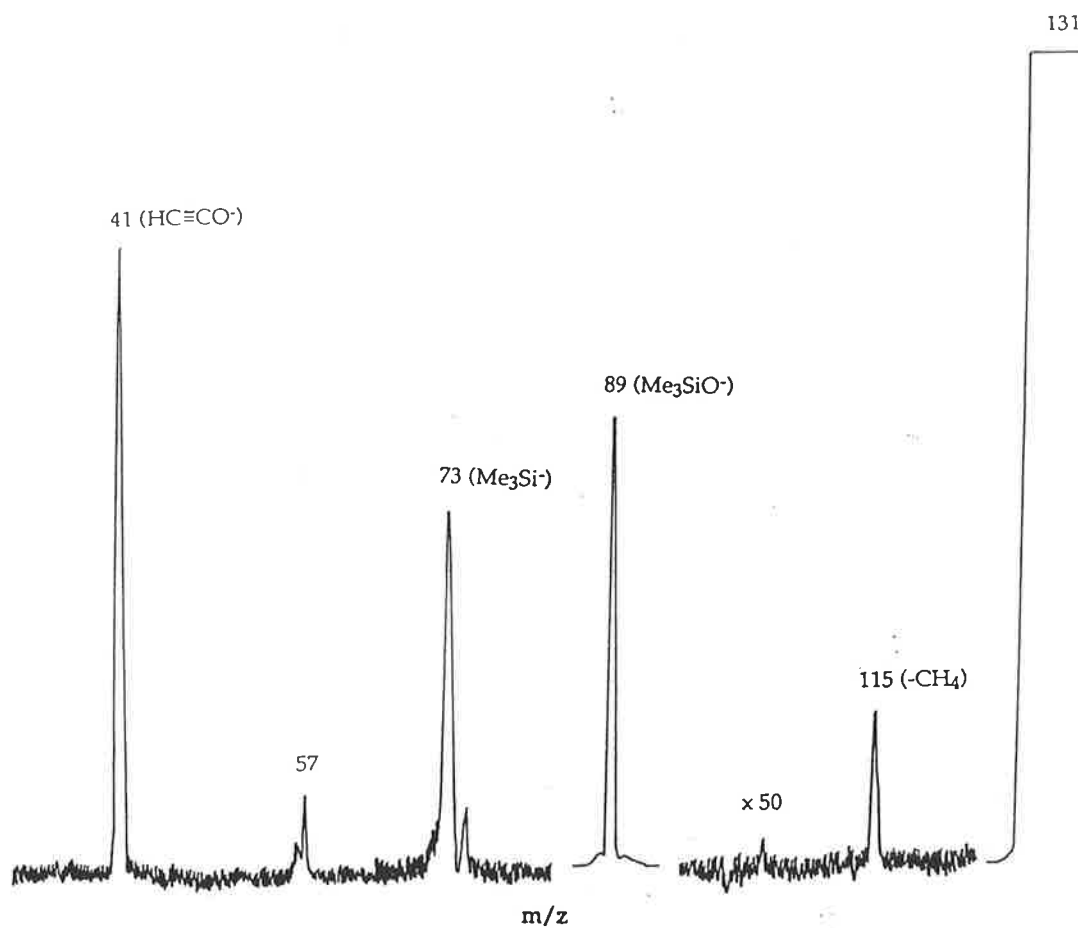


Figure 5.1 Collisional activation mass spectrum of $\text{Me}_3\text{SiCH}_2\text{CO}_2^-$.

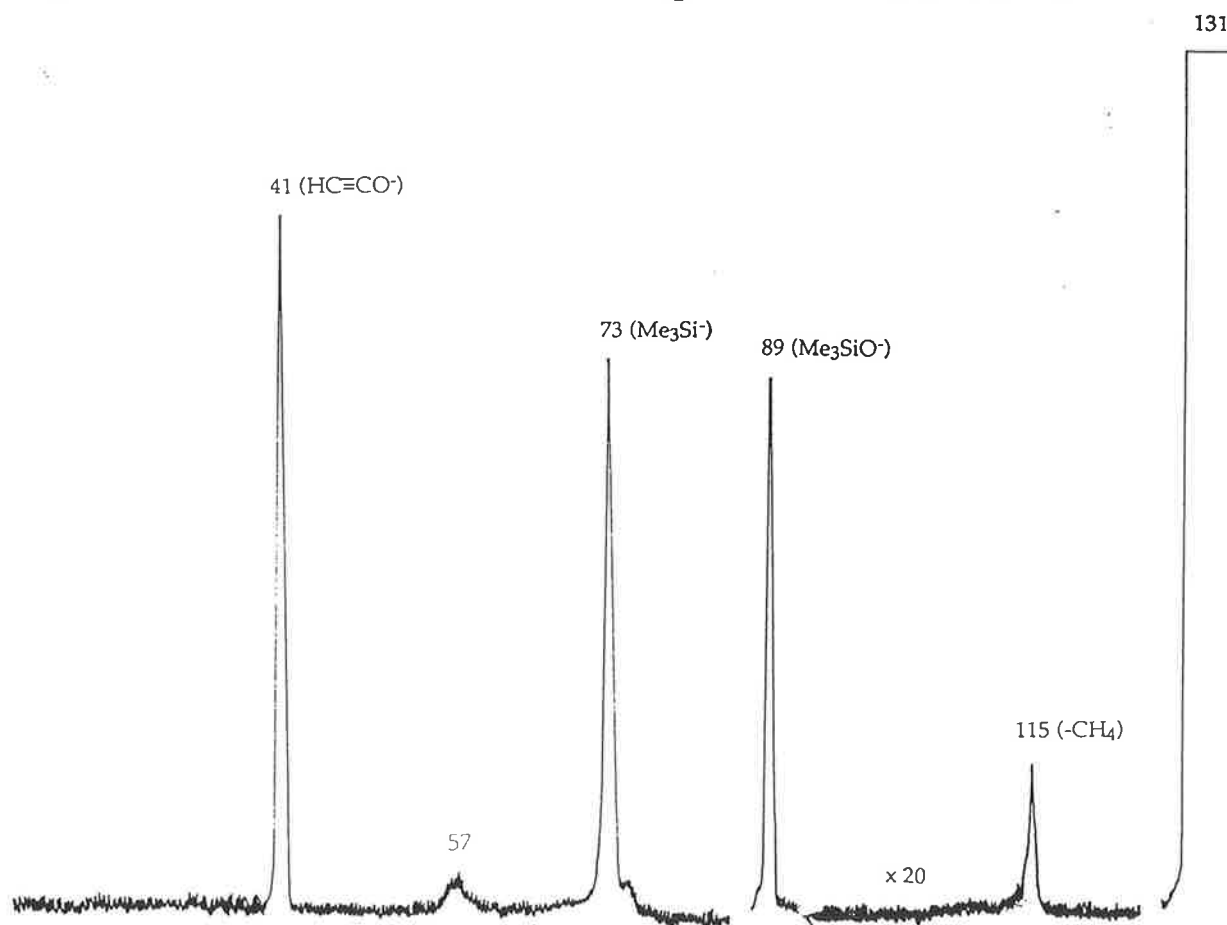
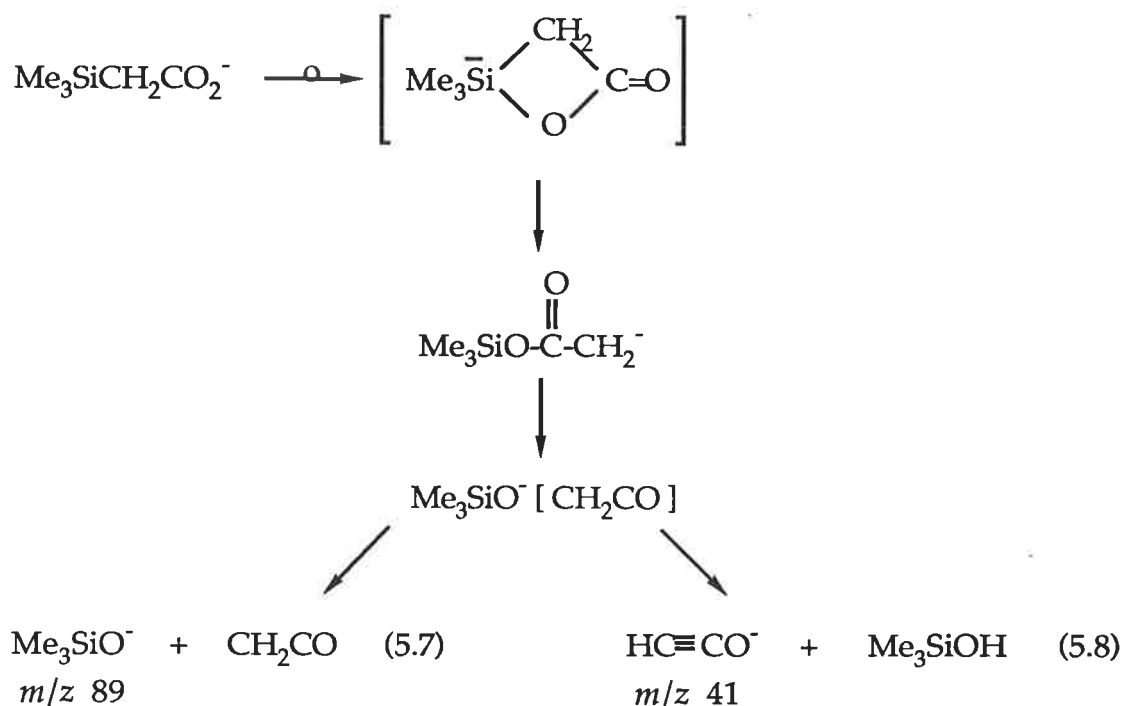


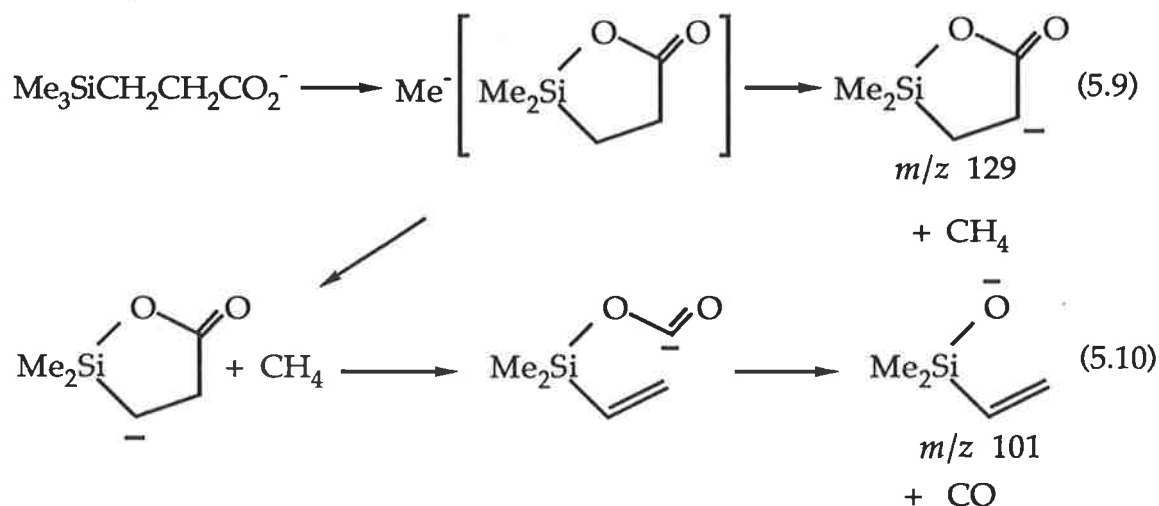
Figure 5.2 Collisional activation mass spectrum of $-\text{CH}_2\text{CO}_2\text{SiMe}_3$.



As with the trimethylsilyl substituted alkoxides (described in Section 5.2), the loss of methane in the C.A. spectra of $\text{Me}_3\text{Si}(\text{CH}_2)_n\text{CO}_2^-$ ($n=1-3$) is more prevalent with an increase in n , whilst the relative abundance of daughter ion Me_3SiO^- decreases with increasing n . Indeed, the C.A. mass spectra of $\text{Me}_3\text{Si}(\text{CH}_2)_n\text{CO}_2^-$ ($n=2,3$) both exhibit base peaks corresponding to the loss of methane.

Of particular note are several minor product ions in the C.A. spectrum of $\text{Me}_3\text{Si}(\text{CH}_2)_2\text{CO}_2^-$ (Table 5.2). Firstly, the spectrum exhibits an ion corresponding to $\text{Me}_3\text{SiH}_2^-$ (m/z 75) formed by a double hydrogen transfer. The mechanism of this process is not understood. Such processes are rare in negative ion chemistry although several examples have been reported¹⁴⁴ (see also Section 5.4). Secondly, the spectrum shows a peak at m/z 101 consistent with the loss of carbon dioxide or consecutive losses of methane and carbon monoxide. The former process is unlikely, given the difficulty in generating β -substituted ethyl anions (see Section 2.3). However, if a direct loss of carbon dioxide does occur it is likely that the resulting

β -trimethylsilyl ethyl anion is unstable to isomerisation to either $\text{Me}_3\text{SiC}(\text{H})\text{CH}_3$ or $^-\text{CH}_2(\text{Me})_2\text{SiCH}_2\text{CH}_3$. A consecutive loss of methane and carbon monoxide, however, appears a more probable mechanism with the formation of the dimethylvinyl siloxide anion (m/z 101) (equation 5.10).



This prediction is supported by the recent work of Squires¹⁰⁰ who has measured the appearance energy of the m/z 101 ion and concluded it is not the product of a decarboxylation reaction.

5.4 Deprotonated trimethylsilyl ketones

Trimethylsilyl ketones are useful precursors for the generation of acyl anions RCO^- in both gas^{148,198} and solution phases.^{199,200} It was reported previously that acyl anions are stable species in the gas phase which fragment directly upon collisional activation rather than undergo isomerisation to a more stable isomer.¹⁴⁸

The preparation of several trimethylsilyl ketones for this earlier study prompted an investigation of the possible silicon rearrangements of the deprotonated neutrals on collisional activation. A plethora of largely

unexpected rearrangements necessitated the elucidation of product ion structures by both MS/MS/MS and deuterium labelling experiments.

5.4.1 Deprotonated alkoyltrimethylsilanes

The C.A. mass spectrum of deprotonated acetyl trimethylsilane is shown in Figure 5.3 and Table 5.3. Its fragmentations are typical of all the alkoyl trimethylsilanes studied. The spectrum is dominated by the ion Me_3SiO^- (m/z 89); the product of a 1,2-anionic rearrangement (equation 5.11). This reaction is similar to that reported in solution.^{201,202} Labelling studies confirm that whilst initial proton abstraction occurs at the methyl substituent α to the carbonyl group [see ion A (Scheme 5.1)], some proton transfer to form the α -silyl anion B also occurs. This is illustrated particularly by the C.A. spectrum of labelled $^{-}\text{CD}_2\text{COSiMe}_3$ (Table 5.3) which shows fragment ions at m/z 90 and 89 corresponding to $\text{Me}_2(\text{CH}_2\text{D})\text{SiO}^-$ and Me_3SiO^- respectively.

The C.A. spectrum of deprotonated acetyl trimethylsilane also shows a loss of carbon monoxide, a process which can be rationalised in one of two ways. The first involves cyclisation of the enolate ion A (Scheme 5.1) to a penta-coordinate silicon intermediate. This intermediate can subsequently ring open to yield the α -trimethylsilylacetyl anion which, in turn, loses carbon monoxide (equation 5.12).^{*} The second possibility involves displacement of the acetyl anion from the α -silyl anion B (Scheme 5.1) to yield a solvated ion complex. Within this complex, the acetyl anion can transfer a methyl anion to the "bound" neutral silene, and in so doing, liberate carbon monoxide (equation 5.18). Deuterium labelling studies are unable to differentiate these processes.

* Acyl anions have previously been reported to fragment directly rather than isomerise (see reference 148). For example, the acetyl anion was observed to lose carbon monoxide in preference to isomerising to the acetaldehyde enolate.

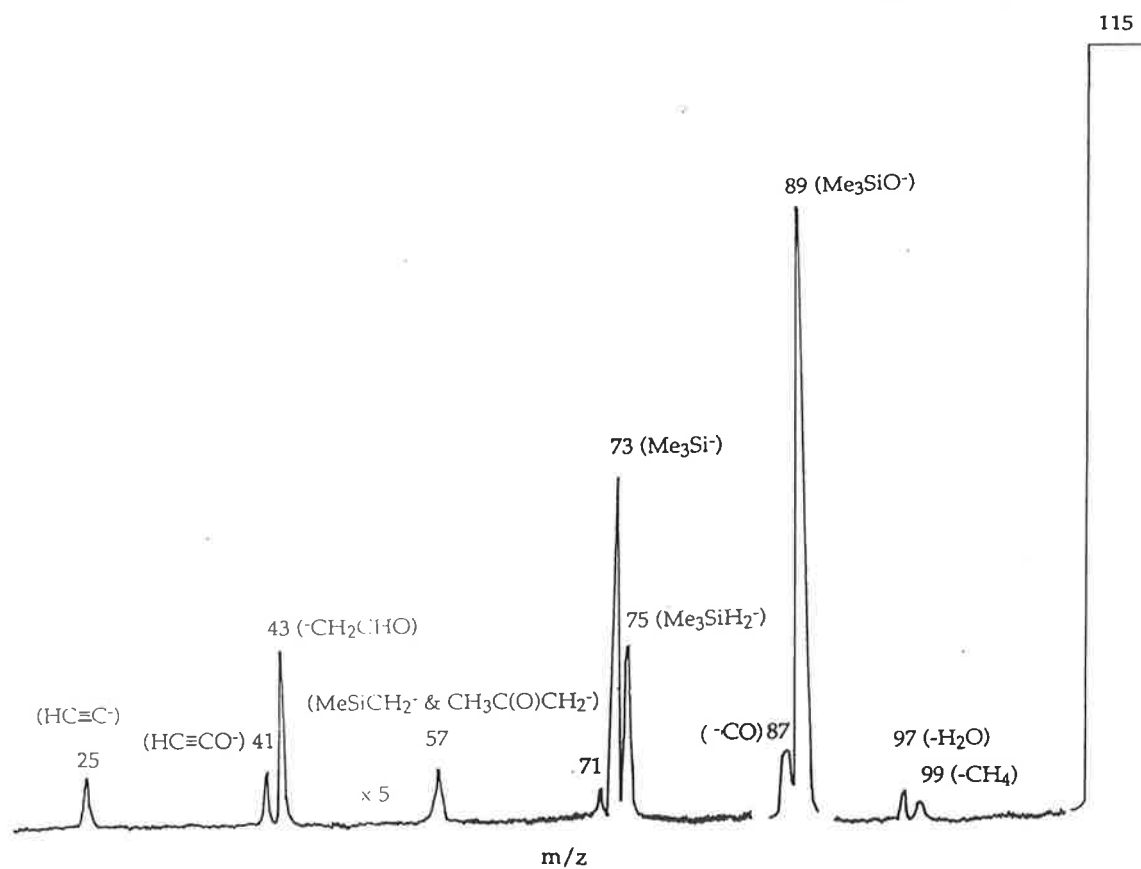


Figure 5.3 Collisional activation mass spectrum of $-\text{CH}_2\text{C}(\text{O})\text{SiMe}_3$.

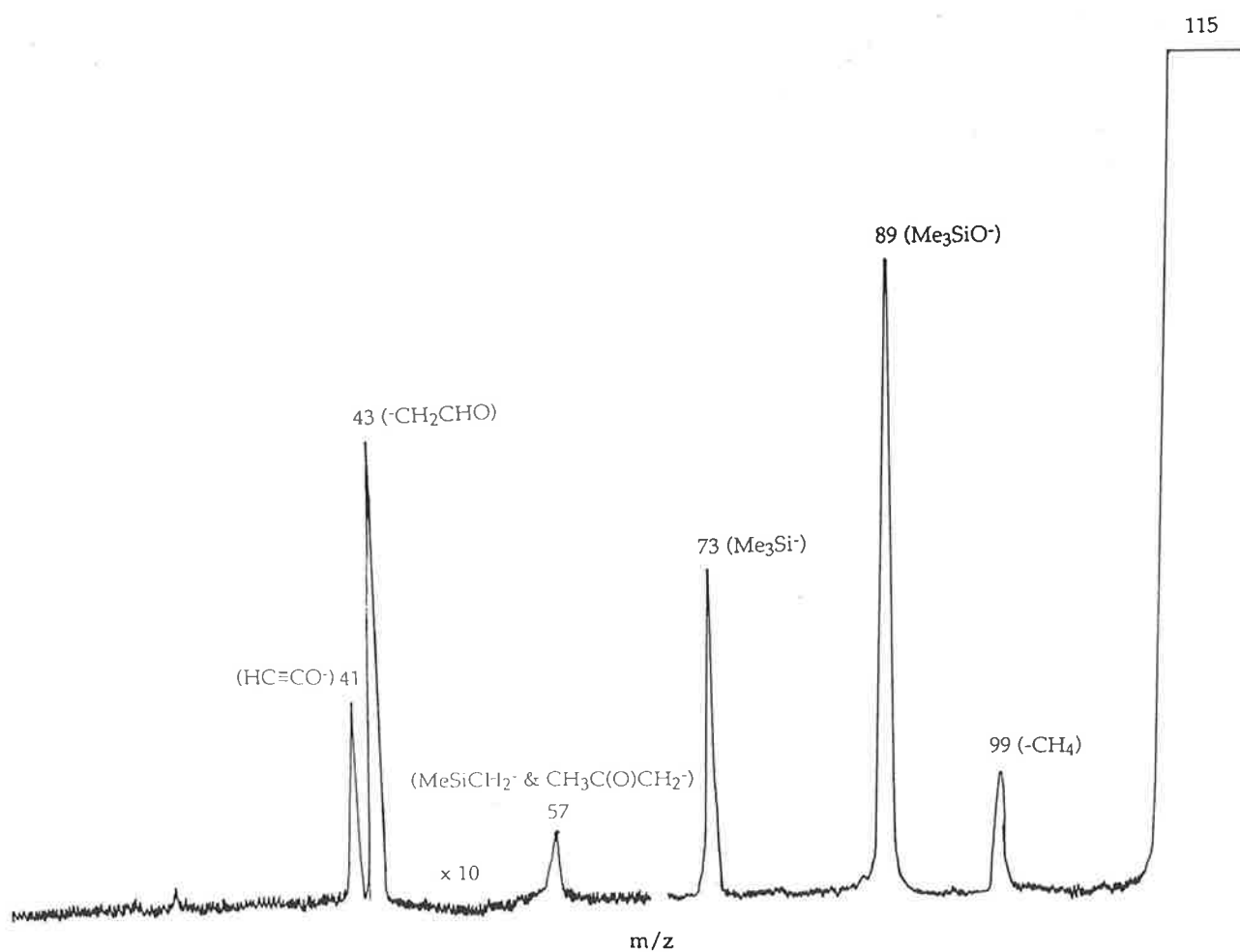
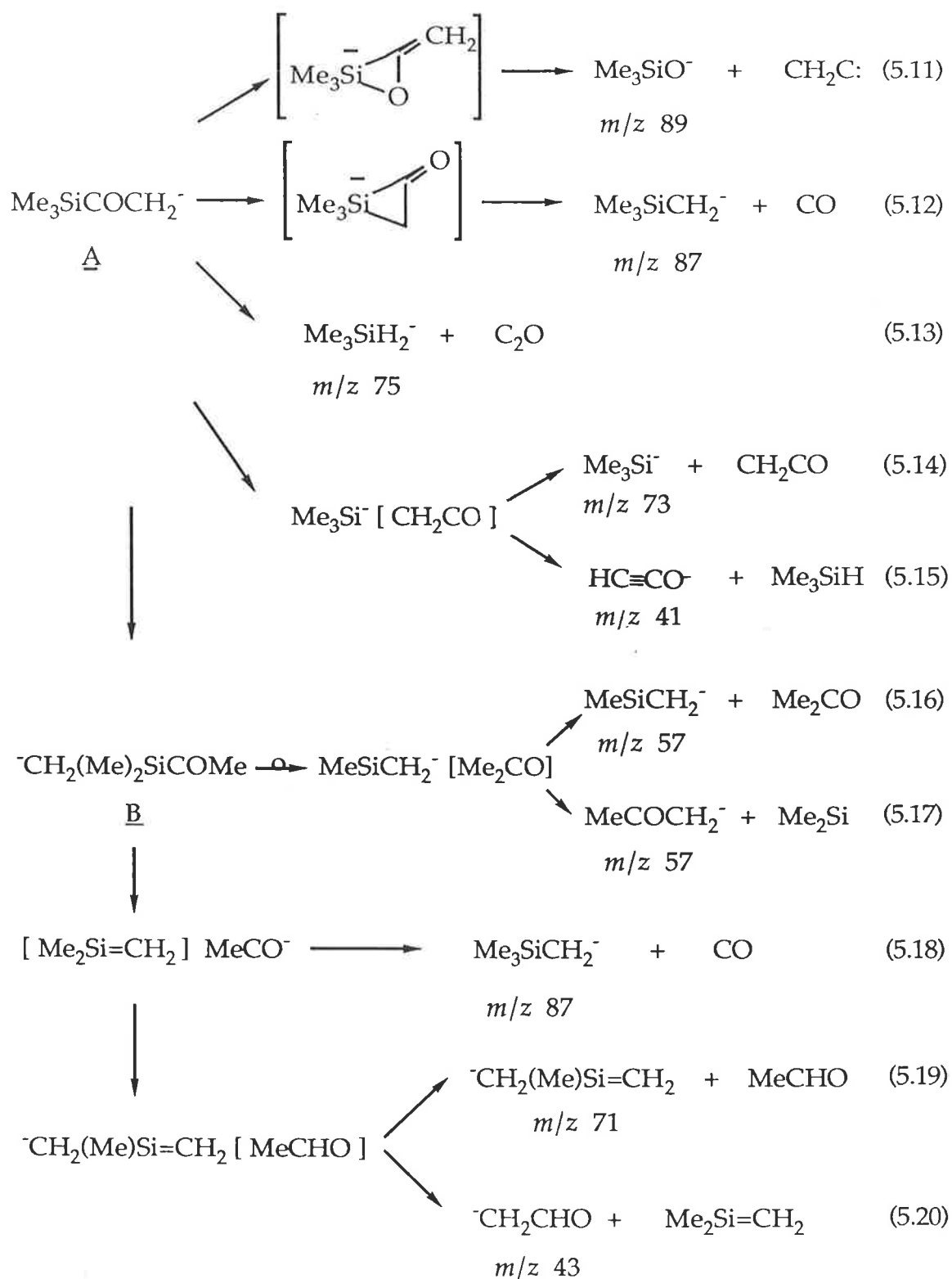


Figure 5.4 Collisional activation mass spectrum of $c(\text{CH}_2\text{OC}^-)\text{SiMe}_3$.

Ion (<i>m/z</i>)	C.A. MS/MS [<i>m/z</i> (loss) abundance in %]
Me ₃ SiCOCH ₂ ⁻ (115)	99(CH ₄)0.5, 97(H ₂ O)1, 89(C ₂ H ₂)100, 87(CO)14, 75(C ₂ O)4, 73(CH ₂ CO)8, 71(MeCHO)1 57(Me ₂ Si and Me ₂ CO)1, 43(Me ₂ SiCH ₂)4, 41(Me ₃ SiH)1.5, 25(Me ₃ SiOH)1
Me ₃ SiCOCD ₂ ⁻ ^a (117)	90(C ₂ HD)100, 89(C ₂ D ₂ or CO)73, 77-73 ^{b(c)} 35, 71(CHD ₂ CHO)5, 59(Me ₂ Si)1, 58(Me(CH ₂ D)Si and Me(CH ₂ D)CO)1, 57(Me(CHD ₂)O)1, 45(Me ₂ SiCH ₂)4, 44(Me ₂ SiCHD)1.5, 42(Me ₃ SiD)1.5, 41(Me ₂ (CH ₂ D)SiD), 26(Me ₃ SiOD)1
Me ₃ Si-c[COCH ₂] ⁻ (115)	99(CH ₄)21, 89(C ₂ H ₂)100, 73(CH ₂ CO)52, 57(Me ₂ Si and Me ₂ CO)1, 43(Me ₂ SiCH ₂)7, 41(Me ₃ SiH)3
Me ₃ SiCOC-(H)Me (129)	128(H)38, 113(CH ₄)3, 111(H ₂ O)3, 101(CO ₂)2, 89(C ₃ H ₄)100, 75(C ₃ H ₂ O)3, 73(MeCHCO)7, 71(MeCH ₂ CHO and Me ₂ Si)3, 57(Me ₂ SiCH ₂ and MeCOCH ₂ Me)15, 55(Me ₃ SiH)2, 39(Me ₃ SiOH)2
Me ₃ SiCOC-(D)Me ^a (130)	128(D)15, 114(CH ₄)4, 112(H ₂ O)4, 102(CO ₂)2, 90(C ₃ H ₄)42, 89(C ₃ H ₃ D)100 76-71 ^{b(d)} 30, 58(Me ₂ SiCH ₂ and MeCOCH ₂ Me)10, 57(Me ₂ SiCHD and MeCHDCHO)3, 39(Me ₃ SiOD)8
-CH ₂ (Me) ₂ SiCOPh (177)	175(H ₂)100, 161(CH ₄)18, 149(CO)67, 119(Me ₂ Si)8, 103(Me ₃ SiH)2, 73(C ₆ H ₄ CO)2

"a" Deprotonation of d₂ or d₃-neutral with DO⁻ (from electron impact of D₂O). "b" Unresolved peak. "c" Linked scan (E/B) shows *m/z* 77 (15%), 73(12%). "d" Linked scan (E/B) shows *m/z* 76(C₃H₂O)14, 75(C₃HDO)16, 73(C₃H₃DO), 72(C₃H₆O)6, 71(C₃H₅DO)5.

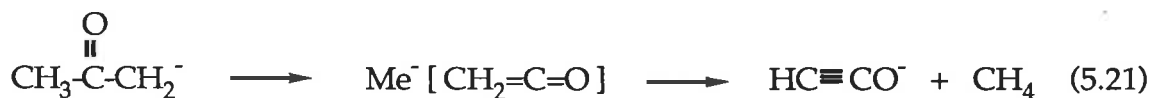


Scheme 5.1

Table 5.4 Collisional activation MS/MS/MS data for product ions from $\text{Me}_3\text{SiC}(\text{O})\text{CH}_2^-$ and $^-\text{CH}_2\text{Si}(\text{Me})_2\text{C}(\text{O})\text{Ph}$, together with CA MS/MS data for $\text{MeC}(\text{O})\text{CH}_2^-$ and $\text{PhC}(\text{O})\text{CH}_2^-$.			
precursor ion (<i>m/z</i>)	product ion (<i>m/z</i>)	spectrum type	spectrum [<i>m/z</i> (abundance in %)]
$\text{Me}_3\text{SiC}(\text{O})\text{CH}_2^-$ (115)	Me_3SiO^- (89)	CA MS/MS/MS CR MS/MS/MS	73(100) 73(23), 59(100), 47(12), 45(88), 43(42), 31(3), 29(3), 15(2)
	$\text{Me}_3\text{SiCH}_2^-$ (87)	CA MS/MS/MS CR MS/MS/MS	71(100) 73(77), 72(98), 71(22), 59(61), 57(28), 55(26), 53(12), 45(20) 44(44), 43(100), 31(8), 29(21)
	$\text{Me}_3\text{SiH}_2^-$ (75)	CA MS/MS/MS CR MS/MS/MS	73(100), 59(11) 59(87), 57(14), 55(10), 45(100), 43(31), 42(16), 41(3), 29(8) 15(4)
	$\text{MeC}(\text{O})\text{CH}_2^- + \text{MeSiCH}_2^-$ (57)	CA MS/MS/MS CR MS/MS/MS	56(78), 55(57), 42(100), 41(8) 55(32), 53(24), 43(46), 42(100), 41(25), 39(12), 29(22), 28(12), 27(20), 15(8), 14(6)
	$^-\text{CH}_2\text{CHO}$ (43)	CA MS/MS/MS CR MS/MS/MS	42(10), 41(100) 42(100), 41(30), 29(81), 28(20), 27(50), 26(25), 15(28), 14(20), 12(2)
	$\text{HC}\equiv\text{CO}^-$ (41)	CA MS/MS/MS CR MS/MS/MS	40(100) 40(100), 25(86), 13(52)
$\text{MeC}(\text{O})\text{CH}_2^-$ (57)		CA MS/MS CR MS/MS	56(100), 41(41) 56(2), 55(10), 54(1), 53(4), 43(68), 42(100), 41(22), 40(8), 39(57), 38(11), 37(5), 29(43), 28(11), 27(49), 26(20), 25(3), 15(10), 14(8)
$^-\text{CH}_2\text{Si}(\text{Me})_2\text{C}(\text{O})\text{Ph}$ (177)	$\text{Ph}(\text{Me})_2\text{SiCH}_2^-$ (149)	CA MS/MS/MS CR MS/MS/MS	No fragmentations detected 134(78), 132(52), 130(35), 120(65), 118(100), 105(92), 93(34), 91(22), 53(18), 43(21)
	$\text{PhC}(\text{O})\text{CH}_2^-$ (119)	CA MS/MS/MS CR MS/MS/MS	118(100), 101(5), 77(80), 41(18) 105(38), 103(40), 102(38), 91(74), 89(40), 77(100), 74(10) 65(23), 63(20), 51(42), 42(6), 39(12), 27(2)
$\text{PhC}(\text{O})\text{CH}_2^-$ (119)		CA MS/MS CR MS/MS	118(100), 101(3), 77(78), 41(15) 105(29), 103(35), 102(38), 91(62), 89(36), 77(100), 74(12) 65(26), 63(18), 51(46), 42(6), 39(12), 27(2)

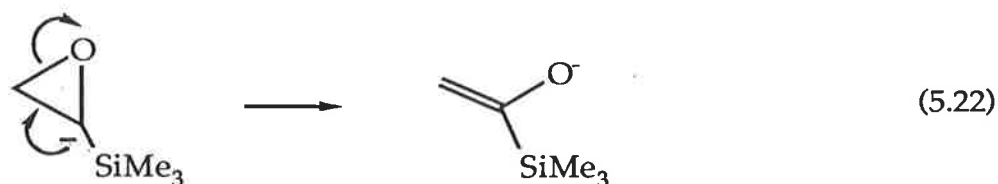
Minor products of note are observed at m/z 57. The C.A. MS/MS/MS spectrum of m/z 57 (Table 5.4) and the C.A. MS/MS spectrum of the labelled parent ${}^{-}\text{CD}_2\text{COSiMe}_3$ (Table 5.3) identify two products; the acetone enolate $\text{CH}_3\text{COCH}_2^-$ and deprotonated dimethyl silane MeSiCH_2^- . These ionic species can be formed by the rearrangement processes shown in equations 5.16 and 5.17, and involve methyl anion transfer. The C.A. spectrum of ${}^{-}\text{CD}_2\text{COSiMe}_3$ (Table 5.3) shows product ions at m/z 57, 58 and 59 consistent with the formation of MeSiCH_2^- , $\text{CH}_3\text{COCHD}^-$ and $\text{Me}_3\text{SiCHD}^-$, and $\text{CH}_3\text{COCD}_2^-$ respectively.

A comparison of the C.A. MS/MS spectrum of authentic $\text{CH}_3\text{COCH}_2^-$ (prepared from the deprotonation of acetone by amide ion in the ion source) with the C.A. MS/MS/MS spectrum of the product ions at m/z 57 (Table 5.4) reveals the spectra to be dissimilar. The grand-daughter ions in the latter spectrum at m/z 41 and m/z 56, corresponding to the losses of methane (equation 5.21) and atomic hydrogen respectively, clearly arise from the fragmentation of the acetone enolate ion.



The grand-daughter ions at m/z 42 and 55 result from the fragmentation of MeSiCH_2^- by loss of methyl radical and molecular hydrogen respectively. A contribution from the fragmentation of MeSiCH_2^- to the products at m/z 41 and 56 cannot be ruled out.

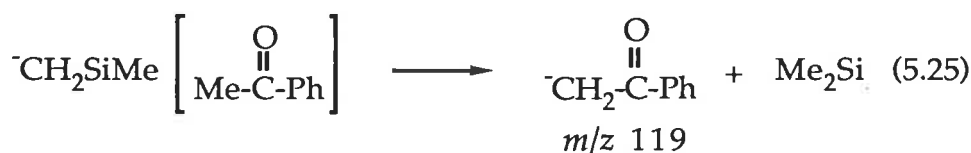
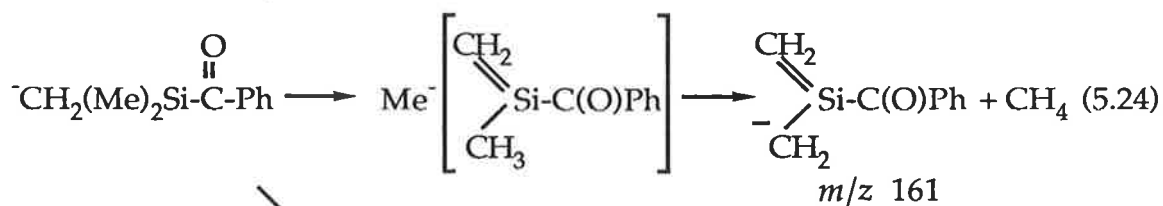
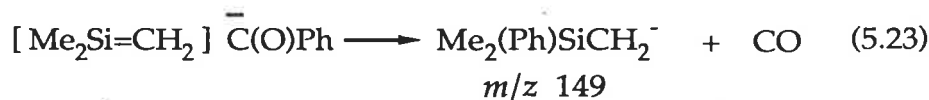
Finally, a comparison of the C.A. mass spectrum of deprotonated acetyl trimethylsilane with that of its isomeric epoxide $\text{c}(\text{CH}_2\text{OC}^-)\text{SiMe}_3$ (Figure 5.4) suggests that the majority of fragmentations of the deprotonated epoxide occur following a transformation to the enolate ion (equation 5.22).



5.4.2 Deprotonated benzoyltrimethylsilane

Whilst the C.A. spectrum of deprotonated propionyltrimethylsilane (Table 5.3) exhibits fragment ions which are analogous to those produced on collisional activation of $^-\text{CH}_2\text{COSiMe}_3$ (Scheme 5.1), the C.A. spectrum of deprotonated benzoyltrimethylsilane is quite different. Unlike the alkyltrimethylsilanes, deprotonated PhCOSiMe_3 shows no rearrangement product ion Me_3SiO^- (m/z 89) in its C.A. mass spectrum (Table 5.3) This is a consequence of benzoyltrimethylsilane bearing no α -hydrogens, resulting in its inability to form an enolate ion on deprotonation. Deprotonation can occur either on the phenyl group or on a methyl group attached to silicon (resulting in the formation of a α -silyl anion).

The C.A. spectrum of deprotonated benzoyltrimethylsilane (Table 5.3) is dominated by losses of molecular hydrogen, carbon monoxide (equation 5.23) and methane (equation 5.24) all of which can be rationalised as fragmentations of the α -silyl anion .



A further decomposition involves methyl anion migration from silicon to the carbonyl group. Subsequent proton transfer within the resulting ion complex, followed by dissociation, yields deprotonated acetophenone [m/z 119 (equation 5.25)]. The C.A. MS/MS/MS and CR MS/MS/MS spectra of this daughter ion are identical to those of authentic deprotonated acetophenone (Table 5.4).

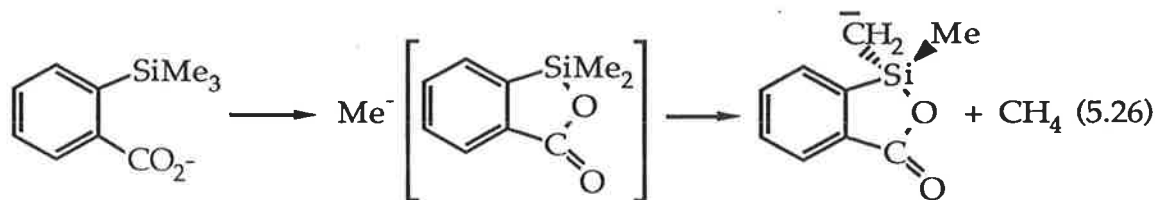
5.5 Trimethylsilylaryl carboxylates

The collisional activation mass spectra of several trimethylsilylsubstituted aryl carboxylates are shown in Table 5.5.

The simplest ions studied are deprotonated *ortho*- and *para*- trimethylsilylbenzoic acid. The spectrum of the *ortho* isomer (Table 5.5) is dominated by the loss of methane. This is rationalised through Si-O bond formation and ejection of a methyl anion which subsequently deprotonates the solvated neutral of the ion-molecule complex (equation 5.26).

Table 5.5 Collisional activation mass spectra of trimethylsilyl substituted aryl carboxylates	
Ion (m/z) ^a	C.A. MS/MS [m/z (loss) abundance in %]
<i>o</i> -Me ₃ Si(C ₆ H ₄)CO ₂ ⁻ (193)	192(H·)100, 177(CH ₄)66, 149(CO ₂)31, 121(Me ₂ SiCH ₂)15
<i>p</i> -Me ₃ Si(C ₆ H ₄)CO ₂ ⁻ (193)	192(H·)100, 178(Me·)18, 149(CO ₂)98
<i>o</i> -Me ₃ SiCH ₂ (C ₆ H ₄)CO ₂ ⁻ (207)	206(H·)65, 191(CH ₄)92, 163(CO ₂)100, 135(Me ₂ SiCH ₂)43, 117(Me ₃ SiOH)28, 91(Me ₂ SiCH ₂ + CO ₂)29, 89(C ₈ H ₆ O)42
<i>o</i> -Me ₃ SiCH ₂ CH ₂ (C ₆ H ₄)CO ₂ ⁻ (221)	220,219 ^b (H·,H ₂)100, 205(CH ₄)5, 177(CO ₂)18, 161(HCO ₂ Me)90, 147(Me ₃ SiH)9, 131(Me ₃ SiOH)1, 103(C ₄ H ₁₀ SiO ₂)9, 89(C ₉ H ₈ O)1, 73(C ₉ H ₈ O ₂)12
<i>p</i> -Me ₃ SiCH ₂ CH ₂ (C ₆ H ₄)CO ₂ ⁻ (221)	220(H·)20, 219(H ₂)4, 205(CH ₄)18, 191(C ₂ H ₆)2, 177(CO ₂)100, 147(Me ₃ SiH)39, 103(C ₄ H ₁₀ SiO ₂)7, 73(C ₉ H ₈ O ₂)2

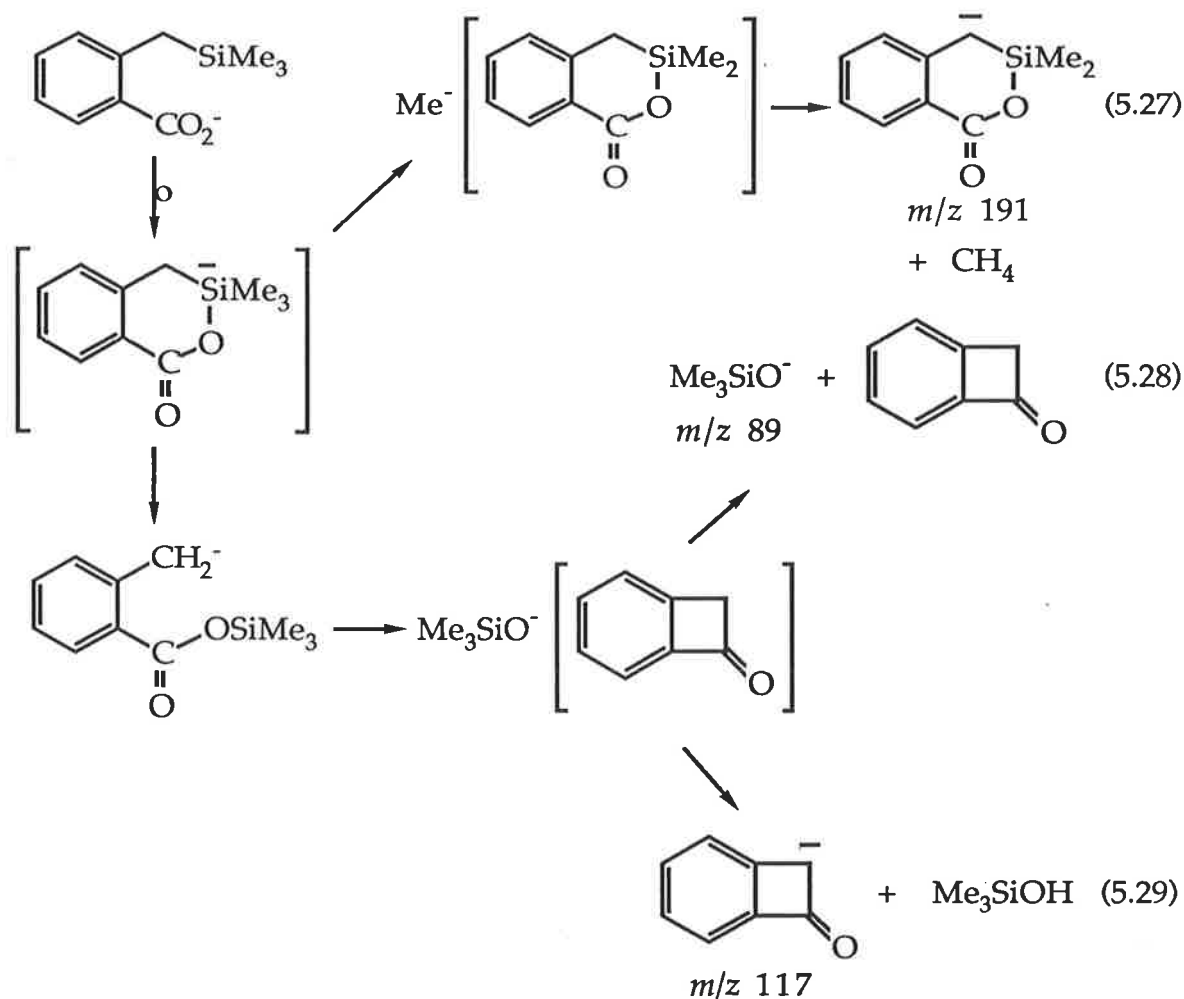
"a" Deprotonation is effected solely on the carboxyl group by the reaction of DO⁻ (from D₂O) with d₁-trimethylsilyl-substituted aryl carboxylic acid. "b" Unresolved peak



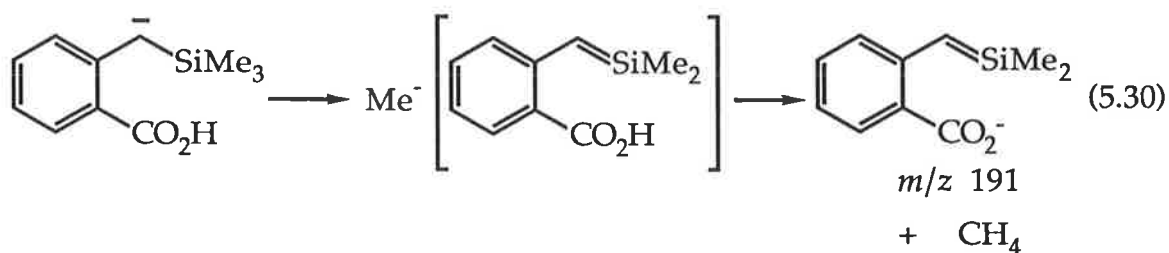
The *para* isomer, in which the trimethylsilyl and carboxylate groups are rigidly separated by the benzene ring, shows no loss of methane in its C.A. mass spectrum (Table 5.5). Instead, the spectrum exhibits a peak at m/z 78 corresponding to a loss of methyl radical by a simple cleavage process.

Fragmentations common to both isomers are the losses of atomic and molecular hydrogen and carbon dioxide, the latter giving rise to the formation of trimethylsilylsubstituted phenyl anions (m/z 149).

The C.A. mass spectrum of deprotonated *ortho*-(trimethylsilylmethyl)-benzoic acid (Table 5.5) shows approximately equal losses of methane and carbon dioxide (to yield m/z 191 and 163 respectively) the latter by a simple cleavage. Peaks at m/z 89 and 117 in the spectrum correspond to the formation of Me_3SiO^- and loss of Me_3SiOH respectively. These product ions are consistent with an intramolecular silicon migration from carbon to oxygen through a penta-coordinate intermediate. Ring opening affords a resonance stabilised benzyl anion which can subsequently eliminate Me_3SiOH (to yield m/z 117) (equation 5.29) and also form Me_3SiO^- (m/z 89) (equation 5.28). This same intermediate can also account for the loss of methane (equation 5.27).

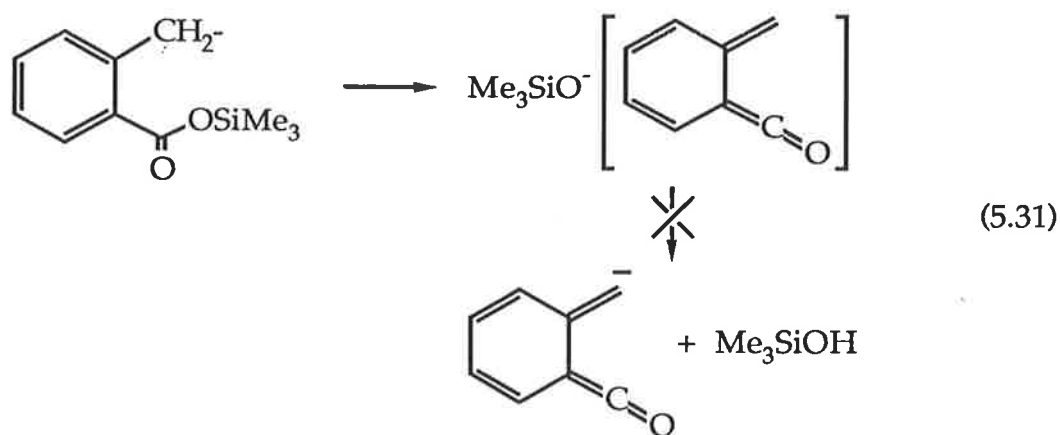


The loss of methane can alternatively be rationalised through a mechanism shown in equation 5.30 from a benzylic anion formed from a competing deprotonation of the parent.

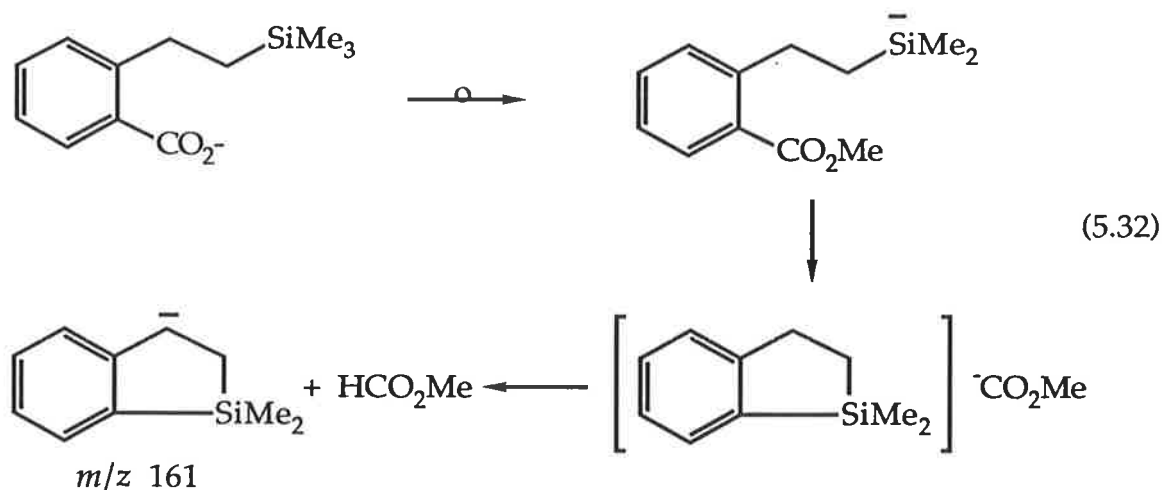


The formation of Me_3SiO^- and elimination of Me_3SiOH from the benzylic anion could be envisaged to occur through nucleophilic addition of the benzylic centre to the carbonyl group (see equations 5.28, 5.29) or by electron

transfer through the aromatic ring (equation 5.31). However, deprotonation of the substituted ketene by Me_3SiO^- in this latter process is not favoured based on estimated acidities [$\Delta H^\circ_{\text{acid}}(\text{CH}_2=\text{CH}_2) = 1699 \text{ kJ mol}^{-1}$ ⁷⁰, predict $\Delta H^\circ_{\text{acid}}(\text{Me}_3\text{SiOH}) \approx 1570 \text{ kJ mol}^{-1}$].



The C.A. spectrum of deprotonated *ortho*-trimethylsilyl ethylbenzoic acid is given in Table 5.5. Whilst the base peak of the spectrum is a result of hydrogen loss, the second most abundant peak (at m/z 161) corresponds to either the loss of methyl formate or to consecutive losses of carbon dioxide and methane. However the abundance of this peak (90%), suggests that the ion at m/z 161 is produced by a single loss from the parent. The loss of methyl formate is best rationalised through the process shown in equation 5.32. Methyl migration from silicon to oxygen followed by cyclisation and ejection of the methoxycarbonyl anion MeOC(O)^- precedes proton transfer within the resulting ion-molecule complex.



The C.A. spectrum of deprotonated *para*-trimethylsilylethyl-benzoic acid (Table 5.5), exhibits no product ion at m/z 161. In the *para* isomer, the trimethylsilyl and carboxylate groups are rigidly separated sufficiently by the aromatic ring and hence the loss of the HCO_2Me does not occur.

5.6 Trimethylsilyl benzyl carboxylates

Deprotonated α -trimethylsilylphenylacetic acid has a C.A. mass spectrum (Figure 5.5, Table 5.6) dominated by the loss of Me_3SiOH consistent with the migration of silicon from carbon to oxygen through a cyclopenta-coordinate silicon intermediate (equations 5.33 and 5.34).

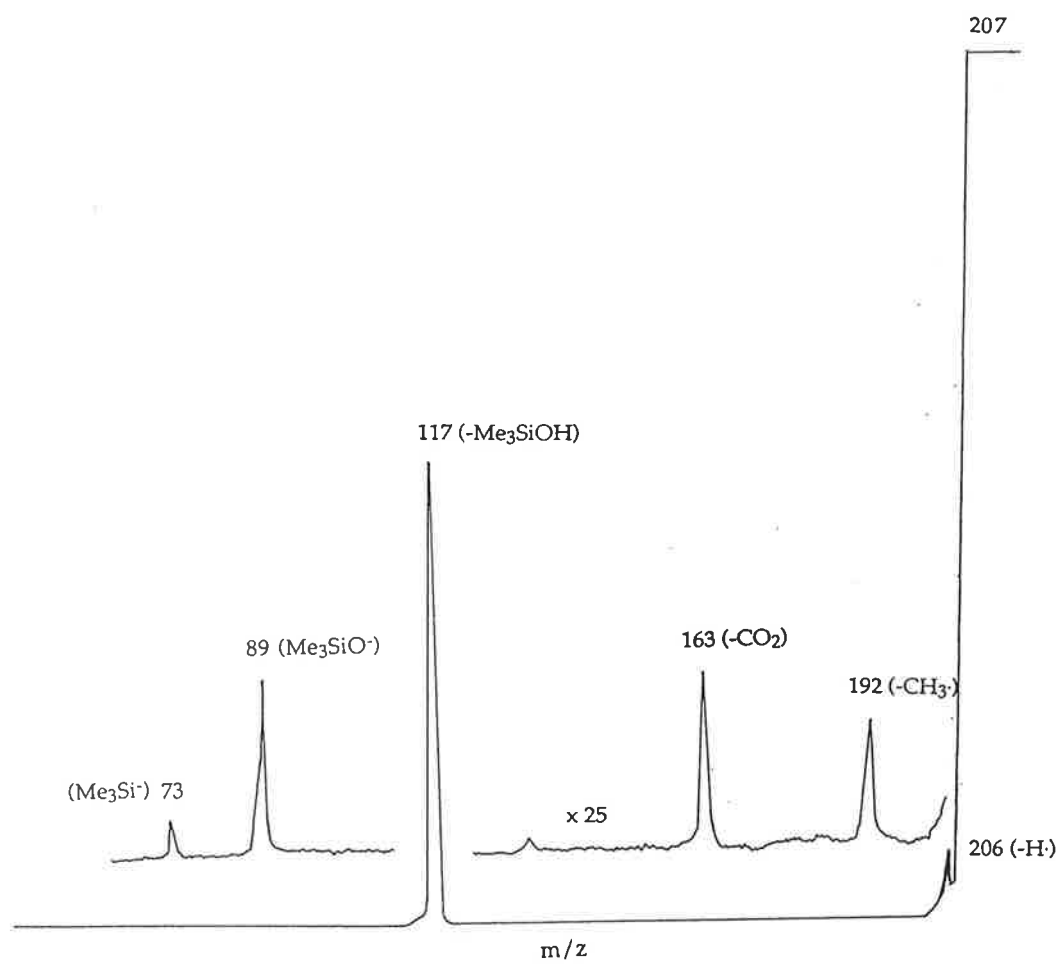
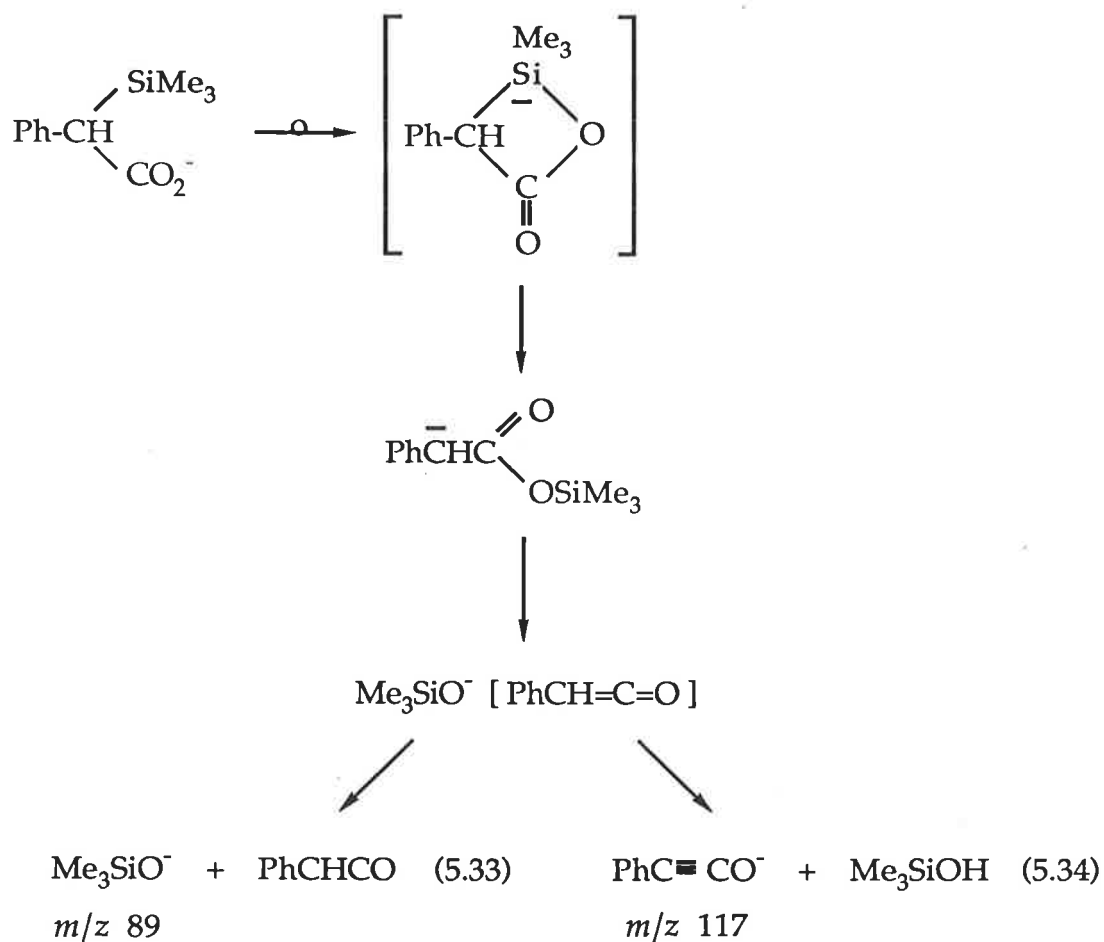


Figure 5.5 Collisional activation mass spectrum of deprotonated α -trimethylsilylphenylacetic acid.

Table 5.6 Collisional activation mass spectra α -trimethylsilylbenzyl carboxylates	
Ion (m/z)	C.A. MS/MS [m/z (loss) abundance in %]
Ph(Me ₃ Si)CHCO ₂ ⁻ (m/z 207)	206(H·)10, 192(Me·)1, 191(CH ₄)1, 163(CO ₂)1.5, 117(Me ₃ SiOH)100 89(PhCHCO)1.5, 73(C ₈ H ₆ O ₂)0.2
Ph(Me ₃ SiCH ₂)CHCO ₂ ⁻ (m/z 221)	220(H·)10, 205(CH ₄)3, 177(CO ₂)100, 161(HCO ₂ Me or CO ₂ + CH ₄)2, 147(Me ₃ SiH)1, 103(C ₄ H ₁₀ SiO ₂)2, 89(C ₉ H ₈ O)0.5, 73(Me ₃ SiH)1
Ph(Me ₃ SiCH ₂)CDCO ₂ ⁻ (m/z 222)	221(H·)6, 220(D·)2, 205(CH ₃ D)2, 178(CO ₂)100, 161(DCO ₂ Me or CO ₂ + CH ₃ D)2, 147(Me ₃ SiD)1, 104(C ₄ H ₁₀ SiO ₂)1, 89(C ₉ H ₇ DO)0.3, 73(C ₉ H ₇ DO ₂)5



Interestingly, this spectrum exhibits no loss of methane. This is likely a result of the instability of the four-centred pentacoordinate silicon intermediate to decomposition by decyclisation.

In contrast, the C.A. spectrum of deprotonated α -trimethylsilylmethylphenylacetic acid (Table 5.6) exhibits only minor fragmentations involving an intramolecular migration of silicon from carbon to oxygen. Instead, $\text{Ph}(\text{Me}_3\text{SiCH}_2)\text{CHCO}_2^-$ fragments predominantly by the loss of carbon dioxide. The stability of the resulting resonance stabilised benzyl anion, over the di-substituted β -ethyl anion produced by silicon migration to oxygen, accounts for the preferential loss of CO_2 .

5.7 Summary and conclusions

The results presented in this chapter suggest that the intramolecular migration of silicon to a formal negatively charged oxygen atom occurs extensively in the gas phase. Two properties which are thought to catalyse such rearrangements are the empty d-orbitals of silicon (which can accept electrons of sterically accessible charged centres) and the large dissociation energy of the subsequently produced silicon-oxygen bond (525 kJ mol^{-1} 188).

The *extent* of silicon migration to oxygen in the gas phase, however, varies within the organosilicon systems studied. In some instances, silicon migration accompanies the formation of an ion which represents the base peak of a spectrum (see for example Figures 5.1-5.4). In other cases, however, such an ion represents only a minor fragmentation [see the C.A. spectrum of deprotonated *o*-(trimethylsilylethyl)-benzoic acid (Table 5.5)] or does not appear at all [see the C.A. spectrum of *p*-trimethylsilylbenzoic acid (Table 5.5)]. The extent of silicon migration appears to be dependent on several factors:

- (i) the intramolecular distance which separates the silicon and oxygen centres

For example, consider the C.A. spectrum of deprotonated *o*-trimethylsilylbenzoic acid (Table 5.5). The spectrum is dominated by the loss of methane [a process rationalised by initial silicon-oxygen bond formation (equation 5.26)]. Collisional activation of its *para*-isomer (in which the silicon and oxygen centres are rigidly separated by the aromatic ring), however, affords only fragment ions produced by simple cleavage processes (Table 5.5).

(ii) the activation energy of the rearrangement process

Fragment ions resulting from silicon-oxygen bond formation are observed to predominate in systems which are expected to form relatively low energy transition states. Note that in the C.A. spectrum of deprotonated *o*-trimethylsilylmethylbenzoic acid (Table 5.5) the formation of Me_3SiO^- (m/z 89) occurs in greater abundance than in the C.A. spectrum of deprotonated *o*-trimethylsilylethyl-benzoic acid (Table 5.5). This is consistent with the lower energy expected to form the six-centred cyclic transition state of the former parent ion.

(iii) the relative stability of the products produced on rearrangement and those produced from other processes

The C.A. spectrum of deprotonated α -trimethylsilylphenylacetic acid (Figure 5.5, Table 5.6) is dominated by the formation of $\text{PhC}\equiv\text{CO}^-$ (m/z 117); the result of an initial silicon migration to afford a benzylic anion (equation 5.34). By comparison, silicon migration from carbon to oxygen in deprotonated α -trimethylsilylmethylphenylacetic acid yields an unstable di-substituted β -ethyl anion. Consequently, the C.A. spectrum of α -trimethylsilylmethyl-phenylacetic acid (Table 5.6) is dominated by the loss of carbon dioxide which results in the production of a more stabilised benzylic anion.

Summary and conclusions

It has been realised for some time that "the interior of a mass spectrometer...provides an ideal laboratory for studying the interplay of theory and experiment."²⁰³ Over recent years, an increasing number of studies have made use of both theoretical and experimental approaches to solve a chemical problem. In these laboratories alone, theory has been combined with experiment on numerous occasions to determine the structure and stability of a gas phase ion, or to investigate the mechanism of a gas phase reaction.^{148,150,204} With the continual improvements in computing "power", undoubtedly more complex problems will be within the realm of theoretical investigations and this relationship will further flourish.

The results presented in this thesis continue to exploit this alliance. In chapter 2, the results of experimental attempts to detect selected α - and β -substituted alkyl carbanions have been presented together with independent theoretical calculations. These calculations enable the basicity of the carbanions and their stability to electron detachment to be predicted; two properties important to their detection. In the case of the α -hetero substituted carbanions $RXCH_2^-$ ($X = O, S, NH, NCH_3$; $R = H, CH_3$), the high level *ab initio* calculations presented provide a reliable estimate of these parameters.

Consider for example the calculations presented in Section 2.2.3.1. The methylene thiol anion was predicted to have a basicity given by $\Delta H^\circ_{\text{acid}}(\text{CH}_3\text{SH}) = 1669 \text{ kJ mol}^{-1}$ and is estimated to be stable to electron detachment by 23 kJ mol^{-1} . In accord with these calculations, the methylene

thiol anion was successfully generated in the gas phase, with its basicity subsequently bracketted (Section 2.2.3.3.1) at 1661 ± 17 kJ mol⁻¹. Unlike their sulphur analogue, the highly basic carbanions HOCH₂⁻ and NH₂CH₂⁻ were not detected, consistent with their predicted instability to electron loss. Similar agreement between theory and experiment was found for the systems CH₃XCH₂⁻ (X = O, S, NH, NCH₃).

Whilst theoretical calculations for the "larger" β-ethyl anions were beyond those possible with the available facilities, the experimental results enable some conclusions regarding their stability to be discussed. All the β-substituted ethyl anions investigated, except one, were found to isomerise to a more stable isomer under the experimental conditions employed. In the case of the β-methoxycarbonyl ethyl anion (where no isomer was detected), the β-ethyl anion is either not produced from the neutral precursors or is unstable to electron detachment.

In chapter 3, the structure of the HN₂O⁻ ion produced by the addition of hydride ion to nitrous oxide is scrutinised theoretically. In this instance, two stable isomers are theoretically plausible, though the experimental approach has been unable to differentiate between them. The chemistry of the HN₂O⁻ ion was explored within the flowing afterglow - S.I.F.T. instrument. Reaction products, branching ratios, reaction rates and efficiencies and postulated reaction mechanisms are presented.

The loss of ethene on the collisional activation of deprotonate ethyl methyl sulphoxide is the subject of chapter 4. The product ion was identified experimentally to be the methyl sulphinyl anion whose ion-molecule chemistry was subsequently investigated. The favoured formation of this isomer, over ⁻CH₂S-OH and ⁻CH₂S(O)H, has been rationalised based on thermodynamic considerations.

Finally, chapter 5 presents a preliminary study of intramolecular gas phase anionic rearrangements involving the migration of silicon. Rearrangements involving the production of silicon-oxygen bonds are reported to predominate in most of the organosilicon systems. This study compliments the large number of gas phase rearrangements of organic anions already reported in these laboratories.^{35-38,205} In many cases, the rearrangements mirror those observed in solution.

CHAPTER 6

EXPERIMENTAL6.1 Instrumentation

Collision activation and charge reversal mass spectra were recorded on a Vacuum Generators ZAB 2HF reverse-geometry mass spectrometer²⁹ operating in the negative chemical ionisation mode. All slits were fully open to maximise sensitivity and to minimise energy resolution effects.²⁰⁶

The chemical ionisation slit was used in the ion-source; ionizing energy 70eV (tungsten filament); ion-source temperature 150°C; accelerating voltage -7 kV. Anions were generated by nucleophilic displacement reactions or proton or deuterium abstraction from the appropriate substrates using NH_2^- (from the chemical ionisation of NH_3), HO^- (from H_2O) or MeO^- (from dissociative resonance capture of MeONO ²⁰⁷ or from MeOH). The source pressure of NH_3 , H_2O , MeOH or MeONO was typically measured at 5×10^{-4} Torr. The *estimated* total source pressure was 10^{-1} Torr. The pressure of helium in the collision cell was 2×10^{-7} Torr measured by an ion gauge situated between the electric sector and the collision cell. These conditions produced a decrease in the main beam signal of approximately 10% corresponding to essentially single ion-helium collisions. Similar conditions were employed for the charge-reversal spectra⁴⁰⁻⁴² except that the polarity of the electric sector voltage was reversed. CA/MS/MS/MS and CR/MS/MS/MS Spectra were recorded by Dr. Roger N. Hayes using a triple sector Kratos MS 50-TA instrument at The University of Nebraska, Lincoln employing operating procedures that have been previously described⁴⁸. Deprotonation was effected using MeO^- (from MeONO ²⁰⁷) in a Kratos Mark IV CI source: ion source temperature 100°C, electron energy 280

eV, emission current $500\mu\text{A}$, accelerating voltage -8 kV , with measured source pressures of compound ($2 \times 10^{-5}\text{ Torr}$) and methyl nitrite ($1 \times 10^{-6}\text{ Torr}$). The estimated total source pressure was 10^{-1} Torr . The helium pressure in each collision cell was $2 \times 10^{-6}\text{ Torr}$ producing a decrease in the main beam signal of 30%.

Ion-molecule reactions, rates and efficiencies and branching ratios were measured using the flowing afterglow-S.I.F.T. instrument at The University of Colorado at Boulder within the laboratories of Professor Charles H. DePuy. The instrument design and capabilities have been discussed in detail elsewhere.⁶⁷ Briefly, the instrument consists of four regions: (i) a flow tube for ion preparation, (ii) a quadrupole mass filter for ion selection, (iii) a second flow tube for ion-molecule reactions, and (iv) an ion detection region.

Ions are prepared in the first flow tube. Five fixed inlets and two movable inlets fitted with diffusors provide a means of introducing buffer and neutral gases. The movable ioniser consists of a thoriated-iridium filament, a repeller plate and an extracting grid. Primary reagent ions can be sampled directly into the quadrupole or allowed to react with a suitable neutral, added downstream, to produce secondary ions. All ions are formed in a helium buffer gas (introduced at pressures $0.3 - 1.5\text{ Torr}$) having an average velocity of approximately 40 m sec^{-1} .

Ions produced in the first flow tube proceed into the ion selection region via a 2 mm orifice in the nose cone. The quadrupole mass filter, free of buffer gas and neutrals, operates at low pressures (typically 10^{-6} Torr). The desired ion is mass selected, electrostatically focussed via a series of lenses and injected into the second flow tube by means of an electric potential.

The second flow tube (filled with a helium buffer gas to pressures of approximately $0.4 - 0.5\text{ Torr}$ at a flow velocity of 90 m sec^{-1}) is 120 cm in length

and is fitted with seven, equally spaced, fixed inlets. Neutral reagent gases are introduced into the flow tube through any inlet (via a vacuum rack) to enable chemical reactions to be performed amidst the buffer gas.

The detection region samples ions through a 1 mm orifice to a differentially pumped high vacuum region. Ions are focussed by three electrostatic lenses, mass analysed with a quadrupole mass filter and detected by an electron multiplier. Data acquisition and analysis is achieved using a micro-computer.

Reaction rates were determined by measuring the change in reactant ion concentration as a function of inlet position (or reaction distance) of the neutral reagent. The decay in reactant ion concentration was monitored by adding the neutral reagent (at constant flow) to each of the seven inlets successively, using an average of two measurements at each inlet. The rate coefficients reported represent an average of, at least, three independent measurements recorded at different neutral flow rates.

Branching ratios were determined from a plot of the decrease in reactant ion concentration (which provides a measure of the extent of reaction) vs. the relative concentrations of product ions averaged at three different neutral flows. A smooth curve is drawn through the set of points associated with each product and extrapolated to zero extent. Each intercept value represents the branching ratio of a particular product ion. A branching ratio determination is typically accurate to $\pm 15\%$. Secondary product ions will have a branching ratio of zero.

Electron impact (positive ion) mass spectra were recorded routinely on a AEI MS-30 mass spectrometer.

All ^1H n.m.r. spectra were recorded on a Varian TS-60 (60 MHz) n.m.r. or a JEOL PMX60 (60 MHz) spectrometer. The spectra were measured in p.p.m.

downfield from internal standard tetramethylsilane in CDCl_3 or CCl_4 , or upfield from residual CHCl_3 in CDCl_3 where appropriate.

Infrared spectra were recorded on a Hitachi 270-30 infrared spectrometer. Samples were prepared, using solvent nujol where appropriate, on NaCl plates.

Melting points were measured on a Reichert-Kofler hot stage melting point apparatus and are uncorrected.

Microanalyses were carried out by Canadian Microanalytical Service Ltd., Delta, British Columbia.

6.2 Synthesis

6.2.1 Commercial samples used for experiments discussed in Chapter 2

The following compounds are commercial reagents which were used without further purification: ethylene glycol, glycolic acid, ethane dithiol, thioglycolic acid, 1,2-diamino-ethane, glycine, 2-methoxyethanol, 2-methylamino-ethanol, sarcosine, 2,2-dimethylamino-ethanol, propionaldehyde, acetone, 3-acetylpropionic acid, butan-2-one, butyraldehyde, propiophenone, phenylpropan-2-one, 4-hydroxypropionic acid, succinic acid, propionic acid, methyl acetate, 4-penten-1-ol and but-2-ene.

6.2.2 Synthesis of unlabelled compounds for chapter 2

Trimethylsilylmethanol was prepared by a reported procedure.²⁰⁸

Yield 50%, b.p. 120-121°C / 760 mm Hg (lit.²⁰⁹ 121.6°C / 760 mmHg)

^1H n.m.r. $\delta(\text{CDCl}_3)$: 0.2,s,9H; 2.1,s,2H; 3.9,s,1H.

Trimethylsilylmethane thiol was prepared by the procedure of Noller and Post.²¹⁰

Yield 36%, b.p. 118-120°C / 760mm Hg (lit.²¹⁰ 115-115.5°C / 749 mm Hg)

¹H n.m.r. δ (CDCl₃): 0.1,s,9H; 0.6,s,2H; 0.7,s,1H.

Trimethylsilylmethylamine was prepared from the hydrochloride salt by a procedure of Sommer and Rockett.²¹¹

Yield 38%, b.p. 94-94.5°C / 760mm (lit.²¹¹ 94°C / 729 mm Hg)

¹H n.m.r. δ (CDCl₃): 0.0,s,9H; 2.1,s,2H.

ν_{\max} (liquid film) 3350 cm⁻¹ (NH)

Methylthioacetic acid was prepared by the methylation of thioglycolic acid following a reported procedure.²¹²

Yield 73%, b.p. 200-250°C / 15 mm Hg (Kugelrohr) (lit.²¹² 130-131°C / 0.27 mm Hg)

¹H n.m.r. δ (CDCl₃): 2.3,s,3H; 3.2,s,2H; 10.3,s,1H

ν_{\max} (liquid film) 1720 (C=O) cm⁻¹

2-Methylthioethanol was synthesised according to a reported method.²¹³

Yield 64%, b.p. 63-65°C / 15 mm Hg (lit.²¹⁴ 80.5-81°C / 30 mm Hg)

¹H n.m.r. δ (CDCl₃): 2.1,s,3H; 2.6-2.9,m,4H; 3.8,s,1H

ν_{\max} (liquid film) 3400 (OH) cm⁻¹

α -Methylthiomethyltrimethylsilane was prepared by the method of Peterson.²¹⁵

Yield 99%, b.p. 130-150°C / 760 mm Hg (Kugelrohr) (lit.²¹⁵ 50-130°C / 760 mm Hg)

¹H n.m.r. δ (CDCl₃): 0.0,s,9H; 1.7,s,2H; 2.1,s,3H

Methoxyacetic acid was prepared from chloroacetic acid by a general procedure.²¹⁶

Yield 42%, b.p. 98-99°C / 17 mm Hg (lit.²¹⁷ 96.5°C / 13 mm Hg)

¹H n.m.r. δ (CDCl₃): 3.6,s,3H; 4.2,s,2H

ν_{\max} (nujol) 1760 (C=O) cm⁻¹

Methoxymethyltrimethylsilane was prepared by the procedure of Speier.²¹⁸

Yield 36%, b.p. 83-84°C / 760 mm Hg (lit.²¹⁸ 83°C / 740 mm Hg)

¹H n.m.r. δ (CDCl₃): 0.0,s,9H; 3.1,s,2H; 3.2,s,3H

N-Methyltrimethylsilylmethylamine was synthesised following a reported method.²¹⁹

Yield 48%, b.pt. 104-105°C / 760 mm Hg (lit.²¹⁹ 93°C / 736.8 mm Hg)

¹H n.m.r. δ (CDCl₃): 0.0,s,9H; 2.3,s,2H; 2.7,s,3H

N,N-Dimethylglycine was prepared according to the procedure of Clarke, Gillespie and Weisshaus.²²⁰

Yield 71%, m.pt. 186-189°C (lit.²²⁰ 189-190°C)

¹H n.m.r. δ (CDCl₃): 3.0,s,6H; 4.2,s,2H

ν_{\max} (nujol) 3400 (OH), 1615 (C=O) cm⁻¹

N,N-Dimethyltrimethylsilylmethylamine was prepared by a published method.²¹⁹

Yield 58%, b.pt. 108-110°C / 760 mm Hg (lit.²¹⁹ 101.6°C / 735 mm Hg)

¹H n.m.r. $\delta(\text{CDCl}_3)$: 0.0,s,9H; 2.2,s,2H; 2.7,s,6H

3-Formylpropanol was prepared by the ozonolysis of 4-pentenol following a general procedure.²²¹

Yield 74%, b.p. 82-84°C / 26 mm Hg (lit.²²² 98-99°C / 35 mm Hg)

¹H n.m.r. $\delta(\text{CDCl}_3)$: 2.1,m,2H; 2.7,m,2H; 4.0,m,2H; 9.9,t (J=4 Hz),1H

ν_{max} (liquid film) 3300 (O-H), 2725 (C(O)-H), 1720 (C=O) cm^{-1}

Succinic semialdehydic acid was prepared by a reported procedure.²²³

Yield 50%, m.p. 146-147°C [lit.²²⁴ 147°C (dimer)]

¹H n.m.r. $\delta(\text{CDCl}_3)$ 2.2,m,2H; 2.7,m,2H; 7.6,t (J=2 Hz),1H; 10.4,s,1H

β -Trimethylsilylpropionaldehyde was prepared by a standard chromium trioxide-pyridine oxidation²²⁵ of β -trimethylsilylpropanol.

Yield 87%, b.p. 58-60°C / 30 mm Hg (lit.²²⁶ 58°C / 30 mm Hg)

¹H n.m.r. $\delta(\text{CDCl}_3)$: 0.3,s,9H; 0.8,t (J=10 Hz)2H; 2.4,m,2H; 7.9,t (J=4 Hz)1H

ν_{max} (liquid film) 2750 [C(O)-H], 1730 (C=O) cm^{-1}

Cyclopropyl acetate was prepared by P.C.H. Eichinger for another study.¹⁷⁶

3-Acetylpropanol was prepared by a procedure analogous to that reported for the preparation of 3-benzoylpropanol.²²⁷

Yield 33%, b.p. 90-100°C (Kugelrohr) / 16 mm Hg (lit.²²⁸ 116-118°C / 33 mm Hg)

¹H n.m.r. $\delta(\text{CDCl}_3)$: 1.17,m,2H; 1.87,t (J=12 Hz),2H; 2.13,s,3H; 2.60,s,1H; 4.57,t (J=12 Hz),2H

ν_{\max} (liquid film) 3500 (OH), 1720 (C=O) cm^{-1}

4-Trimethylsilylbutan-2-one was prepared by a procedure reported by Sommer and Marans.²²⁹

Yield 46%, b.p. 80-82°C / 65 mm Hg (lit.²²⁹ 84°C / 65 mm Hg)

^1H n.m.r. $\delta(\text{CDCl}_3)$: 0.0,s,9H; 0.7,t (J=8 Hz),2H; 2.2,s,3H; 2.3,t (J=8 Hz),2H

3-Benzoylpropanol was prepared following the procedure of Ward and Sherman.²²⁷

Yield 25%, m.p. 31-33°C (lit.²³⁰ 32-33°C)

^1H n.m.r. $\delta(\text{CDCl}_3)$: 2.1,t (J=14 Hz)2H; 2.1,s,1H; 3.1,t (J=14 Hz),2H; 3.7,t (J=14 Hz),2H; 7.13-7.73,m,3H; 7.97-8.20,m,2H

ν_{\max} (liquid film) 3460 (OH), 1690 (C=O) cm^{-1}

3-Benzoylpropionic acid was prepared following a routine procedure.²³¹

Yield 78%, m.p. 117-119°C (lit.²³² 116.5°C)

^1H n.m.r. $\delta(\text{CDCl}_3)$: 2.9,t (J=12 Hz),2H; 3.3,t (J=12 Hz),2H; 7.2-7.6,m,3H, 7.9-8.1,m,2H

ν_{\max} (nujol) 1695 (C=O) cm^{-1}

β -Trimethylsilyl ethyl phenyl ketone was prepared by the photolysis of vinyltrimethylsilane and benzaldehyde by a reported procedure.²³³

28%, b.pt. 113-115°C / 4 mm Hg (lit.²²⁹ 115°C / 4 mm Hg)

^1H n.m.r. $\delta(\text{CDCl}_3)$: 0.0,s,9H; 0.77,m,2H; 2.83,m,2H; 7.3-8.0,m,5H

ν_{\max} (liquid film) 1695 (C=O) cm^{-1}

M.S. (+ve) m/z 205(M^+)9, 204($\text{M}^+ - \text{H}$)34, 190($\text{M}^+ - \text{CH}_3$)33, 117($\text{M}^+ - \text{C}_4\text{H}_{12}\text{Si}$)45, 105(PhCO^+)29, 73(Me_3Si^+)100

β -Trimethylsilylpropionic acid was prepared by a standard chromic oxidation²³⁴ of γ -trimethylsilylpropanol.

Yield 96%, b.p. 110-112°C / 28 mm Hg (lit.²³⁵ 147°C / 65 mm Hg)

¹H n.m.r. δ (CDCl₃): 0.0,s,9H; 1.7,m,2H; 2.3,m,2H; 10.4,s,1H

Methyl 4-hydroxybutyrate was prepared from γ -butyrolactone by the procedure of Brown and Keblys.²³⁶

Yield 15%, b.p. 117-120°C / 16 mm Hg (lit.²³⁶ 45-46°C / 0.2 mm Hg)

¹H n.m.r. δ (CDCl₃): 2.0,m,2H; 2.5,m,2H; 3.7,s,3H, 3.7,t (J=6 Hz),2H

ν_{\max} (liquid film) 3450 (O-H), 1740 (C=O) cm⁻¹

Methyl β -trimethylsilylpropanoate was prepared by an analogous procedure reported by Sommer and Marans²²⁹ using methyl acetoacetate as the starting material.

58%, b.p. 70-72°C / 20 mm Hg (lit.²³⁷ 69°C / 17 mm Hg)

¹H n.m.r. δ (CDCl₃): 0.0,s,9H; 0.8,m,2H, 2.3,m,2H; 3.6,s,3H

4-Pentenoic acid was prepared by a standard oxidation²³⁴ of 4-pentenol.

Yield 98%, b.p. 82-84°C / 12 mm Hg (lit.²²⁸ 93°C / 20 mm Hg)

¹H n.m.r. δ (CDCl₃): 2.4,m,4H; 4.8-5.1,m,2H; 5.5-6.1,m,1H; 9.7,s,1H

ν_{\max} (liquid film) 3000 (O-H), 1720 (C=O) cm⁻¹

4-Trimethylsilylbutene was prepared by the method of Hauser and Hance²³⁸ except that the Grignard reagent of chloromethyltrimethylsilane was used.

Yield 39%, b.p. 112-114°C / 760 mm Hg (lit.²³⁸ 112-113°C / 760 mm Hg)

¹H n.m.r. δ (CDCl₃): -0.1,s,9H; 0.6,m,2H; 2.1,m,2H; 4.8-5.2,m,2H; 5.6-6.3,m,1H

ν_{\max} (liquid film) 1640 (C=O) cm^{-1}

M.S. (+ve) m/z 128(M^+)1, 113(M^+ - Me)43, 85(M^+ - C_3H_7)22, 73(Me_3Si^+)100

1-butene was prepared by a reported procedure.²³⁹

Cyclopropylacetic acid was prepared according to a reported procedure.²⁴⁰

33%, b.p. 87-89°C / 15 mm Hg (lit.²⁴¹ 189-191°C / 750 mm Hg)

^1H n.m.r. $\delta(\text{CDCl}_3)$: 0.7-0.9,m,5H; 2.2,m,2H; 10.4,s,1H

6.2.3 Synthesis of labelled compounds for chapter 2

d_2 -Ethylene glycol, d_2 -ethanedithiol, d_1 -trimethylsilylmethanol, d_1 -trimethylsilylmethane thiol and β -(d_5 -acetyl)-propionic acid were all prepared by stirring the unlabelled compound (ca 0.1 g) in D_2O (1 ml) for 1 hour. The labelled compound was separated by extraction with dichloromethane (3 x 10 ml) with the organic extracts combined and dried over magnesium sulphate. Removal of the solvent yielded the labelled compound which was used directly without further purification. Deuterium incorporation (d_1 , d_2 or d_5) was greater than 90% in all cases by ^1H n.m.r. and positive ion mass spectrometry.

3-(d_5 -Benzoyl)-propionic acid was prepared by the acylation of d_6 -benzene following an identical procedure to that for the unlabelled compound.²³¹

Deuterium incorporation $\text{d}_5 = 99\%$

^1H n.m.r. $\delta(\text{CDCl}_3)$: 2.9,t (J=12 Hz),2H; 3.3,t (J=12 Hz),2H

*d*₃-Methoxyacetic acid was prepared in 28% yield by an identical procedure to that of its unlabelled analogue²¹⁷ using *d*₃-sodium deuterioxide prepared from *d*₄-methanol.

Deuterium incorporation *d*₃ = 99%

¹H n.m.r. δ (CDCl₃): 3.2,s,2H, 10.3,s,1H

*N,N-d*₆-Dimethylglycine was prepared by the reaction of *d*₆-dimethylamine and chloroacetic acid in 54% yield.

Deuterium incorporation *d*₆ = 98%

¹H nm.r. δ (CDCl₃): 4.2,s,2H

6.2.4 Synthesis of compounds for chapter 3

Neo-pentyl nitrite was prepared in 87% yield from the reaction of *neo* pentyl alcohol and sodium nitrite according to the general procedure of Noyes²⁴² and was used without further purification.

6.2.5 Synthesis of compounds for chapter 4

Ethyl methyl sulphoxide was prepared by the oxidation of ethyl methyl sulphide with sodium metaperiodate following a general procedure.²⁴³

Yield 92%, b.p. 114-115°C / 14 mm Hg ²⁴⁴

¹H n.m.r. δ (CDCl₃): 1.4,t (J=7 Hz),3H; 2.9,s,3H; 3.1,t (J=7 Hz),2H

α,α -d₂-ethyl d₃-methyl sulphoxide was prepared from the unlabelled sulphoxide by the following method.

Ethyl methyl sulphoxide (124 mg, 1.35 mmol) in a solution of sodium deuterioxide [sodium (0.20g, 6.75 mmol) in D₂O (15 ml)] was heated at 100°C for 3 days. The solution was acidified with concentrated d₂-sulphuric acid and extracted with anhydrous chloroform (3 x 15 ml). The combined organic extracts were dried over magnesium sulphate and the solvent removed *in vacuo* to yield d₂-ethyl d₃-methyl sulphoxide (120 mg, 92%, ²H₅ = 98%).

¹H n.m.r. δ(CDCl₃): 3.1,s,3H

6.2.6 Synthesis of unlabelled compounds for chapter 5

Trimethylsilylmethanol was prepared as described in Section 6.2.2

β-Trimethylsilylethanol was a commercial sample and used without further purification.

γ-Trimethylsilylpropanol was prepared by a reported procedure.²⁴⁵

Yield 75%, b.p. 64-67°C / 15 mm Hg (lit.²⁴⁶ 83°C / 27 mm Hg)

¹H n.m.r. δ(CDCl₃): 0.0,s,9H; 0.6,m,2H; 1.6,m,2H; 2.5,s,1H; 3.8,m,2H.

δ-Trimethylsilylbutanol was prepared by the reaction of the Grignard reagent of chloromethyltrimethylsilane and oxetane according to a reported procedure.²⁴⁷

45%, b.p. 88-90°C / 22 mm Hg (lit.²⁴⁷ 96°C / 25 mm Hg)

¹H n.m.r. δ(CDCl₃): 0.0,s,9H; 0.6,m,2H; 1.6-2.0,m,4H; 3.8,m,2H; 3.8,s,1H

Oxetane (trimethylene oxide) was prepared by a reported procedure.²⁴⁸

Yield 19%, b.p. 47-49°C / 760 mm Hg (lit.²⁴⁸ 47.8°C / 760 mm Hg)

^1H n.m.r. $\delta(\text{CDCl}_3)$: 2.7,q (J=8 Hz),2H; 4.6,t (J=8 Hz),4H

ϵ -Trimethylsilylpentanol

β -Bromoethyltrimethylsilane (2.0g, 11.0 mmol) was added dropwise to magnesium turnings (0.30g, 12.2 mmol) in anhydrous diethyl ether (5 ml) with iodine (*ca* 5mg) to maintain a steady reflux. After complete addition, the mixture was heated at reflux for 2 hours. The mixture was cooled on ice, trimethylene oxide was added dropwise and the resulting mixture refluxed for 24 hours. The mixture was poured onto ice cold aqueous sulphuric acid (10%, 20 ml) and extracted with ether (3 x 50 ml). The combined ethereal extracts were washed with saturated sodium chloride solution (100 ml) and dried over magnesium sulphate. Removal of the solvent *in vacuo* followed by fractional distillation afforded ϵ -trimethylsilylpentanol as a colourless oil (0.53 g, 30%). b.p. 62-65°C / 10 mm Hg (lit.²⁴⁶ 85°C / 8mm Hg)

^1H n.m.r. $\delta(\text{CDCl}_3)$: 0.0,s,9H; 0.5,m,4H; 1.4,m,4H; 2.1,s,1H; 3.8,m,2H

α -Trimethylsilylacetic acid was a commercial sample and used without further purification.

Trimethylsilylacetate was prepared by R.A.J. O'Hair for another study.²⁴⁹

β -Trimethylsilylpropanoic acid was prepared as described in Section 6.2.2

γ -Trimethylsilylbutanoic acid was prepared by a standard chromic acid oxidation²³⁴ of δ -trimethylsilylbutanol.

Yield 98%, b.p. 117-118°C / 10mm Hg (lit.²⁵⁰ 118°C / 10 mm Hg)

^1H n.m.r. $\delta(\text{CDCl}_3)$: 0.0,s,9H; 0.50,m,2H; 1.9,m,2H; 3.8,m,2H.

Acetyl trimethylsilane was prepared according to the method of Soderquist.²⁵⁰

Yield 49%, b.p. 111-112°C / 760 mm Hg (lit.²⁵² 112°C / 760 mm Hg)

¹H n.m.r. δ (CDCl₃): 0.3,s,9H; 2.4,s,3H

ν_{\max} (liquid film) 1640 (C=O) cm⁻¹

M.S. (+ve) m/z 116(M⁺)14, 73(Me₃Si⁺)100, 43(MeCO⁺)31

Ethylepoxytrimethylsilane was synthesised by the epoxidation of vinyl-trimethylsilane by a published method.²⁵³

Yield 68%, b.p. 108-110°C / 760 mm Hg (lit.²⁵³ 109-110°C / 760 mm Hg)

¹H n.m.r. δ (CDCl₃): 0.0,s,9H; 2.1,t (J=4 Hz)1H; 2.5,t (J=4 Hz),1H; 2.9,t (J=4 Hz)1H

Propionyl trimethylsilane was prepared following the general procedure of Corey.²⁵⁴

Yield 43%, b.p. 56-58°C / 40 mm Hg (lit.²⁵⁵ 82-83°C / 118 mm Hg)

¹H n.m.r. δ (CDCl₃): 0.3,s,9H; 1.1,t (J=7 Hz),3H, 2.8,q (J=7 Hz),2H

M.S. (+ve) m/z 130(M⁺)6, 73(Me₃Si⁺)100, 57(CH₃CH₂CO⁺)94, 29(CH₃CH₂⁺)100

Benzoyl trimethylsilane was prepared by the procedure of Corey.²⁵⁴

Yield 40%, b.p. 109-110°C / 22 mm Hg (lit.²⁵⁶ 42-44°C / 0.02 mm Hg)

¹H n.m.r. δ (CDCl₃): 0.3,s,9H; 7.5,m,3H; 7.8,m,2H

ν_{\max} (liquid film) 1610 (C=O) cm⁻¹

M.S. (+ve) m/z 178(M⁺)21, 105(PhCO⁺)100, 77(Ph⁺)75

o-Trimethylsilylbenzoic acid was prepared by the method of Benkeser and Krysiak.²⁵⁷

Yield 23%, m.p. 98-100°C (lit.²⁵⁷ 97-98.5°C)

^1H n.m.r. $\delta(\text{CDCl}_3)$: 0.0,s,9H; 7.3,m,2H, 7.9,m,2H

ν_{max} (nujol) 2500-3200 (O-H), 1680 (C=O) cm^{-1}

p-Trimethylsilylbenzoic acid was prepared from *p*-bromobenzoic acid by the same procedure reported for the *ortho* isomer.²⁵⁷

Yield 22%, m.p. 117-119°C (lit.²⁵⁷ 117-118°C)

^1H n.m.r. $\delta(\text{CDCl}_3)$: 0.0,s,9H; 7.4,m,2H; 7.8,m,2H

ν_{max} (nujol) 2500-3400 (O-H), 1690 (C=O) cm^{-1}

o-Trimethylsilylmethylbenzoic acid was prepared by the procedure reported by Coughlin and Salomon.²⁵⁸

Yield 64%, m.p. 77-78°C (lit.ref 77.5°C)

^1H n.m.r. $\delta(\text{CDCl}_3)$: 0.0,s,9H; 2.8,s,2H; 7.3,m,3H, 8.2,m,1H

ν_{max} (nujol) 2500-3400 (O-H), 1670 (C=O) cm^{-1}

M.S. (+ve) m/z 222(M^+)16, 207(M^+ - Me)100, 73(Me_3Si^+)58

o-Trimethylsilylethylbenzoic acid was prepared by an identical procedure to that of *o*-trimethylsilylmethylbenzoic acid except that the alkylation was carried out at 0°C with chloromethyltrimethylsilane and a reaction time of 48 hours.

Yield 37%, m.p. 68-69°C

Found C 66.3%, H 8.4%, $\text{C}_{12}\text{H}_{18}\text{SiO}_2$ requires C 66.8%, H 8.1%

^1H n.m.r. $\delta(\text{CDCl}_3)$: 0.0,s,9H; 0.8,m,2H; 3.0,m,2H; 7.3,m,3H; 8.0,m,1H

ν_{max} (nujol) 2500-3200 (O-H), 1685 (C=O) cm^{-1}

M.S. (+ve) m/z 222(M^+)9, 193(M^+ - Me)99, 104(C_8H_8^+)41, 73(Me_3Si^+)100

p-Trimethylsilylethylbenzoic acid was prepared by an identical procedure to its *ortho* isomer using *p*-toluic acid as starting material.

Yield 32%, m.p. 173-175°C

Found C 66.5%, H 7.9%, C₁₂H₁₈SiO₂ requires C 66.8%, H 8.1%

¹H n.m.r. δ(CDCl₃): 0.0,s,9H; 0.90,m,2H; 2.7,m,2H; 7.2-8.1,m,4H

M.S. (+ve) *m/z* 222(M⁺)16, 207(M⁺ - Me)100, 205(M⁺ - ·OH)41, 73(Me₃Si⁺)92

α-Trimethylsilylphenylacetic acid was prepared by P.C.H. Eichinger by a reported procedure.²⁵⁹

α-Trimethylsilylmethylphenylacetic acid

n-Butyl lithium in anhydrous diethylether (0.83M, 45 mmol, 54.2 ml) was added dropwise to a mixture of anhydrous diisopropylamine (6.3 ml, 45 mmol) in anhydrous tetrahydrofuran (45 ml) at -20°C. The solution was warmed to 0°C, stirred for 30 min. and re-cooled to -20°C. Sodium dried hexamethylphosphoric triamide (7.8 ml, 45 mmol) was added dropwise followed by the addition of phenylacetic acid (3.0g, 22.1 mmol) in anhydrous tetrahydrofuran (10 ml). The solution was allowed to warm to room temperature, stirred for 30 min. and re-cooled to 0°C. Chloromethyltrimethylsilane (6.3 ml, 45 mmol) was added dropwise and the mixture allowed to warm to room temperature. The solution was poured onto aqueous hydrogen chloride (5%, 100 ml), extracted with diethyl ether (2 x 50 ml), the organic phase was washed with aqueous hydrogen chloride (5%, 4 x 100 ml), water (200 ml), saturated sodium chloride solution (200 ml) and dried over magnesium sulphate. Removal of the solvent *in vacuo* followed by distillation afforded *α*-trimethylsilylmethylphenylacetic acid (1.39g, 28%).
b.p. 198-200°C / 2.0 mm Hg

Found: C 66.4%, H 7.8% ; C₁₂H₁₈SiO₂ requires C 66.8%, H 8.1%)

¹H n.m.r. δ(CCl₄): 0.6,s,9H; 1.4,t (J=8 Hz)2H, 3.7,t (J=8 Hz),1H; 7.4,s,5H; 11.8,s,1H

ν_{max} (liquid film) 2500-3200 (O-H), 1700 (C=O) cm⁻¹

M.S. (+ve) m/z 207(M⁺ - Me·)100, 73(Me₃Si⁺)92

6.2.7 Synthesis of labelled compounds for chapter 5

The d₁-trimethylsilylalcohols were prepared by stirring the unlabelled compounds (*ca* 0.1g) in D₂O (1 ml) for 1 hour. The labelled compound was extracted with anhydrous dichloromethane (3 x 10 ml) with the combined extracts dried over magnesium sulphate. Removal of the solvent afforded the labelled compound which was used without further purification. In all cases, deuterium incorporation (d₁) was better than 90% by ¹H n.m.r. and positive ion mass spectrometry.

The deuterium labelled alkyltrimethylsilanes were prepared by stirring the unlabelled precursors (*ca* 0.1g) in a solution of sodium deuterioxide (1 M, 10 ml) heated at 100°C for 1 hour. The solution was acidified with concentrated d₂-sulphuric acid and extracted with anhydrous chloroform. The combined extracts were dried over magnesium sulphate and the solvent removed *in vacuo* to yield the labelled alkyltrimethylsilanes which was used without further purification. d₃ or d₅-deuterium (as appropriate) incorporation was 98% in each case by ¹H n.m.r. and positive ion mass spectrometry.

α-Trimethylsilylmethylphenyl-α-d₁-acetic acid was prepared by the alkylation of d₂-phenylacetic acid by an identical procedure for the unlabelled

compound. d_2 -Phenylacetic acid was prepared by an exchange reaction of phenylacetic acid in a solution of sodium deuterioxide (0.25 M) heated at 85°C for 1 hour.

Deuterium incorporation $d_1 = 99\%$

^1H n.m.r. $\delta(\text{CDCl}_3)$: 0.6,s,9H; 1.4,s,2H; 7.4,s,5H; 11.8,s,1H

References

- (1) F.W. Aston, "Mass Spectra of Isotopes", p27, Edward Arnold, London, 1933
- (2) R. Large, H. Knof, *Org. Mass Spectrom.*, 1976, **11**, 582
- (3) R.T. Aplin, H. Budzikiewicz, C. Djerassi, *J. Am. Chem. Soc.*, 1965, **87**, 3180
- (4) K.R. Jennings, Mass Spectrometry Specialist Reports, Chem. Soc., London, 1979, **5**, 203
- (5) A.G. Harrison, "Chemical Ionisation Mass Spectrometry", C.R.C Press Inc., Boca Raton, Florida, 1983
- (6) H. Budzikiewicz, *Mass Spectrom. Rev.*, 1986, **5**, 345
- (7) M. Barber, R.S. Bordoli, R.D. Sedgwick, A.N. Tyler, *J. Chem. Soc Chem. Commun.*, 1981, 325.
- (8) K.L. Rinehart, L.A. Gaudioso, M.L. Moore, R.C. Pandey, J.C. Cook, M. Barber, R.D. Sedgwick, R.S. Bordoli, A.N. Tyler, B.N. Green, *J. Am. Chem. Soc.*, 1981, **103**, 6517.
- (9) D.H. Williams, C. Bradley, G. Bojesen, S. Santikarn, L.C.E. Taylor, *J. Am. Chem. Soc.*, 1981, **103**, 5700.
- (10) M. Barber, R.S. Bordoli, R.D. Sedgwick, A.N. Tyler, B.N. Green, V. Parr, J.L. Gower, *Biomed. Mass Spectrom.*, 1982, **9**, 11.
- (11) M. Anbar, G. St. John, *Science*, 1975, **190**, 781.
- (12) J.G. Dillard, *Chem. Rev.*, 1973, **73**, 589
- (13) J.H. Bowie, B.D. Williams in *M.T.P. Int. Rev. Sci. Phys. Chem.*, Serial 2, Ed. MacColl, pp89-129, Butterworth, London, 1975.
- (14) H. Budzikiewicz, *Angew. Chem. Int. Ed. (Engl.)*, 1981, **20**, 624.

- (15) E.W. McDaniel, "Collision Phenomena in Ionised Gases", Wiley, New York, N.Y., 1964
- (16) L.G. Christophorou, "Atomic and Molecular Radiation Physics", Wiley-Interscience, London, 1971.
- (17) C.E. Melton, "Principles of Mass Spectrometry and Negative Ions", Marcel Dekker, New York, N.Y., 1970.
- (18) J.D. Baldeschwieler, S.S. Woodgate, *Acc. Chem. Res.*, 1971, **4**, 114.
- (19) J.L. Beauchamp, *Annu. Rev. Phys. Chem.*, 1971, **22**, 527.
- (20) E.E. Ferguson, F.C. Fehsenfeld, A.L. Schmeltekopf, *Advan. At. Mol. Phys.*, 1969, **5**, 1
- (21) C.E. Melton, "Mass Spectrometry of Organic Ions", Chapter 4, Ed. F.W. McLafferty, Acad. Press, N.Y., 1963.
- (22) J.H. Bowie, A.C. Ho, *Aust. J. Chem.*, 1973, **26**, 2009
- (23) T. McAllister, *J. Chem. Soc. Chem. Commun.*, 1972, 245
- (24) R.N. Hayes, J.H. Bowie, *Spectrosc. Int. J.*, 1982, **1**, 98.
- (25) C.H. DePuy, V.M. Bierbaum, L.A. Flippin, J.J. Grabowski, G.K. King, R.J. Schmitt, *J. Am. Chem. Soc.*, 1979, **101**, 6443
- (26) C.H. DePuy, V.M. Bierbaum, L.A. Flippin, J.J. Grabowski, G.K. King, R.J. Schmitt, S.A. Sullivan, *J. Am. Chem. Soc.*, 1980, **102**, 5012.
- (27) G. Klass, V.C. Trenerry, J.C. Sheldon, J.H. Bowie, *Aust. J. Chem.*, 1981, **34**, 519.
- (28) H.P. Tannenbaum, J.D. Roberts, R.C. Dougherty, *Anal. Chem.*, 1975, **47**, 49.
- (29) V.G. Instruments Model ZAB 2HF, Wythenshawe, Manchester, M23 9LE, U.K.
- (30) J.H. Beynon, R.G. Cooks, J.W. Amy, W.E. Baitinger, T.Y. Ridley, *Anal. Chem.*, 1973, **45**, 1023A.
- (31) C.J. Porter, J.H. Beynon, T. Ast, *Org. Mass Spectrom.*, 1981, **16**, 101.
- (32) J.H. Bowie, *Mass Spectrom. Rev.*, 1990, **9**, 349.
- (33) P.C.H. Eichinger, J.H. Bowie, *J. Org. Chem.*, 1986, **51**, 5078.

- (34) M.J. Raftery, J.H. Bowie, *Int. J. Mass Spectrom. Ion. Proc.*, 1988, **85**, 167.
- (35) P.C.H. Eichinger, J.H. Bowie, R.N. Hayes, *J. Am. Chem. Soc.*, 1989, **111**, 4224.
- (36) P.C.H. Eichinger, J.H. Bowie, *J. Chem. Soc. Perkin Trans. II*, 1988, 497.
- (37) M.D. Rozeboom, J.P. Kiplinger, J.E. Bartmess, *J. Am. Chem. Soc.*, 1984, **106**, 1025.
- (38) P.C.H. Eichinger, J.H. Bowie, R.N. Hayes, *J. Org. Chem.*, 1987, **52**, 5224.
- (39) N.J. Jensen, K.B. Tomer, M.L. Gross, *J. Am. Chem. Soc.*, 1985, **107**, 1863.
- (40) R.G. Cooks, J.H. Beynon, R.M. Caprioli, G. Lester, "Metastable Ions", pp 57-77, Elsevier, Amsterdam, 1973.
- (41) J.H. Bowie, *Mass Spectrom. Rev.*, 1984, **3**, 1.
- (42) T. Ast, "Advances in Mass Spectrometry", Part A, p471, Ed. J.F.J. Todd, John Wiley & Sons, 1985.
- (43) J.H. Bowie, P.Y. White, J.C. Wilson, F.C.V. Larsson, S.-O. Lawesson, J.Ø. Madsen, C. Nolde, G. Schroll, *Org. Mass Spectrom.*, 1977, **12**, 191.
- (44) T. Sürig, H.-F. Grützmacher, *Org. Mass Spectrom.*, 1990, **25**, 446.
- (45) J.H. Bowie, P.Y. White, *Aust. J. Chem.*, 1978, **31**, 1511.
- (46) K.L. Busch, G.L. Glish, S.A. McLuckey, "Mass Spectrometry/Mass Spectrometry", VCH, Federal Republic of Germany, 1988.
- (47) D.J. Burinsky, R.G. Cooks, E.K. Chess, M.L. Gross, *Anal. Chem.*, 1982, **54**, 295.
- (48) M.L. Gross, E.K. Chess, P.A. Lyon, F.W. Crow, S. Evans, H. Tudge, *Int. J. Mass Spectrom. Ion Phys.*, 1982, **42**, 243.
- (49) A. Comte, *Course de Philosophie Positive*, Volume III, Bachelier, Paris, 1830.
- (50) E. Schrödinger, *Ann. Physik*, 1926, **79**, 361.

- (51) M. Born, J.R. Oppenheimer, *Ann. Physik.*, 1927, **84**, 457.
- (52) I.N. Levine, "Quantum Chemistry", 3rd Edition, pp 172-192, Allyn & Bacon, Boston, 1983.
- (53) S.F. Boys, *Proc. Roy. Soc.*, 1950, p452, London
- (54) C.C.J. Roothaan, *Rev. Mod. Phys.*, 1960, **32**, 179.
- (55) J.S. Binkley, J.A. Pople, P.A. Dobarh, *Mol. Phys.*, 1974, **28**, 1423.
- (56) J.A. Pople, R.K. Nesbet, *J. Chem. Phys.*, 1954, **22**, 571.
- (57) C. Møller, M.S. Plesset, *Phys. Rev.*, 1934, **46**, 618.
- (58) I.N. Levine, "Quantum Chemistry", 3rd Edition, pp 193, Allyn & Bacon, Boston, 1983.
- (59) R. Krishnan, M.J. Frisch, J.A. Pople, *J. Chem. Phys.*, 1980, **72**, 4244.
- (60) W.J. Hehre, L. Radom, P.v.R. Schleyer, J.A. Pople, "Ab Initio Molecular Orbital Theory", Chapter 4, Wiley, New York, 1986 and references cited therein.
- (61) L. Radom, "Modern Theoretical Chemistry", Vol. 4, p333, (Ed. H.F. Schaefer III) Plenum Press, N.Y. 1977
- (62) C. Reichardt, "Solvents and Solvent Effects in Organic Chemistry", 2nd Edition, VCH, Federal Republic of Germany, 1988.
- (63) C.H. DePuy, J.J. Grabowski, V.M. Bierbaum, *Science*, 1982, **218**, 955.
- (64) C.H. DePuy, V.M. Bierbaum, *Acc. Chem. Res.*, 1981, **14**, 146.
- (65) D.K. Bohme, L.B. Young, *J. Am. Chem. Soc.*, 1970, **92**, 3301.
- (66) N.G. Adams, D. Smith, *Int. J. Mass Spectrom. Ion. Phys.*, 1976, **21**, 349.
- (67) J.M. Van Doren, S.E. Barlow, C.H. DePuy, V.M. Bierbaum, *Int. J Mass Spectrom. Ion Proc.*, 1987, **81**, 85.
- (68) N.G. Adams, D. Smith in "Techniques for the Study of Ion Molecule Reactions", Chapter 4, Ed. J.M. Farrar and W.M. Saunders Jr., Wiley, New York, 1988.
- (69) D.K. Bohme, E. Lee-Ruff, L. B. Young, *J. Am. Chem. Soc.*, 1972, **94**, 5153.

- (70) C.H. DePuy, V.M. Bierbaum, R. Damrauer; *J. Am. Chem. Soc.*, 1984, **106**, 4051.
- (71) C.H. DePuy, S. Gronert, S.E. Barlow, V.M. Bierbaum, R. Damrauer, *J. Am. Chem. Soc.*, 1989, **111**, 1968.
- (72) R.W. Higgins, J.H. Cahn, *J. Appl. Phys.*, 1967, **38**, 180.
- (73) V.M. Bierbaum, C.H. DePuy, R.H. Shapiro, J.H. Stewart, *J. Am. Chem. Soc.*, 1976, **98**, 4229.
- (74) Y. Ikezoe, S. Matsuoka, M. Takebe, A. Viggiano, "Gas Phase Ion Molecule Reaction Rate Constants Through 1986", Ion Reaction Research Group of the Mass Spectrometry Society of Japan, Tokyo, 1987.
- (75) N.G. Adams, D. Smith, *J. Phys. B: Atom. Mol. Phys.*, 1976, **9**, 1439.
- (76) D. Smith, N.G. Adams, *Adv. At. Mol. Phys.*, 1988, **24**.
- (77) T. Su, M.T. Bowers, *Int. J. Mass Spectrom. Ion Phys.*, 1973, **12**, 347.
- (78) G. Gioumouisis, D.P. Stevenson, *J. Chem. Phys.*, 1958, **29**, 294.
- (79) D.J. Cram, "Fundamentals of Carbanion Chemistry", Academic Press New York, N.Y., 1965
- (80) J.C. Stowell, "Carbanions in Organic Synthesis", Wiley-Interscience, New York, N.Y., 1979
- (81) E. Bunce, "Carbanions: Mechanistic and Isotopic Aspects", Elsevier, Amsterdam, 1975
- (82) E. Bunce, T. Durst, "Comprehensive Carbanion Chemistry, Part A: Structure and Reactivity", Elsevier, Amsterdam, 1980.
- (83) R.B. Bates, C.A. Ogle, "Carbanion Chemistry", Springer-Verlag, Berlin, 1983.
- (84) J. Hine, "Structural Effects on Equilibria in Organic Chemistry", Wiley-Interscience, New York, N.Y. 1975.
- (85) R.W. Taft, "Steric Effects in Organic Chemistry", Chapter 13, Ed. M.S. Newman, Wiley, New York, N.Y., 1956

- (86) F.G. Bordwell, J.E. Bartmess, J.A. Hautala, *J. Org. Chem.*, 1978, **43**, 3095.
- (87) F. Bernadi, I.G. Csizamadia, A. Mangini, H.B. Schlegel, M.-H. Whangbo, S. Wolfe, *J. Am. Chem. Soc.*, 1975, **97**, 2209.
- (88) J.-M. Lehn, G. Wipff, *J. Am. Chem. Soc.*, 1976, **98**, 7498.
- (89) A.C. Hopkinson, M.H. Lien, K. Yates, P.G. Mezey, I.G. Csizmadia, *J. Chem. Phys.*, 1977, **67**, 517.
- (90) D.W. Boerth, A. Streitweiser, *J. Am. Chem. Soc.*, 1978, **100**, 750.
- (91) G.I. Mackay, M.H. Lien, A.C. Hopkinson, D.K. Bohme, *Can. J. Chem.*, 1978, **56**, 131.
- (92) A. Pross, D.J. DeFrees, B.A. Levi, S.K. Pollack, L. Radom, W.J. Hehre, *J. Org. Chem.*, 1981, **46**, 1693.
- (93) J. Chandrasekhar, J. G. Andrade, P.v.R. Schleyer, *J. Am. Chem. Soc.*, 1981, **103**, 5609.
- (94) R. Hoffmann, L. Radom, J.A. Pople, P.v.R. Schleyer, W.J. Hehre, L. Salem, *J. Am. Chem. Soc.*, 1972, **94**, 6221.
- (95) A. Pross, L. Radom, *Aust. J. Chem.*, 1980, **33**, 241.
- (96) P.v.R. Schleyer, T. Clark, A.J. Kos, G. W. Spitznagel, C. Rohde, D. Arad, K.N. Houk, N.G. Rondan, *J. Am. Chem. Soc.*, 1984, **106**, 6467.
- (97) A. Streitweiser, J.E. Williams, *J. Am. Chem. Soc.*, 1975, **97**, 191.
- (98) Most gas phase studies refer to the generation of a single substituted alkyl carbanion and ignore the effect of a substituent on carbanion stability. For exceptions, see references 98 - 100: A. J. Noest, N.M.M. Nibbering, *J. Am. Chem. Soc.*, 1980, **102**, 6427.
- (99) S.T. Graul, R.R. Squires, *J. Am. Chem. Soc.*, 1988, **110**, 607.
- (100) S.T. Graul, R.R. Squires, *J. Am. Chem. Soc.*, 1990, **112**, 2506.
- (101) F.R. Cruickshank, S.W. Benson, *J. Phys. Chem.*, 1969, **73**, 733.
- (102) F.R. Cruickshank, S.W. Benson. *Int. J. Chem. Kinet.*, 1969, **1**, 381.
- (103) M.J.S. Dewar, M.A. Fox, D.J. Nelson, *J. Organomet. Chem.*, 1980, **185**, 157.

- (104) M. Rossi, D.M. Golden, *J. Am. Chem. Soc.*, 1979, **101**, 1230.
- (105) J.C. Sheldon, J.H. Bowie, D.E. Lewis, *New J. Chem.*, 1988, **12**, 269.
- (106) E. Block "Reactions of Organosulphur Compounds", Chapter 2, Volume 37, Ed. A.T. Blomquist and H.H. Wasserman, Academic Press, New York, 1978.
- (107) M.J. Frisch, J.S. Binkley, H.B. Schlegel, K. Raghavachari, C.F. Melius, R.L. Martin, J.J.P. Stewart, F.W. Bodrowicz, C.M. Rohlfling, L.R. Kahn, D.J. Frees, R. Seeger, R.A. Whiteside, D.J. Fox, E.M. Fleuder, J.A. Pople, "GAUSSIAN 86", Release C, Carnegie-Mellon Quantum Chemistry Publishing Unit, Pittsburgh, Pennsylvania.
- (108) S.W. Froelicher, B.S. Freiser, R.R. Squires, *J. Am. Chem. Soc.*, 1986, **108**, 2853.
- (109) J.C. Sheldon, J.H. Bowie, *J. Am. Chem. Soc.*, 1990, **112**, 2424.
- (110) D. Thomas, J.E. Bartmess, unpublished work.
- (111) G.I. Mackay, R.S. Hemsworth, D.K. Bohme, *Can. J. Chem.*, 1976, **54**, 1624.
- (112) J.E. Bartmess, J.A. Scott, R.T. McIver Jr., *J. Am. Chem. Soc.*, 1979, **101**, 6046.
- (113) S.R. Kass, H. Guo, G.D. Dahlke, *J. Am. Soc. Mass Spectrom.*, 1990, **1**, 366.
- (114) A.L.C. Smit, F.H. Field, *J. Am. Chem. Soc.*, 1977, **99**, 6471.
- (115) M. Meot-Ner, L.W. Sieck, *J. Phys. Chem.*, 1986, **90**, 6687.
- (116) P.A. Schulz, R.D. Mead, P.L. Jones, W.C. Lineberger, *J. Chem. Phys.*, 1982, **77**, 1153.
- (117) A.H. Zimmerman, J.I. Brauman, *J. Am. Chem. Soc.*, 1977, **99**, 3565.
- (118) C.H. DePuy, V.M. Bierbaum, R.J. Schmitt, R.H. Shapiro, *J. Am. Chem. Soc.*, 1978, **100**, 2920.
- (119) S.R. Kass, C.H. DePuy, *J. Org. Chem.*, 1985, **50**, 2874.
- (120) G.K. King, M.M. Maricq, V.M. Bierbaum, C.H. DePuy, *J. Am. Chem. Soc.*, 1981, **103**, 7133.

- (121) V.M. Bierbaum, J.J. Grabowski, C.H. DePuy, *J. Phys. Chem.*, 1984, **88**, 1389.
- (122) C.H. DePuy, *Org. Mass Spectrom.*, 1985, **20**, 556.
- (123) M. Nimlos, Ph.D. thesis, University of Colorado, Boulder, 1986.
- (124) M. Travers, D. Cowles, G.B. Ellison, *Chem. Phys. Lett.*, 1989, **164**, 449.
- (125) D.G. Hopper, A.C. Wahl, R.L.C. Wu, T.O. Tiernan, *J. Chem. Phys.*, 1976, **65**, 5474.
- (126) C.F. Bernasconi, M.W. Stronach, C.H. DePuy, S. Gronert, *J. Am. Chem. Soc.*, 1990, **112**, 9044.
- (127) S.G. Lias, J.E. Bartmess, J.F. Liebmann, J.L. Holmes, R.D. Levin, W.G. Mallard, *J. Phys. Chem. Ref. Data*, 1988, **17**, Supp. 1.
- (128) R.E. Lee, R.R. Squires, *J. Am. Chem. Soc.*, 1986, **108**, 5078.
- (129) M. Eckersley, J.H. Bowie, R.N. Hayes, *Int. J. Mass Spectrom. Ion Proc.*, 1989, **93**, 199.
- (130) S. Moran, G.B. Ellison, *J. Phys. Chem.*, 1988, **92**, 1794.
- (131) L.G.S. Shum, S.W. Benson, *Int. J. Chem. Kinet.*, 1983, **15**, 433.
- (132) S. Ingemann, N.M.M. Nibbering, *Can. J. Chem.*, 1984, **62**, 2273.
- (133) G.B. Ellison, P.C. Engelking, W.C. Lineberger, *J. Am. Chem. Soc.*, 1978, **100**, 2556.
- (134) D.M. Golden, S.W. Benson, *Chem. Rev.*, 1969, **69**, 125.
- (135) D. Griller, F.P. Loring, *J. Am. Chem. Soc.*, 1981, **103**, 1586.
- (136) R.C. Bingham, *J. Am. Chem. Soc.*, 1975, **97**, 6743.
- (137) P.v.R. Schleyer, E. Kaufmann, A.J. Kos, H. Mayr, J. Chandrasekhar, *J. Chem. Soc. Chem. Commun.*, 1986, 1583.
- (138) A. Streitwieser, C.M. Berke, G.W. Schriver, D. Grier, J.B. Collins, *Tetrahedron Supplement 1*, 1981, **37**, 345.
- (139) P.v.R. Schleyer, A.J. Kos, *Tetrahedron*, 1983 **39**, 1141.
- (140) J.D. Roberts, R.L. Webb, E.A. McElhill, *J. Am. Chem. Soc.*, 1950, **72**, 408.
- (141) Y. Apeloig, Z. Rappoport, *J. Am. Chem. Soc.*, 1979, **101**, 5095.

- (142) R. Peerboom, S. Ingemann, N.M.M. Nibbering, *Recl. Trav. Chim. Pays-Bas*, 1985, **104**, 74.
- (143) W.P.M. Maas, P.A. vanVeelen, N.M.M. Nibbering, *Org. Mass Spectrom.*, 1989, **24**, 546.
- (144) M.J. Raftery, J.H. Bowie, J.C. Sheldon, *J. Chem. Soc. Perkin Trans. II*, 1988, 563.
- (145) C.H. DePuy, R. Damrauer, *Organometallics*, 1984, **3**, 362.
- (146) M.B. Stringer, D.J. Underwood, J.H. Bowie, J.L. Holmes, A.A. Mommers, J.A. Szulejko, *Can. J. Chem.*, 1986, **64**, 764.
- (147) S.R. Kass, J. Filley, J.M. Van Doren, C.H. DePuy, *J. Am. Chem. Soc.*, 1986, **108**, 2849.
- (148) K.M. Downard, J.C. Sheldon, J.H. Bowie, *Int. J. Mass Spectrom. Ion. Proc.*, 1988, **86**, 217.
- (149) R.H. Nobes, D. Poppinger, W.-K. Li, L. Radom, "Comprehensive Carbanion Chemistry", Ed. E. Buncl and T. Burst, Part C, Elsevier, Amsterdam, 1987.
- (150) J.C. Sheldon, G.J. Currie, J. Lahnstein, R.N. Hayes, J.H. Bowie, *Nouv. J. Chim.*, 1985, **9**, 205.
- (151) J.C. Sheldon - private communication.
- (152) J.B. Pedley, J. Rylance, Sussex-N.P.L. Computer Analysed Thermochemical Data, University of Sussex, 1977.
- (153) J.G. Dillard, J.L. Franklin, *J. Chem. Phys.*, 1968, **48**, 2353.
- (154) C.H. DePuy, V.M. Bierbaum, *Tetrahedron Lett.*, 1981, **22**, 5129.
- (155) J.H. Bowie, C.H. DePuy, S.A. Sullivan, V.M. Bierbaum, *Can. J. Chem.*, 1986, **64**, 1046.
- (156) C.J. Casewit, W.A. Goddard III, *J. Am. Chem. Soc.*, 1982, **104**, 3280.
- (157) D.L. Baulch, R.A. Cox, P.J. Crutzen, R.F. Hampson Jr., J.A. Kerr, J. Troe, R.T. Watson, *J. Phys. Chem Ref. Data*, 1982, **11**, 493.
- (158) S. Wolfe, A. Rauk, I.G. Csizmadia, *J. Am. Chem. Soc.*, 1967, **89**, 5710.
- (159) A. Rauk, S. Wolfe, I.G. Csizmadia, *Can. J. Chem.*, 1969, **47**, 113.

- (160) S. Wolfe, A. Stolow, L.A. LaJohn, *Can. J. Chem.*, 1984, **62**, 1470.
- (161) R.E. Penn, E. Block, L.K. Revelle, *J. Am. Chem. Soc.*, 1978, **100**, 3622.
- (162) F. Turecek, L. Brabec, T. Vondrak, V. Hanus, J. Hajicek, Z. Havlas, *Collect. Czech. Chem. Comm.*, 1988, **53**, 2140.
- (163) F.A. Davis, R.L. Billmers, *J. Org. Chem.*, 1985, **50**, 2593.
- (164) J.L. Kice, *Adv. Phys. Org. Chem.*, 1980, **17**, 65.
- (165) D.R. Hogg, *Compr. Org. Chem.*, 1979, **4**, 261.
- (166) E. Wenschuh, W. Radeck, A. Porzel, A. Kolbe, S. Edelmann, *Z. Anorg. Allg. Chem.*, 1985, **528**, 138.
- (167) D.P. Ridge, J.L. Beauchamp, *J. Am. Chem. Soc.*, 1974, **96**, 637.
- (168) S.A. Sullivan, J.L. Beauchamp, *J. Am. Chem. Soc.*, 1976, **98**, 1160.
- (169) S.A. Sullivan, J.L. Beauchamp, *J. Am. Chem. Soc.*, 1977, **99**, 5017.
- (170) R vanDoorn, K.R. Jennings, *Org. Mass Spectrom.*, 1981, **16**, 397.
- (171) C.H. DePuy, V.M. Bierbaum, *J. Am. Chem. Soc.*, 1981, **103**, 5034.
- (172) C.H. DePuy, E.C. Beedle, V.M. Bierbaum, *J. Am. Chem. Soc.*, 1982, **104**, 6483.
- (173) V.M. Bierbaum, J. Filley, C.H. DePuy, M.F. Jarrold, M.T. Bowers, *J. Am. Chem. Soc.*, 1985, **107**, 2818.
- (174) L.J. deKoning, N.M.M. Nibbering, *J. Am. Chem. Soc.*, 1987, **109**, 1715.
- (175) W.W. van Berkel, L.J. deKoning, N.M.M. Nibbering, *J. Am. Chem. Soc.*, 1987, **109**, 7602.
- (176) R.J. Waugh, R.N. Hayes, P.C.H. Eichinger, K.M. Downard, J.H. Bowie, *J. Am. Chem. Soc.*, 1990, **112**, 2537.
- (177) C.H. DePuy, S. Gronert, A. Mullin, V.M. Bierbaum, *J. Am. Chem. Soc.*, 1990, **112**, 8650.
- (178) S. Gronert, R.A.J. O'Hair, S. Prodnuk, D. Sülzle, R. Damrauer, C.H. DePuy, *J. Am. Chem. Soc.*, 1990, **112**, 997.
- (179) S.A. Wolfe, A. Stolow, L.A. LaJohn, *Tetrahedron Lett.*, 1983, **24**, 4071.
- (180) E. Magnusson, *Tetrahedron.*, 1985, **41**, 2939.
- (181) C.A. Wight, J.L. Beauchamp, *J. Phys. Chem.*, 1980, **84**, 2503.

- (182) S.W. Benson, "Thermochemical Kinetics", Wiley-Interscience, New York, 1976.
- (183) J.B. Cumming, P. Kebarle, *Can. J. Chem.*, 1978, **56**, 1.
- (184) J.J. Grabowski, L. Zhang, *J. Am. Chem. Soc.*, 1989, **111**, 1193.
- (185) J.H. Bowie, M.B. Stringer, R.N. Hayes, *Rapid Commun. Mass Spectrom.*, 1990, **4**, 129.
- (186) R.A.J. O'Hair, K.E. Carrigan, V.M. Bierbaum, C.H. DePuy, *Int. J. Mass Spectrom. Ion. Proc.*, 1989, **90**, 295.
- (187) D.A. Thomas, J.E. Bloor, J.E. Bartmess, *J. Am. Soc. Mass Spectrom.*, 1990, **1**, 295.
- (188) A.G. Brook, *Acc. Chem. Res.*, 1974, **7**, 77.
- (189) A.G. Brook, A.R. Bassindale, "Rearrangements in Ground and Excited States", Ed. P. deMayo, Essay 9, pp149-227, Academic Press, New York, 1980.
- (190) L.H. Sommer, "Stereochemistry, Mechanism and Silicon", McGraw-Hill, New York, 1965.
- (191) I. Fleming, *Compr. Org. Chem.*, 1979, **3**, 542.
- (192) R.J.P. Corriu, C. Guerin, *Adv. Organomet. Chem.*, 1982, **20**, 265.
- (193) R. West, *Adv. Organomet. Chem.*, 1977, **16**, 1.
- (194) A.G. Brook, *J. Am. Chem. Soc.*, 1958, **80**, 1886.
- (195) J.C. Sheldon, J.H. Bowie, C.H. DePuy, R. Damrauer, *J. Am. Chem. Soc.*, 1986, **108**, 6794.
- (196) R.A.J. O'Hair, J.C. Sheldon, J.H. Bowie, R. Damrauer, C.H. DePuy, *Aust. J. Chem.*, 1989, **42**, 489.
- (197) A.G. Brook, J.M. Duff, D.G. Anderson, *J. Am. Chem. Soc.*, 1970, **92**, 7567.
- (198) C.H. DePuy, V.M. Bierbaum, R. Damrauer, J.A. Soderquist, *J. Am. Chem. Soc.*, 1985, **107**, 3385.
- (199) A. Degl'Innocenti, S. Pike, D.R.M. Walton, G. Seconi, A. Ricci, M. Fiorenza, *J. Chem. Soc. Chem. Commun.*, 1980, 1201.

- (200) A. Ricci, A. Degl'Innocenti, S. Chimichi, M. Fiorenza, G. Rossini, H.J. Bestmann, *J. Org. Chem.*, 1985, **50**, 130.
- (201) A.G. Brook, W.W. Limburg, D.M. MacRae, S.A. Fieldhouse, *J. Am. Chem. Soc.*, 1967, **89**, 704.
- (202) A.G. Brook, D.M. MacRae, W.W. Limburg, *J. Am. Chem. Soc.*, 1967, **89**, 5493.
- (203) L.Radom, *Org. Mass Spectrom.*, 1991, **26**, 359.
- (204) J.C. Sheldon, R.N. Hayes, J.H. Bowie, C.H. DePuy, *J. Chem. Soc. Perkin Trans. II*, 1987, 275.
- (205) G.W. Adams, J.H. Bowie, R.N. Hayes, *J. Chem. Soc. Perkin Trans. II*, 1989, 2159.
- (206) P.C. Burgers, J.L. Holmes, J.E. Szulejko, A.A. Mommers, J.K. Terlouw, *Org. Mass Spectrom.*, 1983, **18**, 254.
- (207) D.P. Ridge, J.L. Beauchamp, *J. Am. Chem. Soc.*, 1974, **96**, 3595.
- (208) S. Ambasht, S.K. Chiu, P.E. Peterson, J. Queen, *Synthesis*, 1980, 318.
- (209) J.L. Speier, B.F. Daubert, R.R. McGregor, *J. Am. Chem. Soc.*, 1948, **70**, 1117.
- (210) D.C. Noller, H.W. Post, *J. Org. Chem.*, 1952, **17**, 1393.
- (211) L.H. Sommer, J. Rockett, *J. Am. Chem. Soc.*, 1951, **73**, 5130.
- (212) E. Larsson, *Chem. Ber.*, 1930, **63**, 1347.
- (213) P.S. Fitt, L.N. Owen, *J. Chem. Soc.*, 1957, 2250.
- (214) W.R. Kirner, *J. Am. Chem. Soc.*, 1928, **50**, 2446.
- (215) D.J. Peterson, *J. Org. Chem.*, 1967, **32**, 1717.
- (216) R.C. Fuson, B.H. Wojcik, *Org. Syn. Coll. Vol. II*, Ed. A.H. Blatt, pp260, John Wiley & Sons Inc., London, 1944.
- (217) M.H. Palomaa, *Chem. Zentr.*, 1912, **2**, 596.
- (218) J. L. Spier, *J. Am. Chem. Soc.*, 1948, **70**, 4142.
- (219) J.E. Noll, J.L. Spier, B.F. Daubert, *J. Am. Chem. Soc.*, 1951, **73**, 3867.
- (220) H.T. Clarke, H.B. Gillespie, S. Z. Weiss Haus, *J. Am. Chem. Soc.*, 1933, **55**, 4571.

- (221) W.A. Bunnelle, M.A. Rafferty, S.L. Hodges; *J. Org. Chem.*, 1987, **52**, 1603.
- (222) H. Adkins, G Krsek, *J. Am. Chem. Soc.*, 1948, **70**, 383.
- (223) S. Borghero, O. Finsterle, *Gazz. Chim. Ital.*, 1955, **85**, 651
- (224) W.H. Perkin Jr., C.H.G. Sprankling, *J. Chem. Soc.*, 1899, **75**, 11.
- (225) R. Ratcliffe, P. Rodehorst, *J. Org. Chem.*, 1970, **35**, 4000.
- (226) J.-P. Picard, A. Ekouya, J. Dunogues, N. Duffant, R. Calas, *J. Organomet. Chem.*, 1975, **93**, 51.
- (227) H.R. Ward, P.D. Sherman Jr., *J. Am. Chem. Soc.*, 1968, **90**, 3812
- (228) "Handbook of Chemistry and Physics", Ed. R.E. Weast, 56th Edition, C.R.C. Press Inc., Ohio, 1975
- (229) L.H. Sommer, N.S. Marans, *J. Am. Chem. Soc.*, 1950, **72**, 1935
- (230) C.V. Chelintzev, E.D. Osetravo, *Compt. Rend. Acad. Sci. U.R.S.S.*, 1935, **2**, 251
- (231) A.I. Vogel, "Textbook of Practical Organic Chemistry", pp778, 4th Edition, Longman, London, 1978
- (232) E. Kohler, H. Engelbrecht, *J. Am. Chem. Soc.*, 1919, **41**, 764
- (233) N.V. Komarov, V.K. Roman, L.I. Kamarova, *Izv. Akad. Nauk. S.S.S.R. Ser. Khim.*, 1966, **8**, 1464
- (234) L.F. Fieser, M. Fieser, "Reagents in Organic Synthesis", Volume 1, pp142, John Wiley & Sons Inc., New York, 1967
- (235) L.H. Sommer, J.R. Gold, G.M. Goldberg, M.S. Marans, *J. Am. Chem. Soc.*, 1949, **71**, 1509
- (236) H.C. Brown, K.A. Keblys, *J. Org. Chem.*, 1966, **31**, 485
- (237) A.D. Petrov, S.I. Sadykh-Zade, E.I. Filatova, *Zh. Obsch. Khim.*, 1959, **29**, 2936.
- (238) C.R. Hauser, C.R. Hance, *J. Am. Chem. Soc.*, 1952, **74**, 5091
- (239) W.T. Olsen, F.M. Whitacre, *J. Am. Chem. Soc.*, 1943, **65**, 1019
- (240) J.H. Turnbull, E.S. Wallis, *J. Org. Chem.*, 1956, **21**, 663
- (241) L.I. Smith, S. McKenzie Jr., *J. Org. Chem.*, 1950, **15**, 74

- (242) W.A. Noyes, *J. Am. Chem. Soc.*, 1933, **55**, 3888
- (243) R. Bell, P.D. Cottam, J. Davies, D.N. Jones, *J. Chem. Soc. Perkin Trans. I*, 1981, 2106
- (244) Klason, *J. Prakt. Chem.*, 1877, **15**, 175.
- (245) M.F. Shostakovskii, I.A. Shikhiev, *Izvest. Akad. Nauk. S.S.S.R., Otdel. Khim. Nauk.*, 1954, 745
- (246) L.H. Sommer, R.E. Van Strien, F.C. Whitmore, *J. Am. Chem. Soc.*, 1949, **71**, 3056
- (247) W. Steudel, H. Gilman, *J. Am. Chem. Soc.*, 1960, **82**, 6129
- (248) C.G. Derrick, D.W. Bissell, *J. Am. Chem. Soc.*, 1916, **38**, 2478
- (249) R.A.J. O'Hair, S. Gronert, C.H. DePuy, J.H. Bowie, *J. Am. Chem. Soc.*, 1989, **111**, 3105
- (250) L.H. Sommer, R.P. Pioch, N.S. Marans, G.M. Goldberg, J. Rockett, J. Kerlin, *J. Am. Chem. Soc.*, 1953, **75**, 2932
- (251) J.A. Soderquist, G.J.-H. Hsu, *Organometallics*, 1982, **1**, 830
- (252) A.G. Brook, *Adv. Organomet. Chem.*, 1968, **7**, 95
- (253) J.-L. Chow, *Hua. Hsueh. Hsueh. Pao.*, 1958, **24**, 426
- (254) E.J. Corey, D. Seebach, R. Freedman, *J. Am. Chem. Soc.*, 1967, **89**, 434
- (255) C.H. Heathcock, C.T. Buse, W.A. Kleschick, M.C. Pirrung, J.E. Sohn, J. Lampe, *J. Org. Chem.*, 1980, **45**, 1066
- (256) A.G. Brook, M.A. Quigley, G.J.D. Peddle, N.V. Schwartz, C.M. Warner, *J. Am. Chem. Soc.*, 1960, **82**, 5102
- (257) R.A. Benkesser, H.R. Krysiak, *Chemical Abstracts*, 1955, **49**, 3890
- (258) D.J. Coughlin, R.G. Salomon, *J. Org. Chem.*, 1979, **44**, 3784
- (259) W.T. Brady, J.C. Sheng, *J. Organomet. Chem.*, 1977, **137**, 287

Publications

Some of the work described in this thesis has been reported in the following publications:

"Are the Elusive Ions $^{-}\text{CH}_2\text{SH}$, $^{-}\text{CH}_2\text{OH}$, and $^{-}\text{CH}_2\text{NH}_2$ Detectable in the Gas Phase? A Joint Theoretical/Experimental Approach", K. M. Downard, J. C. Sheldon, J. H. Bowie, D.E. Lewis, R.N. Hayes, *J. Am. Chem. Soc.*, 1989, **111**, 8112.

"Collision-Induced Elimination of Alkenes from Deprotonated Unsaturated Ethers in the Gas Phase. Reactions Involving Specific β -Proton Transfer", R.J. Waugh, R.N. Hayes, P.C.H. Eichinger, K.M. Downard, J.H. Bowie, *J. Am. Chem. Soc.*, 1990, **112**, 2537.

"Skeletal Rearrangements of Deprotonated Organosilanes in the Gas Phase. Silicon-Oxygen Bond Formation." K. M. Downard, J.H. Bowie, R.N.Hayes, 1990, **43**, 511.

Other sections of work described in this thesis are in final preparation for publication.

Downard, K. M., Sheldon, J. C., Bowie, J. H., Hayes, Roger N. & Lewis, D. E. (1989). Are the elusive ions $\bar{\text{C}}\text{H}_2\text{SH}$, $\bar{\text{C}}\text{H}_2\text{OH}$, and $\bar{\text{C}}\text{H}_2\text{NH}_2$ detectable in the gas phase? A joint ab initio/experimental approach. *Journal of the American Chemical Society*, *111*(21), 8112-8115.

NOTE:

This publication is included in the print copy of the thesis held in the University of Adelaide Library.

It is also available online to authorised users at:

<http://dx.doi.org/10.1021/ja00203a007>

Waugh, R. J., Eichinger, P. C. H., Downard, K. M., Bowie, J. H. & Hayes, R. N. (1990). Collision-induced elimination of alkenes from deprotonated unsaturated ethers in the gas phase. Reactions involving specific β -proton transfer. *Journal of the American Chemical Society*, 112(7), 2537-2541.

NOTE:

This publication is included in the print copy
of the thesis held in the University of Adelaide Library.

It is also available online to authorised users at:

<http://dx.doi.org/10.1021/ja00163a009>

Downard, K. M., Bowie, J. H. & Hayes, R. N. (1990). Skeletal rearrangements of deprotonated organosilanes in the gas phase. Silicon-oxygen bond formation. *Australian Journal of Chemistry*, 43(3), 511-520.

NOTE:

This publication is included in the print copy of the thesis held in the University of Adelaide Library.

It is also available online to authorised users at:

<http://dx.doi.org/10.1071/CH9900511>